Cape Peninsula University of Technology

DESIGN AND OPTIMISATION OF DOMESTIC-SCALE THERMOACOUSTIC REFRIGERATOR

by

PATRICK KAJA TSHOWA

Thesis submitted in fulfilment of the requirements for the degree.

MASTER OF ENGINEERING IN MECHANICAL ENGINEERING

in the Faculty of Engineering and the Built Environment

at the Cape Peninsula University of Technology

Supervisor: Associate Professor Tiyamike Ngonda

Bellville campus

Thursday, 31 October 2024

DECLARATION

I, Patrick Kaja Tshowa, declare that the contents of this thesis represent my own unaided work, and that the thesis has not previously been submitted for academic examination towards any qualification. Furthermore, it represents my own opinions and not necessarily those of the Cape Peninsula University of Technology.

Patrick Kaja Tshowa (209159332) **Thursday, 31 October 2024**

Signed **Date**

ABSTRACT

This research study aimed to evaluate the performance of a standing wave thermoacoustic refrigerator and optimise the stack length and position for a single stack material. Thermoacoustic refrigerator (TAR) generally has a low coefficient of performance (COP). This has negatively impacted its development. There has been research to improve its COP, which has mostly focused on optimising the system. Numerical and experimental have been used to optimise various components of TAR. This research study combined the experimental work and numerical modelling of the standing wave TAR. Thirty experiments were conducted over three months. The experiments were done for three stack positions of 30 mm, 40 mm, and 50 mm. At each stack position, stacks of lengths of 25 mm, 35 mm, 45 mm, 55 mm, and 65 mm. In addition, numerical modelling of TAR performance was done for the three positions, with the five stack lengths for each position. The numerical modelling was done using the commercial Multiphysics software. The experiments and numerical modelling were followed by optimisation. The optimisation of the experimental data identified the optimal stack configuration as a stack position of 55 mm and a stack length of 25 mm, achieving a COP of 0.33. The optimal configuration yielded ΔT=8°C, COP=0.33, T_C=25.1°C and Q_C=0.0532 W. On the other hand, the optimisation of numerical modelling data identified the optimal stack configuration as a stack position of 30 mm and a stack length of 25 mm, achieving a COP of 1.27. The optimal configuration yielded ΔT=8.5 K and COP=0.33. The experimental work and numerical modelling agreed regarding stack length. They both indicated an optimal stack length of 25 mm, suggesting that short stack lengths are good for a high COP while maintaining other performance metrics within acceptable ranges. The experimental work and numerical modelling differed in the optimal stack position. As a result, this study could not uncover the influence of stack position as far as optimising for a high COP is concerned.

Keywords: *Coefficient of Performance, Cooling Load, Cooling Temperature, Environmentally Friendly, Acoustic Sound Wave, Thermoacoustic Refrigerator.*

ACKNOWLEDGEMENTS

I would like to express my gratitude to:

- The Almighty God for his divine grace.
- The student debtor department for their significant financial support.
- My principal supervisor, Prof Tiyamike Ngonda, for his enduring sacrifice.
- The Department of Mechanical Engineering for their assistance throughout my studies.
- The Department of Industrial and Systems Engineering for their oversight during my tenure as a teaching assistant.

The financial support provided by the Centre for Postgraduate Studies for this research is hereby acknowledged.

DEDICATION

This thesis is dedicated to family members who played a huge role through the course of my life:

- My late mother: Anastasie Mwadi Kasongo. Her education, discipline, and unconditional love had a significant impact on my childhood and motivated me to study further, knowing that one day I would be able to support her financially. It is always about the mother. As quoted by Celia Haddon in the novel titled The Power of Love: When we read of the utter downfall of a man in the newspapers - fallen from a high position, facing imprisonment, bankrupt, disgraced - we often read that he is staying with his mother. May my mother's soul and spirit live forever for the time to come.

- My late grandparents: Augustin Kasongo Ntita and Ernestine Mujinga Ngala. The most valuable lesson I learnt was of them being authentic, hardworking individuals who raised eleven children by earning an honest living from the sweat of their forehead and always advised of being considerate of others.

- My foster uncle and his beloved wife: Kabeya Mwadianvita and Octavie Mbombo Mitonga.

- My sisters: Kanjinga Bibi, Chantal Mujinga, and Annie Mwadi Katshimwena.

- My brothers: Jean Ngoyi Mukola, Ley Katende Buzangu, Carlos Kabanga Mvidia, Billy Mbuyi Mvidia, and Fabrice Kasongo Ntita.

TABLE OF CONTENTS

LIST OF FIGURES

LIST OF TABLES

NOMENCLATURE

English Letters

a	Speed of sound	m/s
C_p	Specific heat capacity at constant pressure	J/kg. K
D	Drive ratio	-
k	Thermal conductivity	W/m. K^2
L_S	Stack length	m
$\dot{m}_C$	Fluid mass flow rate	Kg/s
$\dot{m}_h$	Fluid mass flow rate	Kg/s
P_m	Mean pressure	Pa
P_A	Amplitude pressure	Pa
q	Heat flux by conduction	W/m^2
S_L	Stack length	m
T_m	Mean temperature	K
T_C	Lower temperature	K
u	Velocity vector	m/s
W_{ac}	Acoustic power	W
X_h	Stack position	m
y		

Greek Letters

λ	Wavelength	[m]
γ	Ratio of isobaric-to-isobaric specific heats	[-]
ρ	Density	[Kg/m^3]
β	Flux density	[T]
δ_k	Gas thermal penetration depth	[m]
δ_{kn}	Normalised thermal penetration depth	[m]
δ_v	Viscous penetration depth	[m]
ω	Angular frequency	[rad/sec]
μ	Dynamic viscosity	[N. m/ m^2]
ρ_m	Mean density	[kg/ m^3]
σ	Prandtl number	[---]
η	Overall efficiency	[%]
η_{Carnot}	Carnot efficiency	[%]
Φ	Phase angle	[rad or ^{0}]
Φ_p	Phase angle of acoustic pressure	[rad or ^{0}]
Φ_u	Phase angle of particles	[rad or ^{0}]
Φ	Porosity	[%]

GLOSSARY

AC	Alternative courant
COP	Coefficient of performance
LANL	Los Alamos National Laboratory
TAR	Thermoacoustic refrigerator.

CHAPTER ONE: INTRODUCTION

1.1 Background to the research problem

Thermoacoustic refrigerators (TARs) are devices that utilise sound waves to transfer thermal energy from the cold to the warm side of a stack. In a TAR, an acoustic driver generates sound waves within a resonator tube, causing standing waves to form (Alcock *et al.* 2018). The interaction between the sound waves and the gas inside the tube results in a cyclical compression and expansion of the gas, which creates temperature differences. These temperature differences are harnessed to cool the cold side of the stack while the warm side dissipates heat. The stack, typically made of a porous material, facilitates the heat exchange by allowing the gas to oscillate and transfer thermal energy.

The key components of a TAR include a loudspeaker (acoustic driver), the stack, heat exchangers, and the resonator tube. The loudspeaker driver supplies the acoustic power necessary for the operation of the TAR, converting electrical input power into acoustic waves with high efficiency (Minner *et al.* 1996). Figure 1-1 shows a standing wave TAR. The stack, considered the heart of the TAR, plays a crucial role in storing and transferring energy. Research by Zolpakar *et al.* (2016) showed that the temperature difference across the stack depends on various factors such as stack material, length, position, and plate spacing.

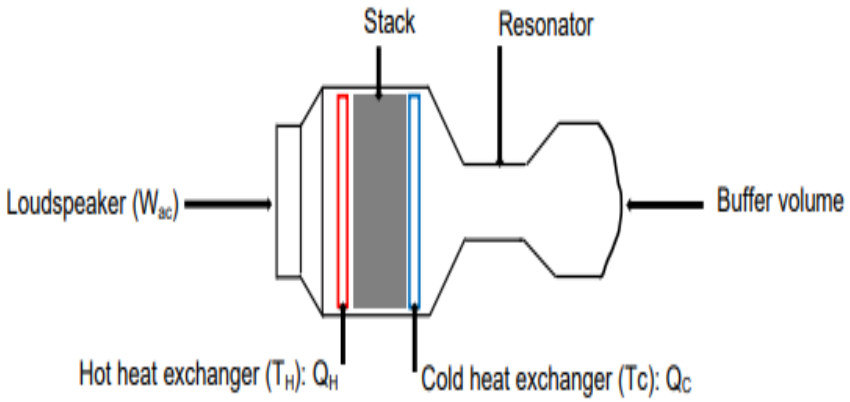

Figure 1-1: Schematic of a standing wave thermoacoustic refrigerator.

The resonator tube, which houses the stack and heat exchangers, is another critical component of the TAR. Studies by Nathad *et al.* (2019) and Kajurek *et al.* (2019) have shown that the resonator tube's length, geometry, and material significantly affect TAR performance. Shorter quarter-wavelength (λ/4) resonators made of materials with lower thermal conductivity have been found to improve TAR efficiency.

The working gas within the TAR, such as helium, argon, xenon, nitrogen, and hydrogen, also plays a crucial role in its performance. Research by Gholamrezaei and Ghorbanian (2016), Kajurek *et al.* (2019), and Rahpeima and Ebrahimi (2022) revealed that gases with a lower Prandtl number enhance the transport coefficient and overall performance of the TAR. Additionally, higher sound intensity in the gas results in a lower cooling temperature.

The performance of TARs is typically evaluated using metrics such as the coefficient of performance (COP), temperature difference across the stack, and the lowest achievable temperature. The COP is a measure of the TAR's efficiency in removing heat from the cold side. Since the invention of the TAR by T.J. Hofler in 1986 at Los Alamos National Laboratory, the low COP has been a persistent issue. Studies aimed at enhancing the COP have focused on using different working gases, with lower Prandtl number gases like He-Xe showing significantly higher COP than helium.

Ongoing research continues to optimise various TAR components, including the loudspeaker driver, stack, heat exchangers, and resonator tube. Several studies have investigated the impact of operating and geometrical parameters on TAR performance. Operating parameters such as mean pressure, pressure amplitude, resonance frequency, acoustic power, blockage ratio, and drive ratio, along with geometrical parameters like stack geometry, length, material, position, pore size or plate spacing, and resonator tube length, geometry, and material, have been examined. For instance, Zolpakar, Mohd-Ghazali and Ahmad (2016) found that the temperature difference across the stack is influenced by these parameters, with increased stack position and shorter stack length with smaller gap spacing yielding better performance. The cooling load, which is the heat extracted from the cold side of the stack, can be improved by using gases with higher Prandtl numbers.

1.2 Statement of the research problem

TAR has a low coefficient of performance (COP). This limitation negatively impacts its development compared to vapour compression and absorption refrigeration cycles and thermoelectric refrigerators. To address this limitation, previous studies have focused on optimising TAR systems to improve COP. Various optimisation methods have been employed, including analytical, mathematical, numerical, and experimental approaches. Researchers have targeted various TAR components for optimisation, such as stack geometry, length, material, the electrodynamic driver, the resonator tube's geometry, length, and material and hot and cold heat exchangers. These efforts are crucial for making TAR a viable alternative to conventional refrigeration and energy conversion technologies. The ongoing research is essential to overcome the current limitations of TAR and achieve a higher COP, thereby making it more competitive with other widely used refrigeration systems.

1.3 Objective of the research

The primary objective of this research study was to evaluate the performance of a standing wave thermoacoustic refrigerator and optimise the stack length and stack position for a single stack material. To achieve the overall goal of the research study, the following secondary objectives were pursued:

- To conduct a literature review of operating parameters and geometrical parameters to enable the design of TAR.
- To construct the standing wave thermoacoustic refrigerator prototype.
- To numerically and experimentally map the performance of a TAR using fixed operating parameters and variable geometrical parameters (stack length and position).
- To determine a viable TAR geometry by optimisation of numerical and experimental data.

1.4 Significance of the research

This study contributes to understanding the influence of stack length and position on COP. An optimal TAR is better positioned to compete and contribute to environmental sustainability as it will reduce reliance on harmful refrigerants.

1.5 Delineation of research

The research was limited to investigating the optimal stack position and length of standing wave TAR. It does not examine the influence of other parameters such as stack material, spacing, resonator length and material. It also investigates a single configuration of TAR, the standing wave TAR.

1.6 Expected outcomes

The outcome of this research study was a prototype standing wave TAR capable of incorporating interchangeable stacks of various lengths at different positions. They could be used to experimentally investigate the influence of stack position and length on COP thereby contributing to the understanding of how these parameters could be used to optimise TAR performance.

1.7 Outline of the thesis

The outline of the thesis was subdivided into six main chapters.

1.8 Chapter One: Introduction

This chapter provides a comprehensive background to the research, establishing the problem statement and objectives. It discusses the challenges of low coefficient of performance (COP) in thermoacoustic refrigerators (TARs) compared to conventional refrigeration systems. The chapter outlines the research methodology, including literature review, numerical modelling, and experimental validation, detailing the systematic approach adopted for the study.

Chapter Two: Literature Review

The literature review explores the theoretical and experimental advancements in TAR technology. It delves into the significance of various components such as the stack, resonator, and working fluid, and their impact on TAR performance. The review highlights previous optimization efforts on TARs, focusing on geometrical and operational parameters to enhance efficiency. This chapter provides a critical analysis of existing research, identifying gaps and setting the context for the current study.

Chapter Three: Research Methodology

This chapter details the methodological approach used in the study, combining experimental and numerical modelling techniques. It describes the experimental setup, including the use of a 5-inch SB Acoustics SATORI MW13P-8 loudspeaker, 3D-printed stacks, and various heat exchangers. The chapter also outlines the numerical modelling process using commercial multiphysics software to simulate different TAR geometries. The systematic experimentation and data collection methods are explained to ensure reproducibility and accuracy. and provides a detailed description of the apparatus and procedures used for data collection. It includes specifics on the construction and assembly of the TAR prototype, the instruments used for measuring temperatures, pressures, and acoustic parameters, and the conditions under which experiments were conducted.

Chapter Four: Results

This chapter presents the findings from both experimental and numerical modelling efforts. It includes data on temperature differences, cooling loads, and COP for various stack configurations. The results are analysed to identify the optimal stack length and position.

Chapter Five: Discussion

The discussion chapter interprets the experimental and numerical results, comparing them with findings from previous studies. It explores the implications of the optimised stack configurations on TAR performance, addressing discrepancies between experimental and

modelling outcomes. The chapter also discusses the limitations of the study and suggests potential areas for further research to enhance TAR efficiency.

Chapter Six: Conclusions and Recommendations

The final chapter summarises the key conclusions drawn from the research, emphasising the significance of optimising stack parameters to improve TAR performance. It provides practical recommendations for future studies and potential applications of the findings in real-world TAR systems. The chapter highlights the contribution of this research to the broader field of thermoacoustic refrigeration, aiming to inspire continued innovation and improvement.

CHAPTER TWO: LITERATURE REVIEW

2.1 Introduction

Thermoacoustic refrigerators (TARs) are reversed heat engines that use sound waves to transport the thermal energy from the cold to the warm side of a stack. The key components of a TAR include an electrodynamic driver, a stack, a resonator tube and two heat exchangers, one in the warm region and the other in the cold region. There are two types of TAR: standing wave and travelling wave TARs. Figure 1-1 presents the general configuration of a standing wave TAR. A standing wave TAR is compact, comprising a resonator tube and a stack as core components. In contrast, a travelling wave TAR, shown in Figure 2-1, is generally large, and its acoustic waves travel in a loop with a regenerator as a core.

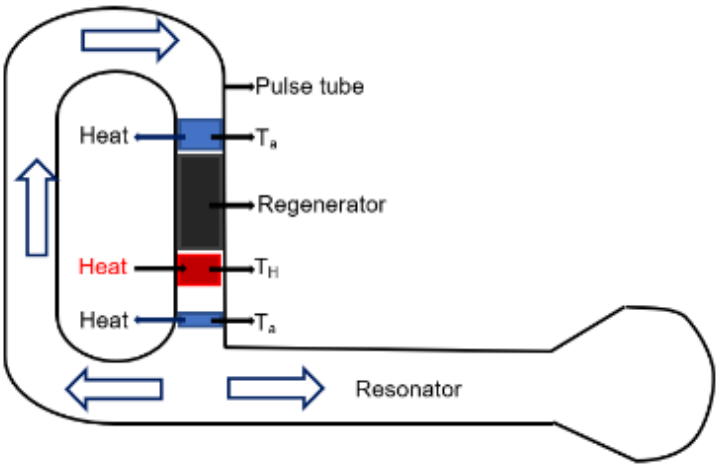

Figure 2-1 Schematic diagram of two stages travelling wave thermoacoustic refrigerator (Alcock *et al.* 2018)

The TAR has a low coefficient of performance (COP), negatively impacting its development. Research to improve the COP of TAR is ongoing and primarily focuses on the optimisation of the system. Several numerical and experimental methods have been developed to optimise the various components of TAR to increase the COP. Optimised components include the stack geometry and material, electrodynamic driver, resonator tube geometry and material, and both heat exchangers (hot and cold).

2.2 Stack

The stack is a crucial TAR component because it increases the gas-solid interface. This increases the possible temperature difference between the TAR's warm and cold regions. Without a stack, the temperature difference would be minimal, compromising the heat-pumping process. Instead, its material temporarily stores the thermal energy while being moved from one point of the stack to another. This happens when the molecule of the gas parcel oscillates back and forth by interfering with one another during the compression and expansion cycles (Kajurek *et al.*, 2019).

2.2.1 Stack geometry

The stack geometry significantly influences the overall efficiency of the TAR by controlling the amount of energy stored and transmitted by the stack. Researchers have demonstrated that the stack shape, pore spacing or plate spacing, and length are critical variables influencing performance. The stack needs to have a large surface area and short distances between the surfaces in the flow channels to maximise the thermal boundary layer, as that is where the thermoacoustic effects occur as collaborated by Zolpakar, Mohd-Ghazali and Ahmad (2016). Figure 2-2 shows stack geometries commonly used in TAR: parallel plate, spiral, honeycomb, Corning Celcor, and pin array. Wantha (2018) studied the spiral, pin array, and circular pore stacks and found that the pin array stack has a lower cold end temperature than the spiral or circular stacks by up to 63% and 70%, respectively. Although the pin array stack is the most effective, it is difficult to manufacture, limiting its use in TAR.

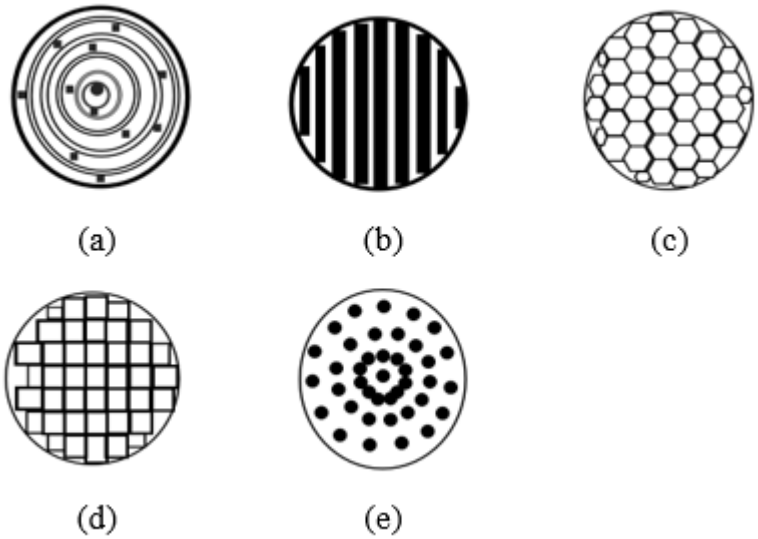

Figure 2-2: Stack geometries: (a) Spiral stack, (b) Parallel plates stack, (c) Honeycomb, (d) Corning celcor, (e) Pin array (Alcock *et al.* 2017).

2.2.2 Plate spacing or pore size.

The gap between the plate spacing or pore size is crucial. It must be large enough to facilitate the gas parcel flow and minimise the viscosity effects of the working fluid, which might prevent the gas parcel from oscillating back and forth (Zolpakar *et al.* 2017). Sarpero *et al.* (2023) evaluated the performance of TAR of three manufactured pores geometry, the square, circular and hexagonal. They found that the square pore geometry was the most effective that had a temperature difference of 18.42 K compared to the other two. Alamir and Elamer (2020) found that increasing the plate spacing in a stack increases the temperature difference between the warm and cold sides up to a point beyond which there is a rapid reduction in the temperature difference. They found that the spacing corresponding to the maximum temperature difference is three times the thermal penetration depth. In their study of the influence of stack plate spacing on TAR performance, Shivakumara and Bheemsha (2021) found that for a TAR that had Helium as a working fluid, a plate spacing of 0.28 mm performed better than plate spacing of 0.33 mm and 0.38 mm. When operating at 1 MPa, 1.6% of drive ratio, 400 Hz and a cooling load of 2 W, the 0.28 mm TAR achieved a maximum temperature difference of 32.9°C, higher

than the 30.75°C and 27.58°C achieved TARs with 0.33 mm and 0.38 mm stacks respectively. The 0.28 mm stack also achieved a higher COP of 2.024 than those of the 0.33 mm (COP = 1.822) and 0.38 mm (COP = 1.656) stack spacing. Shivakumara and Bheemsha (2021) did not present the stack spacing as a function of viscous penetration depth.

2.2.3 Stack material

Table 2-1 presents the thermal properties of some porous materials used as stacks. The stack material is crucial to TAR performance. Nathad *et al.* (2019) asserted that thermal conductivity contributes to the thermal conduction of the working gas and stack material. Zolpakar, Mohd-Ghazali and Ahmad (2016) added that the stack should be designed with a material that has lower thermal conductivity and a higher heat capacity than the working fluid. Ong et al. (2019) collaborated this. They explained that a lower thermal conductivity enables lesser heat loss across the stack while higher heat capacity retains more heat for a slight increase in temperature.

Table 2-1: Thermal properties of porous materials used as stacks (Rahpeima and Ebrahimi 2019; Napolitano *et al.* 2017; Chaiwongsa and Wongwises 2021a; Bhatti and Bashmal 2021).

Porous materials	Thermal conductivity (K) [W/m. K]	Density (ρ) [kg/m^3]	Heat capacity per unit mass [J/Kg K]
Copper scourers	400	8960	385
Stainless steel	14.3-19.0	7918-7801	454-558
Aluminium	5.8	216	895
Celcor ceramic	2.5	2510	730-1017
Glass	1.38	2203	703
VeroWhitePlus	0.23	-	1000
Kapton	0.19-0.20	1419-1394	1394-1394
Mylar sheet	0.16	1347.5	1110
Polylactic acid (PLA)	0.13	1300	1800
RVC	0.033-0.050	49.5	1260

Bhatti *et al.* (2020) compared the temperature difference, energy consumption across the stack and COP of a homogeneous stack with a multi-layered stack where each layer is a different material. They used homogeneous stacks; one was made from Celcor and the other Kapton. For the multi-layered stack, they had two sets of combined stacks, Celcor with RVC and Kapton with RVC. They found that for multi-layered stacks, ΔT increased by as much as 26.14%, COP by 8.5% and the energy reduced by 4.55%. Rahpeima and Ebrahimi (2019) investigated the effect on COP, cooling temperature and drive ratio of different materials in homogenous stacks, Kapton, glass and steel. The drive ratio is the ratio of dynamic pressure amplitude to the mean pressure. They found that Kapton had better performance, followed by glass then steel. The results for cooling temperature, Kapton, glass and steel yielded 11.97 K, 11.8 K and 10.2 K,

respectively. For COP, they yielded 0.28, 0.11 and 0.21, respectively. Finally, the materials yielded drive ratios of 1.4%, 1.45% and 1.7%, respectively. also investigated the effect of stack material. They investigated Mylar and Polylactic Acid (PLA) stacks under the same operating conditions of input power of 20 W, cooling load of 2 W, 150 Hz, and blockage ratio of 0.71. They found that PLA produced better results than Mylar, with a lower cooling temperature of 22.4°C, a temperature difference of 30.5°C, and a COP of 0.93, while Mylar achieved a COP of 0.88. This finding is crucial because stacks made from PLA can be manufactured through 3D printing.

2.2.4 Stack length

Tartibu (2018) and Rahpeima and Ebrahimi (2019) investigated the influence of stack length on COP, and the lowest temperature obtained, the temperature difference between the warm and cold sides of the stack. Zolpakar *et al.* (2017) studied the stack length effects in ceramic Celcor and Mylar stacks as a function of time, temperature, and TAR resonant frequency. They found an optimal stack length of 4 cm which achieved a temperature ranging from 19.2° to 34.2°C with a maximum temperature difference of 15°C. They noted decreasing outcomes with increases in stack length and postulated that this is caused by increasing acoustic impedance and pressure drop. Their results suggest that a long stack should not be preferred. In a later study, Zolpakar *et al.* (2017) investigated the effects of three stack lengths of 3 cm, 4 cm, and 5 cm made of 3D printed VeroWhitePlus Rgd835. They operated the TAR with 101 kPa, 400 Hz, 0.72 blockage ratio with air as a working fluid. They recorded three temperature differences of 16.8°C, 14°C and 12.7°C, respectively. This observation is collaborated by Tartibu (2018), who studied the standing wave TAR and suggested that the best COP is achievable with shorter stacks positioned nearer the closed end of the resonator tube. Rahpeima and Ebrahimi (2019) concurred with Tartibu (2018) that long stacks produce low COP, and short stacks should be preferred. Alamir and Elamer (2020) explain that in long stacks, a larger amount of gas parcels interacts with the stack surfaces, thereby increasing the acoustic power consumption and decreasing TAR performance.

2.2.5 Stack position

The stack position along the resonator length significantly impacts the TAR performance. Zolpakar *et al.* (2016) explained that optimal stack position depends on the acoustic power and thermal relaxation losses across the stack. The thermal relaxation losses are a function of the channel width, Reynolds number, thermal penetration depth, surface roughness in the channel, length, and all minor losses in the resonator. Zolpakar *et al.* (2016) and Tartibu (2018) stated that positioning the stack closer to the pressure antinode instead of the pressure node increases the efficiency and lowers the viscous losses. Thus, a short stack should be positioned nearer the closed end of the resonator, while a longer stack should be placed far away from the closed end of the resonator. Zolpakar *et al.* (2016) considered the influence of stack position on the temperature difference of ceramic Celcor stack. They positioned a 3.5 cm long Celcor stack at 3 cm, 4 cm or 5 cm in a TAR operating 101 kPa, 400 Hz, 0.72 blockage ratio with air as the working fluid. They recorded three temperature differences of 8.8 °C, 10.4 °C and 11 °C for the three stacks positions, respectively, suggesting increasing temperature differences with stack position increases.

2.3 Working fluid.

The TAR uses noble gases such as argon; xenon, nitrogen, and hydrogen (see Table 2-2 for common gasses). Zolpakar *et al.* (2016) explained that cooling load is proportional to the acoustic velocity of the working fluid. Although air is most used in research on TARs, Chaiwongsa and Wongwises (2021) noted that it is not the optimal working fluid because of its high Prandtl number and low specific heat capacity. Zolpakar *et al.* (2016) investigated the effect on TAR performance of using Helium and a gas mixture of He-Xe as working fluids. They operated a TAR at 10 bars, 400 Hz, 0.026 driving ratio and 0.8 blockage ratio. They found that Helium produced a larger cooling load (6.84 W) than the He-Xe mixture (1.93 W) for the same operating conditions, but the He-Xe mixture had a slightly better COP of 1.64 compared with 1.58 for Helium. Ahmed Al-Mufti and Janajreh (2024) investigated the effects of working fluid on the performance of TADR using air, argon, and helium. When argon was utilised with TAE positioned at X_n=0.25 and TAR at X_n=0.58 and acoustic power of 78.3 W. They had discovered

that argon achieved a higher COP and efficiency of 2.66 and 10.068% respectively, however helium achieved the higher cooling power of 60.87 W at ΔT of 5 K.

Table 2-2: Inert gases and binary gas mixtures (Rahpeima and Ebrahimi 2022)

Gas	% of Helium	Prandtl number	Acoustic velocity (m/s)
Air	0	0.70681	347.22
Helium (He)	100	0.6793	1019.2
Argon (Ar)	0	0.6626	322.58
Hydrogen (H2)	0	0.70056	1320.9
Nitrogen (N2)	0	0.71986	353.03
Helium-Argon (He-Ar)	50	0.4178	434.94
Helium-Xenon (He-Xe)	62	0.1945	247.89
Helium-Krypton (He-Kr)	60	0.23	353.6
Helium-Neon (He-Ne)	55	0.53	628.9
Helium-Xenon (He-Xe)	62	0.19516	247.89

2.4 Resonator

The resonator is a crucial component of TAR as it encloses the stack, the hot and cold heat exchangers and contains the working fluid. Nathad *et al.* (2019) explained that a good resonator must be robust, light and have low thermal efficiency to reduce heat losses. Materials with low thermal conductivity, such as PVC (0.19 W/m. K) and acrylic plastic (0.20 W/m. K), are preferred. Additionally, acoustic dissipation losses are a major challenge, particularly for long resonators; hence resonator length as by Nathad *et al.* (2019) needs to be minimal. A long resonator tube accumulates more viscous and thermal penetration losses. Ong *et al.* (2019) explained that the larger losses in long resonators are because the total energy dissipated is proportional to the internal surface area of the resonator.

2.5 Frequency

In a TAR, it is essential to match the frequency of the acoustic waves produced by the speaker with the resonant frequency of the resonator tube. The resonator tube's resonant frequency depends on its length, the working fluid, and boundary conditions. Shivakumara and Bheemsha (2021) investigated the effects of the operating frequency on the achievable maximum temperature difference. They operated a TAR at 200 kPa with a 0.6% drive ratio with Helium as the working fluid. They found that for their TAR, the achievable temperature difference increased as the frequency increased to 400 Hz, but after that decreased as elaborated by Alamir (2019). The decreasing achievable temperature difference would be attributed to the reason that the thermal penetration depth decreased as the frequency increased beyond 400 Hz, thus increasing the viscous losses, and reducing the thermoacoustic effect. Chaiwongsa and Wongwises (2021) studied the impact of the operating frequency on the cooling temperature. They operated a TAR with a 0.71 blockage ratio at varying acoustic frequencies and produced a maximum cooling load of 2 W. They found that the cooling temperature increased as the frequency increased to 150 Hz and then decreased. Their findings suggest that maximum amplitude pressure and thermoacoustic effects can only occur at the resonance frequency, which varies depending on the geometric and operating parameters.

2.6 Average pressure

In a TAR, average pressure, proportional to power density, influences thermal penetration depth (Kajurek *et al.* 2019). The mechanical strength of the resonator limits the achievable average pressure. Alamir and Elamer (2020) found that high average pressure is associated with small thermal penetration depth and temperature difference across the stack. Nevertheless, for experimental purposes, the air at atmospheric pressure is preferred.

2.7 Optimisation of thermoacoustic refrigerator performance

The optimisation of TARs focuses on determining optimal operating and geometrical parameters (Figure 2-3). The operating parameters impact the performance of TAR, which must be well optimised and selected, such as the acoustic power (W_{ac}), frequency, average

pressure, drive ratio (D), blockage ratio (B), and working fluids. The geometrical parameters include stack geometry, stack material, plate spacing, resonator geometry, resonator length, and resonator material.

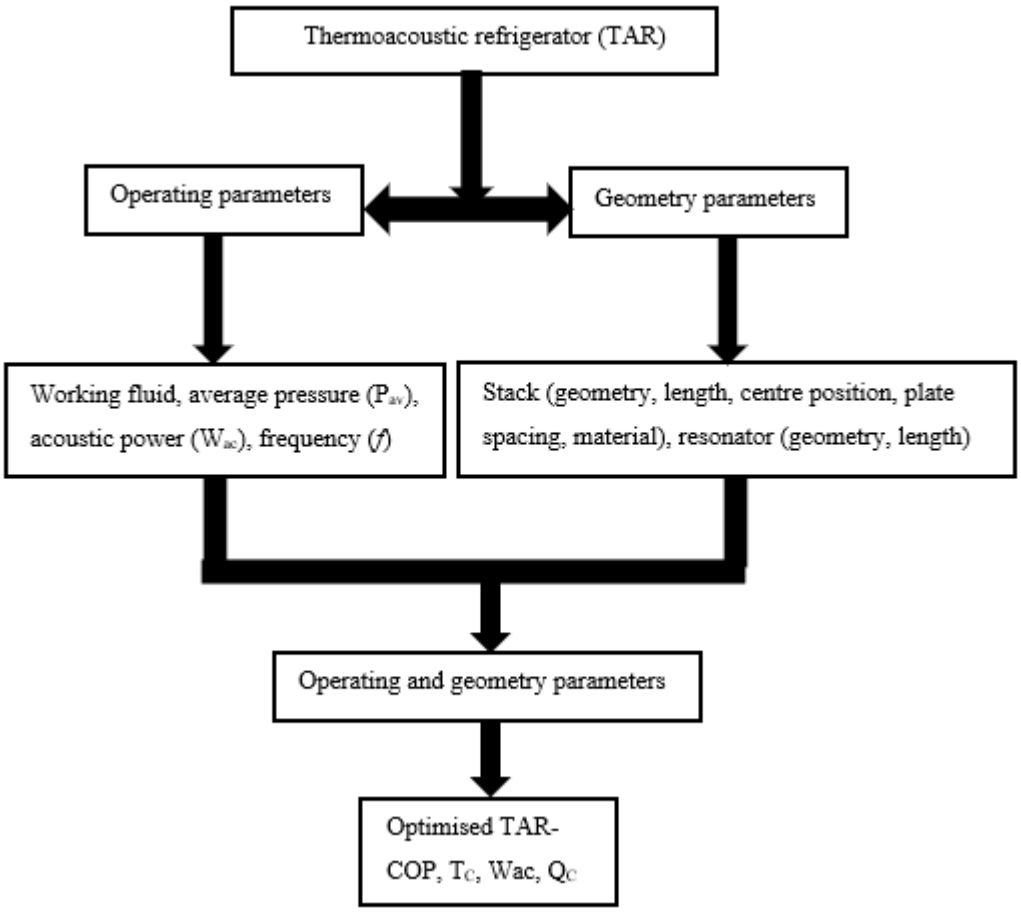

Figure 2-3: Optimisation scheme of thermoacoustic refrigeration.

Table 2-3 summarises literature on studies that optimised TAR using operating and geometrical parameters. The literature covers the period 2016 to 2024. It is evident from the literature that optimisation has substantially increased COP achievable by TAR. Two numerical studies, Ong et al. (2019) and Wang *et al.* (2021) have shown that TAR can achieve COPs greater than 3. Wang *et al.* (2021) numerically studied the characteristics of single and multi-stage travelling-wave TARs. They proposed a multi-stage travelling wave TAR, which

significantly improved the acoustic work utilisation rate from 0.26 to 0.8 and increased the maximum cooling load. Their model, which is yet to be experimentally validated, suggested that a multi-stage travelling wave TAR can achieve a COP of 3.19 and provide cooling up to 6.42 KW. Yuan Ong *et al.* (2019) numerically optimised five design parameters, normalised stack length, blockage ratio, normalised stack centre position and gas thermal penetration depth using the genetic algorithm (GA), with air as the working fluid. After optimisation, they selected a quarter-wavelength resonator of 56.3 cm long made of acrylic and a spiral stack of 2.76 cm long made of Polylactide (PLA), which was positioned at 3.7 cm. They simulated a system that operates at P_m of 1 Bar, 500 s, T_m of 300 K, 154 Hz, and acoustic sound pressure of 160.5 db. The TAR achieved a normalised cooling load (Q_{cn}) of 5.070×10^{-6} and a normalised acoustic power (W_{cn}) of -1.037×10^{-6}, from which they deduced a COP of 4.8904. These numerical results suggest that it is physically possible for TAR to achieve COPs that are comparable to vapour compression refrigeration systems.

However, experimental TARs have not achieved such high COP; most experimental systems have a COP of less than 1. Alamir (2019), Chaiwongsa and Wongwises (2021) and Shivakumara and Bheemsha (2021) compared the performance of TARs with three plate spacings of 0.28 mm, 0.33 mm, and 0.38 mm. They selected a parallel plate stack of 40.5 mm long, 69.03 mm in diameter made of Mylar sheet, an acoustic driver of 120 W, a quarter-wavelength resonator made of PVC, and hot and cold heat exchangers made of hollow coppers tubes whose diameters are 3.866 mm and 1.933 mm respectively. They operated a TAR at 1 MPa, 400 Hz, 1.6% drive ratio, 0.28 – 0.38 mm plate spacings with Helium as the working fluid. They achieved a minimum cooling temperature of - 2.1°C, a cooling load of 2 W and a maximum COP of 2.024, all with the 0.28 mm plate spacing.

Some researchers combined numerical and experimental optimisation of TAR. Nathad *et al.* (2019) optimised a TAR using normalised parameters to find an optimal stack length (7 cm) and stack centre position (16 cm). They constructed a TAR with a parallel plate stack made of Mylar sheet of 2 mm in thickness, a 39 cm long quarter-wavelength stainless steel resonator with an 18.2 cm diameter and an 800W maximum power loudspeaker and 5 W heat pump heat. The TAR achieved a COP of 2.175, an experimental temperature difference of 15.4°C, a cooling temperature of 31°C, and a hot side temperature of 34°C. Zolpakar *et al.* (2016) used

MOGA to numerically optimise three design parameters, the stack length (4 cm), stack centre position (4 cm) and blockage ratio of 0.72, with air as the working fluid. They operated the TAR at an average pressure of 101 kPa, 400 Hz, 500 sec, T_m of 300 K, and ΔT of 30 K. Their TAR produced a COP thermoacoustic core of 2.2 and an experimental cooling temperature of 19.2°C and the hot side temperature of 34.2°C.

Table 2-3: Optimisation work conducted on standing wave and travelling wave thermoacoustic refrigerators.

Authors	Optimization method	Optimization parameters	Outcome
(Shivakumara & Bheemsha, 2021)	Numerical (DeltaeC software) and experiment	Drive ratio; stack plate spacing	COP = 2.024, Tc = -2.1°C, ΔT = 32.9°C
(Chaiwongsa & Wongwises, 2021)	Experiment	Blockage ratios	COP = 0.93, Tc = 22.4°C, ΔT of 30.5°C
(Alamir & Elamer, 2020)	DeltaeC software	Stack length and position, plate spacing, mean pressure and amplitude pressure	COP = 1.24, ΔT = 29.5°C, Q_c = 5 W
(Ong *et al.*, 2019)	Multi-objective genetic algorithm (MOGA)	Normalised stack length and centre position; blockage and drive ratios; normalised gas thermal penetration depth	COP = 4.8904, ΔT = 15.4°C, T_c = 19.3°C
(Alamir, 2019)	Experiment	Stack position, length, and size	COP = 0.377, ΔT of 26.6°C
(Rahpeima & Ebrahimi, 2019)	Numerical (COMSOL Multiphysics)	Stack length, thickness and plate spacing; heat capacity; thermal conductivity	COP = 0.1 (Kapton), COP = 0.11 (glass), COP = 0.21 (steel)

Authors	Optimization method	Optimization parameters	Outcome
(Rahman & Zhang, 2019)	Fruit fly optimisation algorithm (FOA)	Stack length and centre position; blockage ratio; drive ratio	COP = 1.83, Q_c = 1.041 W, W_{ac} = 0.568 W
(Rahman & Zhang, 2019)	Particle swarm optimisation (PSO)	Stack length and centre position; blockage ratio; drive ratio	COP = 1.96, Q_{cn} = 1.32 W, W_{ac} = 0.673 W
(Peng *et al.*, 2018)	Multi-objective genetic algorithm (MOGA)	Stack length, centre position and porosity; plate spacing; acoustic frequency	COP of 1.656
(Tartibu, 2018)	General algebraic modelling system (GAMS)	Stack length and centre position	COP of 0.1601
(Zolpakar & Mohd-Ghazali, 2016)	Genetic algorithm (GA)	Stack length and centre position; blockage ratio; drive ratio	COP = 1.58, W_{ac} of 4.33 W, Q_c of 6.84 W, COP of 1.64, Q_c of 1.93 W, W_{ac} of 1.18 W
(Zolpakar *et al.*, 2016)	Multi-objective genetic algorithm (MOGA) & experiment	Stack length and centre position; and plate spacing	COP = 2.2, ΔT = 15°C

Summary

The study reported in this literature uncovered several strategies that would enhance standing wave TAR performance:

- The pin array stack, with smaller spacing between the holes, is the most effective.
- The stack should be made from low thermal conductivity materials such as Mylar sheet, PLA and RVC, with PLA showing the most promising in previous studies. This finding opens opportunities to make intricate stack geometry as they would be manufactured through 3D printing.
- The stacks should be short and positioned nearer the closed end of the resonator. Fourth, the study found that working fluids with low Prandtl numbers, such as the Helium-Xenon mixture, give better results in terms of coefficient of performance.
- For resonators, short resonators made from low thermal conductivity materials, such as PVC and acrylic plastic, are preferred.
- When designing a standing wave TAR, it is necessary to match the acoustic frequency of the driver with the resonator's natural frequency because a TAR performs better at its resonator's natural frequency.
- The study found that although most previous studies operated the TAR at atmospheric pressure, higher pressures might perform better.

These optimal parameters sometimes operate in a contrary manner, therefore is necessary to optimize TAR's geometric and operating parameters. Numerical studies have shown that when properly optimized, TARs can achieve coefficients of performance comparable to vapor compression systems. However, the numerical results are yet to be compared by experiment.

CHAPTER THREE: RESEARCH METHODOLOGY

3.1 Introduction

This chapter describes the research methods used to conduct the experiments and numerical modelling of the TAR. The operating and geometrical parameters used to design the current TAR were gathered from the literature review of this study.

3.2 Methodological approach

The research study combined the experimental work and numerical modelling of the standing wave TAR.

The study conducted thirty experiments between 3 January 2024 and 5 March 2024. The experiments were conducted for three stack positions of 30 mm, 40 mm, and 50 mm. At each stack position, five stack lengths, 25 mm, 35 mm, 45 mm, 55 mm, and 65 mm, were tested.

Similarly, thirty simulations were done using commercial multiphysics software. The simulations were done on a Windows 10 computer equipped with an Intel (R) core (TM) i5-6500 CPU @ 3.20GHz and 64GB DDR4 RAM.

3.3 Experimental methods

The experimentation took place during the summer season. The temperature of the air conditioning in the laboratory was set to 22°C. Each experiment began when the data logger displayed a temperature of approximately 21.9°C, 22.0°C and so on prior to connecting any temperature sensor to the 20 mm protruded copper tube on the larger resonator.

Figure 3-1 presents the prototype standing wave TAR that was used in the experiments.

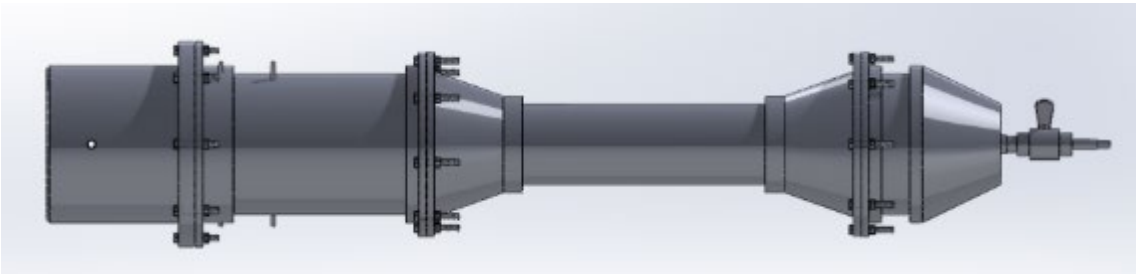

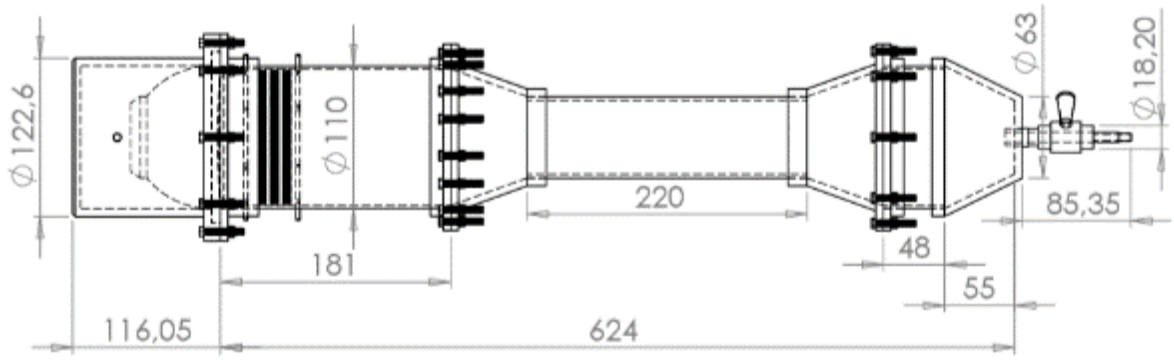

Figure 3-1: Standing wave thermoacoustic refrigerator.

3.3.1 Components of the thermoacoustic refrigerator and ancillary apparatus

The TAR comprised four key components: a 5-inch SATORI MW13P-8 speaker, 3D printed parallel plates stack, heat exchangers (hot and cold) and resonator tube.

3.3.1.1 SATORI MW13P-8: 5 Inch speaker

Figure 3-2 presents the 5-inch SB acoustic speaker with a bandwidth frequency range of 20 to 20 KHz. Table 3-1 shows the design specifications of the SATORI MW13P-8.

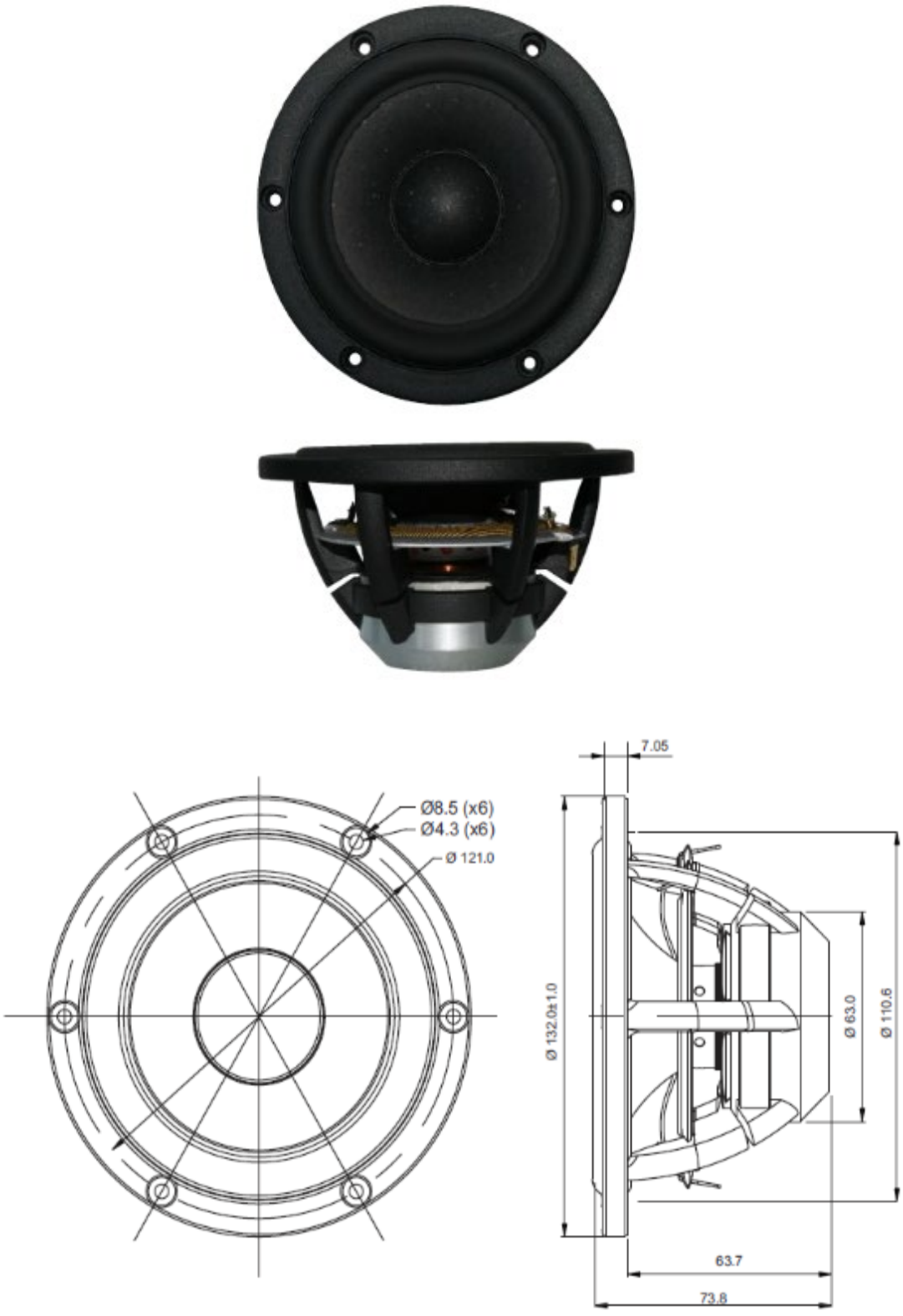

Figure 3-2: SATORI MW13P 8: 5 Inch speaker.

Table 3-1: Design specifications of SATORI MW13P-8: 5 Inch speaker.

Parameters	value	Parameters	value
Nominal Impedance	8 Ω	Free air resonance, Fs	41 Hz
DC resistance, Re	6.0 Ω	Sensitivity (2.83 V / 1 m)	87 dB
Voice coil inductance, Le	$0.15\ mH$	Mechanical Q-factor, Qms	3.55
Effective piston area, Sd	$70\ cm^2$	Electrical Q-factor, Qes	0.33
Voice coil diameter	$30.5\ mm$	Total Q-factor, Qts	0.30
Voice coil height	$15\ mm$	Moving mass incl. air, Mms	6.8 g
Air gap height	$5\ mm$	Force factor, Bl	5.7 Tm
Linear coil travel (p-p)	$10\ mm$	Equivalent value, Vas	15.0 litres
Magnetic flux density	$1.08\ T$	Compliance, Cms	2.16 mm/N
Magnetic weight (NEO)	$0.1\ kg$	Mechanical loss, Rms	0.5 kg/s
Net weight	0.78 kg	Rated power handling	40 W

3.3.1.2 Speaker box.

Figure 3-3 shows a cylindrical box manufactured from polyvinyl chloride (PVC) material closed on one side and opened on the other. It was utilised to sandwich the 5-inch SATORI MW13P-8 speaker. A copper tube of 6.35 mm inserted through the diameter of the cylindrical box underneath of the speaker as heat exchanger to dissipate heat produced.

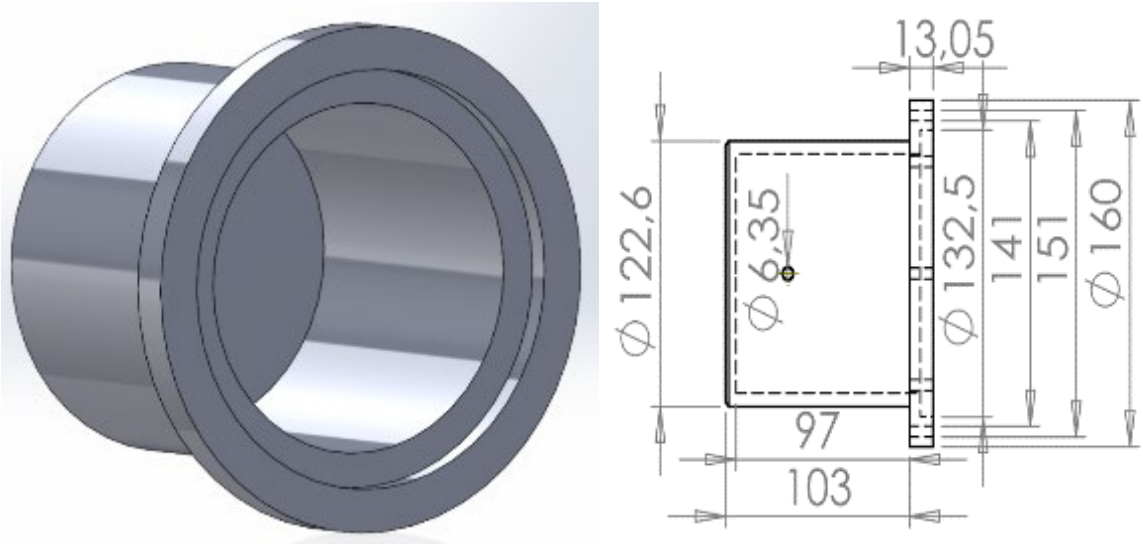

Figure 3-3: Speaker box.

3.3.1.3 The stacks

Figure 3-4 shows the 3D printed parallel plates stack utilised in the standing wave thermoacoustic refrigerator prototype. Its external core diameter was of 104.6 mm and its internal diameter of 102.6 mm, a gap spacing between two plates of $2\gamma_0$ = 0.6 mm and plate thickness (th) of 0.5 mm.

Figure 3-4: 3D printed parallel plates stack.

Figure 3-5 shows five 3D printed parallel plates stack lengths of 25 mm, 35 mm, 45 mm, 55 mm, and 65 mm. Each stack length was individually utilised in TAR to investigate the TAR performance.

Figure 3-5: Five stacks of length ranging from 25-65 mm.

The stacks were made of polylactic acid (PLA). PLA has a lower thermal conductivity (K) of 0.13 W/m. K and a specific heat capacity (Cp) of 1800 J/Kg. K. Table 3-2 presents the material properties of PLA.

Table 3-2: Properties of Polylactic acid (PLA)

Polylactic acid (PLA)		
Thermal conductivity (K)	0.13	[W/ m. K]
Density (ρ)	1300	[Kg/m^3]
Specific heat capacity (Cp)	1800	[J/Kg. K]

Figure 3-6 shows five parallel plates stack positioned at X_h inside of the lager tube. Three stack position of 30 mm, 40 mm, and 50 mm were adopted from the literature of this study. These

positions were relevant to better investigate the performance of the standing wave thermoacoustic refrigerator prototype.

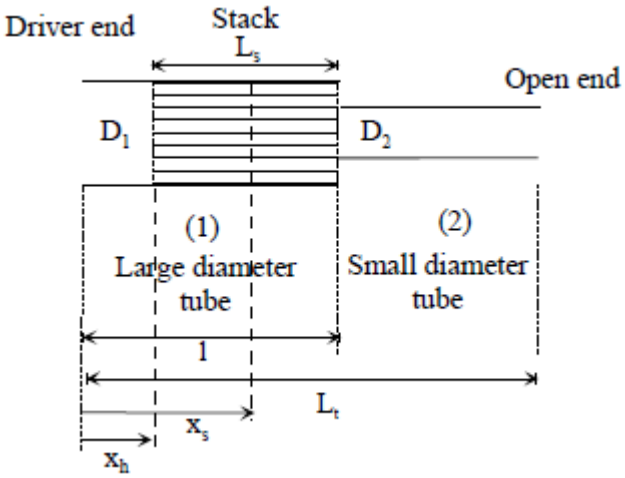

Figure 3-6: Five stacks each positioned at 50 mm.

3.3.1.4 Heat exchangers (hot and cold)

Figures 3-7 and 3-8 show two copper tubes of 3.175 mm and 6.35 mm, respectively. The 3.175 mm copper tube was used as hot and cold heat exchangers on both sides of the stack in the

larger tube while the other 6.35 mm copper tube was used as heat exchanger in the cylindrical box to dissipate heat produced by the speaker.

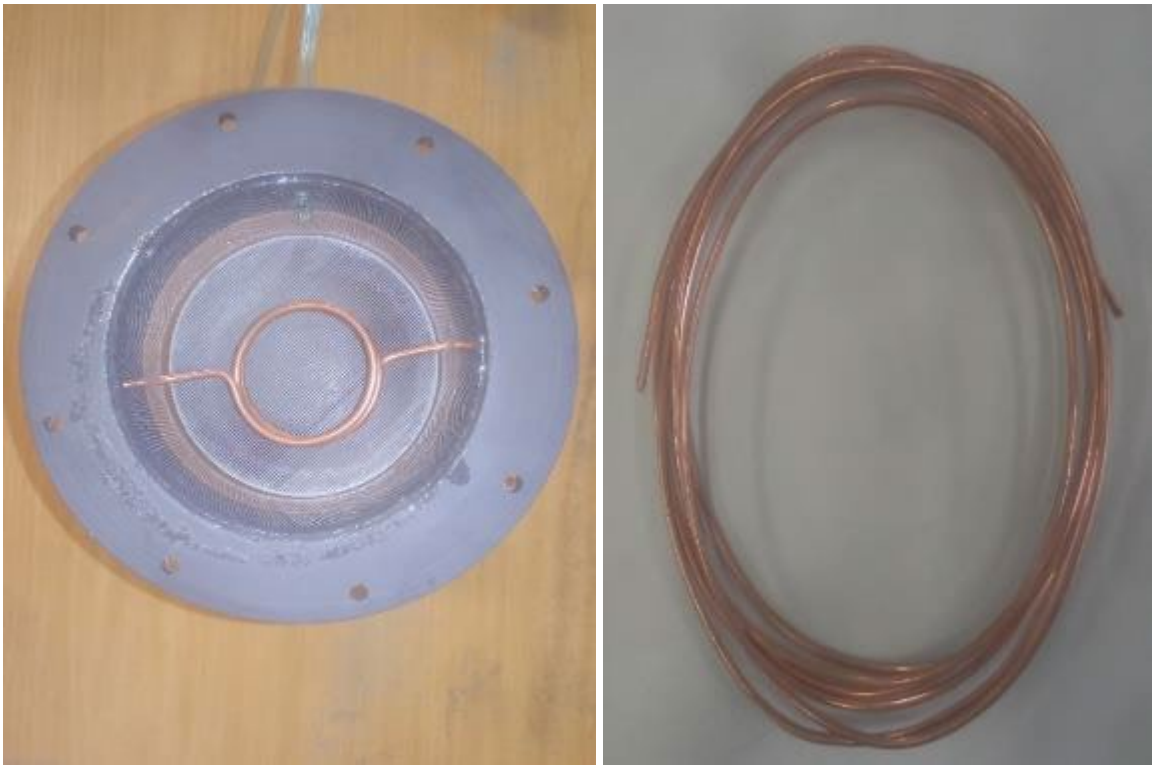

Figure 3-7: Copper tube of 1/8 inch.

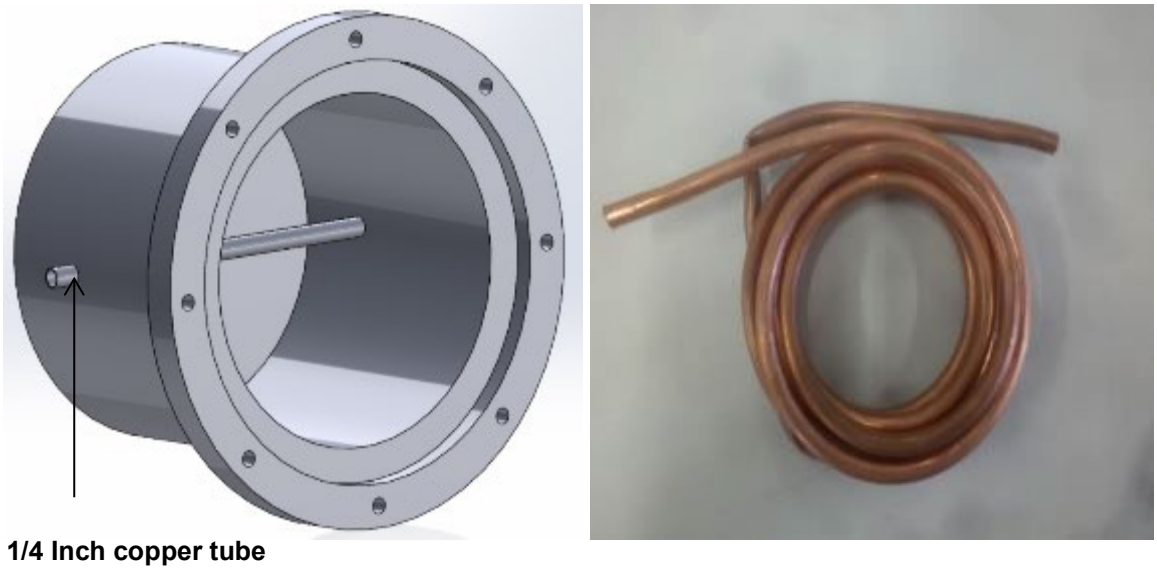

Figure 3-8: Copper tube of 1/4 inch.

3.3.1.5 Larger resonator tube

Figure 3-9 shows a larger polyvinyl chloride (PVC) resonator tube of 181 mm long that has an external diameter (OD) of 110 mm, and an internal diameter (ID) of 105.6 mm. On each end of the larger resonator tube, one flange of the same material as the larger tube was bonded and glued using C2 magma bond. Table 3-3 presents the material properties of the PVC.

Table 3-3: Properties of polyvinyl chloride (PVC)

Thermal conductivity [W/m. K]	Density (ρ) [kg/m^3]	Heat capacity per unit mass [J/Kg K]
0.19	1330	880

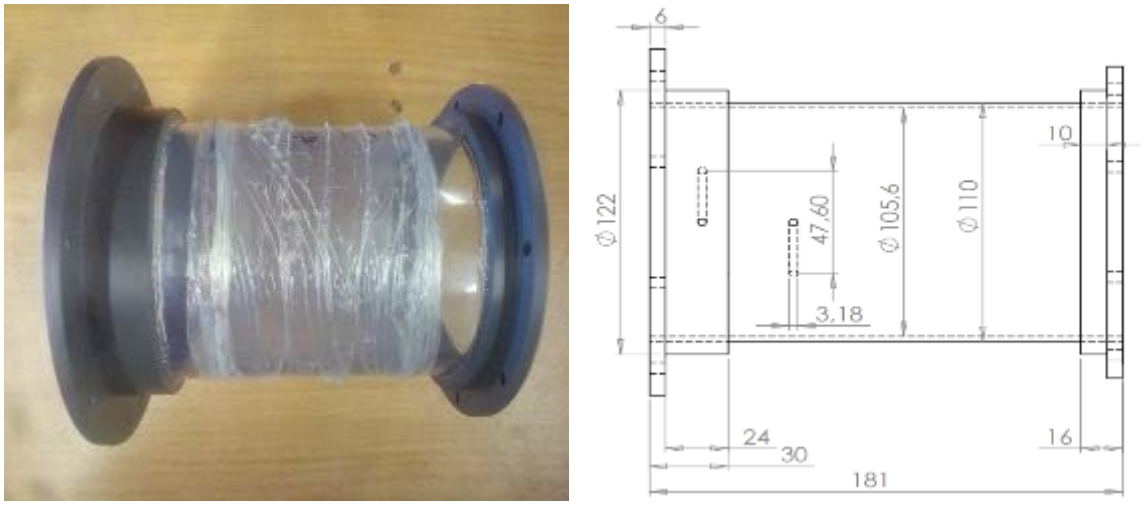

Figure 3-9: Larger resonator tube of 110 mm of external diameter.

3.3.1.6 Smaller resonator tube

Figure 3-10 shows a smaller polyvinyl chloride (PVC) resonator tube of 220 mm long having an external diameter of 63 mm and an internal diameter of 57 mm. The entire resonator tube was a quarter wavelength (λ/4) having the larger diameter reduced to D_2/D_1= 0.54. On each end of the smaller tube, one cone of the same material as the smaller tube was bonded and glued using C2 magma bond.

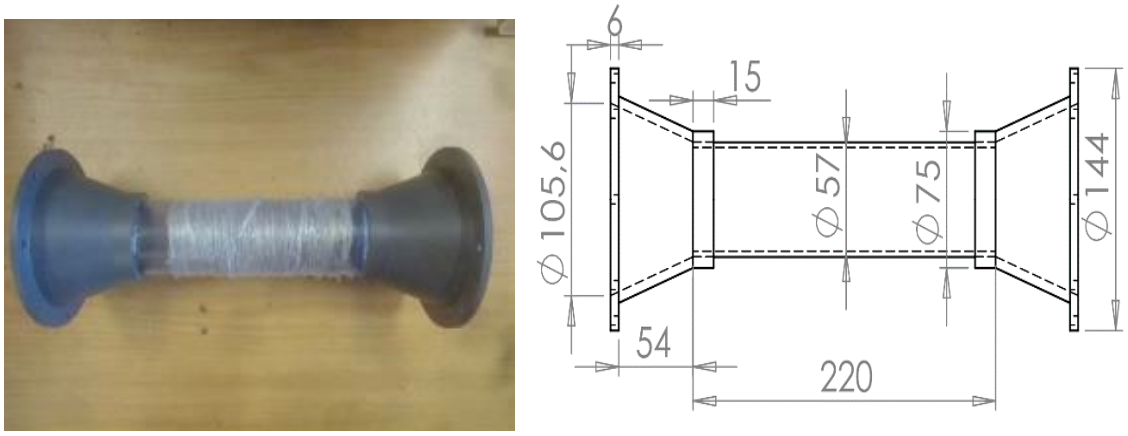

Figure 3-10: Smaller resonator tube.

3.3.1.7 Buffer volume

Figure 3-11 shows the buffer volume manufactured from polyvinyl chloride (PVC) of 103 mm long. A cone of 55 mm long, tube of 48 mm long, and a flange of 16 mm long were bonded and glued using C2 magma bond to make the buffer volume.

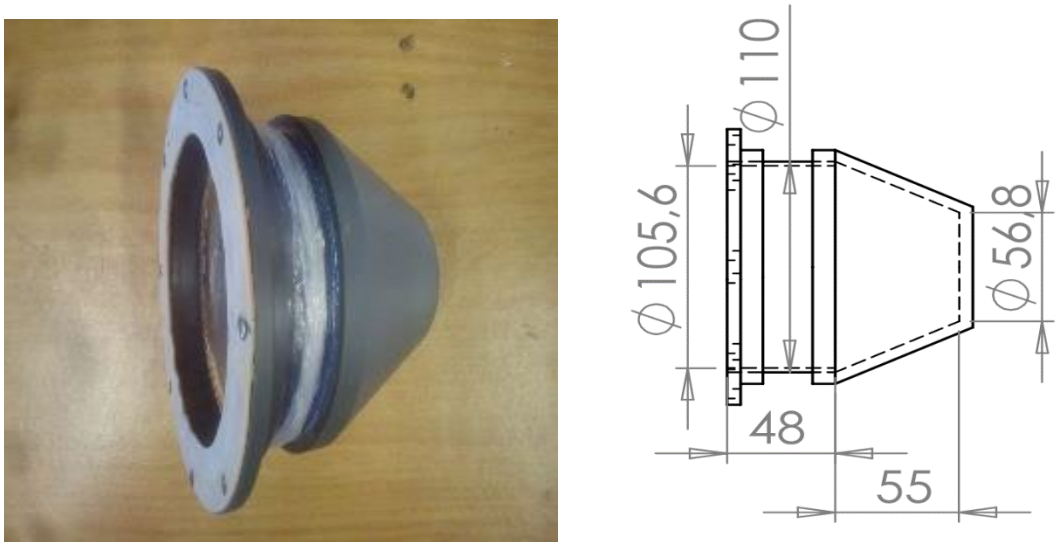

Figure 3-11: Buffer volume and flange.

3.3.1.8 Tightening of components

Each flange had eight drilled holes of 5.5 mm in diameter to enable the assembly of all components. A total of 24 M5 bolts 30 mm long, nuts and washers were utilized to fasten the

whole standing wave thermoacoustic refrigerator. The inner bike tube was used as gasket in between flanges.

3.3.2 Apparatus

The following apparatus have been utilised during experiments for data collection. The purpose of each instrument is elaborated below.

3.3.2.1 Function generator: GFG-8216A

Figure 3-12 shows the function generator of type GFG-8216A utilised to input the operating frequency (f). The purpose of the function generator was to generate a sinewave signal that enabled to drive the speaker by letting the diaphragm vibrate back and forth.

Figure 3-12: Function generator GFG-8216A.

3.3.2.2 Oscilloscope: Tektronix TBS1052B-EDU

Figure 3-13 shows the digital oscilloscope of type Tektronix TBS1052B-EDU coupled to a function generator to display the output signals such as voltage, current, frequency, and amplitude etc.

Figure 3-13: Digital Oscilloscope: Tektronix TBS1052B-EDU.

3.3.2.3 Dixon sound amplifier

Figure 3-14 shows the Dixon sound amplifier of type AV-260 utilised to amplifier the sinewave signal generated by the function generator. The coaxial cable (50 Ω) was plugged into the output of the function generator and connected to the input of the sound amplifier then its output connected to the 5-inch SATORI MW13P-8 speaker. The knob was used to adjust the voltage and current to not exceed the rated handling power of the speaker. The amplifier had these technical specifications: AC110-240 V 50/60 Hz input power, 100 W rated power, S/N ratio: >75 dB, THD: 0.1% (1W), frequency response: 20 Hz-20 KHz, input sensitivity: 300 MV, and output impedance: 4-8 Ω.

Figure 3-14: Dixon sound amplifier : AV-260.

3.3.2.4 AC voltage and current datalogger: MT250

Figure 3-15 shows an AC voltage / current datalogger of type MT250. This datalogger was utilised to measure and record simultaneously both the sinewave voltage and current through a software installed to a PC. The voltage sensor was clipped to both wires powering the speaker while one wire was fed through the current sensor. Each channel of datalogger had a storage capacity of 50022 data. The AC current range from 2 to 200 A with a ± 2% ±1 A accuracy while the AC voltage range from 6 to 600 V with a ± 2% ± 1 V accuracy. The sampling interval ranges from 2 to 24 hours and current and voltage frequencies range from 40 Hz to 1 KHz.

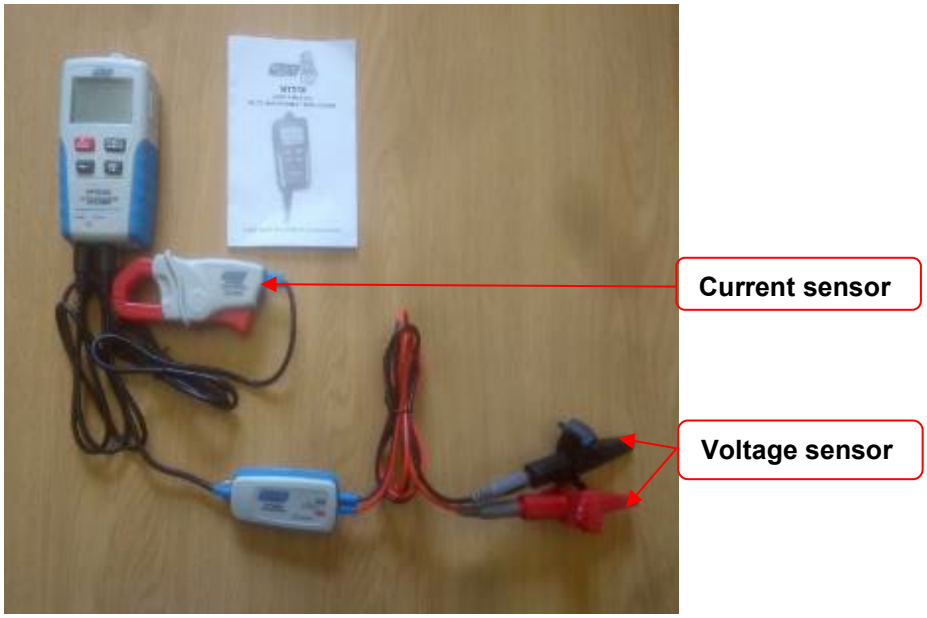

Figure 3-15: AC Voltage / current datalogger : MT250.

3.3.2.5 Four input datalogger thermometer: RS-1384

Figure 3-16 presents the thermometer of type RS-1384 with four input channels for T_1, T_2, T_3, and T_4. The RS PRO 1384 may support K, J, E, T, R, S, N, L, U, B and C type thermocouple as temperature sensor. It has an operating temperature range of 0˚C to +50˚C. Hence two thermometer dataloggers had to be utilised to connect six K-type thermocouples and logged temperature through a RS-232 interface software installed on a computer.

Figure 3-16: 4 Input Data Logging Thermometer: RS-1384.

3.3.2.6 K-type thermocouple

Figure 3-17 presents the K-type thermocouple made from Nickel Aluminium and Nickel Chrome with legs arranged in junction. The twin twisted leads insulated with durable Teflon PFA and capable of measuring a maximum temperature of +250°C. A maximum of six thermocouples were utilised, two inserted into the resonator tube on either side of the stack while four connected to the coiled copper heat exchangers (cold and hot) outside of the resonator tube. A Kapton tape was utilised to insulate the thermocouples.

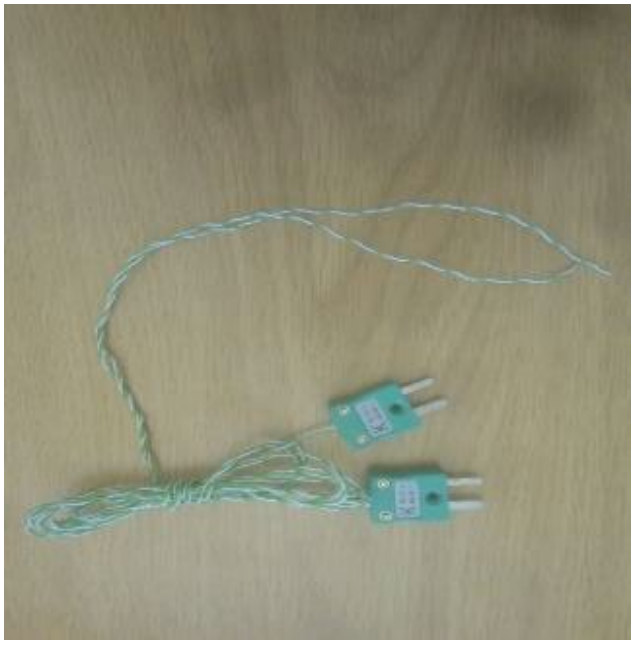

Figure 3-17: K- type thermocouple.

3.3.2.7 Lutron Manometer: PM-9110SD

Figure 3-18 shows the Lutron manometer datalogger of type PM-9110SD utilised to log pressurized helium into the resonator tube. The datalogger recorded data along with time and date on an SD card inserted into the slot. It had two pressure points P1 and P2 if both utilised the pressure difference (ΔP) was determined. A plastic tube of 5 mm in diameter was inserted and glued to the buffer volume end of the resonator then connected directly to one point pressure (P1). The device could read up to ± 200 Kpa, however the range of maximum pressure recorded was from 110 Kpa to 111 Kpa.

Figure 3-18: Lutron Manometer datalogger: PM-9110SD.

3.3.2.8 Industrial gas regulator

Figure 3-19 shows an industrial helium gas regulator bolted to the 20-litre gas cylinder. It was used to regulate the maximum outflow of helium from the gas cylinder into the resonator tube through an LPG hose 8 mm SGH 701 SANS 1156 04/21. It had a maximum flow rate of 25 litre per minute and a maximum regulating capacity of 3500 in PSI and 250 in Kgf/cm^2.

Figure 3-19: Industrial helium Gas regulator.

3.3.2.9 Coolants utilised within the standing wave TAR prototype

Figure 3-20 shows a cylinder that has a capacity of 20 litre pressurised with helium at 3000 PSI. Table 3-4 presents the thermophysical properties of water and helium. Water was fed through the coiled copper heat exchangers (hot and cold) while helium was pressurised within the prototype standing wave thermoacoustic refrigerator.

Table 3-4: Thermophysical properties of coolants

Water (H_2O)		
Temperature (°C)	**Density (Kg/m^3)**	**Specific heat (KJ/Kg. K)**
0	1000	4.22
25	997	4.18
50	988	4.18

Helium (H_e)		
Thermal conductivity (K)	0.15243	[W/ m. K]
Density (ρ)	0.1605	[Kg/m^3]
Specific heat (Cp)	5192.6	[J/Kg. K]
Speed of sound (a)	1019.1	[Pas]
Prandtl number (σ)	0.6793	-
Specific gas constant (R)	2076.9	[J/kg. K]
Specific ratio of the gas (γ)	1.667	-

Figure 3-20: A cylinder of 20 litres pressurised with helium at 3000 PSI.

3.3.2.10 Incorporated heat exchangers within the larger tube

Figure 3-21 shows the 3.175 mm copper tube coiled twice and half to an inner diameter of 48 mm and extended 45 mm long each side. The coiled copper tube was inserted into the larger

tube and positioned 10 mm away on each side of the stack length. A protrusion of 20 mm of the 45 mm extended length was reserved to connect the temperature sensors and admin set.

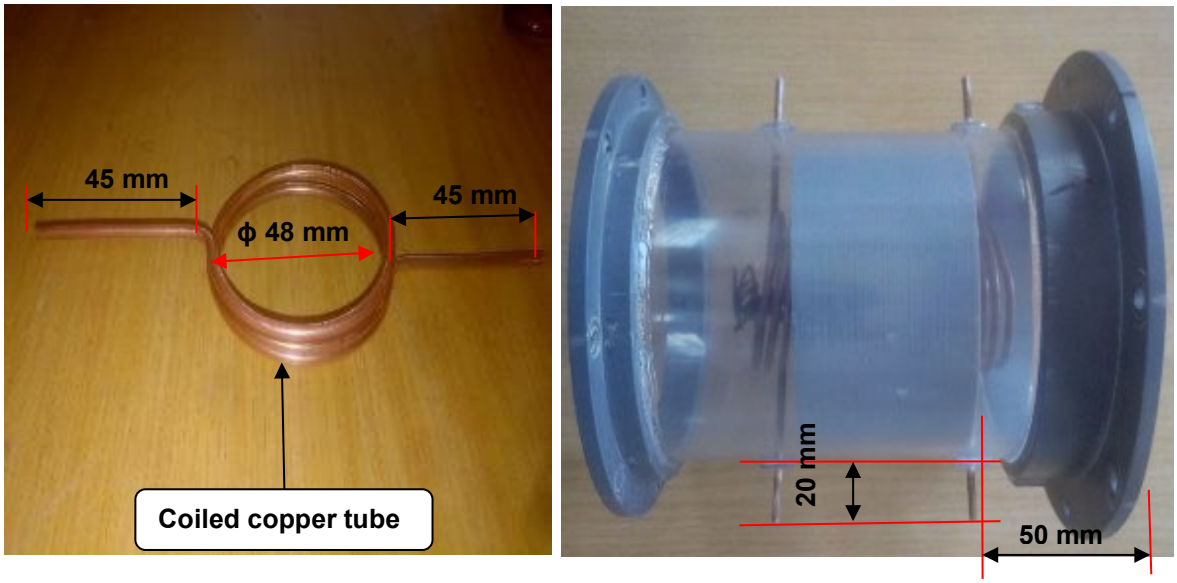

Figure 3-21: Coiled copper heat exchangers (hot and cold).

3.3.2.11 Measurement of temperatures within TAR

Figure 3-22 shows the arrangement of six K-type thermocouples connected to various points of the standing wave TAR prototype. Two thermocouples inserted inside of the resonator tube to measure T_5 and T_6 on each side of the stack length. The T_5 was the temperature on the cooler side while T_6 was the temperature on the warmer side of the stack. Two thermocouples connected to the hot heat exchanger on the warmer side of the stack to measure T_4 and T_2. The T_4 was the inlet temperature of water while T_2 was the outlet temperature of water exiting the coiled copper. Two thermocouples connected to the cold heat exchanger on the cooler side of the stack to measure T_3 and T_1. The T_3 was the inlet temperature of water while T_1 was the outlet temperature of water exiting the coiled copper.

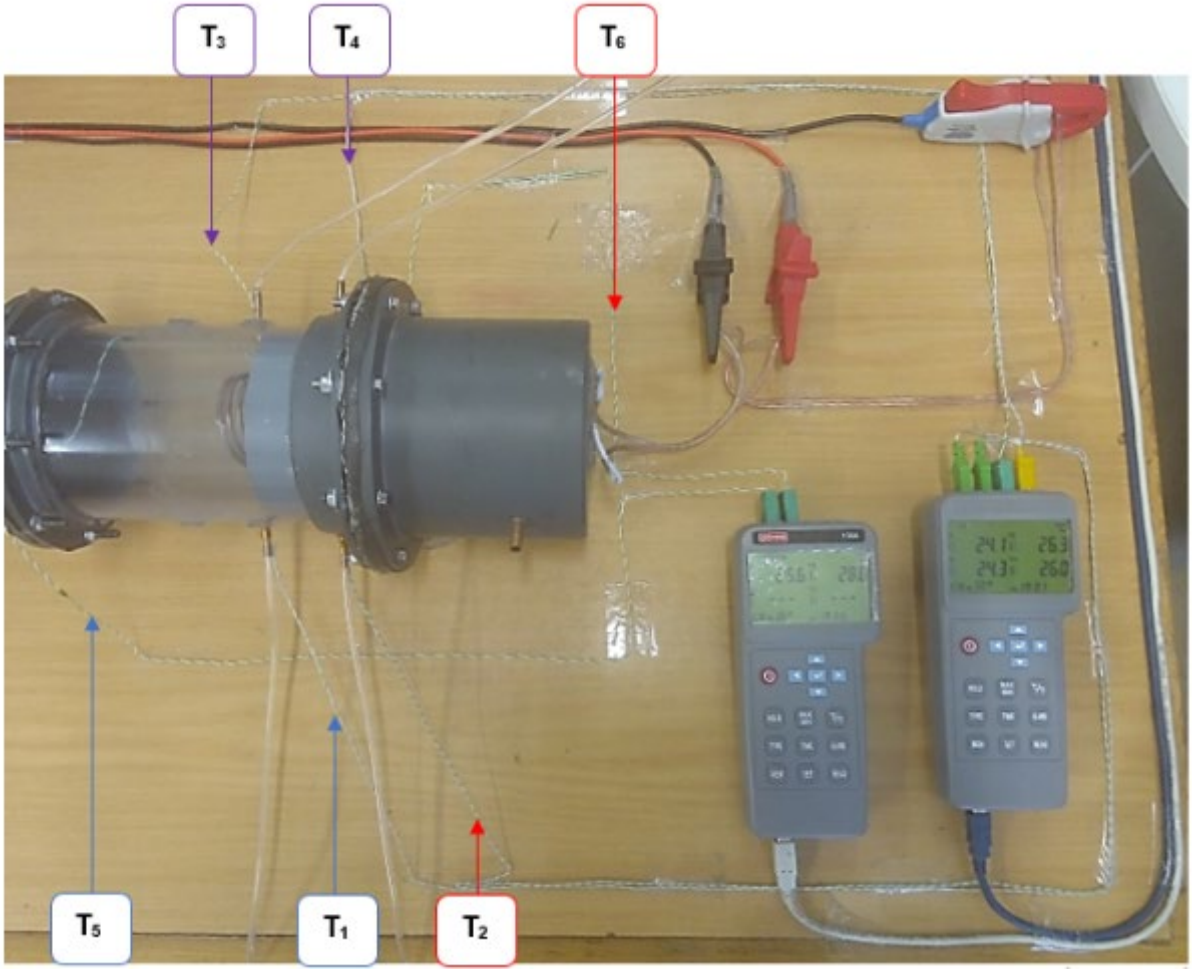

Figure 3-22: Temperature sensors (T_1, T_2, T_3, T_4, T_5 and T_6).

3.3.3 Experimental procedures

Figure 3-23 displayed various instruments illustrated above connected in place. The temperature difference (ΔT) across the stack length, coefficient of performance (COP), cooling load (Q_C), heating load (Q_H), and overall coefficient of performance ($COP_{overall}$) are parameters required in this research study. The following procedure were followed to gather the data:

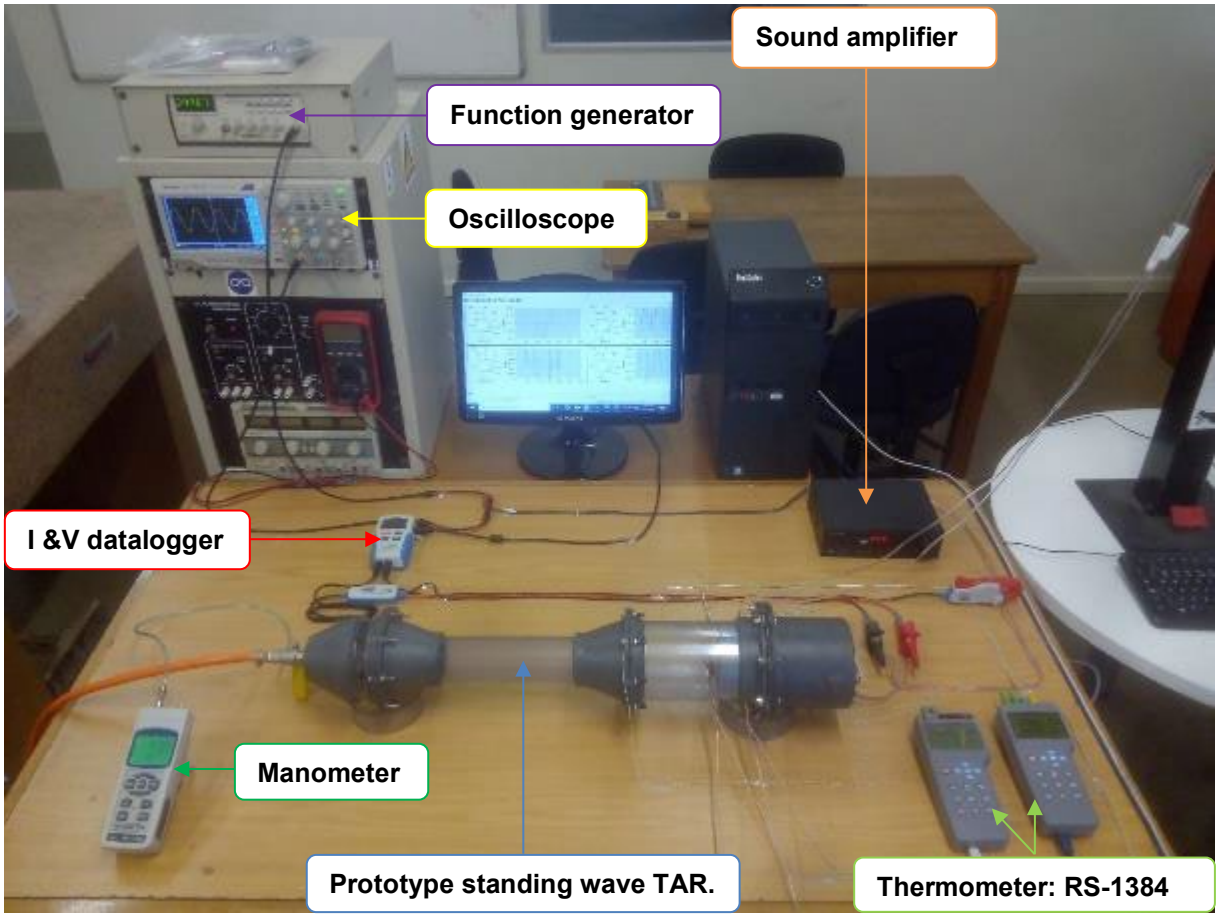

Figure 3-23: Standing wave thermoacoustic refrigerator prototype.

- A frequency of 400 Hz derived from the equation provided in Table 3-8 was set at the function generator,
- The oscilloscope calibrated prior connecting any auxiliary coaxial cable,
- One coaxial cable connected to the function generator output and another coaxial cable connected to the oscilloscope input and both coaxial cables coupled with a third cable which connected to the sound amplifier input to receive the sinewave signal,
- A two-lead cable connected to the sound amplifier output which powered the 5 Inch acoustic speaker sandwiched inside of the speaker box,
- An AC current and voltage datalogger utilised to record the sinewave current (I) and voltage (V), so it was connected to the Desktop PC via a USD cable,
- Two thermometers datalogger utilised to record six different temperatures: T5 and T6 inside of TAR while T1, T2, T3, and T4 at the coiled heat exchangers (cold and hot), so they have been connected to the Desktop PC via a USD cable,

- One manometer datalogger connected to the buffer volume of TAR via a 5 mm diameter plastic tube to record the varying pressure,
- Helium pressurized just once into the TAR at 110 Kpa at the beginning of each experiment,
- A top water reservoir regulated by two admin set which fed water through the coiled copper heat exchangers (cold and hot),
- The produced cold (T5) and warm (T6) temperature at both side of the stack were used to calculate the ΔT across the stack length,
- The produced ΔT at the cold side of the stack was the difference of temperature between the inlet (T3) and outlet (T1) of water fed through the cold copper heat exchanger,
- The produced ΔT at the warm side of the stack was the difference of temperature between the inlet (T4) and outlet (T2) of water fed through the hot copper heat exchanger,
- The cooling load (Q_C) at the cold side of the stack calculated because of fluid mass flow rate (m_C), specific heat capacity (Cp) of water, and temperature difference of water between the inlet and outlet on the cold side of the stack,
- The heating load (Q_H) at the warm side of the stack calculated because of fluid mass flow rate (m_H), specific heat capacity (Cp) of water, and temperature difference of water between the inlet and outlet on the warm side of the stack,
- The COP was the ratio of the cooling load (Q_C) to the difference of both heating load (Q_H) and cooling load,
- The mean pressure (P_m) and amplitude pressure (PA) were the maximum and minimum helium pressure at the end of each experiment,
- The voltage (V) and current (I) regarded were those recorded last at the end of every experiment and used to calculate the electrical input power (Win),
- The $COP_{overall}$ was the ratio of the cooling load (Q_C) to the electrical input power (Win).

3.3.4 Condition of laboratory

The laboratory in which the fifteen experiments were conducted was completely closed from direct entry of ambient air but had a double door, a normal door and two windows all in glass covered by blinds. The room temperature was controlled by an inside mounted air-conditioning operated by a wall remote control as illustrated in Figure 3-24.

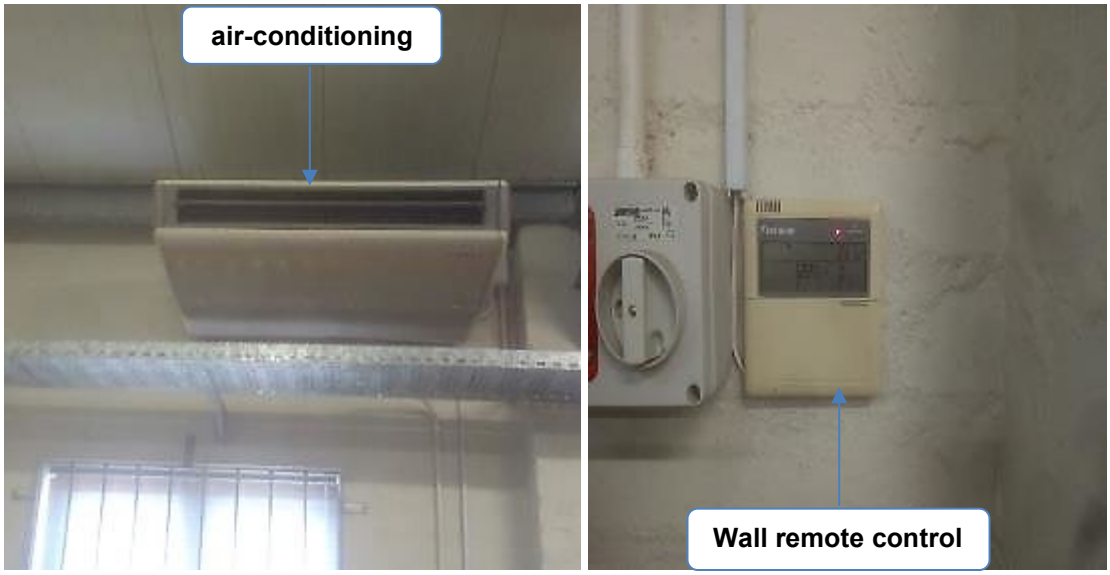

Figure 3-24: air-conditioning inside of laboratory.

3.3.5 Modules assemblage

Figure 3-25 shows the buffer volume, smaller tube, larger tube, 5 Inch acoustic speaker, speaker box and assembled prototype standing wave thermoacoustic refrigerator. Each module had to be fastened with another one by eight bolts using the inner bike tube as gasket sealant between two modules to prevent helium links. As the one opening side of the buffer volume fastened to one side of the smaller tube by eight M5x30 mm bolts. The larger tube was made available for assembly which had already a specific length of 3D printed parallel plates stack inserted between the cold and hot coiled copper heat exchangers. The other side of the smaller tube was fastened to one side of the larger tube by eight M5x30 mm bolts. A two leads wire connected to negative and positive of the 5 Inch acoustic speaker altogether sandwiched in the speaker box then as a whole fastened to the other side of the larger tube by eight M5x30 mm bolts.

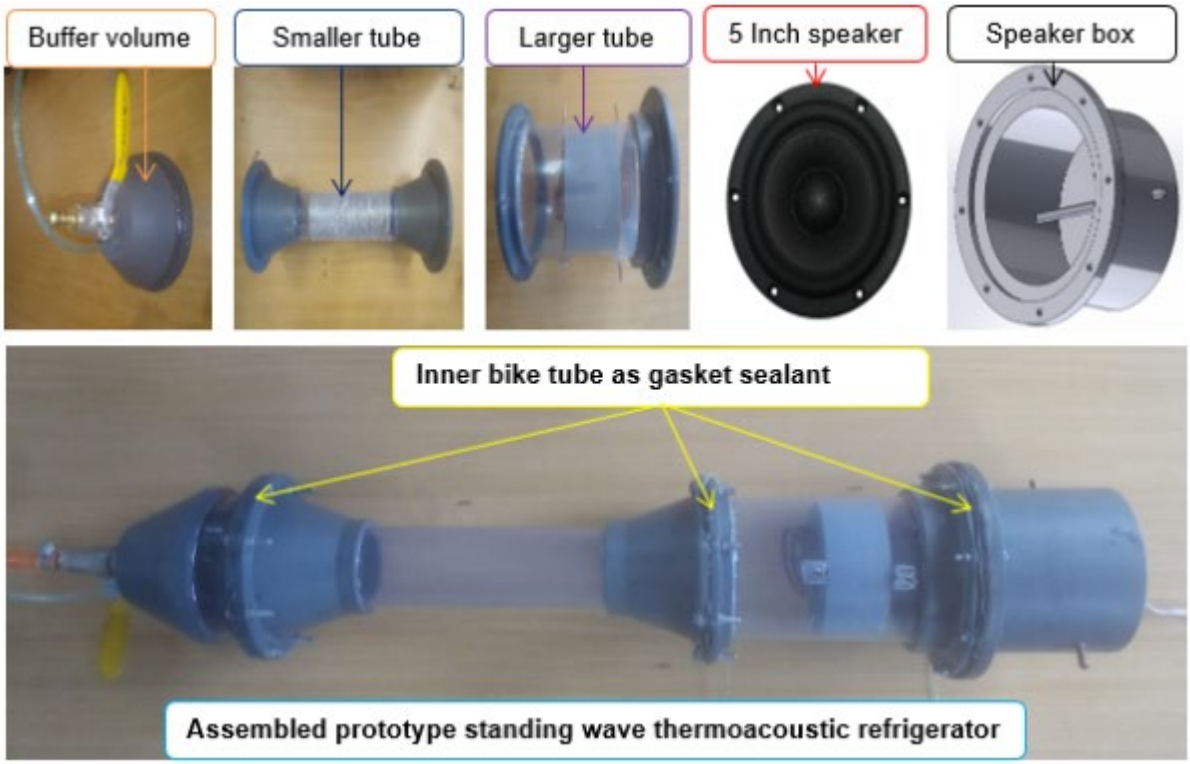

Figure 3-25: Modules of prototype standing wave TAR.

3.3.6 Experimental change over

Figure 3-26 shows one set of five larger tube manufactured from polylactic acid (PLA) made available for each experimental changer over. There was already in each larger tube one 3D printed parallel plates stack made from polyvinyl chloride (PVC) of length of 25 mm, 35 mm, 45 mm, 55 mm, and 65 mm which inserted between the cold and hot coiled copper heat exchangers. The provided set of five larger tube was prior arranged as per stack position of 30 mm, 40 mm, and 50 mm. However, an additional two set of five larger tube had to be arranged to make up fifteen experiments.

Figure 3-26: Five larger tube ready for experimental change over.

3.3.7 Annotations of apparatus of standing wave thermoacoustic refrigerator

Figure 3-27 shows a complete set up of prototype standing wave thermoacoustic refrigerator connected to various instruments. Each apparatus has been labelled with a specific number and a detailed description. Table 3-5 provides the labelling and description of each apparatus.

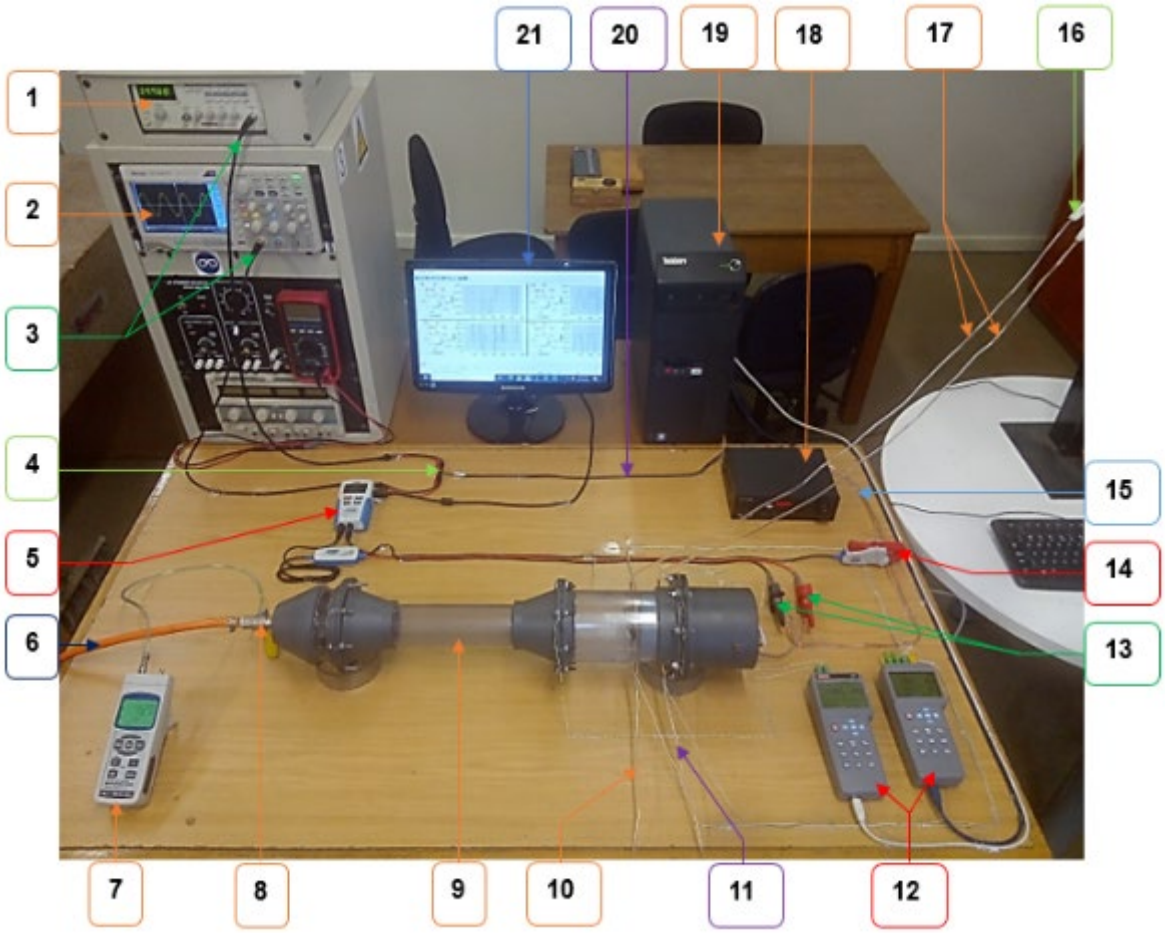

Figure 3-27: Experimental set up of standing wave thermoacoustic refrigerator prototype.

Table 3-5: Apparatus utilised during experiment.

Numbering	Description of apparatus
1	Function generator (1x1)
2	Oscilloscope Tektronix TBS1052B-EDU (1x1)
3	BNC double clam wire : 50 Ω Coaxial Cables (2x1)
4	Coupling of 2 coaxial cables (50 Ω)
5	AC voltage/current datalogger : MT250 (1x1)
6	LPG hose 8 mm SGH 701 SANS 1156 04/21 (1x1)
7	Lutron Manometer datalogger: PM-9110SD (1x1)
8	Gas ball valve (1x1)
9	Prototype standing wave thermoacoustic refrigerator (1x1)
10	Outlet cooled water from coiled copper (1x1)
11	Outlet warmer water (1x1)
12	Four input Data Logging Thermometer: RS-1384 (2x1)
13	Voltage sensor (2x1)
14	Current sensor (1x1)
15	Two ways Wire (1x1)
16	Admin set (2x1)
17	Ambient water to the cold and warmer side of heat exchangers (2x1)
18	Dixon sound amplifier AV-260
19	Computer box (1x1)
20	Two ways Wire (1x1)
21	Monitor (1x1)
22	Kapton tape

3.3.8 Insulator of thermocouple sensors

Figure 3-28 shows a 20 mm protruded copper tube of the cold and hot heat exchanger on either side of the stack length onto which two k-type thermocouple sensors were connected and insulated using a Kapton tape capable of withstanding a temperature between -269°C to 400°C.

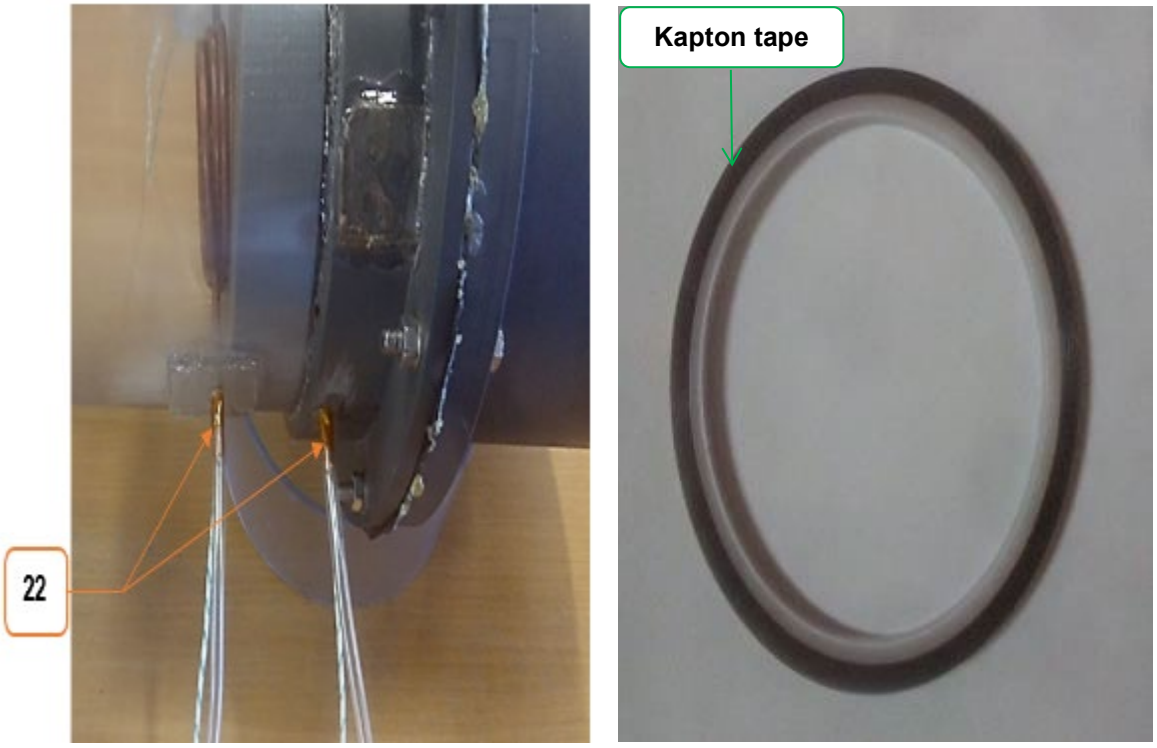

Figure 3-28: Kapton tape used as an insulator.

3.3.9 Set up of apparatus

- Prior to coupling the oscilloscope Tektronix TBS1052B-EDU denoted by (2) with the function generator (1). The device was calibrated by plugging its BNC double clam wire (50 Ω) coaxial cable (3) to channel 1 then connected the red crocodile clips to positive and black to the grind.
- A function generator represented by (1) was used to input the operating frequency (f). It was then coupled to an oscilloscope (2) through BNC double clam wire (50 Ω) coaxial cable (3). The two crocodile clips were joined based on the colour of the insulators: red to red, and black to black as illustrated at point (4). The two-lead cable denoted by (20) was

connected at point (4) and plugged into the input of Dixon sound amplifier AV-260 denoted by (18). The two-lead cable denoted by (15) were connected at the output of the sound amplifier to power the 5 Inch acoustic speaker.

- The AC voltage/current datalogger: MT250 denoted by (5) was used to measure and record the waveform of current and voltage that resembled to a sine curve. The datalogger had two channels, one for voltage sensor and the other for current sensor. The USB socket cable of the datalogger was at all times connected to the port of the PC denoted by (19) for sharing data with software. The voltage sensor denoted by (13) was inserted into the COM of datalogger thereafter clipped the two-lead cable represented by (15) to power the 5 Inch acoustic speaker while one wire fed through the current sensor represented by (14).
- The LPG hose 8 mm SGH 701 SANS 1156 04/21 denoted by (6) was 2 m long connected between the industrial helium gas regulator and the gas ball valve (8) attached to the buffer volume of the resonator tube (9).
- The Lutron manometer datalogger: PM-9110SD represented by (7) was used to monitor and record the pressurised helium into the prototype standing wave TAR denoted by (9). A plastic tube of 5 mm in diameter was inserted into the buffer volume end of the resonator tube and plugged directly to the Manometer (7).
- A plastic tube of 5 mm in diameter represented by (10) was plugged to the outlet of the 20 mm protruded copper tube heat exchanger (cold) on the cold side of the stack to lead the cold water into the container.
- A plastic tube of 5 mm in diameter denoted by (11) was plugged to the outlet of the 20 mm protruded copper tube heat exchanger (hot) on the warm side of the stack to lead the warm water into the container.
- Two thermometers datalogger:RS-1384 denoted by (12) were used to measure and record the temperature. Each datalogger had four input channels. Two K-type thermocouples were plugged into one to record the T_5 and T_6 and four other K-type thermocouples were plugged into the second datalogger to record the T_1, T_2, T_3, and T_4 connected to the four points of both heat exchangers (hot and cold).
- Two admin set denoted by (16) plugged into the top water reservoir positioned at 1,5 m above the experimental table utilised to regulate the ambient fluid flow rate ($\dot{m}_C$ and $\dot{m}_h$) denoted by (17) going through the coiled copper heat exchangers (hot and cold) and the same used water was recycled to the top reservoir.
- A Desktop computer denoted by (19) and (21) was utilised to install the software of the AC voltage/current datalogger and thermometer datalogger.

- Kapton tape denoted by (22) was used as an insulator for all K-type thermocouples connected to the four 20 mm protruded copper tube of the heat exchangers.

3.4 Analysis of results

The temperature difference (ΔT), coefficient of performance (COP), cooling load (Q_C), heating load (Q_h), and overall coefficient of performance ($COP_{overall}$) were calculated value from the gathered data as illustrated in Appendix A. The Taguchi design method in Minitab software was utilised to optimise the performance of TAR and analysed the experimental work and numerical modelling results of the stack length and stack position as by (Nur Ozdemir *et al.* 2023).

3.5 Numerical modelling of standing wave thermoacoustic refrigerator

The numerical modelling of the standing wave thermoacoustic refrigerator were conducted in the following manner:

3.5.1 Methods and materials

A brief description of the standing wave thermoacoustic refrigerator has been provided along with the governing equations that described each mathematical model applied to thermoacoustic phenomena. The method and materials adopted are discussed in the sub-sections. All conducted simulations were done with commercial multiphysics software which run between 6 hours to 15 hours.

3.5.2 Standing wave thermoacoustic refrigerator

A standing wave thermoacoustic refrigerator has been presented in Figure 1-1 which comprised of a loudspeaker driver, resonator tube sandwiching a hot and cold heat exchangers positioned on either side of the stack. The rises and drops of temperature are caused by compression and expansion of gas molecules oscillating back and forth within the length of the resonator tube because of the diaphragm vibrating.

3.5.3 Thermoacoustic governing equations

The oscillatory boundaries utilised in thermoacoustic as low amplitudes have been expounded and summarised by Swift (1988). The pressure (P), velocity (u) and temperature (T) applied

at the inlet of computational domain were expressed in terms of mean component and first order component, which illustrated below:

$$\boldsymbol{P = P_m + R_e\left\{P_1[z]e^{i\omega t}\right\}} \quad \textbf{Equation 1}$$

$$\boldsymbol{u = R_e\left\{u_1[z]\, e^{i\omega t}\right\}} \quad \textbf{Equation 2}$$

$$\boldsymbol{T = T_m + R_e\left\{T_1[z]e^{i\omega t}\right\}} \quad \textbf{Equation 3}$$

Where: P_m and T_m are mean pressure and mean temperature respectively, z = is the geometric direction of 2D axisymmetric model of computational domain, $R_e\{\}$ is the real part, $e^{i\omega t}$ is the time dependency of a particular variable, ω is the angular frequency, and P_1, u_1 and T_1 are oscillating amplitude pressure, velocity, and temperature respectively of the standing wave, which expressed as follows:

$$\boldsymbol{P_1 = P_A\, cos(k_1.z)} \quad \textbf{Equation 4}$$

$$\boldsymbol{u_1 = -i\frac{P_A}{\rho_m .a}\, sin\,(k_1.z)} \quad \textbf{Equation 5}$$

$$\boldsymbol{T_1 = \frac{P_A}{\rho_m C_p} cos(k_1.z)} \quad \textbf{Equation 6}$$

Where: P_A = is the amplitude pressure at pressure antinode, a = is the speed of sound, k_1 = is the wave number, ρ_m = is the mean density and C_p = is the gas specific heat capacity at constant pressure. Then substituted equations (1) to (3) into equations (4) to (6), yielded three final equations (7) to (9) illustrated below:

$$\boldsymbol{P = P_m + P_A\, cos(k_1.z)\, cos\,\omega t.} \quad \textbf{Equation 7}$$

$$\boldsymbol{U = \frac{P_A}{\rho_m .a} sin(k_1.z)\, sin\,\omega t.} \quad \textbf{Equation 8}$$

$$\boldsymbol{T = T_m + \frac{P_A}{\rho_m C_p}\, cos(k_1.z)\, cos\,\omega t.} \quad \textbf{Equation 9}$$

The equations (7) to (9) represent the pressure (P), velocity (U), and temperature (T) respectively, which utilised as the oscillatory boundaries at the inlet of computational domain.

3.5.4 Simulation model and geometrical modelling

Three TAR geometries were designed and pre-simulated using commercial Multiphysics software. The viable geometry was determined based on the lower temperature difference (ΔT) achieved amongst the three simulated.

3.5.4.1 TAR geometry 1

Figure 3-29 shows the TAR geometry 1 created using the method described by Nathad *et al.* (2019). The geometry was 624 mm long, which included the length of smaller and larger diameter, two cones, each 60 mm long, and the length of buffer volume. The length of the larger diameter equalled the length of both, the maximum stack position of 50 mm and the maximum stack length of 65 mm, which made up a total of 115 mm. The buffer volume and larger diameter tube both had the same diameter of 110 mm.

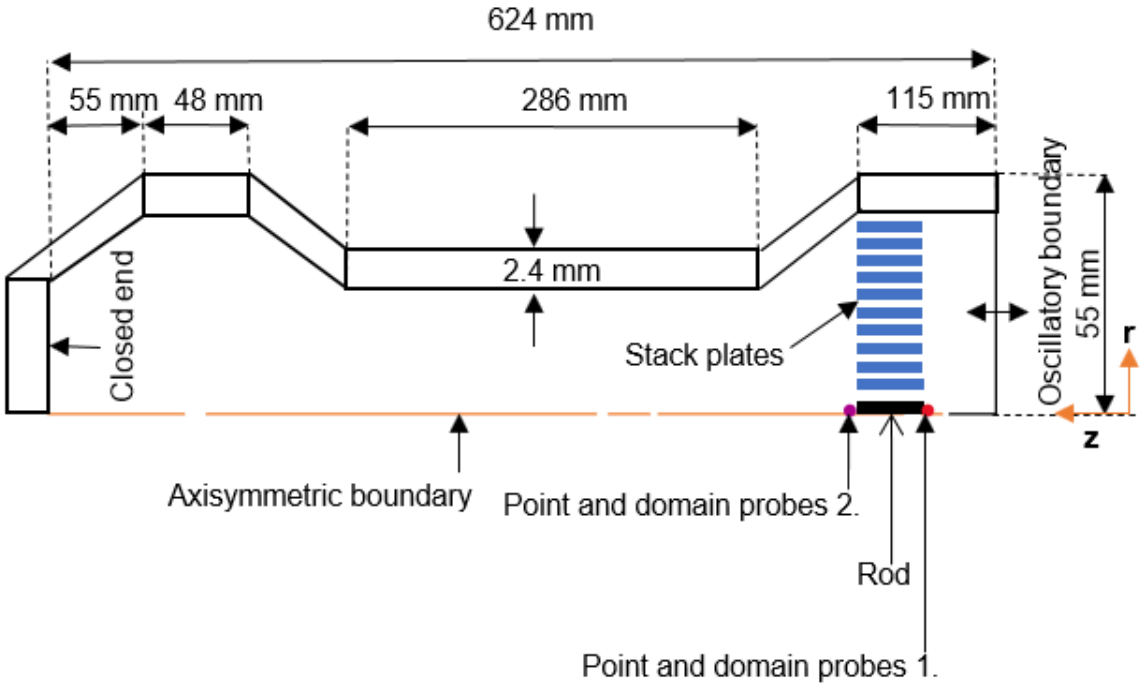

Figure 3-29: TAR geometry 1.

3.5.4.2 TAR geometry 2

Figure 3-30 depicts the TAR geometry 2 designed by adopting the method applied by Nathad *et al.* (2019). The geometry was 624 mm long, which included the length of smaller and larger diameter, two cones, each 60 mm long, and the length of buffer volume. The length of the larger diameter was the length of the maximum stack position (50 mm), maximum stack length of 65 mm and the incorporated hot heat exchanger of (L_{copper}/λ = 0.02625) long as regarded by Rahpeima and Ebrahimi (2022). However, the diameter of the buffer volume was reduced from 110 mm to 76 mm.

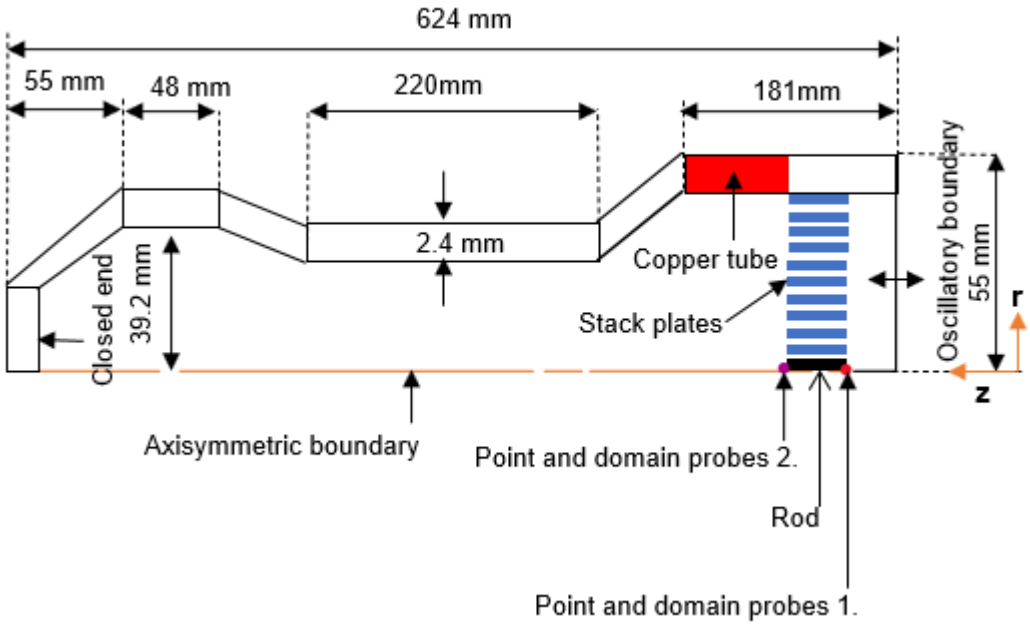

Figure 3-30: TAR geometry 2.

3.5.4.3 TAR geometry 3

Table 3-6 presents various properties of solid materials used in simulation. The modelling was implemented in commercial multiphysics software. Figure 3-31 shows the 2D axisymmetric geometry that was used in the modelling as viable design. The TAR geometry was 624 mm long. The larger diameter (D_1) was 110 mm, which tapered to a ratio of D_2/D_1 = 0.54 to obtain a smaller diameter (D_2). Five stacks made from polylactic acid (PLA) of length range from 25 mm to 65 mm with a gap spacing ($2\gamma_0$ = 0.6 mm), where γ_0 is the half distance between two

stack plates spacing, and stack plate thickness (th) was 0.5 mm. Each stack length positioned at 30 mm, 40 mm, and 50 mm away from the oscillatory boundary of the computational domain. A hot copper heat exchanger of L_{copper} /λ = 0.02625 mm long was embedded in the tube thickness and positioned at the upper end of each stack length to absorb the exhausting heat and dissipated it to the environment. A cold heat exchanger was omitted in the computational domain reason being that no heat generated was utilised externally as elaborated by Rahpeima and Ebrahimi (2022). The total length of the computational domain was set to 0.012λ+0.0238λ m. The lower edge of the stack positioned at 0.012λ m away from the inlet boundary of the computation domain while the distance of the lower edge of the stack to the upper closed end of computation domain was set to 0.0238λ m.

Table 3-6: Properties of various solid materials used in simulation.

Domain	**Materials**	**Thermal conductivity (K)**	**Density (ρ)**	**Heat capacity.**
		[W/m. K]	**[kg/m^3]**	**[J/Kg K]**
Hot heat exchanger	Copper	400	8960	385
Resonator and rod	PVC	0.19	1330	880
Stack	PLA	0.13	1300	1800

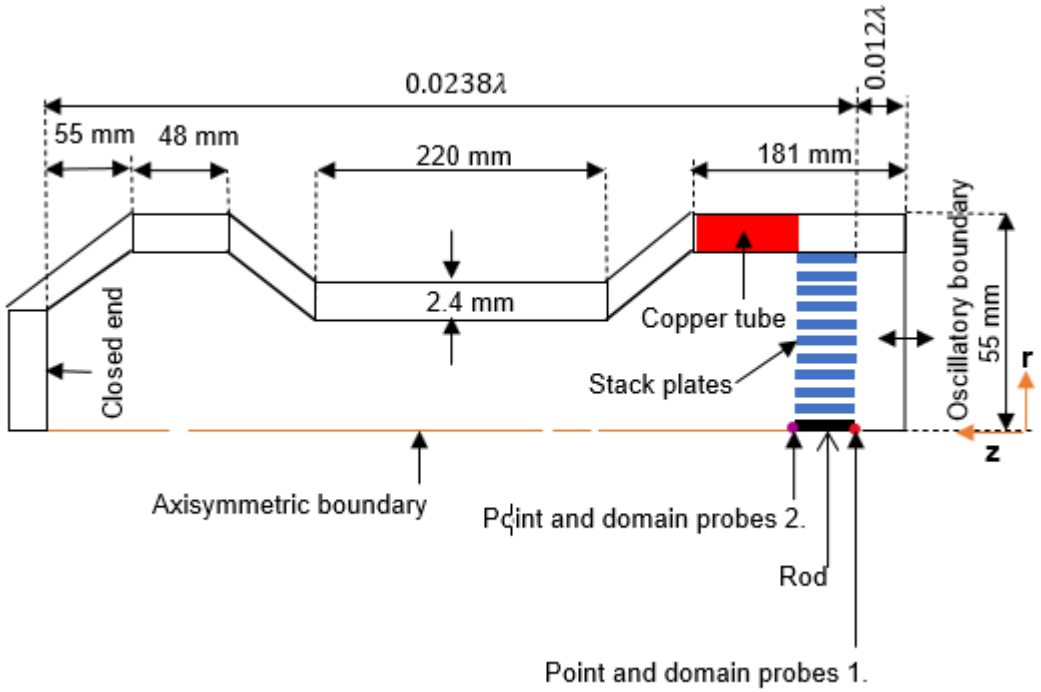

Figure 3-31: Computational domain adopted TAR geometry.

3.5.5 Numerical methodologies and boundary conditions

Table 3-7 presents the operating conditions and thermophysical properties of helium used in one of the fifteen numerical model. For the model, the study used a 2D axisymmetric model, conjugate heat transfer, laminar flow coupled by nonisothermal flow multiphysics. The type of fluid flow was determined by the Reynolds number (R_e) is being referred to as the critical Reynolds number limited to 2300 ($R_{eCr} = 2u_1/\sqrt{V\omega}$) as elaborated by Bhatti *et al.* (2020). A time-dependant solution was utilised. The segregated solver utilised to minimise the computation time. A segregated solver subdivides the solution process into segregated sub-steps and solved each parameter sequentially within a single iteration.

- When $\boldsymbol{t = 0}$ at all r and z cells $\begin{pmatrix} \boldsymbol{u_r = 0} \\ \boldsymbol{u_z = 0} \\ \boldsymbol{T = T_m} \end{pmatrix}$ Equation 10

Where: u_r and u_z are the velocities in r and z directions and T_m is the fluid mean temperature.

- Internal solid boundaries $\begin{pmatrix} \boldsymbol{u_r = 0} \\ \boldsymbol{u_z = 0} \\ \boldsymbol{T_{solid} = T_{fluid}} \end{pmatrix}$ Equation 11
- Horizontal external boundary $\left[-\boldsymbol{k}\frac{\boldsymbol{\partial T}}{\boldsymbol{\partial z}} = \boldsymbol{h}\,(\boldsymbol{T_{ext} - T})\right]$ Equation 12
- Vertical external boundary $\left[-\boldsymbol{k}\frac{\boldsymbol{\partial T}}{\boldsymbol{\partial r}} = \boldsymbol{h}\,(\boldsymbol{T_{ext} - T})\right]$ Equation 13
- Thermal insulation boundary $\begin{bmatrix} \frac{\boldsymbol{\partial T}}{\boldsymbol{\partial r}} = \boldsymbol{0} \\ \frac{\boldsymbol{\partial T}}{\boldsymbol{\partial z}} = \boldsymbol{0} \end{bmatrix}$ Equation 14

Where: $\boldsymbol{T_{ext}}$ = is the ambient temperature of external resonator tube taken to be 288 k, $\boldsymbol{h}$ = is the convection heat transfer coefficient for the external air taken to be 5 w/m^2. k (Rahpeima and Ebrahimi 2022).

Table 3-7: Operating conditions and thermophysical properties of helium.

Operating conditions		
Property	**Value**	**Units**
Mean temperature (T_m)	295.15	K
Mean pressure (P_m)	110500	Pa
Operating frequency (f)	400	Hz
Amplitude pressure (P_A)	68100	Pa
Thermophysical properties of Helium		
Thermal conductivity (K)	0.15243	[W/ m. K]
Density (ρ)	0.1667	[Kg/m^3]
Specific heat (Cp)	5192.6	[J/Kg. K]
Speed of sound (a)	998.6	m/s
Gas constant (R)	2076.9	J/kg. K
Wavelength (λ)	2.4963	m

Table 3-8 presents the geometrical and model parameters utilised in the computation domain. Figure 3-32 shows the boundaries conditions applied to the quarter wavelength designed using the 2D axisymmetric model. A PVC rod of 3 mm in diameter and stack plates positioned at 30 mm away from the oscillatory boundary. A hot heat exchanger embedded was positioned above each stack length as elaborated by Rahpeima and Ebrahimi (2022). The gas used was ideal gas and modelling fluid changed to Newtonian by specifying the density and dynamics viscosity. Three oscillatory boundary conditions applied at the inlet: the temperature, velocity, and pressure respectively.

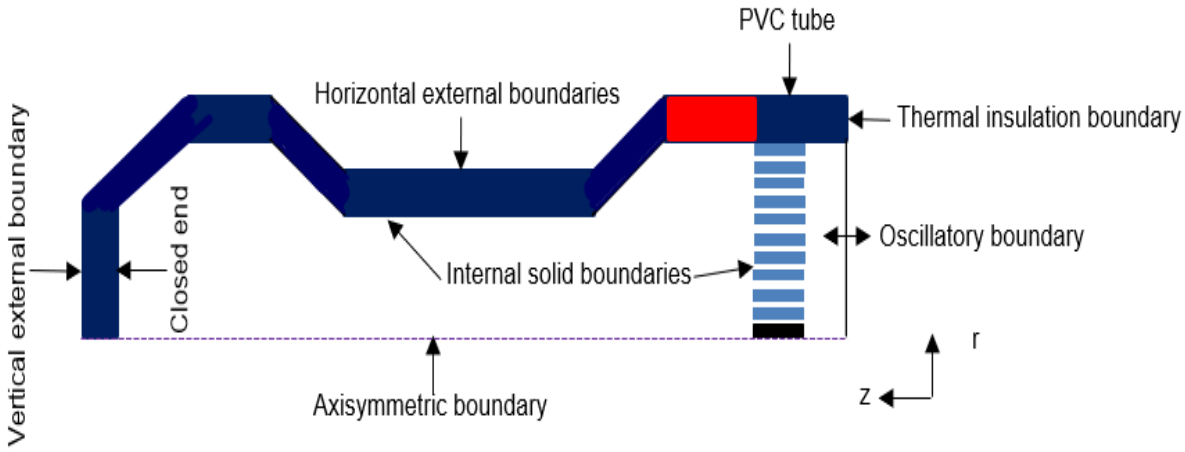

Figure 3-32: Boundaries applied to simulation domain.

Table 3-8: Geometrical parameters and model parameters.

Geometrical parameters			
Name	**Expression**	**Value**	**Description**
Tube-R	52.8[mm]	0.0528 m	Tube radius
Tube-L	624[mm]	0.624 m	Tube length
Tube-RE	55[mm]	0.055 m	Tube external radius
Tube-LE	626[mm]	0.626 m	Tube external length
Stack-w	0.5[mm]	5E-4 m	Stack plate width
Stack-L	15[mm]	0.03 m	Stack length
Stack-G	0.6[mm]	6E-4 m	Stack gap
Stack-z	30[mm]	0.03 m	Stack position
Rod-w	3[mm]	0.003 m	Rod diameter
Copper-L	0.02625*wave-L.	0.06552 m	Copper length
Model parameters			
a	998.6 [m/s]	998.6 m/s	Speed of sound
f	a/ (4*tube_ L)	400.08 1/s	Resonance frequency
k	2*pi/ (4*tube_ L)	2.5173 1/m	Wave number
rho	0.166 [kg/m^3]	0.166 kg/m³	Density
Cp	5200 [J/(kg*K)]	5200 J/ (kg· K)	Heat capacity at constant pressure
T_m	295.15 [K]	295.15 K	Mean temperature
P_m	110500 [Pa]	1.105E5 Pa	Mean pressure
P_A	68100 [Pa]	68100 Pa	Amplitude pressure
tp	1/f	0.0024995 s	Wave period

Geometrical parameters			
Name	**Expression**	**Value**	**Description**
hwall	5 [W/(m^2*K)]	5 W/ (m²· K)	Convection heat coefficient
wave_L	a/f	2.496 m	Wavelength

Figure 3-33 shows the free triangular mesh used for the entire domain with the predefined size set to extremely fine. The time stepping was set to 0.01 second and an output computation time was of 6 seconds.

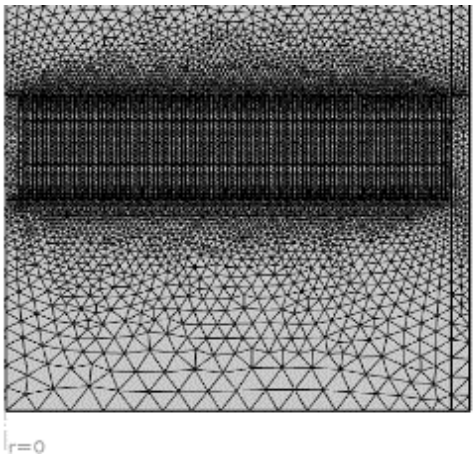

Figure 3-33: Mesh applied to the entire simulation domain.

CHAPTER FOUR: RESULTS

4.1 Introduction

This chapter presents the results of fifteen conducted experiments and fifteen numerical modelling on a standing wave thermoacoustic refrigerator.

4.2 Experimental results

Table 4-1 presents the results of collected data and calculated value. These included five stack length of 25 mm, 35 mm, 45 mm, 55 mm, and 65 mm for a constant stack position of 30 mm. The temperature difference (ΔT) across the stack length increased between the 25 mm and 35 mm stack length of 1.8°C and between the 35 mm and 45 mm stack length of 0.3°C but decreased between the 45 mm and 55 mm stack length of 2.2°C and between the 55 mm and 65 mm stack length of 0.6°C. The COP decreased between the 25 mm and 35 mm stack length of 0.079 and between the 35 mm and 45 mm stack length of 0.015 but increased between the 45 mm and 55 mm stack length of 0.724 and decreased between the 55 mm and 65 mm stack length of 0.41(see Appendix B for detailed results).

Table 4-1: Five experimental results of stack positioned at 30 mm.

Stack Position (mm)	Stack Length (mm)	Temperature Difference (°C)	Temperature on Cold Side (°C)	Cooling Load (W)	Heating Load (W)	Power Input (W)	Coefficient of Performance	Overall Coefficient of Performance
30	25	11	24.3	0.064	0.673	43	0.11	0.00149
30	35	12.8	24.1	0.006	0.199	37.35	0.031	0.00016
30	45	13.1	25	0.0046	0.299	39	0.016	0.00012
30	55	10.9	24.1	0.065	0.153	43	0.74	0.00151
30	65	10.3	23	0.026	0.103	37.5	0.33	0.0007

Figure 4-1 shows the plotted chart of temperature difference (ΔT), coefficient of performance (COP) versus the stack length (S_L). The legend for the ΔT and COP is displayed on top of the chart. The red colour is for the ΔT whereas the black is for the COP. The scatter lines and markers chart were chosen to better visual the trend of data points. The ΔT increased from 11°C to 12.8°C, and then to 13.1°C for the first three stack length of 25 mm, 35 mm, and 45 mm where it decreased from 13.1°C to 10.9°C and then to 10.3°C for the last two stack length of 55 mm and 65 mm respectively. The COP decreased from 0.1 to 0.031and then to 0.016 for the stack length of 25 mm, 35 mm, and 45 mm where it increased to 0.74 and then decreased to 0.33 for the stack length of 55 mm and 65 mm respectively.

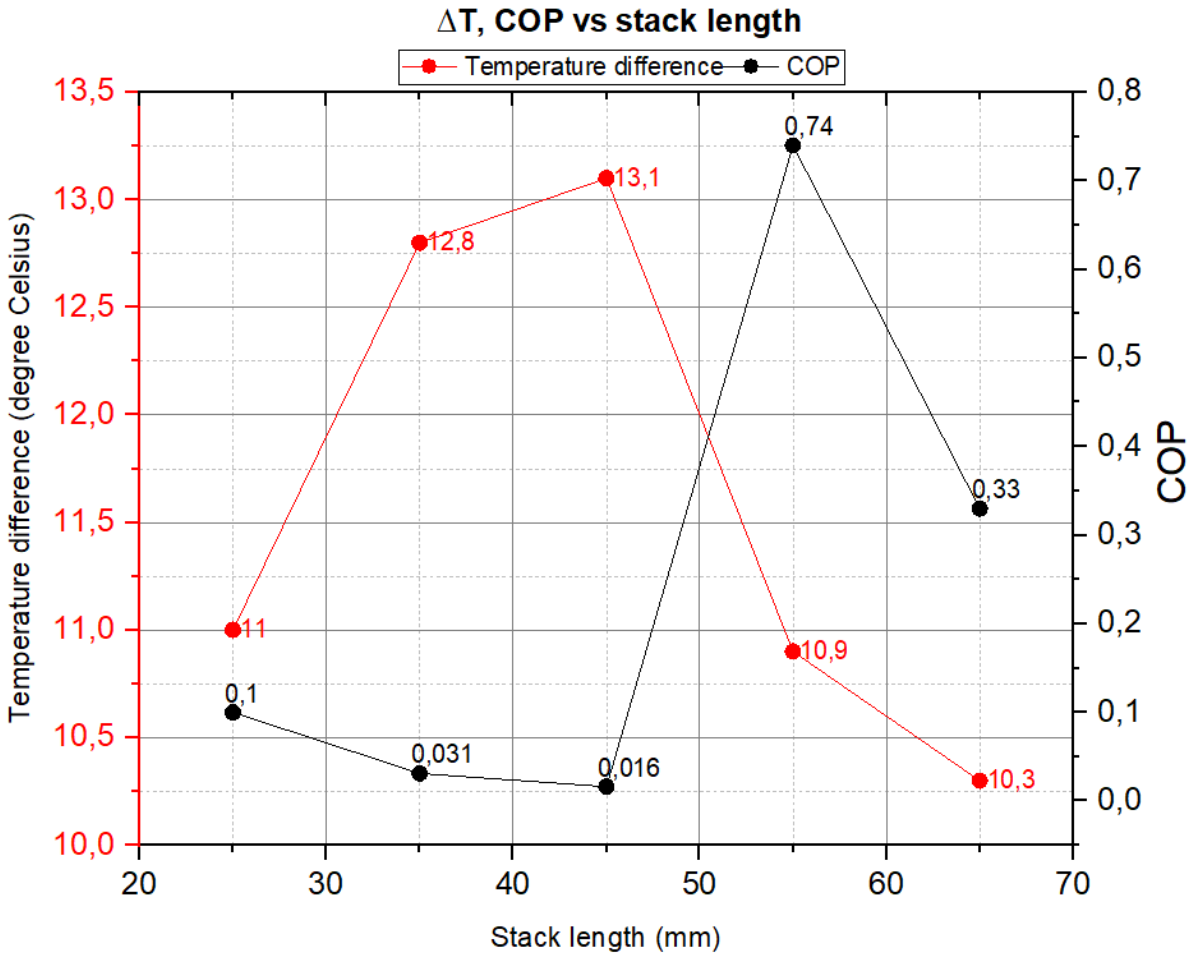

Figure 4-1: Plotted chart of five experiments of stack length positioned at 30 mm.

The outcomes of five experiments are presented in Table 4-2 for the stack length ranges from 25 mm to 65 mm, each positioned at 40 mm. The ΔT across the stack length increased between the 25 mm and 35 mm stack length of 4.7°C but decreased between the 35 mm and

45 mm stack length of 2.7°C and between the 45 mm and 55 mm stack length of 0.9°C and then between the 55 mm and 65 mm stack length of 0.4°C. The COP decreased between the 25 mm and 35 mm stack length of 0.05 and between the 35 mm and 45 mm stack length of 0.03 and then between the 45 mm and 55 mm stack length of 0.2 but increased between the 55 mm and 65 mm stack length of 0.33.

Table 4-2: Five experimental results of stack positioned at 40 mm.

Stack Position (mm)	Stack Length (mm)	Temperature Difference (°C)	Temperature on Cold Side (°C)	Cooling Load (W)	Heating Load (W)	Power Input (W)	Coefficient of Performance	Overall Coefficient of Performance
40	25	7.1	25	0.052	0.194	43	0.37	0.0012
40	35	11.8	23.6	0.039	0.162	43	0.32	0.0009
40	45	9.1	24.4	0.032	0.142	37.5	0.29	0.00086
40	55	8.2	26.3	0.016	0.1826	39	0.09	0.0004
40	65	7.8	25.4	0.054	0.1831	39.1	0.42	0.0013

Figure 4-2 shows the plotted chart of temperature difference (ΔT), coefficient of performance (COP) versus the stack length (S_L). The scatter lines and markers chart were utilised to better visual the pattern of data points. The ΔT increased from 7.1°C to 11.8°C between the 25 mm to 35 mm stack length where it decreased in descended order from 11.8°C to 9.1°C, and then to 8.2°C, and finally to 7.8°C for the three-stack length of 45 mm, 55 mm, and 65 mm. The COP decreased from a higher of 0.37 to a lower of 0.09 for the four consecutive stack length of 25 mm, 35 mm, 45 mm, and 55 mm where it increased to 0.42 at the 65 mm stack length.

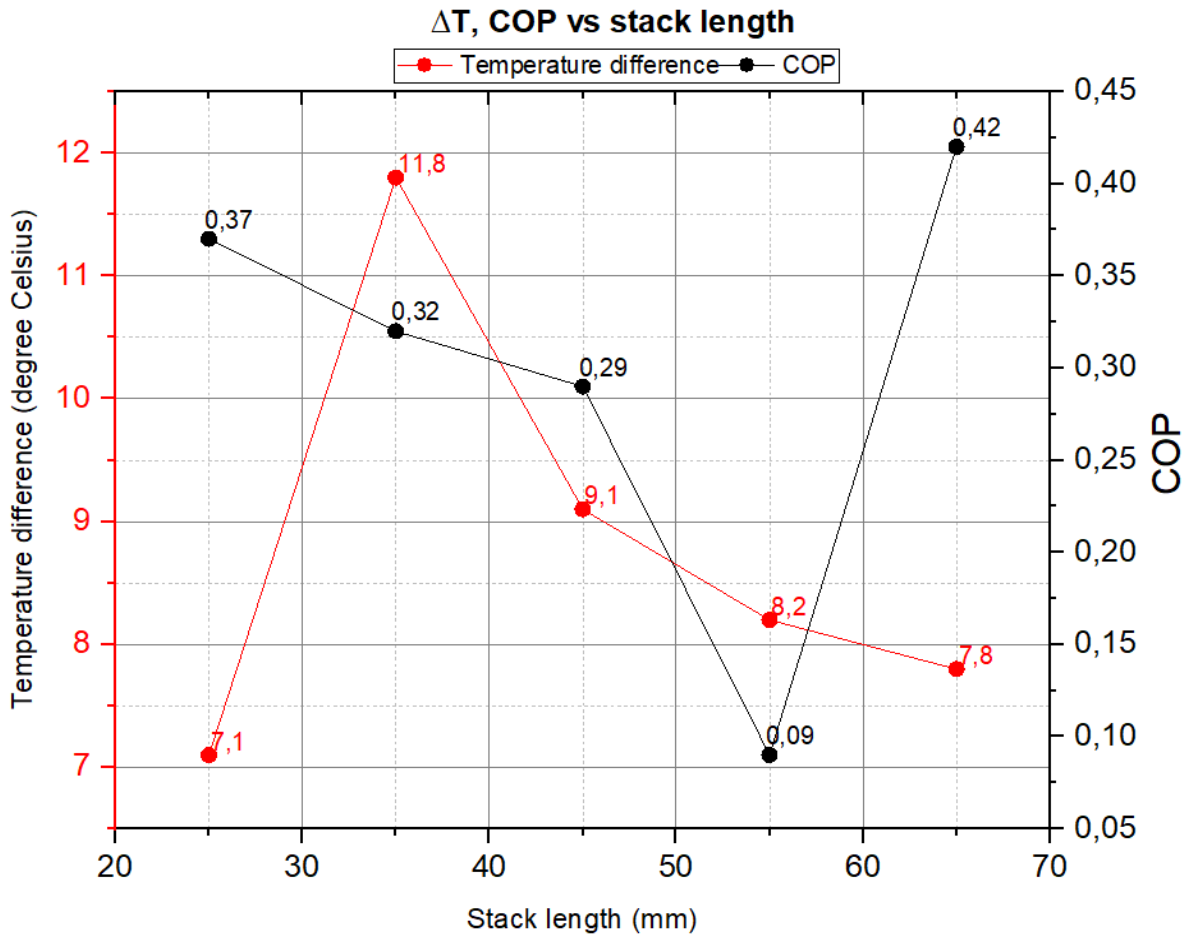

Figure 4-2: Plotted chart of five experiments of stack length positioned at 40 mm.

In Table 4-3 five experimental results are presented for the stack length of 25 mm, 35 mm, 45 mm, 55 mm, and 65 mm for a constant stack position of 50 mm. The ΔT across the stack length decreased by 0.7°C between the 25 mm and 35 mm stack length but increased by an increment of 0.3°C, 2.5°C, and 0.5°C between the 35 mm and 45 mm, 45 mm and 55 mm, and then 55 mm and 65 mm stack length respectively. The COP decreased by 0.01 between the 25 mm and 35 mm stack length and 0.21 between the 35 mm and 45 mm stack length but increased by 0.33 between the 45 mm and 55 mm stack length then decreased by 0.37 between the 55 mm and 65 mm stack length.

Table 4-3: Five experimental results of stack positioned at 50 mm.

Stack Position (mm)	Stack Length (mm)	Temperature Difference (°C)	Temperature on Cold Side (°C)	Cooling Load (W)	Heating Load (W)	Power Input (W)	Coefficient of Performance	Overall Coefficient of Performance
50	25	8	25,1	0,0532	0,216	43	0,33	0,0012
50	35	7,3	24	0,056	0,227	41	0,32	0,00137
50	45	7,6	22,2	0,03	0,306	39,1	0,11	0,00077
50	55	10,1	23,5	0,069	0,226	43	0,44	0,0016
50	65	10,6	23,6	0,021	0,311	43	0,07	0,00049

Figure 4-3 shows the plotted chart of temperature difference (ΔT), coefficient of performance (COP) vs stack length (S_L). The scatter lines and markers chart were used to better visual the trend of data points. The ΔT decreased from 8°C to 7.3°C between the 25 mm and 35 mm stack length where it increased from 7.6°C to 10.1°C, and then to 10.6°C for the last three stack length of 45 mm, 55 mm, and 65 mm. The COP decreased from 0.33 to 0.032, and then to 0.11 for the first stack length of 25 mm, 35 mm, and 45 mm where it deviated by increasing to 0.44 at the 55 mm stack length then decreasing to 0.07 at the 65 mm stack length.

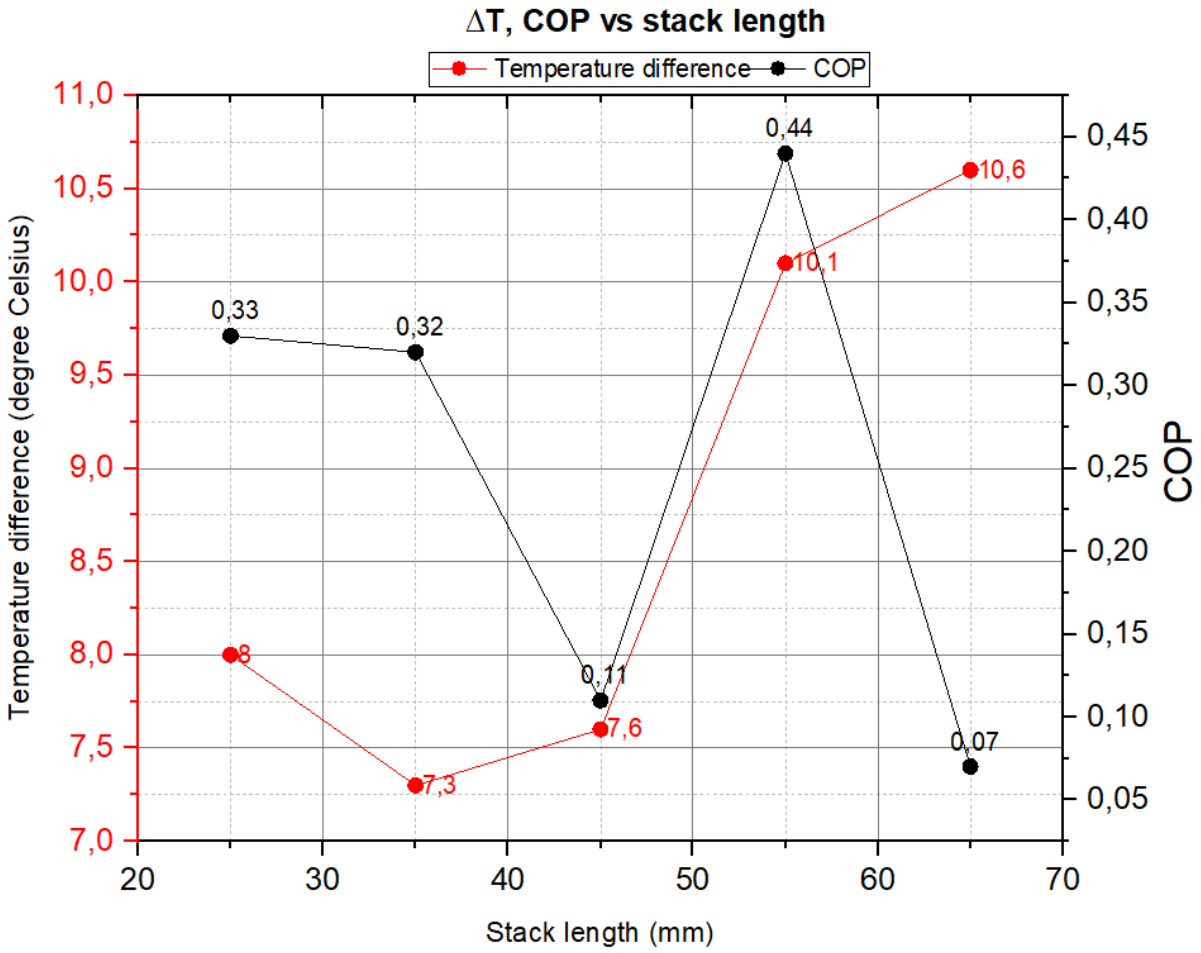

Figure 4-3: Plotted chart of five experiments of stack length positioned at 50 mm.

4.3 Numerical modelling results

Table 4-4 presents the outcomes of five simulated TAR. These comprised of five stack length ranges from 25 mm to 65 mm, each positioned 30 mm away from the oscillatory boundary condition. Each simulated TAR had two rows of collected data, the top and bottom represented the start and end of computation time. The data for top row was not regarded for TAR analysis. Each simulation from the 25 mm to 65 mm stack length lasted 15h32 minutes, 15h41 minutes, 15h35 minutes, 11h47 minutes, and 15h11 minutes respectively. The temperature difference (ΔT) was the difference between the warmer and cooler side of the stack. The coefficient of performance (COP) was the ratio of the total energy flux on the cooler side to the difference of total energy flux between the warmer and cooler side of the stack. Probes 1 and 2 represented the warmer and cooler side of the stack. The temperature difference and total energy flux increased on the warmer side between the 25 mm and 35 mm stack length of 0.40721 K and

3.524 W/m^2 while on the cooler side of the stack decreased of 2.765 K and 6.98 W/m^2 respectively.

Table 4-4: Simulated results of five TARs for stack positioned at 30 mm.

Stack length of 25 mm						
Time (s)	T-probe 1	T-probe 2	Energy flux -Probe 1	Energy flux-Probe 2	**ΔT**	COP
0,002169	371,77598 K	383,65583 K	5345,405704 W/m^2	957,6321151 W/m^2	Start	
6,253863	363,21042 K	354,70023 K	62,01008902 W/m^2	34,77021919 W/m^2	8.5 K	1.27
Stack length of 35 mm						
Time (s)	T-probe 1	T-probe 2	Energy flux -Probe 1	Energy flux-Probe 2	**ΔT**	COP
0,001402	376,87727 K	370,23404 K	10609,29047 W/m^2	260,9670468 W/m^2	Start	
6,34211	363,61763 K	351,93556 K	65,53367607 W/m^2	27,79271655 W/m^2	11.7 K	0.74
Stack length of 45 mm						
Time (s)	T-probe 1	T-probe 2	Energy flux -Probe 1	Energy flux-Probe 2	**ΔT**	COP
0,001232	375,8385 K	360,82695 K	11380,45297 W/m^2	206,9831147 W/m^2	Start	
6,259935	364,05890 K	350,07669 K	66,45143101 W/m^2	20,67540223 W/m^2	13.9 K	0.45
Stack length of 55 mm						
Time (s)	T-probe 1	T-probe 2	Energy flux -Probe 1	Energy flux-Probe 2	**ΔT**	COP
4,98E-04	351,63285 K	316,8338 K	13681,82011 W/m^2	141,0618161 W/m^2	Start	
6,087896	342,23248 K	331,47380 K	50,58384467 W/m^2	9,492054884 W/m^2	10.8 K	0.23
Stack length of 65 mm						
Time (s)	T-probe 1	T-probe 2	Energy flux -Probe 1	Energy flux-Probe 2	**ΔT**	COP
9,69E-04	367,08510 K	332,9455 K	11862,47554 W/m^2	99,7001787 W/m^2	Start	

6,093226	356,69840 K	341,8754 K	60,0917338 W/m^2	9,75075887 W/m^2	14.8 K	0.19

Figure 4-4 shows a generated 3D temperature contour of one of the five simulated TARs. Each simulated TAR from the 25 mm to the 65 mm stack length ($S_{L)}$) had a temperature contour depicting the lower and higher in the following manner: (309 K-374 K), (309 K-375 K), (309 K-375 K), (304 K-352 K), and (307 K-367 K) respectively. This temperature contour was the magnified representation of the temperature region along the stack length within the computation domain. The top is the warm side of the stack at 374 K (101°C) while the bottom is the cold side at 309 K (36°C). This meant that the standing wave TAR reduced the temperature from 101°C to 36°C. For a constant mean temperature (T_m) of 295.15 K (22°C) input in the computation domain. This meant that the TAR increased the temperature by about 14°C.

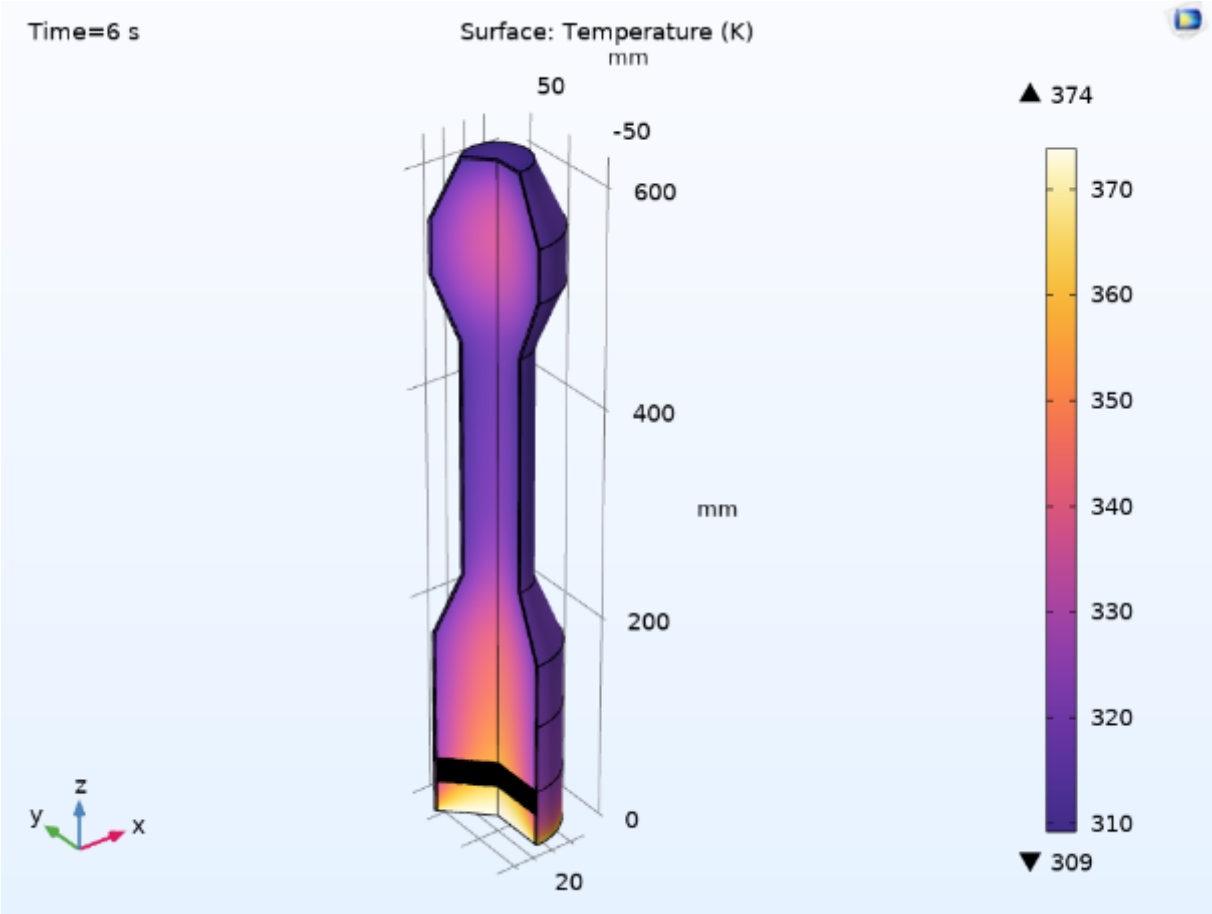

Figure 4-4: Temperature contour of one of the five simulated TARs.

Figure 4-5 shows a generated probe plot chart of temperature and total energy flux versus the time. This chart denoted of one of the five simulated TARs, but all five charts were the same as the one provided below. The output computation time was kept at 6 seconds because of the temperature and total energy flux became constant over that input interval.

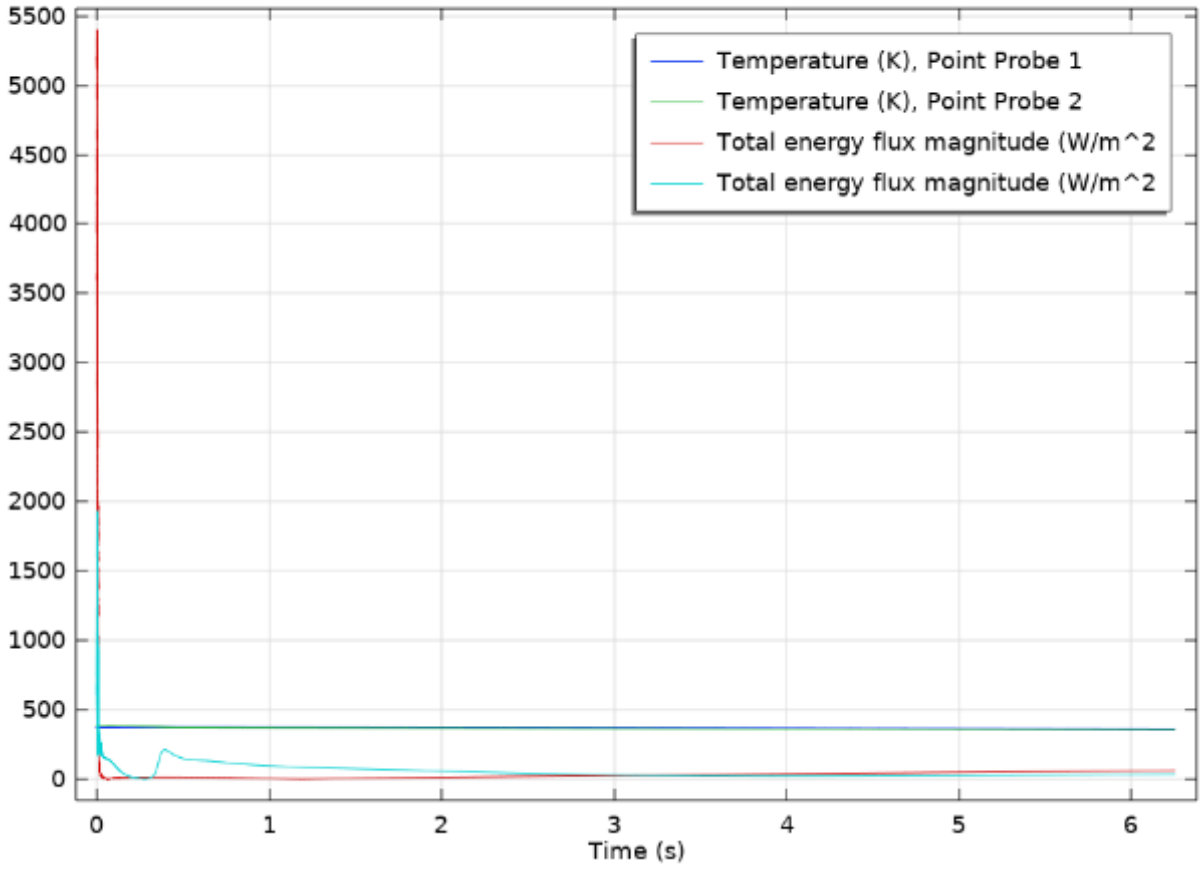

Figure 4-5: Generated probe plot of simulated TAR.

Figure 4-6 shows the plotted chart of temperature difference (ΔT) and coefficient of performance (COP) as function of the stack length (S_L). The scatter lines and markers adopted to better visualize the trend of data points. The legend on top of the chart represented the colour, red for ΔT and black for COP. The ΔT increased from 8.51 K to 11.68 K, and then to 13.98 K for the stack length of 25 mm, 35 mm, and 45 mm where it decreased to 10.76 K at the 55 mm stack length and then increased to 14.82 K at the 65 mm stack length respectively.

The COP decreased in descending order for the five values of 1.3, 0.74, 0.45, 0.23, and 0.19 from the 25 mm to 65 mm stack length respectively.

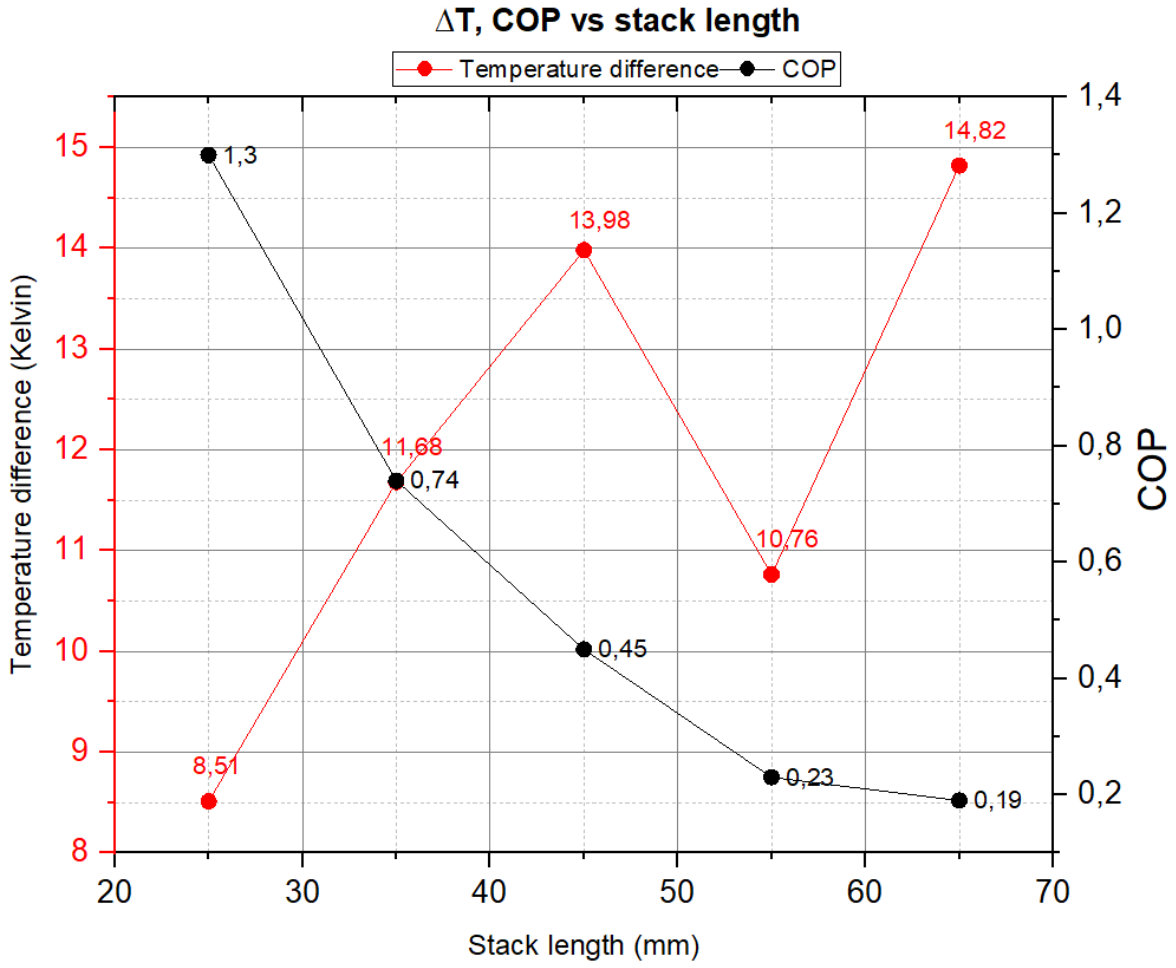

Figure 4-6: Plotted chart of five simulated TARs of stack positioned 30 mm.

Table 4-5 presents five simulation results of TARs. The outcomes were for the stack length of 25 mm, 35 mm, 45 mm, 55 mm and to 65 mm having each stack length positioned 40 mm away from the oscillatory boundary condition of the computation domain. Each simulated TAR lasted 6h57 minutes, 11h53 minutes, 13h7 minutes, 13h33 minutes, and 13h19 minutes respectively. The temperature decreased by 41.45 K and total energy flux by 34.181 W/m^2 between the 25 mm and 35 mm stack length on the warmer side of the stack while on the cooler side the temperature and total energy flux decreased as well by 37.57 K and 17.6 W/m^2 respectively.

Table 4-5: Simulated results of five TARs for stack positioned at 40 mm.

Stack length of 25 mm						
Time (s)	T-probe 1	T-probe 2	Energy flux -Probe 1	Energy flux-Probe 2	**ΔT**	COP
0.0018998	362.62 K	374.45 K	5331.3 W/m^2	739.52 W/m^2	Start	
6.1369	351.94 K	345.58 K	50.896 W/m^2	23.190 W/m^2	6.36 K	0.84
Stack length of 35 mm						
Time (s)	T-probe 1	T-probe 2	Energy flux -Probe 1	Energy flux-Probe 2	**ΔT**	COP
0.0018965	316.50 K	317.66 K	2092.8 W/m^2	381.03 W/m^2	Start	
6.0549	310.49 K	308.01 K	16.715 W/m^2	5.5887 W/m^2	2.48 K	0.50
Stack length of 45 mm						
Time (s)	T-probe 1	T-probe 2	Energy flux -Probe 1	Energy flux-Probe 2	**ΔT**	COP
0.0012873	363.03 K	354.25 K	9179.6 W/m^2	940.08 W/m^2	Start	
6.0917	351.94 K	342.45 K	52.099 W/m^2	11.298 W/m^2	9.49 K	0.28
Stack length of 55 mm						
Time (s)	T-probe 1	T-probe 2	Energy flux -Probe 1	Energy flux-Probe 2	**ΔT**	COP
0.0011576	387.51 K	375.59 K	13636 W/m^2	1279.7 W/m^2	Start	
6.3442	371.65 K	357.09 K	70.040 W/m^2	8.1427 W/m^2	14.6 K	0.132
Stack length of 65 mm						
Time (s)	T-probe 1	T-probe 2	Energy flux -Probe 1	Energy flux-Probe 2	**ΔT**	COP
0.0011153	370.77 K	348.22 K	11742 W/m^2	1216.4 W/m^2	Start	
6.2983	355.55 K	342.64 K	58.101 W/m^2	6.6683 W/m^2	12.9 K	0.129

Figure 4-7 shows the change in temperature difference (ΔT) and coefficient of performance (COP) as function of the stack length (S_L). Each simulated TAR from the 25 mm to 65 mm stack length generated a 3D temperature contour depicting the lower and higher in the following manner: (306 K-365K), (298 K-317K), (306 K-365K), (312 K-387K), and (308 K-370 K) respectively. The COP decreased in descending order for the five values of 0.84, 0.5, 0.28, 0.132, and 0.129 as from the 25 mm to 65 mm stack length respectively. The ΔT decreased from 6.36 K to 2.48 K from the 25 mm to 35 mm stack length then increased to 9.49 K and then to 14.56 K at the 55 mm stack length where it deviated by decreasing to 12.91 K at the 65 mm stack length.

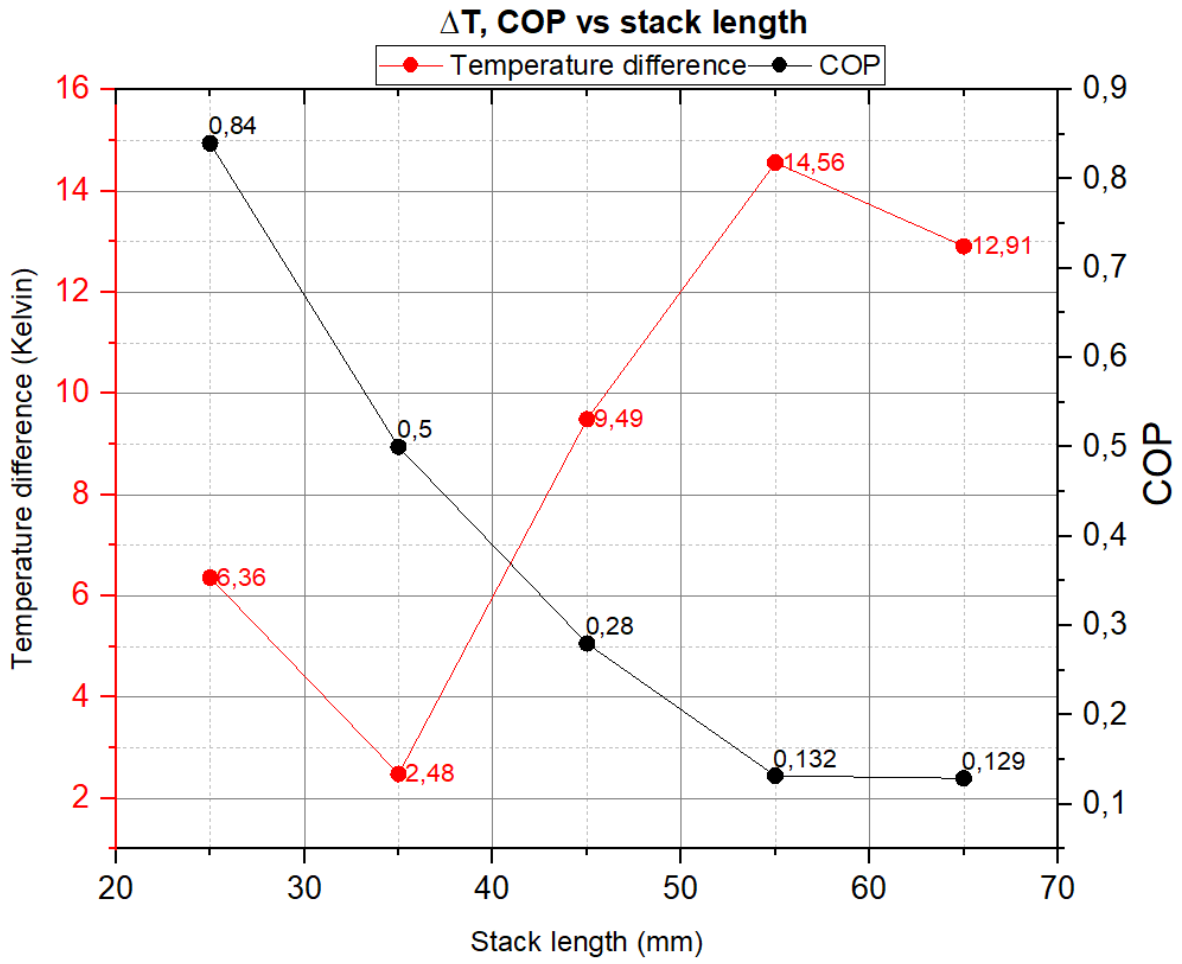

Figure 4-7: Plotted chart of five simulated TARs of stack positioned 40 mm.

In Table 4-6 the results of five simulated TAR are presented. The stack length ranged from 25 mm to 65 mm with each positioned 50 mm away from the oscillatory boundary condition of the computation domain. Each computation time as from the shorter to the larger stack length lasted 13h33 minutes, 14h30 minutes, 14h17 minutes, 13h28 minutes, and 13h14 minutes respectively. The temperature and total energy flux on the warmer side of the stack decreased by 22.09 K and 16.447 W/m^2 this between the 25 mm and 35 mm stack length while on the cooler side of the stack the temperature and total energy flux decreased as well by 20.72 K and 6.82 W/m^2 respectively.

Table 4-6: Simulated results of five TARs for stack positioned at 50 mm.

Stack length of 25 mm						
Time (s)	T-probe 1	T-probe 2	Energy flux -Probe 1	Energy flux-Probe 2	**ΔT**	COP
0.0025047	342.22	351.05	1835.9	176.38	Start	
6.0508	333.94	330.26	32.101	12.027	3.7 K	0.60
Stack length of 35 mm						
Time (s)	T-probe 1	T-probe 2	Energy flux -Probe 1	Energy flux-Probe 2	**ΔT**	COP
0.0035348	318.53	314.13	836.76	35.753	Start	
6.1117	311.85	309.54	15.654	5.2081	2.3 K	0.50
Stack length of 45 mm						
Time (s)	T-probe 1	T-probe 2	Energy flux -Probe 1	Energy flux-Probe 2	**ΔT**	COP
0.0015537	368.16	367.72	8816.2	906.16	Start	
6.1422	350.77	342.76	46.241	8.7400	8 K	0.23
Stack length of 55 mm						
Time (s)	T-probe 1	T-probe 2	Energy flux -Probe 1	Energy flux-Probe 2	**ΔT**	COP
0.0014446	318.01	309.13	2799.9	207.65	Start	

6.0479	310.36	307.40	14.784	3.7626	3 K	0.34

Stack length of 65 mm

Time (s)	T-probe 1	T-probe 2	Energy flux -Probe 1	Energy flux-Probe 2	∆**T**	COP
5.7212E-4	365.07	321.78	13900	7385.6	Start	
6.0566	349.46	339.90	44.476	5.7023	9.6 K	0.15

Figure 4-8 shows the plotted chart of temperature difference (∆T) and coefficient of performance (COP) as function of the stack length (S_L). Each simulated TAR from the 25 mm to 65 mm stack length generated a 3D temperature contour depicting the lower and higher in the following manner: (303 K-347 K), (298 K-320 K), (306 K-366 K), (298 K-318 K), and (307 K-365 K) respectively. The COP decreased from 0.6 to 0.5, and then to 0.23 for the 25 mm, 35 mm, and 45 mm stack length where it deviated by increasing to 0.34 at the 55 mm stack length and then decreased to 0.15 at the 65 mm stack length. The ∆T decreased from 3.68 K to 2.31 K as from the 25 mm to 35 mm stack length where it deviated by increasing to 8.01 K at the 45 mm stack length then decreased to 2.96 K at the 55 mm stack length and then increased to 9.56 K at the 65 mm stack length.

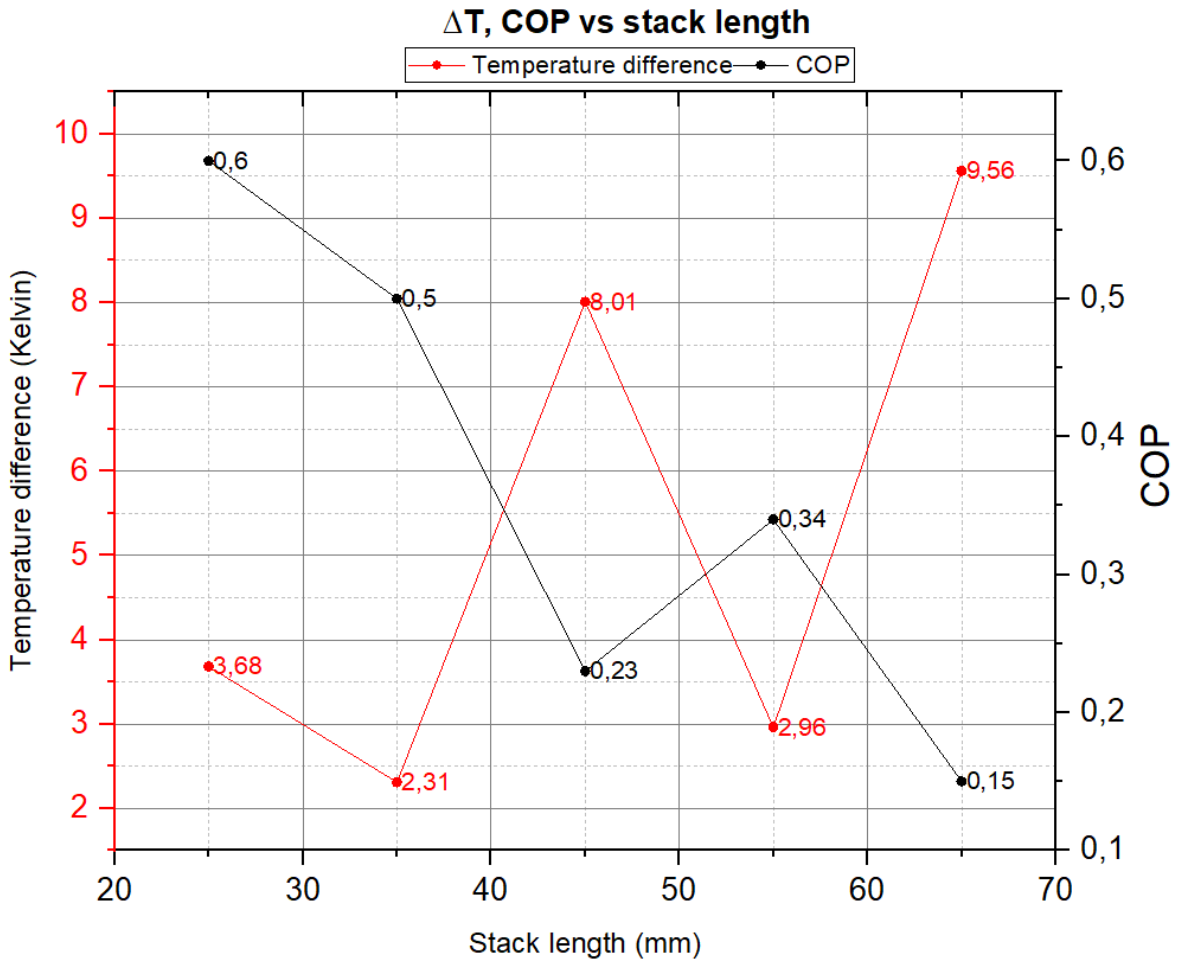

Figure 4-8: Plotted chart of five simulated TARs of stack positioned 50 mm.

4.4 Optimisation of stack length and stack position.

The experimental and simulation results have been analysed using the Taguchi design method in Minitab statistical software as collaborated by Priyanga and Muthadhi (2023). The Taguchi design method (TDM) is a statistical analysis developed by Genichi Taguchi. The method is known to be robust and powerful for optimizing multiple parameters. It can determine the optimal level of the control factor, analysed their effects on the response and revealed the relationship between the controllable and uncontrollable parameters. The optimisation approach was to provide the required number of experiments with a signal to noise ratio. The signal-to-noise ratio is being regarded as a gauge to measure the quality of a system. The quality is said to be better when the signal to noise ratio is higher. There are though three

diverse types of signals to noise ratio for statistical analysis: larger is better, nominal is better, and smaller is better.

4.4.1 Optimisation of experimental results

The objective of the experiment was to optimize the performance of TAR for the two input factors, the stack length and stack position. The larger is better as noise condition adopted to maximize the response.

4.4.1.1 Taguchi analysis: ΔT, COP, T_C, Q_C versus stack length and stack position

Table 4-7 presents the response table for signal to noise ratios for two factors the stack length and stack position. For the design of experiment, five levels were for the stack length ranges from 25 mm to 65 mm while three levels for the stack position of 30 mm, 40 mm, and 50 mm. The delta statistic measured the size of the effect, it is the difference between the higher and lower of a factor while the rank indicated the factor with a higher effect. For the conducted experiments the stack length ranked number 1 with a delta of 10.36 and a higher signal to noise ratio of -19,55 at level one followed second by the stack position with a delta of 6.75 and a higher signal to noise ratio of -21.74 at level three.

Table 4-7: Response table for signal to noise ratio: Larger is better.

Level	Stack length (mm)	Stack position (mm)
1	-19,55	-28,49
2	-26,65	-23,07
3	-29,92	-21,74
4	-21,70	
5	-24,34	
Delta	10,36	6,75

Table 4-8 presents the orthogonal array of the experimental results using the Taguchi design method. The design summary was two factors (2) each for stack length and stack position, 15 total number of runs (15), one base blocks (1), and one total blocks (1). Five levels were for the stack length ranges from 25 mm to 65 mm while three levels for the three-stack position of 30 mm, 40 mm, and 50 mm. The ΔT, COP, lower temperature (T_C), and cooling load (Q_C) were parameters added in Minitab software to determine the signal-to-noise ratios.

Table 4-8: Orthogonal array of experimental using Taguchi design.

Std Order	Run order	PtType	Blocks	Stack length (mm)	Stack position (mm)	ΔT (ºC)	COP	Tc (ºC)	Qc (W)	SNRA1
1	1	1	1	65	30	10,3	0,330	23,0	0,0260	-25,7068
7	2	1	1	35	50	7,3	0,320	24,0	0,0560	-19,1469
13	3	1	1	25	50	8,0	0,330	25,1	0,0532	-19,5728
9	4	1	1	55	30	10,9	0,740	24,1	0,0650	-17,7547
10	5	1	1	45	50	7,6	0,110	22,2	0,0300	-24,7486
14	6	1	1	55	50	10,1	0,440	23,5	0,0690	-17,3082
6	7	1	1	65	50	10,6	0,070	23,6	0,0210	-27,9093
11	8	1	1	35	30	12,8	0,031	24,1	0,0060	-38,5761
15	9	1	1	35	40	11,8	0,320	23,6	0,0390	-22,2222
8	10	1	1	25	30	11,0	0,100	24,3	0,0640	-19,3469
5	11	1	1	55	40	8,2	0,090	26,3	0,0160	-30,0322
12	12	1	1	45	30	13,1	0,016	25,0	0,0046	-41,0691
2	13	1	1	45	40	9,1	0,290	24,4	0,0320	-23,9290
4	14	1	1	65	40	7,8	0,420	25,4	0,0540	-19,4030
3	15	1	1	25	40	7,1	0,370	25,0	0,0520	-19,7445

Figure 4-9 shows the main effects plot for signal to noise ratios for two input factors the stack length and stack position. The generated chart was the signal to noise ratio as function of two factors the stack length and stack position. The y-axis depicted the signal to noise ratio while the x-axis depicted the stack length and stack position. This indicated the effect of the control factors on the response. The higher the signal to noise ratio value meant that the factor performed better. A higher signal to noise ratio of -19,55 occurred at the 25 mm stack length while a signal to noise ratio of -21,74 occurred at the 50 mm stack position.

Figure 4-9: Signal-to-noise ratios for stack length and stack position (Experimental results).

Figure 4-10 shows the probability plot for the temperature difference (ΔT), COP, T_C, and cooling load (Q_C). The probability plot was used to verify the experimental method whether the data points followed the normal distribution. This was determined by comparing the p-value of each parameter to the significance level of 0.05. Two conditions were that when the p-value is less or equal to the significance level, the data points did not follow the normal distribution, then when the p-value is higher than the significance level, the method is said to be effective. The p-value of each parameter (ΔT), COP, T_C, and cooling load (Q_C) were 0.324, 0.104, 0.87,

and 0.377 respectively which being larger than the significance level of 0.05, hence the experimental method was effective having the data points followed the normal distribution.

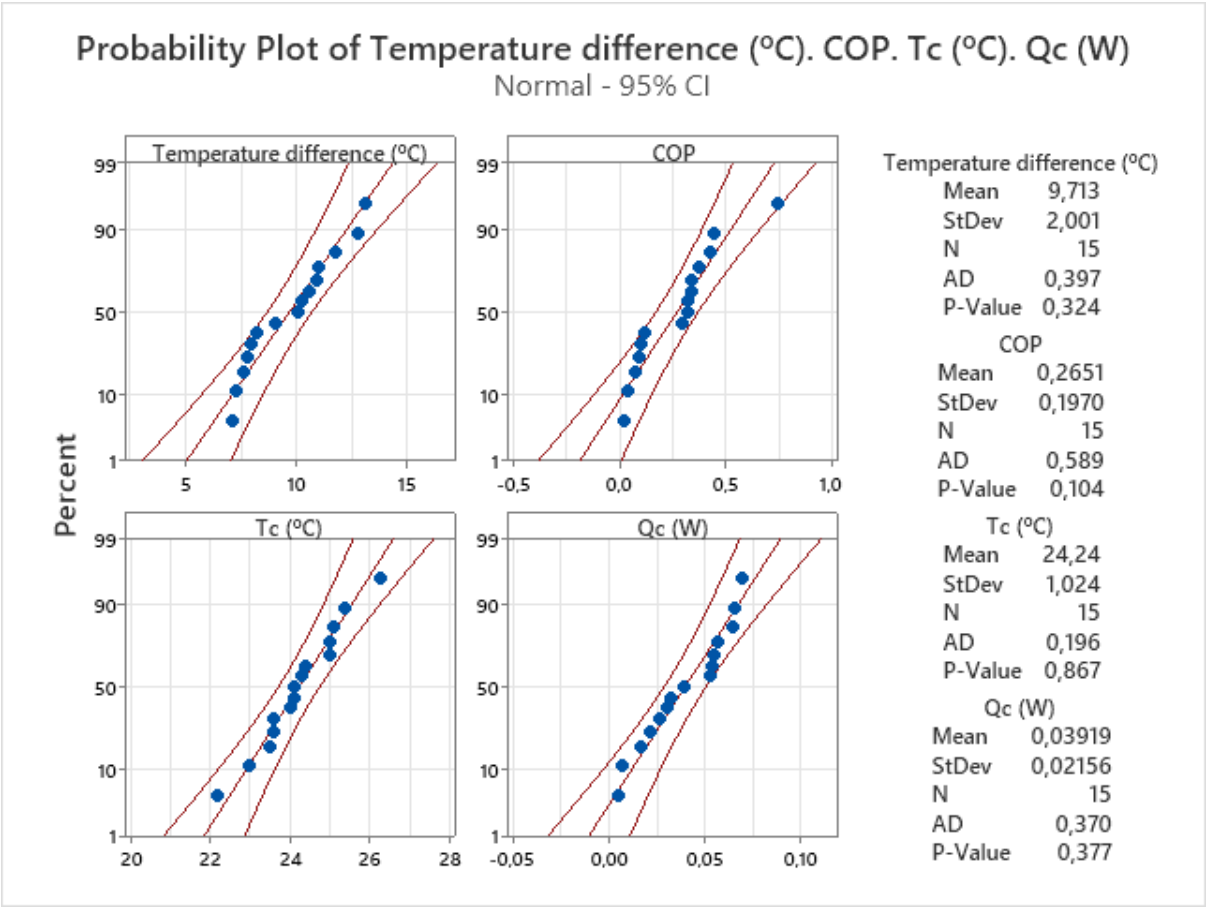

Figure 4-10: Probability plot ΔT, COP, T_C, and Q_C (Experimental results).

4.4.2 Optimisation of numerical modelling results

The Taguchi design method was used as well to optimise the fifteen numerical modelling of TARs.

4.4.2.1 Taguchi analysis: ΔT, COP, T_C, Q_C versus stack length and stack position

Table 4-9 presents the response table for signal to noise ratios. Five levels were for the stack length of 25 mm, 35 mm, 45 mm, 55 mm, and 65 mm while three levels for the three-stack position of 30 mm, 40 mm, and 50 mm. The larger is better signal to noise ratio adopted for the design of numerical modelling. The stack length and stack position had a higher signal to

noise ratio at level 1 of 1,624 and -3,947 respectively, however the stack length was the most influential parameter being ranked number 1 with a delta value of 14,845 followed second by the stack position with a delta value of 3,887.

Table 4-9: Response table for signal to noise ratio: Larger is better.

Level	Stack length (mm)	Stack position (mm)
1	1,624	-3,947
2	-2,006	-7,834
3	-7,246	-6,879
4	-10,250	
5	-13,221	
Delta	14,845	3,887

Table 4-10 presents the orthogonal array of simulation using the Taguchi design method. The design summary was two factors (2) each for the stack length and stack position, 15 total number of runs (15), one base blocks (1), and one total blocks (1). Five levels were for the stack length ranges from 25 mm to 65 mm while three levels were for the three-stack position of 30 mm, 40 mm, and 50 mm. The ΔT, and COP were parameters added in Minitab software to determine the signal-to-noise ratios.

Table 4-10: Orthogonal array of simulation using Taguchi design.

Std Order	Run Order	PtType	Blocks	Stack length (mm)	Stack position (mm)	Temperature difference (K)	COP	SNRA1
8	1	1	1	45	40	9.49	0.28	-8.05032
4	2	1	1	35	30	11.7	0.74	0.377596
6	3	1	1	35	50	2.3	0.5	-3.21084
11	4	1	1	55	40	14.6	0.132	-14.5786
2	5	1	1	25	40	6.36	0.84	1.420781
7	6	1	1	45	30	13.9	0.45	-3.93
10	7	1	1	55	30	10.8	0.23	-9.75711
15	8	1	1	65	50	9.6	0.15	-13.4689
13	9	1	1	65	30	14.8	0.19	-11.4153
3	10	1	1	25	50	3.7	0.6	-1.5394
1	11	1	1	25	30	8.5	1.27	4.990489
12	12	1	1	55	50	3	0.34	-6.41555
14	13	1	1	65	40	12.9	0.129	-14.7783
5	14	1	1	35	40	2.48	0.5	-3.18334
9	15	1	1	45	50	8	0.23	-9.75873

Figure 4-11 shows the main effects plot for the signal to noise ratio for the stack length and stack position. The generated chart illustrated the variation of the signal to noise ratio as function of the stack length and stack position. The stack length of 65 mm had a lower signal to noise ratio of -13,22 while the 25 mm stack length had a higher signal to noise

ratio of 1,624. Another higher signal to noise ratio of -3,947 generated for the 30 mm stack position.

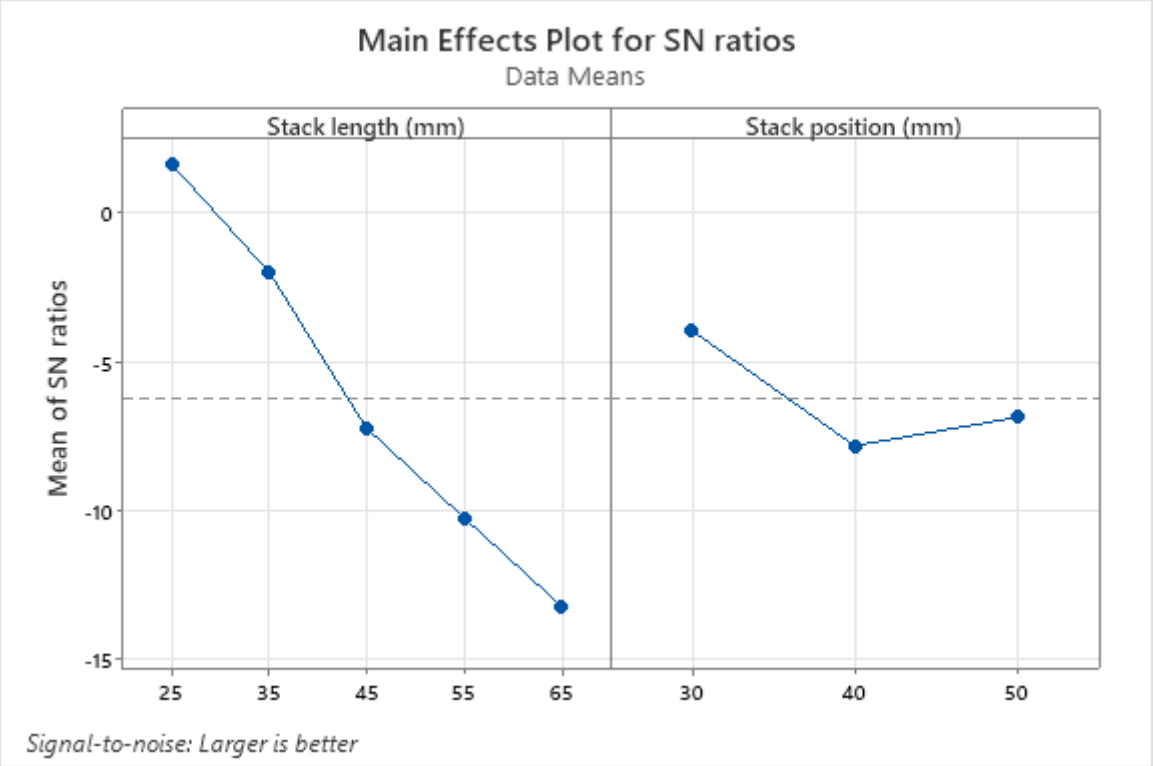

Figure 4-11: Main effects plot for signal-to-noise ratios (Simulation results).

Figure 4-12 presents the probability plot for the temperature difference (ΔT) and COP. To determine whether the numerical modelling method was effective by the data points following the normal distribution. The p-value of each parameter was compared to the significance level of 0.05. The p-value of temperature difference and coefficient of performance were 0.389 and 0.066 respectively which happened to be larger than the significance level of 0.05, hence the simulation method was effective, and the data points appeared to follow the normal distribution.

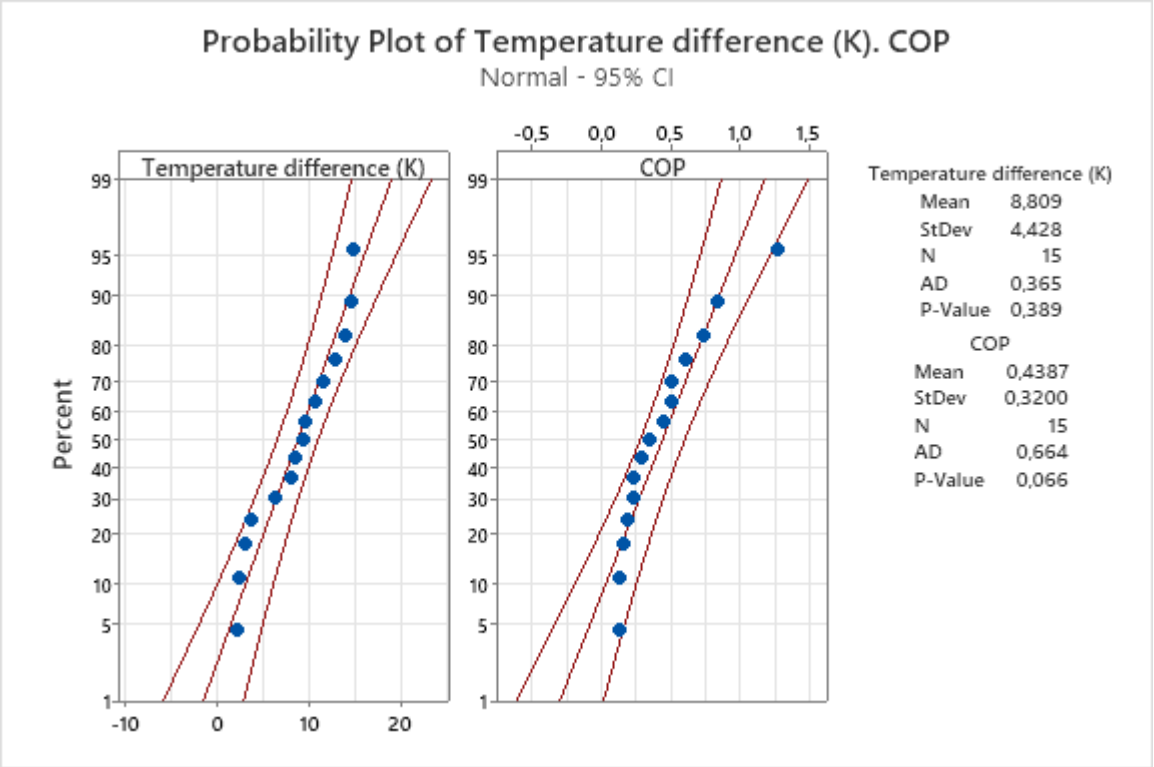

Figure 4-12: Probability plot of temperature difference and COP (Simulation results).

4.5 Summary

The experimental results of collected data and calculated parameters were presented in Tables 4-1, 4-2, and 4-3. The patterns of ΔT and COP are illustrated in Figures 4-1, 4-2, and 4-3. As for the numerical modelling results were presented in Tables 4-4, 4-5, and 4-6 and their patterns of ΔT and COP were illustrated in Figures 4-6, 4-7, and 4-8.

Optimisation based on experimental results is presented in Table 4-8. The main effects plot for signal to noise ratio and probability plot are presented in Figures 4-9, and 4-10. Optimisation based on numerical modelling results is presented in Table 4-10. The main effects plots for signal to noise ratio and probability plot were illustrated in Figures 4-11 and 4-12.

CHAPTER FIVE: DISCUSSIONS

5.1 Introduction

This section presents the discussion of outcomes of chapter four on the experimental work, numerical modelling and optimisation process of the five-stack length of 25 mm, 35 mm, 45 mm, 55 mm, and 65 mm being each positioned at 30 mm, 40 mm, and 50 mm.

5.2 Discussion of experimental results

The experimental discussion is split into three sections with each representing the stack position of 30 mm, 40 mm, and 50 mm.

5.2.1 Stack positioned at 30 mm

The five experiments produced five temperature difference (ΔT) across the stack length of 11°C, 12.8°C, 13.1°C, 10.9°C, and 10.3°C, and five COP of 0.1, 0.031, 0.016, 0.74, and 0.33. Both the ΔT and COP were for the five-stack length of 25 mm, 35 mm, 45 mm, 55 mm, and 65 mm, respectively, positioned each at one stack position of 30 mm. The ΔT increased with increase of stack length for the first three stack length of 25 mm, 35 mm, and 45 mm from 11°C to 12.8°C and then to 13.1°C. The ΔT deviation occurred at the 45 mm stack length where it decreased from 13.1°C to 10.9°C and then to 10.3°C for the last two stack length of 55 mm and 65 mm respectively. The COP decreased with increase of stack length for the first three stack lengths of 25 mm, 35 mm, and 45 mm from 0.1 to 0.031, and then to 0.016, then deviated at the 45 mm stack length where it increased to 0.74 at the 55 mm stack length then decreased to 0.33 at the last 65 mm stack length.

The ΔT and COP pattern variation were in reverse order, but both formed the zigzag shape. However, these outcomes were compared with the literature of this study. According to previous research conducted by Zolpakar *et al.* (2017) who investigated the effects of three different stack length made from the same material but positioned at one optimum stack position. They discovered that the ΔT decreased in descending order with increase of stack length. This was to say that shorter stack length yielded a higher ΔT and vice versa. As for the current experiments, the ΔT for the first three pattern increased instead decreasing which contradicted the findings, but for the last two pattern concurred with the author. Nevertheless, the increases in ΔT with increase of stack length contradicted what research by Zolpakar *et al.*

(2016) who evaluated the influence of three different stack position for one optimum stack length. Their findings revealed that the ∆T increased in ascending order with the increase of stack position that a smaller stack position produced a smaller ∆T and vice versa.

The pattern variation for the first three COP concurred with Rahpeima and Ebrahimi (2019) while the last two patterns did not, so the COP decreased with increase of stack length, thus shorter stack length produced a higher COP and vice versa. In general, the disarray in pattern variation might have been because of one of these parameters: The difference in temperature (T_1 -T_3) of inlet and outlet water fed through the coiled copper heat exchanger (cold) on the cooler side and fluid mass flow rate ($\dot{m}_C$) were (1.3°C, 0.2°C, 0.1°C, 2.2°C, and 0.6°C) and ($11.7.10^{-6}$, $6.9.10^{-6}$, 11.10^{-6}, $7.04.10^{-6}$, and $10.5.\ 10^{-6}$ Kg/s) while the difference in temperature (T_2 -T_4) and fluid mass flow rate ($\dot{m}_h$) on the warmer side were (7.1°C, 6.3°C, 9.3°C, 6°C, and 3.3°C) and ($22.7.10^{-6}$, $7.5.10^{-6}$, $7.7.10^{-6}$, $6.12.10^{-6}$, and $7.5.10^{-6}$ Kg/s) respectively. However, for the five experiments, their higher TAR performance occurred at the 55 mm stack length where the T_C, Q_C, COP, and ∆T were 24.1°C, 0.065 W, 0.74, and 10.9°C respectively.

5.2.2 Stack positioned at 40 mm

The five experiments produced five temperature difference (∆T) across the stack length of 7.1°C, 11.8°C, 9.1°C, 8.2°C, and 7.8°C, and five COP of 0.37, 0.32, 0.29, 0.09, and 0.42. Both the ∆T and COP were for the five-stack length of 25 mm, 35 mm, 45 mm, 55 mm, and 65 mm respectively, positioned each at one stack position of 40 mm. The ∆T increased from 7.1°C to 11.8°C starting at the 25 mm to 35 mm stack length where it deviated by decreasing in descending order from a higher of 11.8°C to a lower of 7.8°C with increase of stack length from 35 mm to 65 mm. The COP decreased in descending order from a higher of 0.37 to a lower of 0.09 with increase of stack length from 25 mm to 55 mm where it deviated by increasing to 0.42 at the 65 mm stack length.

The ∆T and COP had four patterns of data points both decreased as the stack length increased but formed a zigzag shape. The ∆T increased between the 25 mm and 35 mm stack length where it deviated by decreasing in descending order with increase of stack length to its maximum of 65 mm. Regardless of the shape obtained, the four last patterns out of five of ∆T concurred with the literature of this study. As in previous research conducted by Zolpakar *et al.* (2017) who evaluated the influence of three different stack length made from the same material but positioned at one optimum stack position. Their findings revealed what uncover in

the current experiments having the temperature difference across the stack length decreased with increase of stack length, so the smaller stack length produced a higher ΔT and vice and versa. As for the COP the decrease has been in descending order as the stack length increased starting at the 25 mm to 55 mm stack length where it deviated by increasing to the 65 mm stack length. It was noticed that four out of five COP patterns had agreed with Rahpeima and Ebrahimi (2019) who collaborated with Tartibu (2018) that the shorter stack length yielded a higher COP and vice versa.

There still unclear to the results of ΔT and COP to have one out of five patterns not concurring with the findings of the authors. However, the choice to which parameter to prioritize would depend on the circumstances. This might have been because of each of these parameters: the difference in temperature (T_1 -T_3) of inlet and outlet water fed through the coiled copper heat exchanger (cold) on the cooler side and fluid mass flow rate ($\dot{m}_C$) were (1.2°C, 1.8°C, 1.4°C, 0.7°C, and 1.8°C) and ($10.4.10^{-6}$, $5.2.10^{-6}$, $5.4.10^{-6}$, $7.5.10^{-6}$, and $7.2.10^{-6}$ Kg/s) while the difference in temperature (T_2 -T_4) and fluid mass flow rate ($\dot{m}_h$) on the warmer side were (4°C, 6.6°C, 3.4°C, 8.4°C, and 5°C) and ($11.6.10^{-6}$, $5.9.10^{-6}$, 10.10^{-6}, $5.2.10^{-6}$, and $8.76.10^{-6}$ kg/s) respectively. Nevertheless, for the five experiments, one achieved a higher TAR performance to have occurred at the 65 mm stack length where the T_C, Q_C, ΔT, and COP were 25.4°C, 0.054 W, 7.8°C and 0.42 respectively.

5.2.3 Stack positioned at 50 mm

The five experiments produced five temperature difference (ΔT) across the stack length of 8°C, 7.3°C, 7.6°C, 10.1°C, and 10.6°C, and five COP of 0.33, 0.32, 0.11, 0.44, and 0.07. Both the ΔT and COP were for the five-stack length of 25 mm, 35 mm, 45 mm, 55 mm, and 65 mm respectively, positioned each at one stack position of 50 mm. The ΔT decreased from 8°C to 7.3°C starting at the 25 mm to 35 mm stack length where it deviated by increasing to 7.6°C at the 45 mm stack length then to 10.1°C at the 55 mm stack length and finally to 10.6°C at the 65 mm stack length. The COP decreased from 0.33 to 0.32 and then to 0.11 for the first three stack length of 25 mm, 35 mm, and 45 mm where it deviated by increasing to 0.44 at the 55 mm stack length then decreased to its minimum at 0.07 at the 65 mm stack length.

The patterns variation of ΔT and COP increased and decreased as both had a zigzag shape. The outcomes of the current experiments were analysed with the literature of this study. The ΔT decreased between the 25 mm and 35 mm stack length which concurred with previous

research conducted by Zolpakar *et al.* (2017) who investigated the effects of three stack length made of same material but positioned at one optimum stack position. They noted that the temperature difference decreased with increase of stack length. This implied that the shorter stack length produced a higher ΔT and vice and versa. However, the increase in ΔT with increase of stack length between the 35 mm and 65 mm stack length may seem to have agreed with Zolpakar *et al.* (2016) although not. Their findings were that the ΔT increased with increase of stack position, this meant to say that a shorter stack position yielded a smaller ΔT and vice versa. The COP decreased with increase of stack length starting at the 25 mm to 45 mm, so three of five patterns agreed with Rahpeima and Ebrahimi (2019) who asserted that shorter stack length produced a higher COP and vice versa.

Nevertheless, the current findings still unclear but to have somehow contradicted with the literature. The cause of patterns deviation for both the COP and ΔT might have been influenced by one of these parameters: the difference in temperature (T_1 -T_3) of inlet and outlet water fed through the coiled copper heat exchanger (cold) and fluid mass flow rate ($\dot{m}_C$) on the cooler side were (1.5ºC, 1.1ºC, 1.1°C, 1.3°C, and 0.7°C) and ($8.5.10^{-6}$, $12.2.10^{-6}$, $10.4.10^{-6}$, $11.8.10^{-6}$, and $7.29.10^{-6}$ Kg/s) while the difference in temperature (T_2 -T_4) and fluid mass flow rate ($\dot{m}_h$) on the warmer side were (4.3°C, 4°C, 6.2°C, 4.4°C, and 6.2°C) and (12.10^{-6}, $13.6.10^{-6}$, $11.8.10^{-6}$, $12.3.10^{-6}$, and 12.10^{-6} Kg/s) respectively. As for the five experiments, one achieved a higher TAR performance at the 55 mm stack length where the T_C, Q_C, ΔT, and COP were 23.5°C, 0.069 W, 10.1°C, and 0.44 respectively.

5.3 Discussion of numerical modelling results

The numerical modelling of TARs was based on the quasi-steady state instead of transient behaviour. This was because of the boundary equations utilised in the computation domain. The time step was set to 0.01 seconds, and the output computation time was kept at 6 seconds because all simulated TARs became constant over that interval, as illustrated in Figure 4-5. Each computed simulation aimed to verify the experiment results shown in Tables 4-1, 4-2, and 4-3.

5.3.1 Stack positioned at 30 mm

The five simulated TARs with stack length positioned 30 mm away from the oscillatory boundary condition of the computation domain, have produced five temperature difference

(∆T) across the stack length of 8.51 K, 11.68 K, 13.98 K, 10.76 K, and 14.82 K and five COP of 1.27, 0.74, 0.45, 0.23, and 0.19. The ∆T and COP were for the five-stack length of 25 mm, 35 mm, 45 mm, 55 mm, and 65 mm respectively. The temperature difference increased from 8.51 K to 11.68 K and then to 13.98 K for the first three stack length of 25 mm, 35 mm, and 45 mm where it deviated at the last by decreasing to 10.76 K at the 55 mm stack length then increased to 14.82 K at the 65 mm stack length. Unlike the COP decreased in descending order as from a higher of 1.27 to a lower of 0.19 with increase of stack length starting at the 25 mm to 65 mm.

However, both the COP and ∆T did not have the same pattern variation, but in reverse order. It was observed that the patterns of ∆T increased with increase of stack length. The current findings seemed to contradict with Zolpakar *et al.* (2017) who investigated the effects of three different stack length of same material positioned each at one optimum stack position. Their outcomes were that the ∆T decreased in descending order with increase of stack length, as to say a shorter stack length yielded a higher ∆T and vice versa. In contrast with Zolpakar *et al.* (2016) who evaluated the influence of three different stack position for one optimum stack length. They discovered that the ∆T increased in ascending order with increase of stack position, so a smaller stack position produced a smaller ∆T and vice versa. As for the COP the decrease was in descending order to have formed a curve in shape with increase of stack length, as from a higher of 1.27 to a lower of 0.19. These findings concurred with Rahpeima and Ebrahimi (2019) who collaborated with Tartibu (2018) that shorter stack length produced a higher COP and vice versa.

However, to have the ∆T patterns deviated at one stack length might have been because of different amplitude pressure (P_A) input in each computation domain which varied between a lower of 49.2 Kpa to a higher of 69.4 Kpa. Nevertheless, for the five simulated TARs, one achieved a higher TAR performance to have occurred at the 25 mm stack length where the ∆T and COP were 8.51 K and 1.27, respectively.

5.3.2 Stack positioned at 40 mm

The five simulated TARs with stack length positioned 40 mm away from the oscillatory boundary condition of the computation domain, had produced five temperature difference (∆T) across the stack length of 6.36 K, 2.48 K, 9.49 K, 14.56 K and 12.91 K, and five COP of 0.84, 0.5, 0.28, 0.132, and 0.129. The ∆T and COP were for the five-stack length of 25 mm, 35 mm,

45 mm, 55 mm, and 65 mm respectively. The ∆T decreased from 6.36 K to 2.48 K between the 25 mm to 35 mm stack length then increased to 9.49 K and then to 14.56 K at the 55 mm stack length where it deviated by decreasing to 12.91 K at the 65 mm stack length. Unlike the COP decreased in descending order from a higher of 0.84 to a lower of 0.129 with increase of stack length, thus the pattern formed a curve in shape.

The ∆T and COP were in reverse order to the variation of patterns. As observed the temperature difference increased with increase of stack length even though deviated at some stack lengths. The decrease of ∆T between the 25 mm to 35 mm and 55 mm to 65 mm stack length may have agreed with previous research by Zolpakar *et al.* (2017) who investigated the effect of three different stack length positioned at one optimum stack position. They stated that the ∆T decreased in descending order with increase of stack length, so the smaller stack length yielded a higher ∆T and vice versa. As the increase of ∆T with increase of stack length between the 35 mm to 55 mm may have not agreed with previous research by Zolpakar *et al.* (2016) who evaluated the influence of three different stack position for one optimum stack length and stipulated that the ∆T increased in ascending order with increase of stack position, so to say that a smaller stack position produced a smaller ∆T and vice versa. The COP decreased with increase of stack length from shorter to larger with these current findings seemed to concur with the literature of this study by Rahpeima and Ebrahimi (2019) who asserted that a shorter stack length produced a higher COP and vice versa.

However, the deviation of ∆T still sceptical, perhaps that might have been caused by the different amplitude pressure (P_A) input in each computation domain having varied between a lower of 18.5 Kpa to a higher of 79.3 Kpa. As for the five simulated TARs, one achieved a higher TAR performance at the 25 mm stack length where the COP and ∆T were 0.84 and 6.36 K respectively.

5.3.3 Stack positioned at 50 mm

The five simulated TARs with stack length positioned 50 mm away from the oscillatory boundary condition of the computation domain, have produced five temperature difference (∆T) across the stack of 3.68 K, 2.31 K, 8.01 K, 2.96 K, and 9.56 K and five COP of 0.6, 0.5, 0.23, 0.34, and 0.15. The ∆T and COP were for the five-stack length of 25 mm, 35 mm, 45 mm, 55 mm, and 65 mm respectively. The ∆T decreased from 3.68 K to 2.31 K starting at the 25 mm to 35 mm stack length where it deviated by increasing to 8.01 K at the 45 mm stack

length then decreased to 2.96 K at the 55 mm stack length and then increased to 9.56 K at the 65 mm stack length forming a pattern of zigzag shape. In contrast to the COP the decrease from 0.6 to 0.23 noticed with increase of stack length starting at the 25 mm to 35 mm where it deviated by increasing to 0.34 then decreased to a minimum of 0.15 at the 65 mm stack length, hence formed a pattern of zigzag shape.

The ΔT and COP patterns had different variations but formed the zigzag shape. For the ΔT, there were a decrease and an increase occurring at each stack length interval between the 25 mm to 65 mm stack length. As for the decrease in ΔT with increase of stack length between the 25 mm to 35 mm and 45 mm to 55 mm happened to obey what research by Zolpakar *et al.* (2017) who stated the influence of different stack length for one stack position, which had the effect of ΔT decreasing with increase of stack length. This may have concurred with the authors even though not on a full range of stack length. As for the increase in ΔT with increase of stack length between the 35 mm to 45 mm and 55 mm to 65 mm may have contradicted these findings by Zolpakar *et al.* (2016) who stipulated the influence of different stack position for one stack length had the effect that the temperature difference increased with increase of stack position. So regardless of the deviation that occurred at the 45 mm to 55 mm stack length, the COP had four of five patterns agreeing with Rahpeima and Ebrahimi (2019) who collaborated with Tartibu (2018) to assert that shorter stack length produced a higher COP and vice versa.

The deviation of ΔT and COP might have been caused by the input of different amplitude pressure (P_A) in each computation domain which varied between a lower of 19.6 Kpa to a higher of 61.4 Kpa. As for the five simulated TARs, one had achieved a higher TAR performance at the shorter stack length of 25 mm where the COP and ΔT were 0.6 and 3.68 K respectively.

5.4 Discussion of outcomes of the optimisation process

The objective of the experiment was to analyse the performance of the prototype standing wave TAR. The larger is better as noise condition used to maximise the stack length and stack position. The optimisation was to identify among the stack length or stack position the factor with a higher delta value and a higher level of signal-to-noise ratio. The delta value determined the rank of the factor. The stack length ranked number 1 in Table 4-8 with a higher delta value of 10.36 and a higher signal-to-noise ratio of -19.55 at level 1, followed second by the stack position with a delta value of 6.75 and a higher signal-to-noise ratio of -21.74 at level 3. The

optimum performance of the experimental work occurred at the 25 mm stack length at a signal-to-noise ratio of -19,5728, as illustrated in Figure 4-9, where the ∆T, COP, TC and QC were 8°C, 0.33, 25.1°C, 0.0532 W, respectively. These current findings concurred with Tartibu (2018) who researched that shorter stack length produced a higher COP and vice versa, as for its optimum stack position was at 50 mm at a signal to noise ratio of -21.74 at level 3 which agreed with Zolpakar *et al.* (2016) who stipulated that larger stack position yielded a higher temperature difference. The probability plot provided in Figure 4-10 has been used to verify whether the optimisation method was effective. This was done by comparing the generated p-value of respective parameters with the significance level. So, their p-value were (∆T=0,324), (COP=0,104), (TC=0,867), and (Q_C=0,377) which were larger than the significance level of 0.05. Hence, the experimental work method determined to be effective having the data points followed the normal distribution.

Subsequently, to what was explained in the previous section of Taguchi's design of optimisation. So, this was emulated for the numerical modelling. The stack length ranked number 1 in Table 4-10 with a higher delta value of 14.845 and a higher signal-to-noise ratio of 1.624 at level 1, followed second by the stack position with a delta value of 3.887 and a higher signal-to-noise ratio of -3.947, at level 1 respectively. The optimum performance of numerical modelled TARs occurred at the 25 mm stack length at a signal to noise ratio of 1.624 at level 1 as illustrated in Figure 4-11 where the COP and ∆T were 1.27 and 8.5 K respectively. These current outcomes agreed with previous research conducted by Tartibu (2018) who asserted that shorter stack length produced a higher COP and vice versa, as its optimum stack position was at 30 mm at a signal noise ratio of -3.947 at level 1. As to previous research by Zolpakar *et al.* (2016) who investigated the influence of different stack position for one stack length and stipulated that smaller stack position yielded a smaller ∆T and vice versa. The probability plot provided in Figure 4-12 has been used to verify whether the optimisation method was effective. Based on the generated p-value of these two parameters, (∆T=0,389) and (COP=0,066) being larger than the significance level of 0.05. It was affirmed that the simulation method was effective, having the data points followed the normal distribution.

5.5 Summary

The respective stack position of 30 mm, 40 mm, and 50 mm had each five conducted experiments involving stack length ranges from 25 mm to 65 mm. There was one higher achieved TAR performance among each five experiments. However, each higher TAR performance occurred at different stack length of 55 mm, 65 mm, and 55 mm for the respective stack position of 30 mm, 40 mm, and 50 mm.

Each five experiments were compared by numerical modelling using commercial multiphysics software. There was one higher achieved TAR performance among each five simulated which occurred at the 25 mm stack length for the three respective stack position of 30 mm, 40 mm, and 50 mm.

The Taguchi design method used to optimise the stack length and stack position for the fifteen experimental work and numerical modelling. The experimental work had their optimal stack length occurred at the 25 mm stack length with an optimal stack position of 50 mm. As for the numerical modelling their optimal stack length occurred at the 25 mm stack length with an optimal stack position of 30 mm. However, both the experiment work and numerical modelling had a common optimal stack length of 25 mm but different stack position of 50 mm and 30 mm respectively.

CHAPTER SIX: CONCLUSIONS AND RECOMMENDATIONS

6.1 Conclusion

The objective of this research study was to evaluate the performance of a standing wave thermoacoustic refrigerator and optimise the stack length and stack position for a single stack material. Have done so, five 3D printed parallel plates stack manufactured from the polylactic acid (PLA) material had identical external core diameter of 104.6 mm and internal diameter of 102.6 mm, a gap spacing between two plates of 0.6 mm and plate thickness (th) of 0.5 mm. The five-stack length of 25 mm, 35 mm, 45 mm, 55 mm, and 65 mm had been each positioned at three different stack position of 30 mm, 40 mm, and 50 mm within a quarter-wavelength (λ/4) resonator tube manufactured from the polyvinyl chloride (PVC) material of inner diameter of 105.6 mm by 624 mm long. The helium as the working gas was pressurised at 110 Kpa into the resonator tube. Five experiments for the five-stack length had been conducted for each stack position. Each experiment had the coefficient of performance (COP), temperature difference (ΔT), cooling load (Q_C), cooling temperature (T_C) and overall coefficient of performance ($COP_{overall}$) determined.

Each experiment took place in a laboratory at controlled room temperature set to 22°C and lasted ninety minutes. Six temperature probes were utilised to measure and record the temperature variation. T_5 and T_6 on either side of the stack were for determining the temperature difference (ΔT) across the stack length. T_3 and T_1 at the inlet and outlet were for determining the cooling load (Q_C) of water fed through the coiled copper heat exchanger at the cold side of the stack whereas T_4 and T_2 at the inlet and outlet were for determining the heating load (Q_h) of water fed through the coiled copper heat exchanger at the warm side of the stack.

The first five conducted experiments of stack length positioned 30 mm away from the loudspeaker, had their one higher TAR performance occurred at the 55 mm stack length where the COP, ΔT, Q_C, T_C, and $COP_{overall}$ were 0.74, 10.9°C, 0.065 W, 24.1°C, and 0.00151 respectively. Then the second five conducted experiments of stack length positioned 40 mm away from the loudspeaker, had their one higher TAR performance occurred at the 65 mm stack length where the results were: (COP=0.42), (ΔT=7.8°C), (Q_C=0.054 W), (T_C =25.4°C), and ($COP_{overall}$ =0.0013). Lastly, the third five conducted experiments of stack length positioned 50 mm away from the loudspeaker, had their one higher TAR performance occurred at the 55 mm stack length where the results were: (COP=0.44), (ΔT=10.1°C), (Q_C=0.069 W), (T_C

=23.5°C), and ($COP_{overall}$=0.0016). However, each one of these five experiments have been compared by simulation using commercial multiphysics software.

The first five simulated TAR of stack length positioned 30 mm away from the oscillatory boundary condition, had their one higher TAR performance occurred at the 25 mm stack length (COP=1.27 and ΔT=8.5 K). Then the second five simulated TAR of stack length positioned 40 mm away from the oscillatory boundary condition, had their one higher TAR performance occurred at the 25 mm stack length where the COP and ΔT were 0.84 and 6.36 K respectively. Lastly, the third five simulated TAR of stack length positioned 50 mm away from the oscillatory boundary condition, had their one higher TAR performance occurred at the 25 mm stack length where the results were (COP=0.6) and (ΔT=3.7 K). It was concluded that for the fifteen simulated TAR regardless of the stack position, the one higher TAR performance occurred at the 25 mm stack length. Whereas for the fifteen conducted experiments the one higher TAR performance occurred at different stack length of 55 mm, 65 mm, and 55 mm for each of the stack position of 30 mm, 40 mm, and 50 mm respectively.

However, the stack length and stack position for both the experimental and simulation results were optimised using the Taguchi design method. These were evaluated by identifying the higher delta value and signal to noise ratio for either the stack length or stack position on the response table and verified their optimisation method with the probability plot whether effective. The optimum TAR performance for the fifteen conducted experiments occurred at the 25 mm stack length with an optimised stack position of 50 mm where the ΔT, COP, T_C Q_C, and signal-to-noise ratio were 8°C, 0.33, 25.1°C, 0.0532 W, and -19,5728 respectively. As for the fifteen simulated TAR their optimum TAR performance occurred at the 25 mm stack length with an optimised stack position of 30 mm where the ΔT, COP, and signal to noise ratio were 1.27, 8.5 K, and 4.990489 respectively. In summary, the experimental work and numerical modelling agreed regarding stack length. They both indicated an optimal stack length of 25 mm, suggesting that short stack lengths are good for a high COP while maintaining other performance metrics within acceptable ranges. The experimental work and numerical modelling differed on optimal stack position. As a result, this study could not uncover the influence of stack position, as far as optimising for a high COP is concerned.

6.2 Recommendations

- The daytime weather varied most of the time having the temperature not to remain constant. Hence, the experimental work could be further enhanced by incorporating a chamber that would not enable heat in or heat out of the system.
- The TAR design proposed in this research study could be improved by shortening the length of the larger tube to reserve the space uniquely for the stack and both the cold and hot heat exchangers. This may be done by removing the hot copper heat exchanger embedded in the tube thickness positioned at the upper end of each stack length in the computational domain.
- Air could be utilised as coolant in lieu of water which must be ventilated through the coiled copper heat exchangers (cold and hot).

REFERENCES

Ahmed Al-Mufti, O. & Janajreh, I. 2024. High fidelity analysis and optimization of a quarter wavelength thermo-acoustically driven refrigerator. *Energy Conversion and Management*, 299: 117884.

Alamir, M.A. 2019. Experimental study of the stack geometric parameters effect on the resonance frequency of a standing wave thermoacoustic refrigerator. *International Journal of Green Energy*, 16(8): 639–651.

Alamir, M.A. & Elamer, A.A. 2020. A compromise between the temperature difference and performance in a standing wave thermoacoustic refrigerator. *International Journal of Ambient Energy*, 41(13): 1441–1453.

Alcock, A.C., Tartibu, L.K. & Jen, T.C. 2018. Experimental investigation of an adjustable thermoacoustically-driven thermoacoustic refrigerator. *International Journal of Refrigeration*, 94: 71–86. https://doi.org/10.1016/j.ijrefrig.2018.07.015.

Alcock, A.C., Tartibu, L.K. & Jen, T.C. 2017. Experimental Investigation of Ceramic Substrates in Standing Wave Thermoacoustic Refrigerator. *Procedia Manufacturing*, 7: 79–85.

Bhatti, U.N. & Bashmal, S. 2021. Performance evaluation of a standing wave thermoacoustic refrigerator using normalized sensitivity coefficients. *Journal of Thermal Science and Engineering Applications*, 13(3).

Bhatti, U.N., Bashmal, S., Khan, S. & Ben-Mansour, R. 2020. Numerical Modeling and Performance Evaluation of Standing Wave Thermoacoustic Refrigerators with a Multi-Layered Stack. *Energies*, 13(17): 4360.

Chaiwongsa, P. & Wongwises, S. 2021. Effect of the blockage ratios of circular stack on the performance of the air-based standing wave thermoacoustic refrigerator using heat pipe. Case Studies in Thermal Engineering, 24: 100843. https://doi.org/10.1016/j.csite.2021.100843.

Gholamrezaei, M. & Ghorbanian, K. 2016. Thermal analysis of shell-and-tube thermoacoustic heat exchangers. *Entropy*, 18(8).

Kajurek, J., Rusowicz, A. & Grzebielec, A. 2019. Design and simulation of a small capacity thermoacoustic refrigerator. *SN Applied Sciences*, 1(6): 1–9. https://doi.org/10.1007/s42452-019-0569-2.

Napolitano, M., Romano, R. & Dragonetti, R. 2017. Open-cell foams for thermoacoustic applications. *Energy*, 138: 147–156. https://doi.org/10.1016/j.energy.2017.07.042.

Nathad, A., Ahmed, F., Khalid, M.O., Kumar, R. & Hafeez, H. 2019. Experimental Analysis of an Economical Lab Demonstration Prototype of a Thermo Acoustic Refrigerator (TAR). *Energy Procedia*, 157: 343–354.

Nathad, A., Ahmed, F., Osama Khalid, M., Kumar, R. & Hafeez, H. 2019. Experimental analysis of an economical lab demonstration prototype of a thermo acoustic refrigerator (TAR). *Energy Procedia*, 157: 343–354. https://doi.org/10.1016/j.egypro.2018.11.199.

Ong, J.Y., King, J.Y., Saw, L.H.. & Theng, K.K. 2019. Optimization of the Design Parameter for Standing Wave Thermoacoustic Refrigerator using Genetic Algorithm. IOP Conference Series: *Earth and Environmental Science*, 268(1): 012021.

Ozdemir, S.N., Taymaz, I., Okumuş, E., San, F.G.B. and Akgün, F 2023. Experimental investigation on performance evaluation of PEM electrolysis cell by using a Taguchi method. *Fuel*, 344: 128021.

Peng, Y., Feng, H. & Mao, X. 2018. Optimization of standing-wave thermoacoustic refrigerator stack using genetic algorithm. *International Journal of Refrigeration*, 92: 246–255. https://doi.org/10.1016/j.ijrefrig.2018.04.023.

Priyanga, R. & Muthadhi, A. 2023. Optimization of compressive strength of cementitious matrix composition of Textile Reinforced Concrete–Taguchi approach. *Results in Control and Optimization*, 10: 100205.

Rahman, A.A. & Zhang, X. 2019. Single-objective optimization for stack unit of standing wave thermoacoustic refrigerator through fruit fly optimization algorithm. *International Journal of Refrigeration*, 98: 35–41.

Rahpeima, R. & Ebrahimi, R. 2022. A numerical approach for optimization of the working fluid of a standing-wave thermo-acoustic refrigerator. *Engineering with Computers*, (0123456789). https://doi.org/10.1007/s00366-022-01646-1.

Rahpeima, R. & Ebrahimi, R. 2019. Numerical investigation of the effect of stack geometrical parameters and thermo-physical properties on performance of a standing wave thermoacoustic refrigerator. *Applied Thermal Engineering*, 149: 1203–1214. https://doi.org/10.1016/j.applthermaleng.2018.12.093.

Sarpero, E., Gourdon, E. & Borelli, D. 2023. Experimental development and optimization of a standing wave thermoacoustic refrigerator using additive manufactured stacks. *International Journal of Refrigeration*, 146: 63–73.

Shivakumara, N.V. & Bheemsha, A. 2021. Performance Analysis of Thermoacoustic Refrigerator of 10 W Cooling Power made up of Poly-Vinyl-Chloride for Different Parallel Plate Stacks by using Helium as a Working Fluid. *Journal of Thermal Science*, 30(6): 2037–2055.

Tartibu, L. 2018. Mathematical programming formulation for large-scale standing-wave thermo-acoustic refrigerator design optimization. In Proceedings of the International Conference on Industrial Engineering and Operations Management. Pretoria: IEOM Society International: 1165–1175.

Wang, Q., Shen, B., Huang, J., Yang, H., Pei, G. & Yang, H,. 2021. A spectral self-regulating parabolic trough solar receiver integrated with vanadium dioxide-based thermochromic coating. *Applied Energy*, 285.

Wantha, C. 2018. The impact of stack geometry and mean pressure on cold end temperature of stack in thermoacoustic refrigeration systems. *Heat and Mass Transfer/Waerme- und Stoffuebertragung,* 54(7): 2153–2161.

Zolpakar, N.A. & Mohd-Ghazali, N. 2016. Optimization of a thermoacoustic refrigerator with an evolutionary algorithm approach. *Jurnal Teknologi*, 78(9–2): 19–24.

Zolpakar, N.A., Mohd-Ghazali, N. & Ahmad, R. 2016. Experimental investigations of the performance of a standing wave thermoacoustic refrigerator based on multi-objective genetic algorithm optimized parameters. *Applied Thermal Engineering*, 100: 296–303.

Zolpakar, N.A., Mohd-Ghazali, N., Ahmad, R. & Maré, T. 2017. Performance of a 3D-printed Stack in a Standing Wave Thermoacoustic Refrigerator. *Energy Procedia*, 105: 1382–1387.

APPENDIX A: Calculated results of various output parameters

A.1 Stack positioned at 30 mm

- **Stack length of 25 mm**
  - $\dot{m}_{cooling} = 63.18\ g = 11.7.10^{-6}$ kg/s
  - $\dot{m}_{warmer} = 122.6\ g = 22.7\ 10^{-6}$ kg/s
  - $Q_C = \dot{m}_{cooling}.C_p.(T_1\text{-}T_3) = 11.7.10^{-6}.4.18.10^3.\ (297.45\text{-}296.15) = 0.064$ Watt
  - $Q_H = \dot{m}_{warmer.}C_p.(T_2\text{-}T_4) = 22.7\ 10^{-6}.\ 4.18.10^3.\ (306.05\text{-}298.95) = 0.673$ Watt
  - $COP = Q_C / (Q_H - Q_c) = 0.064 / (0.673 - 0.064) = 0.11$
  - $COP_{Overall} = Q_C / W_{electrical\text{-}Speaker} = 0.064 /43 = 0.0015$
- **Stack length of 35 mm**
  - $\dot{m}_{cooling} = 36.8\ g = 6.9.\ 10^{-6}$ kg/s
  - $\dot{m}_{warmer} = 40.5\ g = 7.5.\ 10^{-6}$ kg/s
  - $Q_C = \dot{m}_{cooling}.C_p.(T_1\text{-}T_3) = 6.9.\ 10^{-6}.\ 4.18.10^3.\ (297.25\text{-}297.05) = 0.006$ Watt
  - $Q_H = \dot{m}_{warmer.}C_p.(T_2\text{-}T_4) = 7.5.\ 10^{-6}.\ 4.18.10^3.\ (303.65\text{-}297.35) = 0.198$ Watt
  - $COP = Q_C / (Q_H - Q_c) = 0.006 / (0.0197\text{-}\ 0.006) = 0.031$
  - $COP_{Overall} = Q_C / W_{electrical\text{-}Speaker} = 0.006/37.5 = 0.00016$
- **Stack length of 45 mm**
  - $\dot{m}_{cooling} = 59.3\ g = 11.1.\ 10^{-6}$ kg/s
  - $\dot{m}_{warmer} = 41.7\ g = 7.7.\ 10^{-6}$ kg/s
  - $Q_C = \dot{m}_{cooling}.C_p.(T_1\text{-}T_3) = 11.1.\ 10^{-6}.\ 4.18.10^3.\ (298.15\text{-}298.05) = 0.0046$ Watt
  - $Q_H = \dot{m}_{warmer.}C_p.(T_2\text{-}T_4) = 7.7.\ 10^{-6}.\ 4.18.10^3.\ (307.15\text{-}297.85) = 0.299$ Watt
  - $COP = Q_C / (Q_H - Q_c) = 0.0046 / (0.299\text{-}0.0046) = 0.016$
  - $COP_{Overall} = Q_C / W_{electrical\text{-}Speaker} = 0.0046 / 39 = 0.00012$
- **Stack length of 55 mm**
  - $\dot{m}_{cooling} = 7.04.\ 10^{-6}$ kg/s
  - $\dot{m}_{warmer} = 6.12.\ 10^{-6}$ kg/s
  - $Q_C = \dot{m}_{cooling}.C_p.(T_1\text{-}T_3) = 7.04.\ 10^{-6}.\ 4.18.10^3.(297.25\text{-}295.05) = 0.065$ Watt
  - $Q_H = \dot{m}_{warmer.}C_p.(T_2\text{-}T_4) = 6.12.\ 10^{-6}.\ 4.18.10^3.(304.95\text{-}298.95) = 0.153$ Watt
  - $COP = Q_C / (Q_H - Q_c) = 0.065/ (0.153 - 0.065) = 0.74$
  - $COP_{Overall} = Q_C / W_{electrical\text{-}Speaker} = 0.065/43 = 0.0015$
- **Stack length of 65 mm**
  - $\dot{m}_{cooling} = 10.5.\ 10^{-6}$ kg/s

- $\dot{m}_{warmer} = 7.5.\ 10^{-6}$ kg/s
- $Q_C = \dot{m}_{cooling}.C_p.(T_1\text{-}T_3) = 10.5.\ 10^{-6}.\ 4.18.10^3.\ (296.15\text{-}295.55) = 0.026$ Watt
- $Q_H = \dot{m}_{warmer}.C_p.(T_2\text{-}T_4) = 7.5.\ 10^{-6}.\ 4.18.10^3.\ (303.35\text{-}300.05) = 0.103$ Watt
- $COP = Q_C / (Q_H - Q_c) = 0.026 / (0.103 - 0.026) = 0.33$
- $COP_{Overall} = Q_C / W_{electrical\text{-}Speaker} = 0.026 / 37.5 = 0.0007$

A.2 Stack positioned at 40 mm.

- **Stack length of 25 mm**
- $\dot{m}_{cooling} = 10.4.10^{-6}$ kg/s
- $\dot{m}_{warmer} = 11.6.\ 10^{-6}$ kg/s
- $Q_C = \dot{m}_{cooling}.C_p.(T_1\text{-}T_3) = 10.4.\ 10^{-6}.\ 4.18.10^3.(298.15\text{-}296.95) = 0.052$ Watt
- $Q_H = \dot{m}_{warmer}.C_p.(T_2\text{-}T_4) = 11.6.\ 10^{-6}.\ 4.18.10^3.(303.15\text{-}299.15) = 0.194$ Watt
- $COP = Q_C / (Q_H - Q_c) = 0.052 / (0.194 - 0.052) = 0.37$
- $COP_{Overall} = Q_C / W_{electrical\text{-}Speaker} = 0.052 / 43 = 0.0012$
- **Stack length of 35 mm**
- $\dot{m}_{cooling} = 5.2.\ 10^{-6}$ kg/s
- $\dot{m}_{warmer} = 5.9.\ 10^{-6}$ kg/s
- $Q_C = \dot{m}_{cooling}.C_p.(T_1\text{-}T_3) = 5.2.\ 10^{-6}.\ 4.18.10^3.(296.75\text{-}294.95) = 0.039$ Watt
- $Q_H = \dot{m}_{warmer}.C_p.(T_2\text{-}T_4) = 5.9.\ 10^{-6}.\ 4.18.10^3.(304.95\text{-}298.35) = 0.162$ Watt
- $COP = Q_C / (Q_H - Q_c) = 0.039 / (0.162\text{-}0.039) = 0.32$
- $COP_{Overall} = Q_C / W_{electrical\text{-}Speaker} = 0.039/43 = 0.0009$
- **Stack length of 45 mm**
- $\dot{m}_{cooling} = 5.4.\ 10^{-6}$ kg/s
- $\dot{m}_{warmer} = 10.\ 10^{-6}$ kg/s
- $Q_C = \dot{m}_{cooling}.C_p.(T_1\text{-}T_3) = 5.4.\ 10^{-6}.\ 4.18.10^3.(297.55\text{-}296.15) = 0.032$ Watt
- $Q_H = \dot{m}_{warmer}.C_p.(T_2\text{-}T_4) = 10.\ 10^{-6}.\ 4.18.10^3.(302.05\text{-}298.65) = 0.142$ Watt
- $COP = Q_C / (Q_H - Q_c) = 0.032 / (0.142 - 0.032) = 0.29$
- $COP_{Overall} = Q_C / W_{electrical\text{-}Speaker} = 0.032 / 37.5 = 0.00086$
- **Stack length of 55 mm**
- $\dot{m}_{cooling} = 7.5.\ 10^{-6}$ kg/s
- $\dot{m}_{warmer} = 5.2.\ 10^{-6}$ kg/s
- $Q_C = \dot{m}_{cooling}.C_p.(T_1\text{-}T_3) = 7.5.\ 10^{-6}.\ 4.18.10^3.(299.45\text{-}298.95) = 0.016$ Watt
- $Q_H = \dot{m}_{warmer}.C_p.(T_2\text{-}T_4) = 5.2.\ 10^{-6}.\ 4.18.10^3.(307.35\text{-}298.95) = 0.1826$ Watt

- $COP = Q_C / (Q_H – Q_c) = 0.016/ (0.183-0.016) = 0.09$
- $COP_{Overall} = Q_C / W_{electrical\text{-}Speaker} = 0.016/39 = 0.0004$

- **Stack length of 65 mm**

- $\dot{m}_{cooling} = 7.2.\ 10^{-6}$ kg/s
- $\dot{m}_{warmer} = 8.76.\ 10^{-6}$ kg/s
- $Q_C = \dot{m}_{cooling}.C_p.(T_1\text{-}T_3) = 7.2.\ 10^{-6}.\ 4.18.10^3.(298.55\text{-}296.75) = 0.054$ Watt
- $Q_H = \dot{m}_{warmer}.C_p.(T_2\text{-}T_4) = 8.76.\ 10^{-6}.\ 4.18.10^3.(303.15\text{-}298.15) = 0.1831$ Watt
- $COP = Q_C / (Q_H – Q_c) = 0.054/ (0.183\text{-}0.054) = 0.42$
- $COP_{Overall} = Q_C / W_{electrical\text{-}Speaker} = 0.054/ 43 = 0.0013$

A.3 Stack positioned at 50 mm.

- **Stack length of 25 mm**

- $\dot{m}_{cooling} = 8.5.\ 10^{-6}$ kg/s
- $\dot{m}_{warmer} = 12.\ 10^{-6}$ kg/s
- $Q_C = \dot{m}_{cooling}.C_p.(T_1\text{-}T_3) = 8.5.\ 10^{-6}.\ 4.18.10^3.(298.25\text{-}296.75) = 0.0532$ Watt
- $Q_H = \dot{m}_{warmer}.C_p.(T_2\text{-}T_4) = 12.\ 10^{-6}.\ 4.18.10^3.(304.25\text{-}299.95) = 0.216$ Watt
- $COP = Q_C / (Q_H – Q_c) = 0.0532/ (0.216\text{-}0.0532) = 0.32678$
- $COP_{Overall} = Q_C / W_{electrical\text{-}Speaker} = 0.0532/43 = 0.00123$

- **Stack length of 35 mm**

- $\dot{m}_{cooling} = 12.2.10^{-6}$ kg/s
- $\dot{m}_{warmer} = 13.6.10^{-6}$ kg/s
- $Q_C = \dot{m}_{cooling}.C_p.(T_1\text{-}T_3) = 12.2.\ 10^{-6}.\ 4.18.10^3.(297.15\text{-}296.05) = 0.0561$ Watt
- $Q_H = \dot{m}_{warmer}.C_p.(T_2\text{-}T_4) = 13.6.\ 10^{-6}.\ 4.18.10^3.(301.85\text{-}297.85) = 0.2274$ Watt
- $COP = Q_C / (Q_H – Q_c) = 0.0561 / (0.2274 \text{-}0.0561) = 0.32$
- $COP_{Overall} = Q_C / W_{electrical\text{-}Speaker} = 0.0561/41 = 0.00137$

- **Stack length of 45 mm**

- $\dot{m}_{cooling} = 10.4.10^{-6}$ kg/s
- $\dot{m}_{warmer} = 11.8.\ 10^{-6}$ kg/s
- $Q_C = \dot{m}_{cooling}.C_p.(T_1\text{-}T_3) = 10.4.10^{-6}.\ 4.18.10^3.(296.75\text{-}296.05) = 0.030$ Watt
- $Q_H = \dot{m}_{warmer}.C_p.(T_2\text{-}T_4) = 11.8.10^{-6}.\ 4.18.10^3.(303.25\text{-}297.05) = 0.306$ Watt
- $COP = Q_C / (Q_H – Q_c) = 0.030 / (0.306 \text{-}0.030) = 0.28$
- $COP_{Overall} = Q_C / W_{electrical\text{-}Speaker} = 0.030 / 39.1 = 0.00077$

- **Stack length of 55 mm**

- $\dot{m}_{cooling} = 11.8.\ 10^{-6}$ kg/s
- $\dot{m}_{warmer} = 12.3.\ 10^{-6}$ kg/s
- $Q_C = \dot{m}_{cooling}.C_p.(T_1\text{-}T_3) = 11.8.10^{-6}.\ 4.18.10^3.(296.75\text{-}295.35) = 0.069$ Watt
- $Q_H = \dot{m}_{warmer}.C_p.(T_2\text{-}T_4) = 12.3.10^{-6}.\ 4.18.10^3.(304.15\text{-}299.75) = 0.226$ Watt
- $COP = Q_C / (Q_H - Q_c) = 0.069/ (0.226\text{-}0.069) = 0.44$
- $COP_{Overall} = Q_C / W_{electrical\text{-}Speaker} = 0.069/43 = 0.0016$

- **Stack length of 65 mm**

- $\dot{m}_{cooling} = 7.29.\ 10^{-6}$ kg/s
- $\dot{m}_{warmer} = 12.\ 10^{-6}$ kg/s
- $Q_C = \dot{m}_{cooling}.C_p.(T_1\text{-}T_3) = 7.29.10^{-6}.\ 4.18.10^3.(296.75\text{-}296.05) = 0.021$ Watt
- $Q_H = \dot{m}_{warmer}.C_p.(T_2\text{-}T_4) = 12.10^{-6}.\ 4.18.10^3.(304.55\text{-}298.35) = 0.311$ Watt
- $COP = Q_C / (Q_H - Q_c) = 0.021/ (0.311\text{-}\ 0.021) = 0.072$
- $COP_{Overall} = Q_C / W_{electrical\text{-}Speaker} = 0.021/43 = 0.00049$

APPENDIX B: Details of collected data and calculated results of experimental work.

Table B1: Collected data and calculated experimental results of stack positioned at 30 mm

Stack length of 25 mm							
Start	**End**	**Time**	**I**	**V**	**W_{in}**	**T_{room}**	
10:34	12:04	1h30	1.1 A	39.1 V	43 W	22°C	
T_1	**T_2**	**T_3**	**T_4**	**T_5**	**T_6**	**ΔT**	
22.7	23.3	23.7	23.6	24.8	24.9	**Start**	
24.3	32.9	23	25.8	24.8	35.8	11	
$\dot{m}_C$	**$\dot{m}_h$**	**Q_C**	**Q_H**	**COP**	**$COP_{Overall}$**	**P_m**	**P_A**
11.7. 10^{-6}	22.7. 10^{-6}	0.064 W	0.673 W	0.1	0.00149	110.5 Kpa	68.1 Kpa
Stack length of 35 mm							
Start	**End**	**Time**	**I**	**V**	**W_{in}**	**T_{room}**	
10:19	11:49	1h30	1 A	37.5 V	37.35 W	22°C	
T_1	**T_2**	**T_3**	**T_4**	**T_5**	**T_6**	**ΔT**	
25	25	25.3	24.1	25.7	27.3	**Start**	
24.1	30.5	23.9	24.2	25.1	37.9	12.8	
$\dot{m}_C$	**$\dot{m}_h$**	**Q_C**	**Q_H**	**COP**	**$COP_{Overall}$**	**P_m**	**P_A**
6.9. 10^{-6}	7.5. 10^{-6}	0.006 W	0.199 W	0.031	0.00016	111.3 Kpa	68.9 Kpa

Stack length of 45 mm

Start	End	Time	I	V	W_{in}	T_{room}	
12:41	14:11	1h30	1 A	39 V	39 W	22°C	
T_1	T_2	T_3	T_4	T_5	T_6	ΔT	
23.6	30	23.6	24	25.4	29.2	**Start**	
25	34	24.9	24.7	26	39.1	13.1	
$\dot{m}_C$	$\dot{m}_h$	Q_C	Q_H	COP	$COP_{Overall}$	P_m	P_A
11. 10^{-6}	7.7. 10^{-6}	0.0046 W	0.299 W	0.016	0.00012	110.8 Kpa	69.4 Kpa

Stack length of 55 mm

Start	End	Time	I	V	W_{in}	T_{room}	
14:49	16:38	1h49	1.1 A	39.1 V	43 W	22°C	
T_1	T_2	T_3	T_4	T_5	T_6	ΔT	
23.8	28.3	23.3	25.5	24.5	32.6	**Start**	
24.1	31.8	21.9	25.8	24.6	35.5	10.9	
$\dot{m}_C$	$\dot{m}_h$	Q_C	Q_H	COP	$COP_{Overall}$	P_m	P_A
7.04. 10^{-6}	6.12. 10^{-6}	0.065 W	0.153 W	0.74	0.00151	111 Kpa	49.2 Kpa

Stack length of 65 mm

Start	End	Time	I	V	W_{in}	T_{room}	
11:52	13:38	1h46	1 A	37.5 V	37.5 W	22°C	
T_1	T_2	T_3	T_4	T_5	T_6	ΔT	
22.7	22.7	22.2	23.5	23.7	24.8	**Start**	
23	30.2	22.4	26.9	24.6	34.9	10.3	
$\dot{m}_C$	$\dot{m}_h$	Q_C	Q_H	COP	$COP_{Overall}$	P_m	P_A

10.5. 10^{-6}	7.5. 10^{-6}	0.026 W	0.103 W	0.33	0.0007	110.3 Kpa	62.5 Kpa

Table B2: Collected data and calculated experimental results of stack positioned at 40 mm

Stack length of 25 mm							
Start	**End**	**Time**	**I**	**V**	**W_{in}**	**T_{room}**	
11:38	13:08	1h30	1.1 A	39.1 V	43 W	22°C	
T_1	**T_2**	**T_3**	**T_4**	**T_5**	**T_6**	**ΔT**	
23.8	23.8	24.6	24.4	24.7	25	**Start**	
25	30	23.8	26	24.5	31.6	7.1	
$\dot{m}_C$	**$\dot{m}_h$**	**Q_C**	**Q_H**	**COP**	**$COP_{Overall}$**	**P_m**	**P_A**
$10.4.10^{-6}$	$11.6.10^{-6}$	0.052 W	0.194 W	0.37	0.0012	111 Kpa	60 Kpa
Stack length of 35 mm							
Start	**End**	**Time**	**I**	**V**	**W_{in}**	**T_{room}**	
12:37	14:09	1h32	1.1 A	39.1 V	43 W	22°C	
T_1	**T_2**	**T_3**	**T_4**	**T_5**	**T_6**	**ΔT**	
22.8	22.7	23.6	22.2	24	25.3	**Start**	
23.6	31.8	21.8	25.2	24.3	36.1	11.8	
$\dot{m}_C$	**$\dot{m}_h$**	**Q_C**	**Q_H**	**COP**	**$COP_{Overall}$**	**P_m**	**P_A**
$5.2.10^{-6}$	$5.9.10^{-6}$	0.039 W	0.162 W	0.32	0.0009	111.5 Kpa	18.5 Kpa
Stack length of 45 mm							
Start	**End**	**Time**	**I**	**V**	**W_{in}**	**T_{room}**	
11:24	12:58	1h34	1 A	37.5 V	37.5 W	22°C	

T_1	T_2	T_3	T_4	T_5	T_6	ΔT	
22.5	22.8	23.2	23.2	24	24.5	**Start**	
24.4	28.9	23	25.5	25.1	34.2	9.1	
$\dot{m}_C$	$\dot{m}_h$	Q_C	Q_H	**COP**	$COP_{Overall}$	P_m	P_A
$5.4.10^{-6}$	10.10^{-6}	0.032 W	0.142 W	0.29	0.00086	113 Kpa	60.2 Kpa

Stack length of 55 mm

Start	**End**	**Time**	**I**	**V**	W_{in}	T_{room}	
15:01	16:31	1h30	1 A	39 V	39 W	22°C	
T_1	T_2	T_3	T_4	T_5	T_6	ΔT	
25.7	27.5	25.8	25.5	27.6	30.9	**Start**	
26.3	34.2	25.6	25.8	30.5	38.7	8.2	
$\dot{m}_C$	$\dot{m}_h$	Q_C	Q_H	**COP**	$COP_{Overall}$	P_m	P_A
$7.5.10^{-6}$	$5.2.10^{-6}$	0.016 W	0.1826 W	0.09	0.0004	111.9 Kpa	79.3 Kpa

Stack length of 65 mm

Start	**End**	**Time**	**I**	**V**	W_{in}	T_{room}	
15:19	16:49	1h30	1.1 A	39.1 V	39.1 W	22°C	
T_1	T_2	T_3	T_4	T_5	T_6	ΔT	
21.6	28.5	23	24.7	24.8	32.6	**Start**	
25.4	30	23.6	25	25.4	33.2	7.8	
$\dot{m}_C$	$\dot{m}_h$	Q_C	Q_H	**COP**	$COP_{Overall}$	P_m	P_A
$7.2.10^{-6}$	$8.76.10^{-6}$	0.054 W	0.1831 W	0.42	0.0013	111.1 Kpa	64.4 Kpa

Table B3: Collected data and calculated experimental results of stack positioned at 50 mm.

Stack length of 25 mm							
Start	**End**	**Time**	**I**	**V**	**W_{in}**	**T_{room}**	
12:49	14:19	1h30	1.1 A	39.1 V	43 W	22°C	
T_1	**T_2**	**T_3**	**T_4**	**T_5**	**T_6**	**ΔT**	
24.3	25.7	23	23.3	24.8	28.5	**Start**	
25.1	31.1	23.6	26.8	26.2	34.2	8	
$\dot{m}_C$	**$\dot{m}_h$**	**Q_C**	**Q_H**	**COP**	**$COP_{Overall}$**	**P_m**	**P_A**
$8.5.10^{-6}$	12.10^{-6}	0.0532 W	0.216 W	0.33	0.0012	110.1Kpa	44.7 Kpa
Stack length of 35 mm							
Start	**End**	**Time**	**I**	**V**	**W_{in}**	**T_{room}**	
14:30	16:00	1h30	1.1 A	37.3 V	41 W	22°C	
T_1	**T_2**	**T_3**	**T_4**	**T_5**	**T_6**	**ΔT**	
23.9	25.5	22.7	23.5	24.6	27.9	**Start**	
24	28.7	22.9	24.7	24.8	32.1	7.3	
$\dot{m}_C$	**$\dot{m}_h$**	**Q_C**	**Q_H**	**COP**	**$COP_{Overall}$**	**P_m**	**P_A**
$12.2.10^{-6}$	$13.6.10^{-6}$	0.056 W	0.227 W	0.32	0.00137	111 Kpa	21.4 Kpa
Stack length of 45 mm							
Start	**End**	**Time**	**I**	**V**	**W_{in}**	**T_{room}**	
15:05	16:36	1h36	1 A	39.1 V	39.1 W	22°C	
T_1	**T_2**	**T_3**	**T_4**	**T_5**	**T_6**	**ΔT**	
22.4	23.9	23.6	23.6	25.6	25.3	**Start**	
22.2	30.1	21.1	23.9	23.1	30.7	7.6	

$\dot{m}_C$	$\dot{m}_h$	Q_C	Q_H	COP	$COP_{Overall}$	P_m	P_A
$10.4.10^{-6}$	$11.8.10^{-6}$	0.030 W	0.306 W	0.11	0.00077	111.7Kpa	61.4 Kpa

Stack length of 55 mm

Start	End	Time	I	V	W_{in}	T_{room}	
12:57	14:31	1h34	1.1 A	39.1 V	43 W	22°C	
T_1	T_2	T_3	T_4	T_5	T_6	ΔT	
23.6	23.3	21.8	23	23.7	26.6	**Start**	
23.5	31	22.2	26.6	23.7	33.8	10.1	
$\dot{m}_C$	$\dot{m}_h$	Q_C	Q_H	COP	$COP_{Overall}$	P_m	P_A
$11.8.10^{-6}$	$12.3.10^{-6}$	0.069 W	0.226 W	0.44	0.0016	111.1 Kpa	19.6 Kpa

Stack length of 65 mm

Start	End	Time	I	V	W_{in}	T_{room}	
11:34	13:13	1h39	1.1 A	39.1 V	43 W	22°C	
T_1	T_2	T_3	T_4	T_5	T_6	ΔT	
23.1	23	23.7	23.3	25.2	24.9	**Start**	
23.6	31.4	22.9	25.2	23.7	34.3	10.6	
$\dot{m}_C$	$\dot{m}_h$	Q_C	Q_H	COP	$COP_{Overall}$	P_m	P_A
$7.29.10^{-6}$	12.10^{-6}	0.021 W	0.311 W	0.07	0.00049	110.5 Kpa	60.1 Kpa

APPENDIX C: Excel data for experiments results.

C.1 Stacks positioned at 30 mm.

Table C.1.1: Stack length of 25 mm: Temperature range: T1-T4

5268	2024/02/23 12:02	24.3	32.5	22.7	25.6
5269	2024/02/23 12:02	24.3	32.5	22.7	25.6
5270	2024/02/23 12:02	24.3	32.4	22.7	25.6
5271	2024/02/23 12:02	24.3	32.4	22.7	25.6
5272	2024/02/23 12:02	24.3	32.4	22.7	25.6
5273	2024/02/23 12:02	24.3	32.4	22.7	25.6
5274	2024/02/23 12:03	24.3	32.4	22.7	25.6
5275	2024/02/23 12:03	24.3	32.2	22.7	25.6
5276	2024/02/23 12:03	24.3	32.2	22.7	25.6
5277	2024/02/23 12:03	24.3	32.2	22.7	25.6
5278	2024/02/23 12:03	24.3	32.2	22.7	25.6
5279	2024/02/23 12:03	24.3	32.2	22.7	25.6
5280	2024/02/23 12:03	24.3	32.2	22.7	25.6
5281	2024/02/23 12:03	24.3	32.1	22.7	25.6
5282	2024/02/23 12:03	24.3	32.1	22.7	25.6
5283	2024/02/23 12:03	24.3	32.1	22.7	25.6
5284	2024/02/23 12:03	24.3	32.1	22.7	25.6
5285	2024/02/23 12:03	24.3	32.1	22.7	25.6
5286	2024/02/23 12:03	24.3	32.2	22.7	25.6
5287	2024/02/23 12:03	24.3	32.2	22.7	25.6
5288	2024/02/23 12:03	24.3	32.2	22.7	25.6
5289	2024/02/23 12:03	24.3	32.2	22.7	25.6
5290	2024/02/23 12:03	24.3	32.2	22.7	25.6
5291	2024/02/23 12:03	24.3	32.2	22.7	25.6
5292	2024/02/23 12:03	24.3	32.2	22.7	25.6
5293	2024/02/23 12:03	24.3	32.2	22.7	25.6
5294	2024/02/23 12:03	24.3	32.2	22.7	25.7
5295	2024/02/23 12:03	24.3	32.2	22.7	25.7
5296	2024/02/23 12:03	24.3	32.4	22.7	25.7
5297	2024/02/23 12:03	24.3	32.4	22.7	25.7
5298	2024/02/23 12:03	24.3	32.4	22.7	25.7
5299	2024/02/23 12:03	24.3	32.4	22.7	25.7
5300	2024/02/23 12:03	24.3	32.4	22.7	25.7
5301	2024/02/23 12:03	24.3	32.4	22.7	25.7
5302	2024/02/23 12:03	24.3	32.4	22.7	25.7
5303	2024/02/23 12:03	24.3	32.4	22.7	25.7
5304	2024/02/23 12:03	24.3	32.4	22.7	25.7
5305	2024/02/23 12:03	24.3	32.4	22.7	25.7
5306	2024/02/23 12:03	24.3	32.4	22.7	25.7
5307	2024/02/23 12:03	24.3	32.4	22.7	25.7
5308	2024/02/23 12:03	24.3	32.4	22.7	25.7
5309	2024/02/23 12:03	24.3	32.4	22.7	25.7
5310	2024/02/23 12:03	24.3	32.4	22.7	25.7
5311	2024/02/23 12:03	24.3	32.4	22.7	25.7
5312	2024/02/23 12:03	24.3	32.4	22.7	25.7
5313	2024/02/23 12:03	24.3	32.4	22.7	25.7
5314	2024/02/23 12:03	24.3	32.4	22.7	25.7
5315	2024/02/23 12:03	24.3	32.4	22.7	25.8
5316	2024/02/23 12:03	24.3	32.4	22.7	25.8
5317	2024/02/23 12:03	24.3	32.4	22.7	25.8
5318	2024/02/23 12:03	24.3	32.4	22.8	25.8
5319	2024/02/23 12:03	24.3	32.4	22.8	25.8
5320	2024/02/23 12:03	24.3	32.4	22.8	25.8
5321	2024/02/23 12:03	24.3	32.4	22.8	25.8
5322	2024/02/23 12:03	24.3	32.5	22.8	25.8
5323	2024/02/23 12:03	24.3	32.5	22.8	25.8
5324	2024/02/23 12:03	24.3	32.5	23.0	25.8
5325	2024/02/23 12:03	24.3	32.5	23.0	25.8
5326	2024/02/23 12:03	24.3	32.5	23.0	25.8
5327	2024/02/23 12:03	24.3	32.7	23.0	25.8
5328	2024/02/23 12:03	24.3	32.7	23.0	25.8
5329	2024/02/23 12:03	24.3	32.7	23.0	25.8
5330	2024/02/23 12:03	24.3	32.7	23.0	25.7
5331	2024/02/23 12:03	24.3	32.7	23.0	25.7
5332	2024/02/23 12:03	24.3	32.7	23.0	25.7
5333	2024/02/23 12:03	24.3	32.9	23.0	25.7
5334	2024/02/23 12:04	24.3	32.9	23.0	25.7
5335	2024/02/23 12:04	24.3	32.9	23.0	25.8
5336	2024/02/23 12:04	24.3	32.9	23.0	25.8

Table C.1.2: Stack length of 25 mm: Temperature range: T5-T6

5322	2024/02/23 12:03	24.8	35.7	- - -
5323	2024/02/23 12:03	24.8	35.7	- - -
5324	2024/02/23 12:03	24.8	35.7	- - -
5325	2024/02/23 12:03	24.8	35.7	- - -
5326	2024/02/23 12:03	24.8	35.7	- - -
5327	2024/02/23 12:03	24.8	35.7	- - -
5328	2024/02/23 12:03	24.8	35.7	- - -
5329	2024/02/23 12:03	24.8	35.7	- - -
5330	2024/02/23 12:03	24.8	35.7	- - -
5331	2024/02/23 12:03	24.8	35.7	- - -
5332	2024/02/23 12:03	24.8	35.7	- - -
5333	2024/02/23 12:03	24.8	35.7	- - -
5334	2024/02/23 12:03	24.8	35.7	- - -
5335	2024/02/23 12:03	24.8	35.7	- - -
5336	2024/02/23 12:03	24.8	35.7	- - -
5337	2024/02/23 12:03	24.8	35.7	- - -
5338	2024/02/23 12:03	24.8	35.7	- - -
5339	2024/02/23 12:03	24.8	35.7	- - -
5340	2024/02/23 12:03	24.8	35.7	- - -
5341	2024/02/23 12:03	24.8	35.7	- - -
5342	2024/02/23 12:03	24.8	35.7	- - -
5343	2024/02/23 12:03	24.8	35.7	- - -
5344	2024/02/23 12:03	24.8	35.7	- - -
5345	2024/02/23 12:03	24.8	35.7	- - -
5346	2024/02/23 12:03	24.8	35.7	- - -
5347	2024/02/23 12:03	24.8	35.7	- - -
5348	2024/02/23 12:03	24.8	35.8	- - -
5349	2024/02/23 12:03	24.8	35.8	- - -
5350	2024/02/23 12:03	24.8	35.8	- - -
5351	2024/02/23 12:03	24.8	35.9	- - -
5352	2024/02/23 12:03	24.8	35.9	- - -
5353	2024/02/23 12:03	24.8	35.9	- - -
5354	2024/02/23 12:03	24.8	35.9	- - -
5355	2024/02/23 12:03	24.8	35.9	- - -
5356	2024/02/23 12:03	24.8	35.9	- - -
5357	2024/02/23 12:03	24.8	35.8	- - -
5358	2024/02/23 12:03	24.8	35.8	- - -
5359	2024/02/23 12:03	24.8	35.8	- - -
5360	2024/02/23 12:03	24.8	35.8	- - -
5361	2024/02/23 12:03	24.8	35.8	- - -
5362	2024/02/23 12:03	24.8	35.8	- - -
5363	2024/02/23 12:03	24.8	35.8	- - -
5364	2024/02/23 12:03	24.8	35.8	- - -
5365	2024/02/23 12:03	24.8	35.8	- - -
5366	2024/02/23 12:03	24.8	35.8	- - -
5367	2024/02/23 12:03	24.8	35.8	- - -
5368	2024/02/23 12:03	24.8	35.8	- - -
5369	2024/02/23 12:03	24.8	35.9	- - -
5370	2024/02/23 12:03	24.8	35.9	- - -
5371	2024/02/23 12:03	24.8	35.9	- - -
5372	2024/02/23 12:03	24.8	35.9	- - -
5373	2024/02/23 12:03	24.8	35.9	- - -
5374	2024/02/23 12:03	24.8	35.9	- - -
5375	2024/02/23 12:04	24.8	35.8	- - -
5376	2024/02/23 12:04	24.8	35.8	- - -
5377	2024/02/23 12:04	24.8	35.8	- - -
5378	2024/02/23 12:04	24.8	35.7	- - -
5379	2024/02/23 12:04	24.8	35.7	- - -
5380	2024/02/23 12:04	24.8	35.7	- - -
5381	2024/02/23 12:04	24.8	35.8	- - -
5382	2024/02/23 12:04	24.8	35.8	- - -
5383	2024/02/23 12:04	24.8	35.8	- - -
5384	2024/02/23 12:04	24.8	35.7	- - -
5385	2024/02/23 12:04	24.8	35.7	- - -
5386	2024/02/23 12:04	24.8	35.7	- - -
5387	2024/02/23 12:04	24.8	35.8	- - -

Table C1.3: Stack length of 25 mm: Voltage and current.

479	39.1 V	1.1 A	23/02/24 11:55:16		
480	39.1 V	1.1 A	23/02/24 11:55:26		
481	39.1 V	1.1 A	23/02/24 11:55:36		
482	39.1 V	1.1 A	23/02/24 11:55:46		
483	39.1 V	1.1 A	23/02/24 11:55:56		
484	39.1 V	1.1 A	23/02/24 11:56:06		
485	39.1 V	1.1 A	23/02/24 11:56:16		
486	39.1 V	1.1 A	23/02/24 11:56:26		
487	39.1 V	1.1 A	23/02/24 11:56:36		
488	39.1 V	1.1 A	23/02/24 11:56:46		
489	39.1 V	1.1 A	23/02/24 11:56:56		
490	39.1 V	1.1 A	23/02/24 11:57:06		
491	39.1 V	1.1 A	23/02/24 11:57:16		
492	39.1 V	1.1 A	23/02/24 11:57:26		
493	39.1 V	1.1 A	23/02/24 11:57:36		
494	39.1 V	1.1 A	23/02/24 11:57:46		
495	39.1 V	1.1 A	23/02/24 11:57:56		
496	39.1 V	1.1 A	23/02/24 11:58:06		
497	39.0 V	1.1 A	23/02/24 11:58:16		
498	39.0 V	1.1 A	23/02/24 11:58:26		
499	39.1 V	1.1 A	23/02/24 11:58:36		
500	39.0 V	1.1 A	23/02/24 11:58:46		
501	39.0 V	1.1 A	23/02/24 11:58:56		
502	39.1 V	1.1 A	23/02/24 11:59:06		
503	39.1 V	1.1 A	23/02/24 11:59:16		
504	39.1 V	1.1 A	23/02/24 11:59:26		
505	39.1 V	1.1 A	23/02/24 11:59:36		
506	39.1 V	1.1 A	23/02/24 11:59:46		
507	39.1 V	1.1 A	23/02/24 11:59:56		
508	39.1 V	1.1 A	23/02/24 12:00:06		
509	39.0 V	1.1 A	23/02/24 12:00:16		
510	39.1 V	1.1 A	23/02/24 12:00:26		
511	39.1 V	1.1 A	23/02/24 12:00:36		
512	39.1 V	1.1 A	23/02/24 12:00:46		
513	39.1 V	1.1 A	23/02/24 12:00:56		
514	39.1 V	1.1 A	23/02/24 12:01:06		
515	39.1 V	1.1 A	23/02/24 12:01:16		
516	39.1 V	1.1 A	23/02/24 12:01:26		
517	39.1 V	1.1 A	23/02/24 12:01:36		
518	39.0 V	1.1 A	23/02/24 12:01:46		
519	39.1 V	1.1 A	23/02/24 12:01:56		
520	39.1 V	1.1 A	23/02/24 12:02:06		
521	39.1 V	1.1 A	23/02/24 12:02:16		
522	39.1 V	1.1 A	23/02/24 12:02:26		
523	39.1 V	1.1 A	23/02/24 12:02:36		
524	39.1 V	1.1 A	23/02/24 12:02:46		
525	39.0 V	1.1 A	23/02/24 12:02:56		
526	39.1 V	1.1 A	23/02/24 12:03:06		
527	39.1 V	1.1 A	23/02/24 12:03:16		
528	39.0 V	1.1 A	23/02/24 12:03:26		
529	39.1 V	1.1 A	23/02/24 12:03:36		
530	39.1 V	1.1 A	23/02/24 12:03:46		
531	39.0 V	1.1 A	23/02/24 12:03:56		
532	39.1 V	1.1 A	23/02/24 12:04:06		
533	39.0 V	1.1 A	23/02/24 12:04:16		
534	39.1 V	1.1 A	23/02/24 12:04:26		
535	39.1 V	1.1 A	23/02/24 12:04:36		
536	39.1 V	1.1 A	23/02/24 12:04:46		
537	39.1 V	1.1 A	23/02/24 12:04:56		
538	39.1 V	1.1 A	23/02/24 12:05:06		

Table C1.4: Stack length of 25 mm: Mean pressure.

5941	2/23/2024	12:10:37	65.8	kpa		
5942	2/23/2024	12:10:39	65.8	kpa		
5943	2/23/2024	12:10:41	65.8	kpa		
5944	2/23/2024	12:10:43	65.8	kpa		
5945	2/23/2024	12:10:45	65.8	kpa		
5946	2/23/2024	12:10:47	65.8	kpa		
5947	2/23/2024	12:10:49	65.8	kpa		
5948	2/23/2024	12:10:51	65.7	kpa		
5949	2/23/2024	12:10:53	65.7	kpa		
5950	2/23/2024	12:10:55	65.7	kpa		
5951	2/23/2024	12:10:57	65.7	kpa		
5952	2/23/2024	12:10:59	65.7	kpa		
5953	2/23/2024	12:11:01	65.7	kpa		
5954	2/23/2024	12:11:03	65.7	kpa		
5955	2/23/2024	12:11:05	65.7	kpa		
5956	2/23/2024	12:11:07	65.7	kpa		
5957	2/23/2024	12:11:09	65.7	kpa		
5958	2/23/2024	12:11:11	65.6	kpa		
5959	2/23/2024	12:11:13	65.6	kpa		
5960	2/23/2024	12:11:15	65.6	kpa		
5961	2/23/2024	12:11:17	65.6	kpa		
5962	2/23/2024	12:11:19	65.6	kpa		
5963	2/23/2024	12:11:21	65.6	kpa		
5964	2/23/2024	12:11:23	65.6	kpa		
5965	2/23/2024	12:11:25	65.6	kpa		
5966	2/23/2024	12:11:27	65.5	kpa		
5967	2/23/2024	12:11:29	65.5	kpa		
5968	2/23/2024	12:11:31	65.5	kpa		
5969	2/23/2024	12:11:33	65.5	kpa		
5970	2/23/2024	12:11:35	65.5	kpa		
5971	2/23/2024	12:11:37	65.5	kpa		
5972	2/23/2024	12:11:39	65.5	kpa		
5973	2/23/2024	12:11:41	65.5	kpa		
5974	2/23/2024	12:11:43	65.5	kpa		
5975	2/23/2024	12:11:45	65.4	kpa		
5976	2/23/2024	12:11:47	65.4	kpa		
5977	2/23/2024	12:11:49	65.4	kpa		
5978	2/23/2024	12:11:51	65.4	kpa		
5979	2/23/2024	12:11:53	65.4	kpa		
5980	2/23/2024	12:11:55	65.4	kpa		
5981	2/23/2024	12:11:57	65.4	kpa		
5982	2/23/2024	12:11:59	65.4	kpa		
5983	2/23/2024	12:12:01	65.4	kpa		
5984	2/23/2024	12:12:03	65.4	kpa		
5985	2/23/2024	12:12:05	65.4	kpa		
5986	2/23/2024	12:12:07	65.3	kpa		
5987	2/23/2024	12:12:09	65.3	kpa		
5988	2/23/2024	12:12:11	65.3	kpa		
5989	2/23/2024	12:12:13	65.3	kpa		
5990	2/23/2024	12:12:15	65.3	kpa		
5991	2/23/2024	12:12:17	65.3	kpa		
5992	2/23/2024	12:12:19	65.3	kpa		
5993	2/23/2024	12:12:21	65.3	kpa		
5994	2/23/2024	12:12:23	65.3	kpa		
5995	2/23/2024	12:12:25	65.3	kpa		
5996	2/23/2024	12:12:27	65.2	kpa		
5997	2/23/2024	12:12:29	65.2	kpa		
5998	2/23/2024	12:12:31	65.2	kpa		
5999	2/23/2024	12:12:33	65.2	kpa		
6000	2/23/2024	12:12:35	65.2	kpa		
6001	2/23/2024	12:12:37	65.2	kpa		
6002	2/23/2024	12:12:39	65.1	kpa		
6003	2/23/2024	12:12:41	65.1	kpa		
6004	2/23/2024	12:12:43	65.1	kpa		
6005	2/23/2024	12:12:45	65.1	kpa		
6006	2/23/2024	12:12:47	65.1	kpa		
6007	2/23/2024	12:12:49	65.1	kpa		

Table C1.5: Stack length of 35 mm: Temperature range: T1-T4

5269	2024/02/08 11:48	24,1	30,3	23,9	24,1
5270	2024/02/08 11:48	24,1	30,3	23,9	24,1
5271	2024/02/08 11:48	24,1	30,3	23,9	24,3
5272	2024/02/08 11:48	24,1	30,3	23,9	24,3
5273	2024/02/08 11:48	24,1	30,3	23,9	24,3
5274	2024/02/08 11:48	24,1	30,2	23,9	24,3
5275	2024/02/08 11:48	24,1	30,2	23,9	24,3
5276	2024/02/08 11:48	24,1	30,2	23,9	24,3
5277	2024/02/08 11:48	24,1	30,2	23,9	24,3
5278	2024/02/08 11:48	24,1	30,2	23,9	24,3
5279	2024/02/08 11:48	24,1	30,3	23,9	24,3
5280	2024/02/08 11:48	24,1	30,3	23,9	24,3
5281	2024/02/08 11:48	24,1	30,3	23,9	24,3
5282	2024/02/08 11:48	24,1	30,3	23,9	24,3
5283	2024/02/08 11:48	24,1	30,3	23,9	24,3
5284	2024/02/08 11:48	24,1	30,3	23,9	24,3
5285	2024/02/08 11:48	24,1	30,2	23,9	24,3
5286	2024/02/08 11:48	24,1	30,2	23,9	24,3
5287	2024/02/08 11:48	24,1	30,2	23,9	24,3
5288	2024/02/08 11:48	24,1	30,2	23,9	24,3
5289	2024/02/08 11:48	24,1	30,2	23,9	24,3
5290	2024/02/08 11:48	24,1	30,3	23,9	24,3
5291	2024/02/08 11:48	24,1	30,3	23,9	24,3
5292	2024/02/08 11:48	24,1	30,3	23,9	24,3
5293	2024/02/08 11:48	24,1	30,3	23,9	24,3
5294	2024/02/08 11:48	24,1	30,3	23,9	24,3
5295	2024/02/08 11:48	24,1	30,2	23,9	24,3
5296	2024/02/08 11:48	24,1	30,2	23,9	24,3
5297	2024/02/08 11:48	24,1	30,2	23,9	24,3
5298	2024/02/08 11:48	24,1	30,2	23,9	24,3
5299	2024/02/08 11:48	24,1	30,2	23,9	24,3
5300	2024/02/08 11:48	24,1	30,3	23,9	24,3
5301	2024/02/08 11:48	24,1	30,3	23,9	24,3
5302	2024/02/08 11:48	24,1	30,3	23,9	24,3
5303	2024/02/08 11:48	24,1	30,3	23,9	24,3
5304	2024/02/08 11:48	24,1	30,3	23,9	24,3
5305	2024/02/08 11:48	24,1	30,2	23,9	24,3
5306	2024/02/08 11:48	24,1	30,2	23,9	24,3
5307	2024/02/08 11:48	24,1	30,2	23,9	24,3
5308	2024/02/08 11:48	24,1	30,2	23,9	24,2
5309	2024/02/08 11:48	24,1	30,2	23,9	24,2
5310	2024/02/08 11:48	24,1	30,2	23,9	24,2
5311	2024/02/08 11:48	24,1	30,3	23,9	24,2
5312	2024/02/08 11:48	24,1	30,3	23,9	24,2
5313	2024/02/08 11:48	24,1	30,3	23,9	24,2
5314	2024/02/08 11:48	24,1	30,3	23,9	24,2
5315	2024/02/08 11:48	24,1	30,3	23,9	24,2
5316	2024/02/08 11:48	24,1	30,2	23,9	24,2
5317	2024/02/08 11:48	24,1	30,2	23,9	24,2
5318	2024/02/08 11:48	24,1	30,2	23,9	24,2
5319	2024/02/08 11:48	24,1	30,2	23,9	24,2
5320	2024/02/08 11:48	24,1	30,2	23,9	24,2
5321	2024/02/08 11:48	24,1	30,3	23,9	24,2
5322	2024/02/08 11:48	24,1	30,3	23,9	24,2
5323	2024/02/08 11:48	24,1	30,3	23,9	24,2
5324	2024/02/08 11:48	24,1	30,3	23,9	24,2
5325	2024/02/08 11:48	24,1	30,3	23,9	24,2
5326	2024/02/08 11:48	24,1	30,4	23,9	24,2
5327	2024/02/08 11:49	24,1	30,4	23,9	24,2
5328	2024/02/08 11:49	24,1	30,4	23,9	24,2
5329	2024/02/08 11:49	24,1	30,4	23,9	24,2
5330	2024/02/08 11:49	24,1	30,4	23,9	24,2
5331	2024/02/08 11:49	24,1	30,4	23,9	24,2
5332	2024/02/08 11:49	24,1	30,5	23,9	24,2

Table C1.6: Stack length of 35 mm: Temperature range: T5-T6

5267	2024/02/08 11:48	25	37,8	- - -	- - -
5268	2024/02/08 11:48	25	37,8	- - -	- - -
5269	2024/02/08 11:48	25	37,9	- - -	- - -
5270	2024/02/08 11:48	25	37,9	- - -	- - -
5271	2024/02/08 11:48	25	37,9	- - -	- - -
5272	2024/02/08 11:48	25	37,9	- - -	- - -
5273	2024/02/08 11:48	25	37,9	- - -	- - -
5274	2024/02/08 11:48	25	37,9	- - -	- - -
5275	2024/02/08 11:48	25	37,9	- - -	- - -
5276	2024/02/08 11:48	25	37,9	- - -	- - -
5277	2024/02/08 11:48	25	37,9	- - -	- - -
5278	2024/02/08 11:48	25	37,9	- - -	- - -
5279	2024/02/08 11:48	25	37,9	- - -	- - -
5280	2024/02/08 11:48	25	37,9	- - -	- - -
5281	2024/02/08 11:48	25	37,9	- - -	- - -
5282	2024/02/08 11:48	25	37,9	- - -	- - -
5283	2024/02/08 11:48	25	37,9	- - -	- - -
5284	2024/02/08 11:48	25	37,9	- - -	- - -
5285	2024/02/08 11:48	25	37,9	- - -	- - -
5286	2024/02/08 11:48	25	37,9	- - -	- - -
5287	2024/02/08 11:48	25	37,9	- - -	- - -
5288	2024/02/08 11:48	25	37,9	- - -	- - -
5289	2024/02/08 11:48	25	37,9	- - -	- - -
5290	2024/02/08 11:48	25	37,9	- - -	- - -
5291	2024/02/08 11:48	25	37,9	- - -	- - -
5292	2024/02/08 11:48	25	37,9	- - -	- - -
5293	2024/02/08 11:48	25	37,9	- - -	- - -
5294	2024/02/08 11:48	25	37,9	- - -	- - -
5295	2024/02/08 11:48	25	37,9	- - -	- - -
5296	2024/02/08 11:48	25	37,9	- - -	- - -
5297	2024/02/08 11:48	25	37,9	- - -	- - -
5298	2024/02/08 11:48	25,1	37,9	- - -	- - -
5299	2024/02/08 11:48	25,1	37,9	- - -	- - -
5300	2024/02/08 11:48	25,1	37,9	- - -	- - -
5301	2024/02/08 11:49	25,1	37,9	- - -	- - -
5302	2024/02/08 11:49	25,1	37,9	- - -	- - -
5303	2024/02/08 11:49	25,1	37,9	- - -	- - -
5304	2024/02/08 11:49	25	37,9	- - -	- - -
5305	2024/02/08 11:49	25	37,9	- - -	- - -
5306	2024/02/08 11:49	25	37,9	- - -	- - -
5307	2024/02/08 11:49	25	37,9	- - -	- - -
5308	2024/02/08 11:49	25	37,9	- - -	- - -
5309	2024/02/08 11:49	25	37,9	- - -	- - -
5310	2024/02/08 11:49	25	37,9	- - -	- - -
5311	2024/02/08 11:49	25	37,9	- - -	- - -
5312	2024/02/08 11:49	25	37,9	- - -	- - -
5313	2024/02/08 11:49	25,1	37,9	- - -	- - -

Table C1.7: Stack length of 35 mm: Voltage and current

469	37.3 V	1.0 A	08/02/24 11:38:35		
470	37.3 V	1.0 A	08/02/24 11:38:45		
471	37.3 V	1.0 A	08/02/24 11:38:55		
472	37.3 V	1.0 A	08/02/24 11:39:05		
473	37.5 V	1.0 A	08/02/24 11:39:15		
474	37.3 V	1.0 A	08/02/24 11:39:25		
475	37.3 V	1.0 A	08/02/24 11:39:35		
476	37.3 V	1.0 A	08/02/24 11:39:45		
477	37.3 V	1.0 A	08/02/24 11:39:55		
478	37.3 V	1.0 A	08/02/24 11:40:05		
479	37.3 V	1.0 A	08/02/24 11:40:15		
480	37.3 V	1.0 A	08/02/24 11:40:25		
481	37.5 V	1.0 A	08/02/24 11:40:35		
482	37.5 V	1.0 A	08/02/24 11:40:45		
483	37.3 V	1.0 A	08/02/24 11:40:55		
484	37.3 V	1.0 A	08/02/24 11:41:05		
485	37.3 V	1.0 A	08/02/24 11:41:15		
486	37.3 V	1.0 A	08/02/24 11:41:25		
487	37.3 V	1.0 A	08/02/24 11:41:35		
488	37.5 V	1.0 A	08/02/24 11:41:45		
489	37.3 V	1.0 A	08/02/24 11:41:55		
490	37.3 V	1.0 A	08/02/24 11:42:05		
491	37.3 V	1.0 A	08/02/24 11:42:15		
492	37.3 V	1.0 A	08/02/24 11:42:25		
493	37.3 V	1.0 A	08/02/24 11:42:35		
494	37.5 V	1.0 A	08/02/24 11:42:45		
495	37.3 V	1.0 A	08/02/24 11:42:55		
496	37.3 V	1.0 A	08/02/24 11:43:05		
497	37.3 V	1.0 A	08/02/24 11:43:15		
498	37.3 V	1.0 A	08/02/24 11:43:25		
499	37.3 V	1.0 A	08/02/24 11:43:35		
500	37.3 V	1.0 A	08/02/24 11:43:45		
501	37.3 V	1.0 A	08/02/24 11:43:55		
502	37.3 V	1.0 A	08/02/24 11:44:05		
503	37.3 V	1.0 A	08/02/24 11:44:15		
504	37.5 V	1.0 A	08/02/24 11:44:25		
505	37.3 V	1.0 A	08/02/24 11:44:35		
506	37.3 V	1.0 A	08/02/24 11:44:45		
507	37.5 V	1.0 A	08/02/24 11:44:55		
508	37.5 V	1.0 A	08/02/24 11:45:05		
509	37.3 V	1.0 A	08/02/24 11:45:15		
510	37.3 V	1.0 A	08/02/24 11:45:25		
511	37.3 V	1.0 A	08/02/24 11:45:35		
512	37.3 V	1.0 A	08/02/24 11:45:45		
513	37.3 V	1.0 A	08/02/24 11:45:55		
514	37.3 V	1.0 A	08/02/24 11:46:05		
515	37.3 V	1.0 A	08/02/24 11:46:15		
516	37.3 V	1.0 A	08/02/24 11:46:25		
517	37.3 V	1.0 A	08/02/24 11:46:35		
518	37.3 V	1.0 A	08/02/24 11:46:45		
519	37.3 V	1.0 A	08/02/24 11:46:55		
520	37.3 V	1.0 A	08/02/24 11:47:05		
521	37.3 V	1.0 A	08/02/24 11:47:15		
522	37.3 V	1.0 A	08/02/24 11:47:25		
523	37.3 V	1.0 A	08/02/24 11:47:35		
524	37.3 V	1.0 A	08/02/24 11:47:45		
525	37.5 V	1.0 A	08/02/24 11:47:55		
526	37.3 V	1.0 A	08/02/24 11:48:05		
527	37.3 V	1.0 A	08/02/24 11:48:15		
528	37.3 V	1.0 A	08/02/24 11:48:25		
529	37.3 V	1.0 A	08/02/24 11:48:35		
530	37.3 V	1.0 A	08/02/24 11:48:45		
531	37.5 V	1.0 A	08/02/24 11:48:55		

Table C1.8: Stack length of 35 mm: Mean pressure

15454	2024/02/08	11:50:27	000069.5	kpa
15455	2024/02/08	11:50:29	000069.5	kpa
15456	2024/02/08	11:50:31	000069.5	kpa
15457	2024/02/08	11:50:33	000069.5	kpa
15458	2024/02/08	11:50:35	000069.5	kpa
15459	2024/02/08	11:50:37	000069.5	kpa
15460	2024/02/08	11:50:39	000069.5	kpa
15461	2024/02/08	11:50:41	000069.5	kpa
15462	2024/02/08	11:50:43	000069.4	kpa
15463	2024/02/08	11:50:45	000069.4	kpa
15464	2024/02/08	11:50:47	000069.4	kpa
15465	2024/02/08	11:50:49	000069.4	kpa
15466	2024/02/08	11:50:51	000069.4	kpa
15467	2024/02/08	11:50:53	000069.4	kpa
15468	2024/02/08	11:50:55	000069.4	kpa
15469	2024/02/08	11:50:57	000069.4	kpa
15470	2024/02/08	11:50:59	000069.4	kpa
15471	2024/02/08	11:51:01	000069.3	kpa
15472	2024/02/08	11:51:03	000069.3	kpa
15473	2024/02/08	11:51:05	000069.3	kpa
15474	2024/02/08	11:51:07	000069.3	kpa
15475	2024/02/08	11:51:09	000069.3	kpa
15476	2024/02/08	11:51:11	000069.3	kpa
15477	2024/02/08	11:51:13	000069.3	kpa
15478	2024/02/08	11:51:15	000069.3	kpa
15479	2024/02/08	11:51:17	000069.3	kpa
15480	2024/02/08	11:51:19	000069.3	kpa
15481	2024/02/08	11:51:21	000069.2	kpa
15482	2024/02/08	11:51:23	000069.2	kpa
15483	2024/02/08	11:51:25	000069.2	kpa
15484	2024/02/08	11:51:27	000069.2	kpa
15485	2024/02/08	11:51:29	000069.2	kpa
15486	2024/02/08	11:51:31	000069.2	kpa
15487	2024/02/08	11:51:33	000069.2	kpa
15488	2024/02/08	11:51:35	000069.2	kpa
15489	2024/02/08	11:51:37	000069.1	kpa
15490	2024/02/08	11:51:39	000069.1	kpa
15491	2024/02/08	11:51:41	000069.1	kpa
15492	2024/02/08	11:51:43	000069.1	kpa
15493	2024/02/08	11:51:45	000069.1	kpa
15494	2024/02/08	11:51:47	000069.1	kpa
15495	2024/02/08	11:51:49	000069.1	kpa
15496	2024/02/08	11:51:51	000069.1	kpa
15497	2024/02/08	11:51:53	000069.1	kpa
15498	2024/02/08	11:51:55	000069.1	kpa
15499	2024/02/08	11:51:57	000069.1	kpa
15500	2024/02/08	11:51:59	000069.0	kpa
15501	2024/02/08	11:52:01	000069.0	kpa
15502	2024/02/08	11:52:03	000069.0	kpa
15503	2024/02/08	11:52:05	000069.0	kpa
15504	2024/02/08	11:52:07	000069.0	kpa
15505	2024/02/08	11:52:09	000069.0	kpa
15506	2024/02/08	11:52:11	000069.0	kpa
15507	2024/02/08	11:52:13	000069.0	kpa
15508	2024/02/08	11:52:15	000068.9	kpa
15509	2024/02/08	11:52:17	000068.9	kpa
15510	2024/02/08	11:52:19	000068.9	kpa
15511	2024/02/08	11:52:21	000068.9	kpa
15512	2024/02/08	11:52:23	000068.9	kpa
15513	2024/02/08	11:52:25	000068.9	kpa
15514	2024/02/08	11:52:27	000068.9	kpa
15515	2024/02/08	11:52:29	000068.9	kpa

Table C1.9: Stack length of 45 mm: Temperature rang: T1-T4

3596	2024/02/08 14:10	25.0	34.1	24.9	24.7
3597	2024/02/08 14:10	25.0	34.1	24.9	24.7
3598	2024/02/08 14:10	25.0	34.1	24.9	24.7
3599	2024/02/08 14:10	25.0	34.1	24.9	24.7
3600	2024/02/08 14:10	25.0	34.1	24.9	24.7
3601	2024/02/08 14:10	25.0	34.1	24.8	24.7
3602	2024/02/08 14:11	25.0	34.1	24.8	24.7
3603	2024/02/08 14:11	25.0	34.1	24.8	24.7
3604	2024/02/08 14:11	25.0	34.1	24.8	24.7
3605	2024/02/08 14:11	25.0	34.1	24.8	24.7
3606	2024/02/08 14:11	25.0	34.1	24.8	24.7
3607	2024/02/08 14:11	25.0	34.1	24.8	24.7
3608	2024/02/08 14:11	25.0	34.1	24.8	24.7
3609	2024/02/08 14:11	25.0	34.1	24.8	24.7
3610	2024/02/08 14:11	25.0	34.0	24.8	24.7
3611	2024/02/08 14:11	25.0	34.0	24.8	24.7
3612	2024/02/08 14:11	25.0	34.0	24.8	24.7
3613	2024/02/08 14:11	25.0	34.0	24.8	24.7
3614	2024/02/08 14:11	25.0	34.0	24.8	24.7
3615	2024/02/08 14:11	25.0	34.0	24.8	24.7
3616	2024/02/08 14:11	25.0	33.9	24.8	24.7
3617	2024/02/08 14:11	25.0	33.9	24.8	24.7
3618	2024/02/08 14:11	25.0	33.9	24.8	24.7
3619	2024/02/08 14:11	25.0	33.9	24.8	24.7
3620	2024/02/08 14:11	25.0	33.9	24.8	24.7
3621	2024/02/08 14:11	25.0	33.8	24.8	24.7
3622	2024/02/08 14:11	25.0	33.8	24.8	24.7
3623	2024/02/08 14:11	25.0	33.8	24.8	24.7
3624	2024/02/08 14:11	25.0	33.8	24.8	24.7
3625	2024/02/08 14:11	25.0	33.8	24.8	24.7
3626	2024/02/08 14:11	25.0	33.8	24.8	24.7
3627	2024/02/08 14:11	25.0	33.8	24.9	24.7
3628	2024/02/08 14:11	25.0	33.8	24.9	24.7
3629	2024/02/08 14:11	25.0	33.8	24.9	24.7
3630	2024/02/08 14:11	25.0	33.8	24.9	24.7
3631	2024/02/08 14:11	25.0	33.8	24.9	24.7
3632	2024/02/08 14:11	25.0	33.8	24.9	24.7
3633	2024/02/08 14:11	25.0	33.8	24.9	24.7
3634	2024/02/08 14:11	25.0	33.8	24.9	24.7
3635	2024/02/08 14:11	25.0	33.8	24.9	24.7
3636	2024/02/08 14:11	25.0	33.8	24.9	24.7
3637	2024/02/08 14:11	25.0	33.8	24.9	24.7
3638	2024/02/08 14:11	25.0	33.8	24.9	24.7
3639	2024/02/08 14:11	25.0	33.8	24.9	24.7
3640	2024/02/08 14:11	25.0	33.8	24.9	24.7
3641	2024/02/08 14:11	25.0	33.8	24.9	24.7
3642	2024/02/08 14:11	25.0	33.8	24.9	24.7
3643	2024/02/08 14:11	25.0	33.8	24.9	24.7
3644	2024/02/08 14:11	25.0	33.8	24.9	24.7
3645	2024/02/08 14:11	25.0	33.8	24.9	24.7
3646	2024/02/08 14:11	25.0	33.8	24.9	24.7
3647	2024/02/08 14:11	25.0	33.8	24.9	24.7
3648	2024/02/08 14:11	25.0	33.8	24.9	24.7
3649	2024/02/08 14:11	25.0	33.8	24.9	24.7
3650	2024/02/08 14:11	25.0	33.8	24.9	24.7
3651	2024/02/08 14:11	25.0	33.8	24.9	24.7
3652	2024/02/08 14:11	25.0	34.0	24.9	24.7
3653	2024/02/08 14:11	25.0	34.0	24.9	24.7
3654	2024/02/08 14:11	25.0	34.0	24.9	24.7
3655	2024/02/08 14:11	25.0	34.0	24.9	24.7
3656	2024/02/08 14:11	25.0	34.0	24.9	24.7
3657	2024/02/08 14:11	25.0	34.0	24.9	24.7
3658	2024/02/08 14:11	25.0	34.0	24.9	24.7
3659	2024/02/08 14:11	25.0	34.0	24.9	24.7
3660	2024/02/08 14:11	25.0	34.0	24.9	24.7

Table C1.10: Stack length of 45 mm: Temperature range: T5-T6

5295	2024/02/08 14:10	25.8	39.1	- - -	- - -	
5296	2024/02/08 14:10	25.8	39.1	- - -	- - -	
5297	2024/02/08 14:10	25.8	39.1	- - -	- - -	
5298	2024/02/08 14:10	25.8	39.1	- - -	- - -	
5299	2024/02/08 14:10	25.8	39.1	- - -	- - -	
5300	2024/02/08 14:10	25.8	39.1	- - -	- - -	
5301	2024/02/08 14:10	25.8	39.1	- - -	- - -	
5302	2024/02/08 14:10	25.8	39.1	- - -	- - -	
5303	2024/02/08 14:10	25.8	39.1	- - -	- - -	
5304	2024/02/08 14:10	25.8	39.1	- - -	- - -	
5305	2024/02/08 14:10	25.8	39.1	- - -	- - -	
5306	2024/02/08 14:10	25.8	39.1	- - -	- - -	
5307	2024/02/08 14:10	25.8	39.1	- - -	- - -	
5308	2024/02/08 14:10	25.7	39.1	- - -	- - -	
5309	2024/02/08 14:10	25.7	39.1	- - -	- - -	
5310	2024/02/08 14:10	25.7	39.1	- - -	- - -	
5311	2024/02/08 14:10	25.8	39.1	- - -	- - -	
5312	2024/02/08 14:10	25.8	39.1	- - -	- - -	
5313	2024/02/08 14:11	25.8	39.1	- - -	- - -	
5314	2024/02/08 14:11	25.9	39.1	- - -	- - -	
5315	2024/02/08 14:11	25.9	39.1	- - -	- - -	
5316	2024/02/08 14:11	25.9	39.1	- - -	- - -	
5317	2024/02/08 14:11	26.0	39.1	- - -	- - -	
5318	2024/02/08 14:11	26.0	39.1	- - -	- - -	
5319	2024/02/08 14:11	26.0	39.1	- - -	- - -	
5320	2024/02/08 14:11	26.0	39.1	- - -	- - -	
5321	2024/02/08 14:11	26.0	39.1	- - -	- - -	
5322	2024/02/08 14:11	26.0	39.1	- - -	- - -	
5323	2024/02/08 14:11	26.0	39.1	- - -	- - -	
5324	2024/02/08 14:11	26.0	39.1	- - -	- - -	
5325	2024/02/08 14:11	26.0	39.1	- - -	- - -	
5326	2024/02/08 14:11	25.9	39.1	- - -	- - -	
5327	2024/02/08 14:11	25.9	39.1	- - -	- - -	
5328	2024/02/08 14:11	25.9	39.1	- - -	- - -	
5329	2024/02/08 14:11	25.8	39.1	- - -	- - -	
5330	2024/02/08 14:11	25.8	39.1	- - -	- - -	
5331	2024/02/08 14:11	25.8	39.1	- - -	- - -	
5332	2024/02/08 14:11	25.7	39.1	- - -	- - -	
5333	2024/02/08 14:11	25.7	39.1	- - -	- - -	
5334	2024/02/08 14:11	25.7	39.1	- - -	- - -	
5335	2024/02/08 14:11	25.7	39.1	- - -	- - -	
5336	2024/02/08 14:11	25.7	39.1	- - -	- - -	
5337	2024/02/08 14:11	25.7	39.1	- - -	- - -	
5338	2024/02/08 14:11	25.7	39.1	- - -	- - -	
5339	2024/02/08 14:11	25.7	39.1	- - -	- - -	
5340	2024/02/08 14:11	25.7	39.1	- - -	- - -	
5341	2024/02/08 14:11	25.8	39.1	- - -	- - -	
5342	2024/02/08 14:11	25.8	39.1	- - -	- - -	
5343	2024/02/08 14:11	25.8	39.1	- - -	- - -	
5344	2024/02/08 14:11	26.0	39.1	- - -	- - -	
5345	2024/02/08 14:11	26.0	39.1	- - -	- - -	
5346	2024/02/08 14:11	26.0	39.1	- - -	- - -	
5347	2024/02/08 14:11	26.0	39.1	- - -	- - -	
5348	2024/02/08 14:11	26.0	39.2	- - -	- - -	
5349	2024/02/08 14:11	26.0	39.2	- - -	- - -	
5350	2024/02/08 14:11	26.0	39.2	- - -	- - -	
5351	2024/02/08 14:11	26.0	39.2	- - -	- - -	
5352	2024/02/08 14:11	26.0	39.2	- - -	- - -	
5353	2024/02/08 14:11	26.0	39.2	- - -	- - -	
5354	2024/02/08 14:11	26.0	39.2	- - -	- - -	
5355	2024/02/08 14:11	26.0	39.2	- - -	- - -	
5356	2024/02/08 14:11	26.0	39.2	- - -	- - -	
5357	2024/02/08 14:11	26.0	39.1	- - -	- - -	
5358	2024/02/08 14:11	26.0	39.1	- - -	- - -	

Table C1.11: Stack length of 45 mm: Voltage and current

477	38.8 V	1.1 A	08/02/24 14:01:25		
478	38.8 V	1.1 A	08/02/24 14:01:35		
479	38.8 V	1.1 A	08/02/24 14:01:45		
480	38.8 V	1.0 A	08/02/24 14:01:55		
481	39.0 V	1.1 A	08/02/24 14:02:05		
482	38.8 V	1.1 A	08/02/24 14:02:15		
483	38.8 V	1.1 A	08/02/24 14:02:25		
484	38.8 V	1.0 A	08/02/24 14:02:35		
485	39.0 V	1.1 A	08/02/24 14:02:45		
486	38.8 V	1.1 A	08/02/24 14:02:55		
487	39.0 V	1.1 A	08/02/24 14:03:05		
488	38.8 V	1.1 A	08/02/24 14:03:15		
489	38.8 V	1.1 A	08/02/24 14:03:25		
490	38.8 V	1.1 A	08/02/24 14:03:35		
491	38.8 V	1.1 A	08/02/24 14:03:45		
492	38.8 V	1.1 A	08/02/24 14:03:55		
493	38.8 V	1.1 A	08/02/24 14:04:05		
494	38.8 V	1.1 A	08/02/24 14:04:15		
495	38.8 V	1.1 A	08/02/24 14:04:25		
496	39.0 V	1.1 A	08/02/24 14:04:35		
497	39.0 V	1.0 A	08/02/24 14:04:45		
498	39.0 V	1.1 A	08/02/24 14:04:55		
499	38.8 V	1.1 A	08/02/24 14:05:05		
500	38.8 V	1.1 A	08/02/24 14:05:15		
501	38.8 V	1.1 A	08/02/24 14:05:25		
502	39.0 V	1.1 A	08/02/24 14:05:35		
503	39.0 V	1.1 A	08/02/24 14:05:45		
504	38.8 V	1.0 A	08/02/24 14:05:55		
505	39.0 V	1.1 A	08/02/24 14:06:05		
506	38.8 V	1.1 A	08/02/24 14:06:15		
507	39.0 V	1.0 A	08/02/24 14:06:25		
508	38.8 V	1.0 A	08/02/24 14:06:35		
509	38.8 V	1.1 A	08/02/24 14:06:45		
510	38.8 V	1.1 A	08/02/24 14:06:55		
511	38.8 V	1.1 A	08/02/24 14:07:05		
512	38.8 V	1.1 A	08/02/24 14:07:15		
513	39.0 V	1.1 A	08/02/24 14:07:25		
514	38.8 V	1.1 A	08/02/24 14:07:35		
515	38.8 V	1.0 A	08/02/24 14:07:45		
516	38.8 V	1.1 A	08/02/24 14:07:55		
517	38.8 V	1.1 A	08/02/24 14:08:05		
518	38.8 V	1.1 A	08/02/24 14:08:15		
519	38.8 V	1.1 A	08/02/24 14:08:25		
520	39.0 V	1.1 A	08/02/24 14:08:35		
521	38.8 V	1.1 A	08/02/24 14:08:45		
522	38.8 V	1.1 A	08/02/24 14:08:55		
523	38.8 V	1.1 A	08/02/24 14:09:05		
524	38.8 V	1.1 A	08/02/24 14:09:15		
525	39.0 V	1.0 A	08/02/24 14:09:25		
526	39.0 V	1.1 A	08/02/24 14:09:35		
527	38.8 V	1.0 A	08/02/24 14:09:45		
528	39.0 V	1.1 A	08/02/24 14:09:55		
529	38.8 V	1.0 A	08/02/24 14:10:05		
530	39.0 V	1.1 A	08/02/24 14:10:15		
531	38.8 V	1.1 A	08/02/24 14:10:25		
532	39.0 V	1.1 A	08/02/24 14:10:35		
533	38.8 V	1.1 A	08/02/24 14:10:45		
534	38.8 V	1.0 A	08/02/24 14:10:55		
535	38.8 V	1.1 A	08/02/24 14:11:05		
536	38.8 V	1.0 A	08/02/24 14:11:15		
537	39.0 V	1.1 A	08/02/24 14:11:25		
538	38.8 V	1.0 A	08/02/24 14:11:35		
539	39.0 V	1.0 A	08/02/24 14:11:45		

Table C1.12: Stack length of 45 mm: Mean pressure

18241	2024/02/08	14:13:03	000070.1	kpa		
18242	2024/02/08	14:13:05	000070.1	kpa		
18243	2024/02/08	14:13:07	000070.1	kpa		
18244	2024/02/08	14:13:09	000070.1	kpa		
18245	2024/02/08	14:13:11	000070.1	kpa		
18246	2024/02/08	14:13:13	000070.1	kpa		
18247	2024/02/08	14:13:15	000070.1	kpa		
18248	2024/02/08	14:13:17	000070.1	kpa		
18249	2024/02/08	14:13:19	000070.1	kpa		
18250	2024/02/08	14:13:21	000070.0	kpa		
18251	2024/02/08	14:13:23	000070.0	kpa		
18252	2024/02/08	14:13:25	000070.0	kpa		
18253	2024/02/08	14:13:27	000070.0	kpa		
18254	2024/02/08	14:13:29	000070.0	kpa		
18255	2024/02/08	14:13:31	000070.0	kpa		
18256	2024/02/08	14:13:33	000070.0	kpa		
18257	2024/02/08	14:13:35	000070.0	kpa		
18258	2024/02/08	14:13:37	000069.9	kpa		
18259	2024/02/08	14:13:39	000069.9	kpa		
18260	2024/02/08	14:13:41	000069.9	kpa		
18261	2024/02/08	14:13:43	000069.9	kpa		
18262	2024/02/08	14:13:45	000069.9	kpa		
18263	2024/02/08	14:13:47	000069.9	kpa		
18264	2024/02/08	14:13:49	000069.9	kpa		
18265	2024/02/08	14:13:51	000069.9	kpa		
18266	2024/02/08	14:13:53	000069.9	kpa		
18267	2024/02/08	14:13:55	000069.9	kpa		
18268	2024/02/08	14:13:57	000069.8	kpa		
18269	2024/02/08	14:13:59	000069.8	kpa		
18270	2024/02/08	14:14:01	000069.8	kpa		
18271	2024/02/08	14:14:03	000069.8	kpa		
18272	2024/02/08	14:14:05	000069.8	kpa		
18273	2024/02/08	14:14:07	000069.8	kpa		
18274	2024/02/08	14:14:09	000069.8	kpa		
18275	2024/02/08	14:14:11	000069.8	kpa		
18276	2024/02/08	14:14:13	000069.7	kpa		
18277	2024/02/08	14:14:15	000069.7	kpa		
18278	2024/02/08	14:14:17	000069.7	kpa		
18279	2024/02/08	14:14:19	000069.7	kpa		
18280	2024/02/08	14:14:21	000069.7	kpa		
18281	2024/02/08	14:14:23	000069.7	kpa		
18282	2024/02/08	14:14:25	000069.7	kpa		
18283	2024/02/08	14:14:27	000069.7	kpa		
18284	2024/02/08	14:14:29	000069.6	kpa		
18285	2024/02/08	14:14:31	000069.6	kpa		
18286	2024/02/08	14:14:33	000069.6	kpa		
18287	2024/02/08	14:14:35	000069.6	kpa		
18288	2024/02/08	14:14:37	000069.6	kpa		
18289	2024/02/08	14:14:39	000069.6	kpa		
18290	2024/02/08	14:14:41	000069.6	kpa		
18291	2024/02/08	14:14:43	000069.6	kpa		
18292	2024/02/08	14:14:45	000069.6	kpa		
18293	2024/02/08	14:14:47	000069.6	kpa		
18294	2024/02/08	14:14:49	000069.5	kpa		
18295	2024/02/08	14:14:51	000069.5	kpa		
18296	2024/02/08	14:14:53	000069.5	kpa		
18297	2024/02/08	14:14:55	000069.5	kpa		
18298	2024/02/08	14:14:57	000069.5	kpa		
18299	2024/02/08	14:14:59	000069.5	kpa		
18300	2024/02/08	14:15:01	000069.5	kpa		
18301	2024/02/08	14:15:03	000069.5	kpa		
18302	2024/02/08	14:15:05	000069.4	kpa		
18303	2024/02/08	14:15:07	000069.4	kpa		
18304	2024/02/08	14:15:09	000069.4	kpa		

Table C1.13: Stack length of 55 mm: Temperature range-T1-T4

6381	2024/02/21 16:37	24.0	31.6	21.9	26.0	
6382	2024/02/21 16:37	24.0	31.6	21.9	26.0	
6383	2024/02/21 16:37	24.0	31.6	21.9	26.0	
6384	2024/02/21 16:37	24.0	31.6	21.9	26.0	
6385	2024/02/21 16:37	24.0	31.6	21.9	26.0	
6386	2024/02/21 16:37	24.0	31.5	21.9	26.0	
6387	2024/02/21 16:37	24.0	31.5	21.9	26.0	
6388	2024/02/21 16:37	24.0	31.5	21.9	26.0	
6389	2024/02/21 16:37	24.0	31.5	21.9	26.0	
6390	2024/02/21 16:37	23.8	31.5	21.9	26.0	
6391	2024/02/21 16:37	23.8	31.5	21.9	26.0	
6392	2024/02/21 16:37	23.8	31.6	21.9	26.0	
6393	2024/02/21 16:37	23.8	31.6	21.9	26.0	
6394	2024/02/21 16:38	23.8	31.6	21.9	26.0	
6395	2024/02/21 16:38	23.8	31.6	21.9	26.0	
6396	2024/02/21 16:38	23.6	31.6	21.9	26.0	
6397	2024/02/21 16:38	23.6	31.6	21.9	26.0	
6398	2024/02/21 16:38	23.6	31.6	21.9	26.0	
6399	2024/02/21 16:38	23.6	31.6	21.9	26.0	
6400	2024/02/21 16:38	23.6	31.6	21.9	26.0	
6401	2024/02/21 16:38	23.6	31.6	21.9	26.0	
6402	2024/02/21 16:38	23.6	31.6	21.9	26.0	
6403	2024/02/21 16:38	23.6	31.6	21.9	26.0	
6404	2024/02/21 16:38	23.6	31.6	21.9	26.0	
6405	2024/02/21 16:38	23.6	31.6	21.9	26.0	
6406	2024/02/21 16:38	23.6	31.6	21.9	26.0	
6407	2024/02/21 16:38	23.6	31.5	21.9	26.0	
6408	2024/02/21 16:38	23.6	31.5	21.9	26.0	
6409	2024/02/21 16:38	23.6	31.5	21.9	26.0	
6410	2024/02/21 16:38	23.6	31.5	21.9	26.0	
6411	2024/02/21 16:38	23.6	31.5	21.9	26.0	
6412	2024/02/21 16:38	23.6	31.5	21.9	26.0	
6413	2024/02/21 16:38	23.6	31.6	21.9	26.0	
6414	2024/02/21 16:38	23.6	31.6	21.9	26.0	
6415	2024/02/21 16:38	23.6	31.6	21.9	26.0	
6416	2024/02/21 16:38	23.6	31.6	21.9	26.0	
6417	2024/02/21 16:38	23.6	31.6	21.9	26.0	
6418	2024/02/21 16:38	23.6	31.6	21.9	26.0	
6419	2024/02/21 16:38	23.6	31.6	21.9	26.0	
6420	2024/02/21 16:38	23.6	31.6	21.9	26.1	
6421	2024/02/21 16:38	23.6	31.6	21.9	26.1	
6422	2024/02/21 16:38	23.6	31.6	21.9	26.1	
6423	2024/02/21 16:38	23.6	31.6	21.9	26.1	
6424	2024/02/21 16:38	23.6	31.6	21.9	26.1	
6425	2024/02/21 16:38	23.6	31.6	21.9	26.1	
6426	2024/02/21 16:38	23.6	31.6	21.9	26.1	
6427	2024/02/21 16:38	23.6	31.6	21.9	26.1	
6428	2024/02/21 16:38	23.6	31.7	21.9	26.1	
6429	2024/02/21 16:38	23.6	31.7	21.9	26.1	
6430	2024/02/21 16:38	23.6	31.7	21.9	26.1	
6431	2024/02/21 16:38	23.6	31.7	21.9	26.1	
6432	2024/02/21 16:38	23.8	31.7	21.9	26.1	
6433	2024/02/21 16:38	23.8	31.7	21.9	26.1	
6434	2024/02/21 16:38	23.8	31.8	21.9	26.1	
6435	2024/02/21 16:38	23.8	31.8	21.9	26.1	
6436	2024/02/21 16:38	23.8	31.8	21.9	26.0	
6437	2024/02/21 16:38	23.9	31.8	21.9	26.0	
6438	2024/02/21 16:38	23.9	31.8	21.9	26.0	
6439	2024/02/21 16:38	23.9	31.8	21.9	26.0	
6440	2024/02/21 16:38	23.9	31.8	21.9	26.0	
6441	2024/02/21 16:38	23.9	31.8	21.9	25.8	
6442	2024/02/21 16:38	23.9	31.8	21.9	25.8	
6443	2024/02/21 16:38	24.1	31.8	21.9	25.8	
6444	2024/02/21 16:38	24.1	31.8	21.9	25.8	
6445	2024/02/21 16:38	24.1	31.8	21.9	25.8	
6446	2024/02/21 16:38	24.1	31.8	21.9	25.8	

Table C1.14: Stack length of 55 mm: Temperature range-T5-T6

6447	2024/02/21 16:37	24.6	35.5	- - -	- - -
6448	2024/02/21 16:37	24.6	35.5	- - -	- - -
6449	2024/02/21 16:37	24.6	35.5	- - -	- - -
6450	2024/02/21 16:37	24.6	35.5	- - -	- - -
6451	2024/02/21 16:37	24.6	35.5	- - -	- - -
6452	2024/02/21 16:38	24.6	35.5	- - -	- - -
6453	2024/02/21 16:38	24.6	35.5	- - -	- - -
6454	2024/02/21 16:38	24.6	35.5	- - -	- - -
6455	2024/02/21 16:38	24.6	35.5	- - -	- - -
6456	2024/02/21 16:38	24.6	35.5	- - -	- - -
6457	2024/02/21 16:38	24.6	35.5	- - -	- - -
6458	2024/02/21 16:38	24.6	35.5	- - -	- - -
6459	2024/02/21 16:38	24.6	35.5	- - -	- - -
6460	2024/02/21 16:38	24.6	35.5	- - -	- - -
6461	2024/02/21 16:38	24.6	35.5	- - -	- - -
6462	2024/02/21 16:38	24.6	35.5	- - -	- - -
6463	2024/02/21 16:38	24.6	35.5	- - -	- - -
6464	2024/02/21 16:38	24.6	35.5	- - -	- - -
6465	2024/02/21 16:38	24.6	35.5	- - -	- - -
6466	2024/02/21 16:38	24.6	35.5	- - -	- - -
6467	2024/02/21 16:38	24.6	35.5	- - -	- - -
6468	2024/02/21 16:38	24.6	35.5	- - -	- - -
6469	2024/02/21 16:38	24.6	35.5	- - -	- - -
6470	2024/02/21 16:38	24.6	35.5	- - -	- - -
6471	2024/02/21 16:38	24.6	35.5	- - -	- - -
6472	2024/02/21 16:38	24.6	35.5	- - -	- - -
6473	2024/02/21 16:38	24.6	35.5	- - -	- - -
6474	2024/02/21 16:38	24.6	35.5	- - -	- - -
6475	2024/02/21 16:38	24.6	35.5	- - -	- - -
6476	2024/02/21 16:38	24.6	35.5	- - -	- - -
6477	2024/02/21 16:38	24.6	35.5	- - -	- - -
6478	2024/02/21 16:38	24.6	35.5	- - -	- - -
6479	2024/02/21 16:38	24.6	35.4	- - -	- - -
6480	2024/02/21 16:38	24.6	35.4	- - -	- - -
6481	2024/02/21 16:38	24.6	35.4	- - -	- - -
6482	2024/02/21 16:38	24.6	35.4	- - -	- - -
6483	2024/02/21 16:38	24.6	35.4	- - -	- - -
6484	2024/02/21 16:38	24.6	35.4	- - -	- - -
6485	2024/02/21 16:38	24.6	35.4	- - -	- - -
6486	2024/02/21 16:38	24.6	35.4	- - -	- - -
6487	2024/02/21 16:38	24.6	35.4	- - -	- - -
6488	2024/02/21 16:38	24.6	35.4	- - -	- - -
6489	2024/02/21 16:38	24.6	35.4	- - -	- - -
6490	2024/02/21 16:38	24.6	35.4	- - -	- - -
6491	2024/02/21 16:38	24.6	35.5	- - -	- - -
6492	2024/02/21 16:38	24.6	35.5	- - -	- - -
6493	2024/02/21 16:38	24.6	35.5	- - -	- - -
6494	2024/02/21 16:38	24.6	35.5	- - -	- - -
6495	2024/02/21 16:38	24.6	35.5	- - -	- - -

Table C1.15: Stack length of 55 mm: Voltage and current

536	39.1 V	1.1 A	21/02/24 13:58:32		
537	39.1 V	1.1 A	21/02/24 13:58:42		
538	39.1 V	1.1 A	21/02/24 13:58:52		
539	39.1 V	1.1 A	21/02/24 13:59:02		
540	39.1 V	1.1 A	21/02/24 13:59:12		
541	39.1 V	1.1 A	21/02/24 13:59:22		
542	39.1 V	1.1 A	21/02/24 13:59:32		
543	39.1 V	1.1 A	21/02/24 13:59:42		
544	39.1 V	1.1 A	21/02/24 13:59:52		
545	39.1 V	1.1 A	21/02/24 14:00:02		
546	39.1 V	1.1 A	21/02/24 14:00:12		
547	39.1 V	1.1 A	21/02/24 14:00:22		
548	39.1 V	1.1 A	21/02/24 14:00:32		
549	39.1 V	1.1 A	21/02/24 14:00:42		
550	39.1 V	1.1 A	21/02/24 14:00:52		
551	39.1 V	1.1 A	21/02/24 14:01:02		
552	39.1 V	1.1 A	21/02/24 14:01:12		
553	39.1 V	1.1 A	21/02/24 14:01:22		
554	39.1 V	1.1 A	21/02/24 14:01:32		
555	39.1 V	1.1 A	21/02/24 14:01:42		
556	39.1 V	1.1 A	21/02/24 14:01:52		
557	39.1 V	1.1 A	21/02/24 14:02:02		
558	39.1 V	1.1 A	21/02/24 14:02:12		
559	39.1 V	1.1 A	21/02/24 14:02:22		
560	39.1 V	1.1 A	21/02/24 14:02:32		
561	39.1 V	1.1 A	21/02/24 14:02:42		
562	39.1 V	1.1 A	21/02/24 14:02:52		
563	39.1 V	1.1 A	21/02/24 14:03:02		
564	39.1 V	1.1 A	21/02/24 14:03:12		
565	39.1 V	1.1 A	21/02/24 14:03:22		
566	39.1 V	1.1 A	21/02/24 14:03:32		
567	39.1 V	1.1 A	21/02/24 14:03:42		
568	39.1 V	1.1 A	21/02/24 14:03:52		
569	39.1 V	1.1 A	21/02/24 14:04:02		
570	39.1 V	1.1 A	21/02/24 14:04:12		
571	39.1 V	1.1 A	21/02/24 14:04:22		
572	39.1 V	1.1 A	21/02/24 14:04:32		
573	39.1 V	1.1 A	21/02/24 14:04:42		
574	39.1 V	1.1 A	21/02/24 14:04:52		
575	39.1 V	1.1 A	21/02/24 14:05:02		
576	39.1 V	1.1 A	21/02/24 14:05:12		
577	39.1 V	1.1 A	21/02/24 14:05:22		
578	39.1 V	1.1 A	21/02/24 14:05:32		
579	39.1 V	1.1 A	21/02/24 14:05:42		
580	39.1 V	1.1 A	21/02/24 14:05:52		
581	39.1 V	1.1 A	21/02/24 14:06:02		
582	39.1 V	1.1 A	21/02/24 14:06:12		
583	39.1 V	1.1 A	21/02/24 14:06:22		
584	39.1 V	1.1 A	21/02/24 14:06:32		
585	39.1 V	1.1 A	21/02/24 14:06:42		
586	39.1 V	1.1 A	21/02/24 14:06:52		
587	39.1 V	1.1 A	21/02/24 14:07:02		
588	39.1 V	1.1 A	21/02/24 14:07:12		
589	39.1 V	1.1 A	21/02/24 14:07:22		
590	39.1 V	1.1 A	21/02/24 14:07:32		
591	39.1 V	1.1 A	21/02/24 14:07:42		
592	39.1 V	1.1 A	21/02/24 14:07:52		
593	39.1 V	1.1 A	21/02/24 14:08:02		
594	39.1 V	1.1 A	21/02/24 14:08:12		
595	39.1 V	1.1 A	21/02/24 14:08:22		
596	39.1 V	1.1 A	21/02/24 14:08:32		
597	39.1 V	1.1 A	21/02/24 14:08:42		
598	39.1 V	1.1 A	21/02/24 14:08:52		
599	39.1 V	1.1 A	21/02/24 14:09:02		
600	39.1 V	1.1 A	21/02/24 14:09:12		
601	39.1 V	1.1 A	21/02/24 14:09:22		
602	39.1 V	1.1 A	21/02/24 14:09:32		

Table C1.16 Stack length of 55 mm: Mean pressure

27574	2024/02/21	16:45:22	000046.5	kpa		
27575	2024/02/21	16:45:24	000046.5	kpa		
27576	2024/02/21	16:45:26	000046.5	kpa		
27577	2024/02/21	16:45:28	000046.5	kpa		
27578	2024/02/21	16:45:30	000046.5	kpa		
27579	2024/02/21	16:45:32	000046.5	kpa		
27580	2024/02/21	16:45:34	000046.5	kpa		
27581	2024/02/21	16:45:36	000046.5	kpa		
27582	2024/02/21	16:45:38	000046.5	kpa		
27583	2024/02/21	16:45:40	000046.4	kpa		
27584	2024/02/21	16:45:42	000046.4	kpa		
27585	2024/02/21	16:45:44	000046.4	kpa		
27586	2024/02/21	16:45:46	000046.4	kpa		
27587	2024/02/21	16:45:48	000046.4	kpa		
27588	2024/02/21	16:45:50	000046.4	kpa		
27589	2024/02/21	16:45:52	000046.4	kpa		
27590	2024/02/21	16:45:54	000046.4	kpa		
27591	2024/02/21	16:45:56	000046.3	kpa		
27592	2024/02/21	16:45:58	000046.3	kpa		
27593	2024/02/21	16:46:00	000046.3	kpa		
27594	2024/02/21	16:46:02	000046.3	kpa		
27595	2024/02/21	16:46:04	000046.3	kpa		
27596	2024/02/21	16:46:06	000046.3	kpa		
27597	2024/02/21	16:46:08	000046.3	kpa		
27598	2024/02/21	16:46:10	000046.3	kpa		
27599	2024/02/21	16:46:12	000046.3	kpa		
27600	2024/02/21	16:46:14	000046.3	kpa		
27601	2024/02/21	16:46:16	000046.2	kpa		
27602	2024/02/21	16:46:18	000046.2	kpa		
27603	2024/02/21	16:46:20	000046.2	kpa		
27604	2024/02/21	16:46:22	000046.2	kpa		
27605	2024/02/21	16:46:24	000046.2	kpa		
27606	2024/02/21	16:46:26	000046.2	kpa		
27607	2024/02/21	16:46:28	000046.2	kpa		
27608	2024/02/21	16:46:30	000046.1	kpa		
27609	2024/02/21	16:46:32	000046.1	kpa		
27610	2024/02/21	16:46:34	000046.1	kpa		
27611	2024/02/21	16:46:36	000046.1	kpa		
27612	2024/02/21	16:46:38	000046.1	kpa		
27613	2024/02/21	16:46:40	000046.1	kpa		
27614	2024/02/21	16:46:42	000046.1	kpa		
27615	2024/02/21	16:46:44	000046.1	kpa		
27616	2024/02/21	16:46:46	000046.1	kpa		
27617	2024/02/21	16:46:48	000046.0	kpa		
27618	2024/02/21	16:46:50	000046.0	kpa		
27619	2024/02/21	16:46:52	000046.0	kpa		
27620	2024/02/21	16:46:54	000046.0	kpa		
27621	2024/02/21	16:46:56	000046.0	kpa		
27622	2024/02/21	16:46:58	000046.0	kpa		
27623	2024/02/21	16:47:00	000046.0	kpa		
27624	2024/02/21	16:47:02	000045.9	kpa		
27625	2024/02/21	16:47:04	000045.9	kpa		
27626	2024/02/21	16:47:06	000045.9	kpa		
27627	2024/02/21	16:47:08	000045.9	kpa		
27628	2024/02/21	16:47:10	000045.9	kpa		
27629	2024/02/21	16:47:12	000045.9	kpa		
27630	2024/02/21	16:47:14	000045.9	kpa		
27631	2024/02/21	16:47:16	000045.9	kpa		
27632	2024/02/21	16:47:18	000045.9	kpa		
27633	2024/02/21	16:47:20	000045.9	kpa		
27634	2024/02/21	16:47:22	000045.8	kpa		
27635	2024/02/21	16:47:24	000045.8	kpa		
27636	2024/02/21	16:47:26	000045.8	kpa		
27637	2024/02/21	16:47:28	000045.8	kpa		
27638	2024/02/21	16:47:30	000045.8	kpa		

Table C1.17: Stack length of 65 mm: Temperature range-T1-T4

6047	2024/02/22 13:35	23.0	30.2	22.4	26.9	
6048	2024/02/22 13:35	23.0	30.2	22.4	26.9	
6049	2024/02/22 13:35	23.0	30.2	22.4	26.9	
6050	2024/02/22 13:35	23.0	30.2	22.4	26.9	
6051	2024/02/22 13:35	23.0	30.2	22.4	26.9	
6052	2024/02/22 13:35	23.0	30.3	22.4	26.9	
6053	2024/02/22 13:35	23.0	30.3	22.4	26.9	
6054	2024/02/22 13:35	23.0	30.3	22.4	26.9	
6055	2024/02/22 13:35	23.0	30.3	22.4	26.9	
6056	2024/02/22 13:35	23.0	30.3	22.4	26.9	
6057	2024/02/22 13:35	23.0	30.4	22.4	26.9	
6058	2024/02/22 13:35	23.0	30.4	22.4	26.9	
6059	2024/02/22 13:35	23.0	30.4	22.4	26.9	
6060	2024/02/22 13:35	23.0	30.4	22.4	26.9	
6061	2024/02/22 13:35	23.0	30.4	22.4	26.9	
6062	2024/02/22 13:35	23.0	30.5	22.4	26.9	
6063	2024/02/22 13:35	23.0	30.5	22.4	26.9	
6064	2024/02/22 13:35	23.0	30.5	22.4	26.9	
6065	2024/02/22 13:35	23.0	30.5	22.4	26.9	
6066	2024/02/22 13:35	23.0	30.5	22.4	26.9	
6067	2024/02/22 13:35	23.0	30.5	22.4	26.9	
6068	2024/02/22 13:35	23.0	30.4	22.4	26.9	
6069	2024/02/22 13:35	23.0	30.4	22.4	26.9	
6070	2024/02/22 13:35	23.0	30.4	22.4	26.9	
6071	2024/02/22 13:35	23.0	30.4	22.4	26.9	
6072	2024/02/22 13:35	23.0	30.4	22.4	26.9	
6073	2024/02/22 13:35	23.0	30.3	22.4	26.9	
6074	2024/02/22 13:35	23.0	30.3	22.4	26.9	
6075	2024/02/22 13:35	23.0	30.3	22.4	26.9	
6076	2024/02/22 13:35	23.0	30.3	22.4	26.9	
6077	2024/02/22 13:35	23.0	30.3	22.4	26.9	
6078	2024/02/22 13:35	23.0	30.2	22.4	26.9	
6079	2024/02/22 13:35	23.0	30.2	22.4	26.9	
6080	2024/02/22 13:35	23.0	30.2	22.4	26.9	
6081	2024/02/22 13:35	23.0	30.2	22.4	26.9	
6082	2024/02/22 13:35	23.0	30.2	22.4	26.9	
6083	2024/02/22 13:35	23.0	30.2	22.4	26.9	
6084	2024/02/22 13:35	23.0	30.2	22.4	26.9	
6085	2024/02/22 13:35	23.0	30.2	22.4	26.9	
6086	2024/02/22 13:35	23.0	30.2	22.4	26.9	
6087	2024/02/22 13:35	23.0	30.2	22.4	26.9	
6088	2024/02/22 13:35	23.0	30.2	22.4	26.9	
6089	2024/02/22 13:35	23.0	30.2	22.4	26.9	
6090	2024/02/22 13:35	23.0	30.2	22.4	26.9	
6091	2024/02/22 13:35	23.0	30.2	22.4	26.9	
6092	2024/02/22 13:35	23.0	30.2	22.4	26.9	
6093	2024/02/22 13:35	23.0	30.2	22.4	26.9	
6094	2024/02/22 13:35	23.0	30.2	22.4	26.9	
6095	2024/02/22 13:35	23.0	30.2	22.4	26.9	
6096	2024/02/22 13:35	23.0	30.2	22.4	26.9	
6097	2024/02/22 13:35	23.0	30.2	22.4	26.9	
6098	2024/02/22 13:35	23.0	30.2	22.4	26.9	
6099	2024/02/22 13:35	23.0	30.2	22.4	26.9	
6100	2024/02/22 13:35	23.0	30.2	22.4	26.9	
6101	2024/02/22 13:35	23.0	30.2	22.4	26.9	
6102	2024/02/22 13:35	23.0	30.2	22.4	26.9	
6103	2024/02/22 13:35	23.0	30.2	22.4	26.9	
6104	2024/02/22 13:35	23.0	30.2	22.4	26.9	
6105	2024/02/22 13:35	23.0	30.2	22.4	26.9	
6106	2024/02/22 13:35	23.0	30.2	22.4	26.9	
6107	2024/02/22 13:36	23.0	30.2	22.4	26.9	
6108	2024/02/22 13:36	23.0	30.2	22.4	26.9	
6109	2024/02/22 13:36	23.0	30.2	22.4	26.9	

Table C1.18: Stack length of 65 mm: Temperature range-T5-T6

6370	2024/02/22 13:39	24.6	34.8	- - -	- - -	
6371	2024/02/22 13:39	24.6	34.8	- - -	- - -	
6372	2024/02/22 13:39	24.6	34.8	- - -	- - -	
6373	2024/02/22 13:39	24.6	34.8	- - -	- - -	
6374	2024/02/22 13:39	24.6	34.8	- - -	- - -	
6375	2024/02/22 13:39	24.6	34.8	- - -	- - -	
6376	2024/02/22 13:39	24.6	34.8	- - -	- - -	
6377	2024/02/22 13:39	24.6	34.8	- - -	- - -	
6378	2024/02/22 13:39	24.6	34.8	- - -	- - -	
6379	2024/02/22 13:39	24.6	34.8	- - -	- - -	
6380	2024/02/22 13:39	24.6	34.8	- - -	- - -	
6381	2024/02/22 13:39	24.6	34.8	- - -	- - -	
6382	2024/02/22 13:39	24.6	34.8	- - -	- - -	
6383	2024/02/22 13:39	24.6	34.8	- - -	- - -	
6384	2024/02/22 13:39	24.6	34.8	- - -	- - -	
6385	2024/02/22 13:39	24.6	34.8	- - -	- - -	
6386	2024/02/22 13:39	24.6	34.8	- - -	- - -	
6387	2024/02/22 13:39	24.6	34.8	- - -	- - -	
6388	2024/02/22 13:39	24.6	34.8	- - -	- - -	
6389	2024/02/22 13:39	24.6	34.8	- - -	- - -	
6390	2024/02/22 13:39	24.6	34.8	- - -	- - -	
6391	2024/02/22 13:40	24.6	34.8	- - -	- - -	
6392	2024/02/22 13:40	24.6	34.8	- - -	- - -	
6393	2024/02/22 13:40	24.6	34.8	- - -	- - -	
6394	2024/02/22 13:40	24.6	34.8	- - -	- - -	
6395	2024/02/22 13:40	24.6	34.8	- - -	- - -	
6396	2024/02/22 13:40	24.6	34.8	- - -	- - -	
6397	2024/02/22 13:40	24.6	34.8	- - -	- - -	
6398	2024/02/22 13:40	24.6	34.8	- - -	- - -	
6399	2024/02/22 13:40	24.6	34.8	- - -	- - -	
6400	2024/02/22 13:40	24.6	34.8	- - -	- - -	
6401	2024/02/22 13:40	24.6	34.8	- - -	- - -	
6402	2024/02/22 13:40	24.6	34.8	- - -	- - -	
6403	2024/02/22 13:40	24.6	34.8	- - -	- - -	
6404	2024/02/22 13:40	24.6	34.8	- - -	- - -	
6405	2024/02/22 13:40	24.6	34.8	- - -	- - -	
6406	2024/02/22 13:40	24.6	34.8	- - -	- - -	
6407	2024/02/22 13:40	24.6	34.8	- - -	- - -	
6408	2024/02/22 13:40	24.6	34.8	- - -	- - -	
6409	2024/02/22 13:40	24.6	34.8	- - -	- - -	
6410	2024/02/22 13:40	24.6	34.8	- - -	- - -	
6411	2024/02/22 13:40	24.6	34.8	- - -	- - -	
6412	2024/02/22 13:40	24.6	34.8	- - -	- - -	
6413	2024/02/22 13:40	24.6	34.8	- - -	- - -	
6414	2024/02/22 13:40	24.6	34.8	- - -	- - -	
6415	2024/02/22 13:40	24.6	34.8	- - -	- - -	
6416	2024/02/22 13:40	24.6	34.8	- - -	- - -	
6417	2024/02/22 13:40	24.6	34.8	- - -	- - -	
6418	2024/02/22 13:40	24.6	34.9	- - -	- - -	
6419	2024/02/22 13:40	24.6	34.9	- - -	- - -	
6420	2024/02/22 13:40	24.6	34.9	- - -	- - -	
6421	2024/02/22 13:40	24.6	34.9	- - -	- - -	
6422	2024/02/22 13:40	24.6	34.9	- - -	- - -	
6423	2024/02/22 13:40	24.6	34.9	- - -	- - -	
6424	2024/02/22 13:40	24.6	34.8	- - -	- - -	
6425	2024/02/22 13:40	24.6	34.8	- - -	- - -	
6426	2024/02/22 13:40	24.6	34.8	- - -	- - -	
6427	2024/02/22 13:40	24.6	34.8	- - -	- - -	
6428	2024/02/22 13:40	24.6	34.8	- - -	- - -	
6429	2024/02/22 13:40	24.6	34.8	- - -	- - -	
6430	2024/02/22 13:40	24.6	34.9	- - -	- - -	
6431	2024/02/22 13:40	24.6	34.9	- - -	- - -	
6432	2024/02/22 13:40	24.6	34.9	- - -	- - -	
6433	2024/02/22 13:40	24.6	35.0	- - -	- - -	
6434	2024/02/22 13:40	24.6	35.0	- - -	- - -	
6435	2024/02/22 13:40	24.6	35.0	- - -	- - -	
6436	2024/02/22 13:40	24.6	34.9	- - -	- - -	

Table C1.19: Stack length of 65 mm: Voltage and current

581	37.5 V	1.0 A	22/02/24 13:31:16		
582	37.5 V	1.1 A	22/02/24 13:31:26		
583	37.5 V	1.0 A	22/02/24 13:31:36		
584	37.5 V	1.0 A	22/02/24 13:31:46		
585	37.5 V	1.1 A	22/02/24 13:31:56		
586	37.5 V	1.0 A	22/02/24 13:32:06		
587	37.5 V	1.0 A	22/02/24 13:32:16		
588	37.5 V	1.1 A	22/02/24 13:32:26		
589	37.5 V	1.1 A	22/02/24 13:32:36		
590	37.5 V	1.0 A	22/02/24 13:32:46		
591	37.5 V	1.0 A	22/02/24 13:32:56		
592	37.5 V	1.0 A	22/02/24 13:33:06		
593	37.5 V	1.0 A	22/02/24 13:33:16		
594	37.5 V	1.1 A	22/02/24 13:33:26		
595	37.5 V	1.1 A	22/02/24 13:33:36		
596	37.5 V	1.1 A	22/02/24 13:33:46		
597	37.5 V	1.1 A	22/02/24 13:33:56		
598	37.5 V	1.0 A	22/02/24 13:34:06		
599	37.5 V	1.0 A	22/02/24 13:34:16		
600	37.5 V	1.0 A	22/02/24 13:34:26		
601	37.5 V	1.0 A	22/02/24 13:34:36		
602	37.5 V	1.1 A	22/02/24 13:34:46		
603	37.5 V	1.0 A	22/02/24 13:34:56		
604	37.5 V	1.0 A	22/02/24 13:35:06		
605	37.5 V	1.0 A	22/02/24 13:35:16		
606	37.5 V	1.0 A	22/02/24 13:35:26		
607	37.5 V	1.1 A	22/02/24 13:35:36		
608	37.5 V	1.0 A	22/02/24 13:35:46		
609	37.5 V	1.0 A	22/02/24 13:35:56		
610	37.5 V	1.0 A	22/02/24 13:36:06		
611	37.5 V	1.1 A	22/02/24 13:36:16		
612	37.5 V	1.1 A	22/02/24 13:36:26		
613	37.5 V	1.0 A	22/02/24 13:36:36		
614	37.5 V	1.0 A	22/02/24 13:36:46		
615	37.5 V	1.0 A	22/02/24 13:36:56		
616	37.5 V	1.0 A	22/02/24 13:37:06		
617	37.5 V	1.1 A	22/02/24 13:37:16		
618	37.5 V	1.0 A	22/02/24 13:37:26		
619	37.5 V	1.0 A	22/02/24 13:37:36		
620	37.3 V	1.0 A	22/02/24 13:37:46		
621	37.5 V	1.0 A	22/02/24 13:37:56		
622	37.5 V	1.1 A	22/02/24 13:38:06		
623	37.5 V	1.0 A	22/02/24 13:38:16		
624	37.5 V	1.1 A	22/02/24 13:38:26		
625	37.5 V	1.0 A	22/02/24 13:38:36		
626	37.5 V	1.1 A	22/02/24 13:38:46		
627	37.5 V	1.0 A	22/02/24 13:38:56		
628	37.5 V	1.1 A	22/02/24 13:39:06		
629	37.5 V	1.1 A	22/02/24 13:39:16		
630	37.3 V	1.0 A	22/02/24 13:39:26		
631	37.3 V	1.1 A	22/02/24 13:39:36		
632	37.5 V	1.0 A	22/02/24 13:39:46		
633	37.5 V	1.0 A	22/02/24 13:39:56		
634	37.5 V	1.1 A	22/02/24 13:40:06		
635	37.5 V	1.0 A	22/02/24 13:40:16		
636	37.5 V	1.1 A	22/02/24 13:40:26		
637	37.5 V	1.1 A	22/02/24 13:40:36		
638	37.5 V	1.1 A	22/02/24 13:40:46		
639	37.5 V	1.1 A	22/02/24 13:40:56		
640	37.5 V	1.1 A	22/02/24 13:41:06		
641	37.5 V	1.1 A	22/02/24 13:41:16		
642	37.5 V	1.0 A	22/02/24 13:41:26		
643	37.5 V	1.1 A	22/02/24 13:41:36		
644	37.5 V	1.0 A	22/02/24 13:41:46		

C.2 Stacks positioned at 40 mm.

Table C.2.1: Stack length of 25 mm: Temperature range-T1-T4

5352	2024/02/29 13:07	25.0	29.9	23.8	26.0	
5353	2024/02/29 13:07	25.0	29.8	23.8	26.0	
5354	2024/02/29 13:07	25.0	29.8	23.8	26.0	
5355	2024/02/29 13:07	25.0	29.8	23.8	26.0	
5356	2024/02/29 13:07	25.0	29.8	23.8	26.0	
5357	2024/02/29 13:07	25.0	29.8	23.8	26.0	
5358	2024/02/29 13:07	25.0	29.8	23.8	26.0	
5359	2024/02/29 13:07	25.0	29.8	23.8	26.0	
5360	2024/02/29 13:07	25.0	29.8	23.6	26.0	
5361	2024/02/29 13:08	25.0	29.8	23.6	25.8	
5362	2024/02/29 13:08	25.0	29.8	23.6	25.8	
5363	2024/02/29 13:08	24.8	29.8	23.6	25.8	
5364	2024/02/29 13:08	24.8	29.8	23.6	25.8	
5365	2024/02/29 13:08	24.8	29.8	23.6	25.8	
5366	2024/02/29 13:08	24.8	29.8	23.6	25.8	
5367	2024/02/29 13:08	24.8	29.8	23.6	25.8	
5368	2024/02/29 13:08	24.8	29.8	23.6	25.8	
5369	2024/02/29 13:08	24.8	29.7	23.6	25.8	
5370	2024/02/29 13:08	24.8	29.7	23.6	25.8	
5371	2024/02/29 13:08	24.8	29.7	23.6	25.8	
5372	2024/02/29 13:08	24.8	29.7	23.6	25.8	
5373	2024/02/29 13:08	24.9	29.7	23.6	25.8	
5374	2024/02/29 13:08	24.9	29.7	23.6	25.8	
5375	2024/02/29 13:08	24.9	29.7	23.6	25.8	
5376	2024/02/29 13:08	24.9	29.7	23.8	25.8	
5377	2024/02/29 13:08	24.9	29.7	23.8	25.8	
5378	2024/02/29 13:08	25.0	29.7	23.8	25.8	
5379	2024/02/29 13:08	25.0	29.7	23.8	25.8	
5380	2024/02/29 13:08	25.0	29.7	23.8	25.8	
5381	2024/02/29 13:08	25.0	29.7	23.8	25.8	
5382	2024/02/29 13:08	25.0	29.7	23.8	25.8	
5383	2024/02/29 13:08	25.0	29.7	23.8	25.8	
5384	2024/02/29 13:08	25.0	29.7	23.8	25.8	
5385	2024/02/29 13:08	25.0	29.8	23.8	25.8	
5386	2024/02/29 13:08	25.0	29.8	23.8	25.8	
5387	2024/02/29 13:08	25.0	29.8	23.8	25.8	
5388	2024/02/29 13:08	25.0	29.8	23.8	25.8	
5389	2024/02/29 13:08	25.0	29.8	23.8	25.8	
5390	2024/02/29 13:08	25.0	30.0	23.8	25.8	
5391	2024/02/29 13:08	25.0	30.0	23.8	25.8	
5392	2024/02/29 13:08	25.0	30.0	23.8	25.8	
5393	2024/02/29 13:08	25.0	30.0	23.8	25.8	
5394	2024/02/29 13:08	25.0	30.0	23.8	25.8	
5395	2024/02/29 13:08	25.0	30.0	23.8	25.8	
5396	2024/02/29 13:08	25.0	30.0	23.8	25.8	
5397	2024/02/29 13:08	25.0	30.0	23.8	25.8	
5398	2024/02/29 13:08	25.0	30.0	23.8	26.0	
5399	2024/02/29 13:08	25.0	30.0	23.8	26.0	
5400	2024/02/29 13:08	25.0	30.0	23.8	26.0	
5401	2024/02/29 13:08	25.0	30.0	23.8	26.0	

Table C.2.2: Stack length of 25 mm; Temperature range-T5-T6

5370	2024/02/29 13:07	24.5	31.5	- - -	- - -
5371	2024/02/29 13:07	24.5	31.5	- - -	- - -
5372	2024/02/29 13:07	24.5	31.5	- - -	- - -
5373	2024/02/29 13:08	24.5	31.5	- - -	- - -
5374	2024/02/29 13:08	24.5	31.5	- - -	- - -
5375	2024/02/29 13:08	24.5	31.5	- - -	- - -
5376	2024/02/29 13:08	24.5	31.5	- - -	- - -
5377	2024/02/29 13:08	24.5	31.5	- - -	- - -
5378	2024/02/29 13:08	24.5	31.5	- - -	- - -
5379	2024/02/29 13:08	24.5	31.5	- - -	- - -
5380	2024/02/29 13:08	24.5	31.5	- - -	- - -
5381	2024/02/29 13:08	24.5	31.5	- - -	- - -
5382	2024/02/29 13:08	24.5	31.5	- - -	- - -
5383	2024/02/29 13:08	24.5	31.5	- - -	- - -
5384	2024/02/29 13:08	24.5	31.5	- - -	- - -
5385	2024/02/29 13:08	24.5	31.5	- - -	- - -
5386	2024/02/29 13:08	24.5	31.5	- - -	- - -
5387	2024/02/29 13:08	24.5	31.5	- - -	- - -
5388	2024/02/29 13:08	24.5	31.5	- - -	- - -
5389	2024/02/29 13:08	24.5	31.5	- - -	- - -
5390	2024/02/29 13:08	24.5	31.5	- - -	- - -
5391	2024/02/29 13:08	24.5	31.5	- - -	- - -
5392	2024/02/29 13:08	24.5	31.5	- - -	- - -
5393	2024/02/29 13:08	24.5	31.5	- - -	- - -
5394	2024/02/29 13:08	24.5	31.5	- - -	- - -
5395	2024/02/29 13:08	24.5	31.5	- - -	- - -
5396	2024/02/29 13:08	24.5	31.5	- - -	- - -
5397	2024/02/29 13:08	24.5	31.5	- - -	- - -
5398	2024/02/29 13:08	24.5	31.5	- - -	- - -
5399	2024/02/29 13:08	24.5	31.5	- - -	- - -
5400	2024/02/29 13:08	24.5	31.5	- - -	- - -
5401	2024/02/29 13:08	24.5	31.5	- - -	- - -
5402	2024/02/29 13:08	24.5	31.5	- - -	- - -
5403	2024/02/29 13:08	24.5	31.5	- - -	- - -
5404	2024/02/29 13:08	24.5	31.5	- - -	- - -
5405	2024/02/29 13:08	24.5	31.5	- - -	- - -
5406	2024/02/29 13:08	24.5	31.5	- - -	- - -
5407	2024/02/29 13:08	24.5	31.5	- - -	- - -
5408	2024/02/29 13:08	24.5	31.5	- - -	- - -
5409	2024/02/29 13:08	24.5	31.5	- - -	- - -
5410	2024/02/29 13:08	24.5	31.5	- - -	- - -
5411	2024/02/29 13:08	24.5	31.5	- - -	- - -
5412	2024/02/29 13:08	24.5	31.5	- - -	- - -
5413	2024/02/29 13:08	24.5	31.5	- - -	- - -
5414	2024/02/29 13:08	24.5	31.5	- - -	- - -
5415	2024/02/29 13:08	24.5	31.5	- - -	- - -
5416	2024/02/29 13:08	24.5	31.5	- - -	- - -
5417	2024/02/29 13:08	24.5	31.5	- - -	- - -
5418	2024/02/29 13:08	24.5	31.6	- - -	- - -
5419	2024/02/29 13:08	24.5	31.6	- - -	- - -
5420	2024/02/29 13:08	24.5	31.6	- - -	- - -
5421	2024/02/29 13:08	24.5	31.6	- - -	- - -

Table C.2.3: Stack length of 25 mm: Voltage and current

477	39.1 V	1.1 A	29/02/24 12:59:26
478	39.1 V	1.1 A	29/02/24 12:59:36
479	39.1 V	1.2 A	29/02/24 12:59:46
480	39.1 V	1.1 A	29/02/24 12:59:56
481	39.1 V	1.2 A	29/02/24 13:00:06
482	39.1 V	1.2 A	29/02/24 13:00:16
483	39.1 V	1.1 A	29/02/24 13:00:26
484	39.1 V	1.1 A	29/02/24 13:00:36
485	39.1 V	1.2 A	29/02/24 13:00:46
486	39.1 V	1.1 A	29/02/24 13:00:56
487	39.1 V	1.1 A	29/02/24 13:01:06
488	39.1 V	1.1 A	29/02/24 13:01:16
489	39.1 V	1.2 A	29/02/24 13:01:26
490	39.1 V	1.2 A	29/02/24 13:01:36
491	39.1 V	1.1 A	29/02/24 13:01:46
492	39.1 V	1.1 A	29/02/24 13:01:56
493	39.1 V	1.1 A	29/02/24 13:02:06
494	39.1 V	1.1 A	29/02/24 13:02:16
495	39.1 V	1.2 A	29/02/24 13:02:26
496	39.1 V	1.1 A	29/02/24 13:02:36
497	39.1 V	1.1 A	29/02/24 13:02:46
498	39.1 V	1.1 A	29/02/24 13:02:56
499	39.1 V	1.1 A	29/02/24 13:03:06
500	39.1 V	1.1 A	29/02/24 13:03:16
501	39.1 V	1.1 A	29/02/24 13:03:26
502	39.1 V	1.1 A	29/02/24 13:03:36
503	39.1 V	1.1 A	29/02/24 13:03:46
504	39.1 V	1.1 A	29/02/24 13:03:56
505	39.1 V	1.2 A	29/02/24 13:04:06
506	39.1 V	1.1 A	29/02/24 13:04:16
507	39.1 V	1.1 A	29/02/24 13:04:26
508	39.1 V	1.1 A	29/02/24 13:04:36
509	39.1 V	1.1 A	29/02/24 13:04:46
510	39.1 V	1.1 A	29/02/24 13:04:56
511	39.1 V	1.1 A	29/02/24 13:05:06
512	39.1 V	1.1 A	29/02/24 13:05:16
513	39.1 V	1.1 A	29/02/24 13:05:26
514	39.1 V	1.1 A	29/02/24 13:05:36
515	39.1 V	1.1 A	29/02/24 13:05:46
516	39.1 V	1.1 A	29/02/24 13:05:56
517	39.1 V	1.1 A	29/02/24 13:06:06
518	39.1 V	1.1 A	29/02/24 13:06:16
519	39.1 V	1.1 A	29/02/24 13:06:26
520	39.1 V	1.1 A	29/02/24 13:06:36
521	39.1 V	1.1 A	29/02/24 13:06:46
522	39.1 V	1.1 A	29/02/24 13:06:56
523	39.1 V	1.1 A	29/02/24 13:07:06
524	39.1 V	1.1 A	29/02/24 13:07:16
525	39.1 V	1.1 A	29/02/24 13:07:26
526	39.1 V	1.1 A	29/02/24 13:07:36
527	39.1 V	1.1 A	29/02/24 13:07:46
528	39.1 V	1.1 A	29/02/24 13:07:56
529	39.1 V	1.2 A	29/02/24 13:08:06
530	39.1 V	1.1 A	29/02/24 13:08:16
531	39.1 V	1.1 A	29/02/24 13:08:26
532	39.1 V	1.1 A	29/02/24 13:08:36
533	39.1 V	1.1 A	29/02/24 13:08:46
534	39.1 V	1.1 A	29/02/24 13:08:56
535	39.1 V	1.1 A	29/02/24 13:09:06
536	39.1 V	1.1 A	29/02/24 13:09:16
537	39.1 V	1.1 A	29/02/24 13:09:26
538	39.1 V	1.1 A	29/02/24 13:09:36
539	39.1 V	1.1 A	29/02/24 13:09:46
540	39.1 V	1.1 A	29/02/24 13:09:56
541	39.1 V	1.1 A	29/02/24 13:10:06

Table C.2.4: Stack length of 25 mm: Mean pressure

8764	2024/02/29	13:06:33	000060.8	kpa
8765	2024/02/29	13:06:35	000060.8	kpa
8766	2024/02/29	13:06:37	000060.8	kpa
8767	2024/02/29	13:06:39	000060.7	kpa
8768	2024/02/29	13:06:41	000060.7	kpa
8769	2024/02/29	13:06:43	000060.7	kpa
8770	2024/02/29	13:06:45	000060.7	kpa
8771	2024/02/29	13:06:47	000060.7	kpa
8772	2024/02/29	13:06:49	000060.7	kpa
8773	2024/02/29	13:06:51	000060.7	kpa
8774	2024/02/29	13:06:53	000060.7	kpa
8775	2024/02/29	13:06:55	000060.6	kpa
8776	2024/02/29	13:06:57	000060.6	kpa
8777	2024/02/29	13:06:59	000060.6	kpa
8778	2024/02/29	13:07:01	000060.6	kpa
8779	2024/02/29	13:07:03	000060.6	kpa
8780	2024/02/29	13:07:05	000060.6	kpa
8781	2024/02/29	13:07:07	000060.6	kpa
8782	2024/02/29	13:07:09	000060.6	kpa
8783	2024/02/29	13:07:11	000060.5	kpa
8784	2024/02/29	13:07:13	000060.5	kpa
8785	2024/02/29	13:07:15	000060.5	kpa
8786	2024/02/29	13:07:17	000060.5	kpa
8787	2024/02/29	13:07:19	000060.5	kpa
8788	2024/02/29	13:07:21	000060.5	kpa
8789	2024/02/29	13:07:23	000060.5	kpa
8790	2024/02/29	13:07:25	000060.5	kpa
8791	2024/02/29	13:07:27	000060.5	kpa
8792	2024/02/29	13:07:29	000060.4	kpa
8793	2024/02/29	13:07:31	000060.4	kpa
8794	2024/02/29	13:07:33	000060.4	kpa
8795	2024/02/29	13:07:35	000060.4	kpa
8796	2024/02/29	13:07:37	000060.4	kpa
8797	2024/02/29	13:07:39	000060.4	kpa
8798	2024/02/29	13:07:41	000060.3	kpa
8799	2024/02/29	13:07:43	000060.3	kpa
8800	2024/02/29	13:07:45	000060.3	kpa
8801	2024/02/29	13:07:47	000060.3	kpa
8802	2024/02/29	13:07:49	000060.3	kpa
8803	2024/02/29	13:07:51	000060.3	kpa
8804	2024/02/29	13:07:53	000060.3	kpa
8805	2024/02/29	13:07:55	000060.3	kpa
8806	2024/02/29	13:07:57	000060.3	kpa
8807	2024/02/29	13:07:59	000060.2	kpa
8808	2024/02/29	13:08:01	000060.2	kpa
8809	2024/02/29	13:08:03	000060.2	kpa
8810	2024/02/29	13:08:05	000060.2	kpa
8811	2024/02/29	13:08:07	000060.2	kpa
8812	2024/02/29	13:08:09	000060.2	kpa
8813	2024/02/29	13:08:11	000060.2	kpa
8814	2024/02/29	13:08:13	000060.1	kpa
8815	2024/02/29	13:08:15	000060.1	kpa
8816	2024/02/29	13:08:17	000060.1	kpa
8817	2024/02/29	13:08:19	000060.1	kpa
8818	2024/02/29	13:08:21	000060.1	kpa
8819	2024/02/29	13:08:23	000060.1	kpa
8820	2024/02/29	13:08:25	000060.1	kpa
8821	2024/02/29	13:08:27	000060.1	kpa
8822	2024/02/29	13:08:29	000060.1	kpa
8823	2024/02/29	13:08:31	000060.1	kpa
8824	2024/02/29	13:08:33	000060.0	kpa
8825	2024/02/29	13:08:35	000060.0	kpa
8826	2024/02/29	13:08:37	000060.0	kpa
8827	2024/02/29	13:08:39	000060.0	kpa
8828	2024/02/29	13:08:41	000060.0	kpa
8829	2024/02/29	13:08:43	000060.0	kpa

Table C.2.5: Stack length of 35 mm: Temperature range-T1-T4

5313	2024/02/16 14:08	23.6	31.9	25.2	21.9	
5314	2024/02/16 14:08	23.6	31.9	25.2	21.9	
5315	2024/02/16 14:08	23.6	31.9	25.2	21.9	
5316	2024/02/16 14:08	23.6	31.8	25.2	21.9	
5317	2024/02/16 14:08	23.6	31.8	25.0	21.9	
5318	2024/02/16 14:08	23.6	31.8	25.0	21.9	
5319	2024/02/16 14:08	23.6	31.8	25.0	21.9	
5320	2024/02/16 14:08	23.6	31.8	25.0	21.9	
5321	2024/02/16 14:08	23.6	31.8	25.0	21.9	
5322	2024/02/16 14:08	23.6	31.8	25.0	21.9	
5323	2024/02/16 14:08	23.6	31.8	25.0	21.9	
5324	2024/02/16 14:08	23.6	31.8	25.0	22.2	
5325	2024/02/16 14:08	23.6	31.8	25.0	22.2	
5326	2024/02/16 14:08	23.6	31.8	25.0	22.2	
5327	2024/02/16 14:08	23.6	31.8	25.0	22.2	
5328	2024/02/16 14:08	23.6	31.8	25.0	22.2	
5329	2024/02/16 14:08	23.6	31.8	25.0	22.1	
5330	2024/02/16 14:08	23.6	31.8	25.0	22.1	
5331	2024/02/16 14:08	23.6	31.8	25.0	22.1	
5332	2024/02/16 14:08	23.6	31.8	25.0	22.1	
5333	2024/02/16 14:08	23.6	31.8	25.0	22.1	
5334	2024/02/16 14:08	23.6	31.8	25.0	21.9	
5335	2024/02/16 14:08	23.6	31.8	25.0	21.9	
5336	2024/02/16 14:08	23.6	31.8	25.0	21.9	
5337	2024/02/16 14:08	23.6	31.8	25.0	21.9	
5338	2024/02/16 14:08	23.6	31.8	25.0	21.9	
5339	2024/02/16 14:08	23.6	31.8	25.0	21.9	
5340	2024/02/16 14:08	23.6	31.8	25.0	21.9	
5341	2024/02/16 14:08	23.6	31.8	25.0	21.9	
5342	2024/02/16 14:08	23.6	31.8	25.0	21.9	
5343	2024/02/16 14:08	23.6	31.8	25.0	21.9	
5344	2024/02/16 14:08	23.6	31.8	25.0	21.9	
5345	2024/02/16 14:08	23.6	31.8	25.0	21.9	
5346	2024/02/16 14:08	23.6	31.8	25.0	21.9	
5347	2024/02/16 14:08	23.6	31.8	25.0	21.9	
5348	2024/02/16 14:08	23.6	31.7	25.0	21.9	
5349	2024/02/16 14:08	23.6	31.7	24.9	21.9	
5350	2024/02/16 14:09	23.6	31.7	24.9	21.9	
5351	2024/02/16 14:09	23.6	31.7	24.9	21.9	
5352	2024/02/16 14:09	23.6	31.7	24.9	21.9	
5353	2024/02/16 14:09	23.6	31.6	24.9	21.9	
5354	2024/02/16 14:09	23.6	31.6	24.9	21.9	
5355	2024/02/16 14:09	23.6	31.6	24.9	21.8	
5356	2024/02/16 14:09	23.6	31.6	24.9	21.8	
5357	2024/02/16 14:09	23.6	31.6	24.9	21.8	
5358	2024/02/16 14:09	23.6	31.7	24.9	21.8	
5359	2024/02/16 14:09	23.6	31.7	24.9	21.8	
5360	2024/02/16 14:09	23.6	31.7	24.9	21.8	
5361	2024/02/16 14:09	23.6	31.7	24.9	21.8	
5362	2024/02/16 14:09	23.6	31.7	24.9	21.8	
5363	2024/02/16 14:09	23.6	31.8	24.9	21.8	
5364	2024/02/16 14:09	23.6	31.8	25.0	21.8	
5365	2024/02/16 14:09	23.6	31.8	25.0	21.8	
5366	2024/02/16 14:09	23.6	31.8	25.0	21.8	
5367	2024/02/16 14:09	23.6	31.8	25.0	21.8	
5368	2024/02/16 14:09	23.6	31.8	25.0	21.8	
5369	2024/02/16 14:09	23.6	31.8	25.0	21.8	
5370	2024/02/16 14:09	23.6	31.8	25.2	21.8	
5371	2024/02/16 14:09	23.6	31.8	25.2	21.9	
5372	2024/02/16 14:09	23.6	31.8	25.2	21.9	
5373	2024/02/16 14:09	23.6	31.8	25.2	21.9	
5374	2024/02/16 14:09	23.6	31.8	25.2	21.9	
5375	2024/02/16 14:09	23.6	31.8	25.2	21.9	
5376	2024/02/16 14:09	23.6	31.8	25.2	21.8	
5377	2024/02/16 14:09	23.6	31.8	25.2	21.8	

Table C.2.6: Stack length of 35 mm: Temperature range-T5-T6

5422	2024/02/16 14:08	24.6	36.0	- - -	- - -	
5423	2024/02/16 14:08	24.6	36.0	- - -	- - -	
5424	2024/02/16 14:08	24.6	36.0	- - -	- - -	
5425	2024/02/16 14:08	24.6	36.0	- - -	- - -	
5426	2024/02/16 14:08	24.6	36.0	- - -	- - -	
5427	2024/02/16 14:08	24.6	36.0	- - -	- - -	
5428	2024/02/16 14:08	24.6	36.0	- - -	- - -	
5429	2024/02/16 14:08	24.6	36.0	- - -	- - -	
5430	2024/02/16 14:08	24.6	36.0	- - -	- - -	
5431	2024/02/16 14:08	24.6	36.0	- - -	- - -	
5432	2024/02/16 14:08	24.6	36.0	- - -	- - -	
5433	2024/02/16 14:08	24.6	36.0	- - -	- - -	
5434	2024/02/16 14:08	24.6	36.0	- - -	- - -	
5435	2024/02/16 14:08	24.6	36.0	- - -	- - -	
5436	2024/02/16 14:08	24.6	36.0	- - -	- - -	
5437	2024/02/16 14:08	24.6	36.0	- - -	- - -	
5438	2024/02/16 14:08	24.6	36.0	- - -	- - -	
5439	2024/02/16 14:08	24.6	36.0	- - -	- - -	
5440	2024/02/16 14:08	24.6	36.0	- - -	- - -	
5441	2024/02/16 14:08	24.6	36.0	- - -	- - -	
5442	2024/02/16 14:08	24.6	36.0	- - -	- - -	
5443	2024/02/16 14:08	24.6	36.0	- - -	- - -	
5444	2024/02/16 14:08	24.6	36.0	- - -	- - -	
5445	2024/02/16 14:08	24.6	36.0	- - -	- - -	
5446	2024/02/16 14:08	24.6	36.0	- - -	- - -	
5447	2024/02/16 14:08	24.6	36.0	- - -	- - -	
5448	2024/02/16 14:08	24.6	36.0	- - -	- - -	
5449	2024/02/16 14:08	24.6	36.0	- - -	- - -	
5450	2024/02/16 14:08	24.6	36.0	- - -	- - -	
5451	2024/02/16 14:08	24.6	36.0	- - -	- - -	
5452	2024/02/16 14:08	24.6	36.0	- - -	- - -	
5453	2024/02/16 14:08	24.6	36.0	- - -	- - -	
5454	2024/02/16 14:08	24.6	36.0	- - -	- - -	
5455	2024/02/16 14:08	24.6	36.0	- - -	- - -	
5456	2024/02/16 14:08	24.6	36.0	- - -	- - -	
5457	2024/02/16 14:08	24.6	36.0	- - -	- - -	
5458	2024/02/16 14:08	24.6	36.0	- - -	- - -	
5459	2024/02/16 14:08	24.6	36.0	- - -	- - -	
5460	2024/02/16 14:08	24.6	36.0	- - -	- - -	
5461	2024/02/16 14:08	24.6	36.0	- - -	- - -	
5462	2024/02/16 14:08	24.6	36.0	- - -	- - -	
5463	2024/02/16 14:08	24.6	36.0	- - -	- - -	
5464	2024/02/16 14:08	24.6	36.0	- - -	- - -	
5465	2024/02/16 14:08	24.6	36.0	- - -	- - -	
5466	2024/02/16 14:09	24.6	36.0	- - -	- - -	
5467	2024/02/16 14:09	24.6	36.0	- - -	- - -	
5468	2024/02/16 14:09	24.6	36.0	- - -	- - -	
5469	2024/02/16 14:09	24.6	36.0	- - -	- - -	
5470	2024/02/16 14:09	24.6	36.0	- - -	- - -	
5471	2024/02/16 14:09	24.6	36.0	- - -	- - -	
5472	2024/02/16 14:09	24.6	36.0	- - -	- - -	
5473	2024/02/16 14:09	24.6	36.0	- - -	- - -	
5474	2024/02/16 14:09	24.6	36.0	- - -	- - -	
5475	2024/02/16 14:09	24.6	36.0	- - -	- - -	
5476	2024/02/16 14:09	24.6	36.1	- - -	- - -	
5477	2024/02/16 14:09	24.6	36.1	- - -	- - -	
5478	2024/02/16 14:09	24.6	36.1	- - -	- - -	
5479	2024/02/16 14:09	24.6	36.1	- - -	- - -	
5480	2024/02/16 14:09	24.6	36.1	- - -	- - -	
5481	2024/02/16 14:09	24.5	36.1	- - -	- - -	
5482	2024/02/16 14:09	24.5	36.1	- - -	- - -	
5483	2024/02/16 14:09	24.5	36.1	- - -	- - -	
5484	2024/02/16 14:09	24.3	36.1	- - -	- - -	

Table C.2.7: Stack length of 35 mm: Voltage and current

479	39.1 V	1.1 A	16/02/24 13:59:33		
480	39.1 V	1.1 A	16/02/24 13:59:43		
481	39.1 V	1.1 A	16/02/24 13:59:53		
482	39.1 V	1.1 A	16/02/24 14:00:03		
483	39.1 V	1.1 A	16/02/24 14:00:13		
484	39.1 V	1.1 A	16/02/24 14:00:23		
485	39.1 V	1.1 A	16/02/24 14:00:33		
486	39.1 V	1.1 A	16/02/24 14:00:43		
487	39.1 V	1.1 A	16/02/24 14:00:53		
488	39.1 V	1.1 A	16/02/24 14:01:03		
489	39.1 V	1.1 A	16/02/24 14:01:13		
490	39.1 V	1.1 A	16/02/24 14:01:23		
491	39.1 V	1.1 A	16/02/24 14:01:33		
492	39.1 V	1.1 A	16/02/24 14:01:43		
493	39.1 V	1.1 A	16/02/24 14:01:53		
494	39.1 V	1.1 A	16/02/24 14:02:03		
495	39.1 V	1.0 A	16/02/24 14:02:13		
496	39.1 V	1.1 A	16/02/24 14:02:23		
497	39.1 V	1.1 A	16/02/24 14:02:33		
498	39.1 V	1.1 A	16/02/24 14:02:43		
499	39.1 V	1.1 A	16/02/24 14:02:53		
500	39.1 V	1.1 A	16/02/24 14:03:03		
501	39.1 V	1.1 A	16/02/24 14:03:13		
502	39.1 V	1.1 A	16/02/24 14:03:23		
503	39.1 V	1.1 A	16/02/24 14:03:33		
504	39.1 V	1.1 A	16/02/24 14:03:43		
505	39.1 V	1.1 A	16/02/24 14:03:53		
506	39.1 V	1.1 A	16/02/24 14:04:03		
507	39.1 V	1.1 A	16/02/24 14:04:13		
508	39.1 V	1.1 A	16/02/24 14:04:23		
509	39.1 V	1.0 A	16/02/24 14:04:33		
510	39.1 V	1.1 A	16/02/24 14:04:43		
511	39.1 V	1.1 A	16/02/24 14:04:53		
512	39.1 V	1.0 A	16/02/24 14:05:03		
513	39.1 V	1.1 A	16/02/24 14:05:13		
514	39.1 V	1.1 A	16/02/24 14:05:23		
515	39.1 V	1.1 A	16/02/24 14:05:33		
516	39.1 V	1.1 A	16/02/24 14:05:43		
517	39.1 V	1.1 A	16/02/24 14:05:53		
518	39.1 V	1.1 A	16/02/24 14:06:03		
519	39.1 V	1.1 A	16/02/24 14:06:13		
520	39.1 V	1.1 A	16/02/24 14:06:23		
521	39.1 V	1.1 A	16/02/24 14:06:33		
522	39.1 V	1.1 A	16/02/24 14:06:43		
523	39.1 V	1.1 A	16/02/24 14:06:53		
524	39.1 V	1.1 A	16/02/24 14:07:03		
525	39.1 V	1.1 A	16/02/24 14:07:13		
526	39.1 V	1.1 A	16/02/24 14:07:23		
527	39.1 V	1.1 A	16/02/24 14:07:33		
528	39.1 V	1.1 A	16/02/24 14:07:43		
529	39.1 V	1.1 A	16/02/24 14:07:53		
530	39.1 V	1.1 A	16/02/24 14:08:03		
531	39.1 V	1.1 A	16/02/24 14:08:13		
532	39.1 V	1.1 A	16/02/24 14:08:23		
533	39.1 V	1.0 A	16/02/24 14:08:33		
534	39.1 V	1.1 A	16/02/24 14:08:43		
535	39.1 V	1.1 A	16/02/24 14:08:53		
536	39.1 V	1.1 A	16/02/24 14:09:03		
537	39.1 V	1.1 A	16/02/24 14:09:13		
538	39.1 V	1.0 A	16/02/24 14:09:23		
539	39.1 V	1.1 A	16/02/24 14:09:33		
540	39.1 V	1.1 A	16/02/24 14:09:43		
541	39.1 V	1.1 A	16/02/24 14:09:53		

Table C.2.8: Stack length of 35 mm: Mean pressure

12530	2024/02/16	14:15:48	000018.9	kpa		
12531	2024/02/16	14:15:50	000018.9	kpa		
12532	2024/02/16	14:15:52	000018.9	kpa		
12533	2024/02/16	14:15:54	000018.8	kpa		
12534	2024/02/16	14:15:56	000018.8	kpa		
12535	2024/02/16	14:15:58	000018.8	kpa		
12536	2024/02/16	14:16:00	000018.8	kpa		
12537	2024/02/16	14:16:02	000018.8	kpa		
12538	2024/02/16	14:16:04	000018.8	kpa		
12539	2024/02/16	14:16:06	000018.8	kpa		
12540	2024/02/16	14:16:08	000018.8	kpa		
12541	2024/02/16	14:16:10	000018.8	kpa		
12542	2024/02/16	14:16:12	000018.8	kpa		
12543	2024/02/16	14:16:14	000018.8	kpa		
12544	2024/02/16	14:16:16	000018.8	kpa		
12545	2024/02/16	14:16:18	000018.8	kpa		
12546	2024/02/16	14:16:20	000018.7	kpa		
12547	2024/02/16	14:16:22	000018.7	kpa		
12548	2024/02/16	14:16:24	000018.7	kpa		
12549	2024/02/16	14:16:26	000018.7	kpa		
12550	2024/02/16	14:16:28	000018.7	kpa		
12551	2024/02/16	14:16:30	000018.7	kpa		
12552	2024/02/16	14:16:32	000018.7	kpa		
12553	2024/02/16	14:16:34	000018.7	kpa		
12554	2024/02/16	14:16:36	000018.7	kpa		
12555	2024/02/16	14:16:38	000018.7	kpa		
12556	2024/02/16	14:16:40	000018.7	kpa		
12557	2024/02/16	14:16:42	000018.7	kpa		
12558	2024/02/16	14:16:44	000018.7	kpa		
12559	2024/02/16	14:16:46	000018.7	kpa		
12560	2024/02/16	14:16:48	000018.7	kpa		
12561	2024/02/16	14:16:50	000018.7	kpa		
12562	2024/02/16	14:16:52	000018.7	kpa		
12563	2024/02/16	14:16:54	000018.7	kpa		
12564	2024/02/16	14:16:56	000018.7	kpa		
12565	2024/02/16	14:16:58	000018.6	kpa		
12566	2024/02/16	14:17:00	000018.6	kpa		
12567	2024/02/16	14:17:02	000018.6	kpa		
12568	2024/02/16	14:17:04	000018.6	kpa		
12569	2024/02/16	14:17:06	000018.6	kpa		
12570	2024/02/16	14:17:08	000018.6	kpa		
12571	2024/02/16	14:17:10	000018.6	kpa		
12572	2024/02/16	14:17:12	000018.6	kpa		
12573	2024/02/16	14:17:14	000018.6	kpa		
12574	2024/02/16	14:17:16	000018.6	kpa		
12575	2024/02/16	14:17:18	000018.6	kpa		
12576	2024/02/16	14:17:20	000018.6	kpa		
12577	2024/02/16	14:17:22	000018.5	kpa		
12578	2024/02/16	14:17:24	000018.6	kpa		
12579	2024/02/16	14:17:26	000018.6	kpa		
12580	2024/02/16	14:17:28	000018.5	kpa		
12581	2024/02/16	14:17:30	000018.5	kpa		
12582	2024/02/16	14:17:32	000018.5	kpa		
12583	2024/02/16	14:17:34	000018.5	kpa		
12584	2024/02/16	14:17:36	000018.5	kpa		
12585	2024/02/16	14:17:38	000018.5	kpa		
12586	2024/02/16	14:17:40	000018.5	kpa		
12587	2024/02/16	14:17:42	000018.5	kpa		
12588	2024/02/16	14:17:44	000018.5	kpa		
12589	2024/02/16	14:17:46	000018.5	kpa		
12590	2024/02/16	14:17:48	000018.5	kpa		
12591	2024/02/16	14:17:50	000018.5	kpa		
12592	2024/02/16	14:17:52	000018.5	kpa		
12593	2024/02/16	14:17:54	000018.4	kpa		
12594	2024/02/16	14:17:56	000018.5	kpa		

Table C.2.9: Stack length of 45 mm positioned at 40 mm: T1-T4

5553	2024/03/01 12:57	24.2	28.8	23.0	25.2
5554	2024/03/01 12:57	24.2	28.8	23.0	25.2
5555	2024/03/01 12:57	24.2	28.8	23.0	25.2
5556	2024/03/01 12:57	24.2	28.8	23.0	25.2
5557	2024/03/01 12:57	24.2	28.8	23.0	25.2
5558	2024/03/01 12:57	24.2	28.8	23.0	25.2
5559	2024/03/01 12:57	24.2	28.8	23.0	25.2
5560	2024/03/01 12:57	24.2	28.8	23.0	25.2
5561	2024/03/01 12:57	24.2	28.8	23.0	25.2
5562	2024/03/01 12:57	24.2	28.8	23.0	25.1
5563	2024/03/01 12:57	24.2	28.8	23.0	25.1
5564	2024/03/01 12:57	24.4	28.8	23.0	25.1
5565	2024/03/01 12:57	24.4	28.8	23.0	25.1
5566	2024/03/01 12:57	24.4	28.8	23.0	25.1
5567	2024/03/01 12:57	24.4	28.8	23.0	25.1
5568	2024/03/01 12:57	24.4	28.8	23.0	25.2
5569	2024/03/01 12:57	24.2	28.8	23.0	25.2
5570	2024/03/01 12:57	24.2	28.8	23.0	25.2
5571	2024/03/01 12:57	24.2	28.8	23.0	25.2
5572	2024/03/01 12:57	24.2	28.8	23.0	25.2
5573	2024/03/01 12:57	24.2	28.8	23.0	25.2
5574	2024/03/01 12:57	24.2	28.8	23.0	25.2
5575	2024/03/01 12:57	24.2	28.9	23.0	25.2
5576	2024/03/01 12:57	24.2	28.9	23.0	25.2
5577	2024/03/01 12:57	24.2	28.9	23.0	25.2
5578	2024/03/01 12:57	24.2	28.9	23.0	25.2
5579	2024/03/01 12:57	24.1	28.9	23.0	25.2
5580	2024/03/01 12:57	24.1	28.9	23.0	25.2
5581	2024/03/01 12:57	24.1	28.9	23.0	25.2
5582	2024/03/01 12:57	24.1	28.9	23.0	25.2
5583	2024/03/01 12:57	24.1	28.9	23.0	25.3
5584	2024/03/01 12:57	24.1	28.9	23.0	25.3
5585	2024/03/01 12:57	24.2	28.9	23.0	25.3
5586	2024/03/01 12:57	24.2	29.0	23.0	25.3
5587	2024/03/01 12:57	24.2	29.0	23.0	25.3
5588	2024/03/01 12:57	24.2	29.0	23.0	25.3
5589	2024/03/01 12:58	24.2	29.0	23.0	25.4
5590	2024/03/01 12:58	24.4	29.0	23.0	25.4
5591	2024/03/01 12:58	24.4	29.0	23.0	25.4
5592	2024/03/01 12:58	24.4	29.0	23.0	25.4
5593	2024/03/01 12:58	24.4	29.0	23.0	25.4
5594	2024/03/01 12:58	24.4	29.0	23.0	25.5
5595	2024/03/01 12:58	24.4	29.0	23.0	25.5
5596	2024/03/01 12:58	24.4	28.9	23.0	25.5
5597	2024/03/01 12:58	24.4	28.9	23.0	25.5
5598	2024/03/01 12:58	24.4	28.9	23.0	25.5

Table C.2.10: Stack length of 45 mm positioned at 40 mm: T5-T6

5572	2024/03/01 12:57	25.1	34.1	---	---
5573	2024/03/01 12:57	25.1	34.1	---	---
5574	2024/03/01 12:57	24.8	34.1	---	---
5575	2024/03/01 12:57	24.8	34.1	---	---
5576	2024/03/01 12:57	24.8	34.1	---	---
5577	2024/03/01 12:57	24.8	34.1	---	---
5578	2024/03/01 12:57	24.8	34.1	---	---
5579	2024/03/01 12:57	24.8	34.1	---	---
5580	2024/03/01 12:57	24.8	34.1	---	---
5581	2024/03/01 12:57	24.8	34.1	---	---
5582	2024/03/01 12:57	24.8	34.1	---	---
5583	2024/03/01 12:57	24.8	34.1	---	---
5584	2024/03/01 12:57	24.8	34.1	---	---
5585	2024/03/01 12:57	24.8	34.1	---	---
5586	2024/03/01 12:57	24.8	34.1	---	---
5587	2024/03/01 12:57	24.8	34.1	---	---
5588	2024/03/01 12:57	24.8	34.1	---	---
5589	2024/03/01 12:57	24.8	34.1	---	---
5590	2024/03/01 12:57	24.8	34.1	---	---
5591	2024/03/01 12:57	24.8	34.1	---	---
5592	2024/03/01 12:57	25.1	34.1	---	---
5593	2024/03/01 12:57	25.1	34.1	---	---
5594	2024/03/01 12:57	25.1	34.1	---	---
5595	2024/03/01 12:57	25.1	34.1	---	---
5596	2024/03/01 12:57	25.1	34.1	---	---
5597	2024/03/01 12:57	25.1	34.1	---	---
5598	2024/03/01 12:57	25.1	34.1	---	---
5599	2024/03/01 12:57	25.1	34.1	---	---
5600	2024/03/01 12:57	25.1	34.1	---	---
5601	2024/03/01 12:57	25.1	34.1	---	---
5602	2024/03/01 12:57	25.1	34.1	---	---
5603	2024/03/01 12:57	25.1	34.1	---	---
5604	2024/03/01 12:57	25.1	34.1	---	---
5605	2024/03/01 12:57	25.1	34.1	---	---
5606	2024/03/01 12:57	25.1	34.1	---	---
5607	2024/03/01 12:57	25.1	34.1	---	---
5608	2024/03/01 12:57	25.1	34.1	---	---
5609	2024/03/01 12:57	25.1	34.1	---	---
5610	2024/03/01 12:57	25.1	34.1	---	---
5611	2024/03/01 12:57	25.1	34.2	---	---
5612	2024/03/01 12:57	25.1	34.2	---	---
5613	2024/03/01 12:57	25.1	34.2	---	---
5614	2024/03/01 12:57	25.1	34.2	---	---
5615	2024/03/01 12:58	25.1	34.2	---	---
5616	2024/03/01 12:58	25.1	34.2	---	---
5617	2024/03/01 12:58	25.1	34.2	---	---

Table C.2.11: Stack length of 45 mm positioned at 40 mm: Voltage and current.

305	37.5 V	1.1 A	01/03/24 12:17:41		
306	37.5 V	1.1 A	01/03/24 12:17:51		
307	37.5 V	1.1 A	01/03/24 12:18:01		
308	37.5 V	1.1 A	01/03/24 12:18:11		
309	37.5 V	1.1 A	01/03/24 12:18:21		
310	37.5 V	1.1 A	01/03/24 12:18:31		
311	37.5 V	1.1 A	01/03/24 12:18:41		
312	37.3 V	1.1 A	01/03/24 12:18:51		
313	37.3 V	1.1 A	01/03/24 12:19:01		
314	37.5 V	1.1 A	01/03/24 12:19:11		
315	37.5 V	1.1 A	01/03/24 12:19:21		
316	37.5 V	1.1 A	01/03/24 12:19:31		
317	37.5 V	1.1 A	01/03/24 12:19:41		
318	37.5 V	1.1 A	01/03/24 12:19:51		
319	37.5 V	1.1 A	01/03/24 12:20:01		
320	37.5 V	1.1 A	01/03/24 12:20:11		
321	37.5 V	1.1 A	01/03/24 12:20:21		
322	37.5 V	1.1 A	01/03/24 12:20:31		
323	37.5 V	1.0 A	01/03/24 12:20:41		
324	37.5 V	1.1 A	01/03/24 12:20:51		
325	37.5 V	1.1 A	01/03/24 12:21:01		
326	37.5 V	1.1 A	01/03/24 12:21:11		
327	37.5 V	1.1 A	01/03/24 12:21:21		
328	37.5 V	1.1 A	01/03/24 12:21:31		
329	37.5 V	1.1 A	01/03/24 12:21:41		
330	37.5 V	1.0 A	01/03/24 12:21:51		
331	37.5 V	1.1 A	01/03/24 12:22:01		
332	37.5 V	1.1 A	01/03/24 12:22:11		
333	37.5 V	1.0 A	01/03/24 12:22:21		
334	37.5 V	1.1 A	01/03/24 12:22:31		
335	37.5 V	1.1 A	01/03/24 12:22:41		
336	37.5 V	1.1 A	01/03/24 12:22:51		
337	37.5 V	1.0 A	01/03/24 12:23:01		
338	37.5 V	1.1 A	01/03/24 12:23:11		
339	37.5 V	1.1 A	01/03/24 12:23:21		
340	37.5 V	1.0 A	01/03/24 12:23:31		
341	37.5 V	1.1 A	01/03/24 12:23:41		
342	37.5 V	1.1 A	01/03/24 12:23:51		
343	37.5 V	1.1 A	01/03/24 12:24:01		
344	37.5 V	1.1 A	01/03/24 12:24:11		
345	37.3 V	1.1 A	01/03/24 12:24:21		
346	37.5 V	1.1 A	01/03/24 12:24:31		
347	37.5 V	1.1 A	01/03/24 12:24:41		
348	37.3 V	1.1 A	01/03/24 12:24:51		
349	37.5 V	1.1 A	01/03/24 12:25:01		
350	37.5 V	1.1 A	01/03/24 12:25:11		
351	37.5 V	1.1 A	01/03/24 12:25:21		
352	37.5 V	1.1 A	01/03/24 12:25:31		
353	37.5 V	1.1 A	01/03/24 12:25:41		
354	37.5 V	1.1 A	01/03/24 12:25:51		
355	37.5 V	1.1 A	01/03/24 12:26:01		
356	37.5 V	1.1 A	01/03/24 12:26:11		
357	37.5 V	1.1 A	01/03/24 12:26:21		
358	37.5 V	1.1 A	01/03/24 12:26:31		
359	37.5 V	1.1 A	01/03/24 12:26:41		
360	37.5 V	1.0 A	01/03/24 12:26:51		

Table C.2.12: Stack length of 45 mm positioned at 40 mm: Mean and amplitude pressure.

14360	2024/03/01	12:56:34	000060.7	kpa
14361	2024/03/01	12:56:36	000060.7	kpa
14362	2024/03/01	12:56:38	000060.7	kpa
14363	2024/03/01	12:56:40	000060.6	kpa
14364	2024/03/01	12:56:42	000060.6	kpa
14365	2024/03/01	12:56:44	000060.6	kpa
14366	2024/03/01	12:56:46	000060.6	kpa
14367	2024/03/01	12:56:48	000060.6	kpa
14368	2024/03/01	12:56:50	000060.6	kpa
14369	2024/03/01	12:56:52	000060.6	kpa
14370	2024/03/01	12:56:54	000060.6	kpa
14371	2024/03/01	12:56:56	000060.6	kpa
14372	2024/03/01	12:56:58	000060.6	kpa
14373	2024/03/01	12:57:00	000060.5	kpa
14374	2024/03/01	12:57:02	000060.5	kpa
14375	2024/03/01	12:57:04	000060.5	kpa
14376	2024/03/01	12:57:06	000060.5	kpa
14377	2024/03/01	12:57:08	000060.5	kpa
14378	2024/03/01	12:57:10	000060.5	kpa
14379	2024/03/01	12:57:12	000060.5	kpa
14380	2024/03/01	12:57:14	000060.4	kpa
14381	2024/03/01	12:57:16	000060.4	kpa
14382	2024/03/01	12:57:18	000060.4	kpa
14383	2024/03/01	12:57:20	000060.4	kpa
14384	2024/03/01	12:57:22	000060.4	kpa
14385	2024/03/01	12:57:24	000060.4	kpa
14386	2024/03/01	12:57:26	000060.4	kpa
14387	2024/03/01	12:57:28	000060.4	kpa
14388	2024/03/01	12:57:30	000060.3	kpa
14389	2024/03/01	12:57:32	000060.3	kpa
14390	2024/03/01	12:57:34	000060.3	kpa
14391	2024/03/01	12:57:36	000060.3	kpa
14392	2024/03/01	12:57:38	000060.3	kpa
14393	2024/03/01	12:57:40	000060.3	kpa
14394	2024/03/01	12:57:42	000060.3	kpa
14395	2024/03/01	12:57:44	000060.3	kpa
14396	2024/03/01	12:57:46	000060.3	kpa
14397	2024/03/01	12:57:48	000060.2	kpa
14398	2024/03/01	12:57:50	000060.2	kpa
14399	2024/03/01	12:57:52	000060.2	kpa
14400	2024/03/01	12:57:54	000060.2	kpa
14401	2024/03/01	12:57:56	000060.2	kpa
14402	2024/03/01	12:57:58	000060.2	kpa
14403	2024/03/01	12:58:00	000060.2	kpa
14404	2024/03/01	12:58:02	000060.2	kpa

Table C.2.13: Stack length of 55 mm positioned at 40 mm: T1-T4

5310	2024/02/06 16:30	26,1	33,9	25,5	25,8
5311	2024/02/06 16:30	26,1	34,1	25,5	25,8
5312	2024/02/06 16:30	26,1	34,1	25,5	25,8
5313	2024/02/06 16:30	26,1	34,1	25,5	25,8
5314	2024/02/06 16:30	26,1	34,1	25,5	25,8
5315	2024/02/06 16:30	26,2	34,1	25,5	25,8
5316	2024/02/06 16:30	26,2	34,1	25,5	25,8
5317	2024/02/06 16:30	26,2	34,1	25,5	25,8
5318	2024/02/06 16:30	26,2	34,1	25,5	25,8
5319	2024/02/06 16:30	26,2	34,1	25,5	25,8
5320	2024/02/06 16:30	26,2	34,1	25,5	25,8
5321	2024/02/06 16:30	26,2	34,1	25,5	25,8
5322	2024/02/06 16:30	26,2	34,1	25,5	25,8
5323	2024/02/06 16:30	26,2	34,1	25,6	25,8
5324	2024/02/06 16:30	26,2	34,1	25,6	25,8
5325	2024/02/06 16:30	26,2	34,1	25,6	25,8
5326	2024/02/06 16:30	26,2	34,1	25,6	25,8
5327	2024/02/06 16:30	26,2	34,1	25,6	25,8
5328	2024/02/06 16:30	26,2	34,1	25,6	25,8
5329	2024/02/06 16:30	26,2	34,1	25,6	25,8
5330	2024/02/06 16:30	26,2	34,1	25,6	25,8
5331	2024/02/06 16:30	26,2	34,1	25,6	25,8
5332	2024/02/06 16:30	26,2	34,1	25,6	25,8
5333	2024/02/06 16:30	26,2	34,1	25,6	25,8
5334	2024/02/06 16:30	26,2	34,1	25,6	25,8
5335	2024/02/06 16:30	26,2	34,1	25,6	25,8
5336	2024/02/06 16:30	26,2	34,1	25,6	25,8
5337	2024/02/06 16:30	26,2	34,1	25,6	25,8
5338	2024/02/06 16:30	26,2	34,1	25,6	25,8
5339	2024/02/06 16:30	26,2	34,1	25,6	25,8
5340	2024/02/06 16:30	26,2	34,1	25,6	25,8
5341	2024/02/06 16:30	26,2	34,1	25,6	25,8
5342	2024/02/06 16:30	26,2	34,1	25,6	25,8
5343	2024/02/06 16:30	26,2	34,1	25,6	25,8
5344	2024/02/06 16:30	26,2	34,1	25,6	25,8
5345	2024/02/06 16:30	26,2	34,1	25,6	25,8
5346	2024/02/06 16:30	26,2	34,1	25,6	25,8
5347	2024/02/06 16:30	26,3	34,1	25,6	25,8
5348	2024/02/06 16:30	26,3	34,1	25,6	25,8
5349	2024/02/06 16:30	26,3	34,1	25,6	25,8
5350	2024/02/06 16:30	26,3	34,1	25,6	25,8
5351	2024/02/06 16:30	26,3	34,1	25,6	25,8
5352	2024/02/06 16:30	26,3	34,1	25,6	25,8
5353	2024/02/06 16:30	26,3	34,1	25,6	25,8
5354	2024/02/06 16:30	26,3	34,2	25,6	25,8
5355	2024/02/06 16:30	26,3	34,2	25,6	25,8

Table C.2.14:Stack length of 55 mm positioned at 40 mm: T5-T6

5318	2024/02/06 16:30	30,4	38,7	---	---
5319	2024/02/06 16:30	30,4	38,7	---	---
5320	2024/02/06 16:30	30,3	38,7	---	---
5321	2024/02/06 16:30	30,3	38,7	---	---
5322	2024/02/06 16:30	30,3	38,7	---	---
5323	2024/02/06 16:30	30,3	38,7	---	---
5324	2024/02/06 16:30	30,3	38,7	---	---
5325	2024/02/06 16:30	30,3	38,7	---	---
5326	2024/02/06 16:30	30,4	38,7	---	---
5327	2024/02/06 16:30	30,4	38,7	---	---
5328	2024/02/06 16:30	30,4	38,7	---	---
5329	2024/02/06 16:30	30,4	38,7	---	---
5330	2024/02/06 16:30	30,4	38,7	---	---
5331	2024/02/06 16:30	30,4	38,7	---	---
5332	2024/02/06 16:30	30,5	38,7	---	---
5333	2024/02/06 16:30	30,5	38,7	---	---
5334	2024/02/06 16:30	30,5	38,7	---	---
5335	2024/02/06 16:30	30,6	38,7	---	---
5336	2024/02/06 16:30	30,6	38,7	---	---
5337	2024/02/06 16:30	30,6	38,7	---	---
5338	2024/02/06 16:30	30,6	38,7	---	---
5339	2024/02/06 16:30	30,6	38,7	---	---
5340	2024/02/06 16:30	30,6	38,7	---	---
5341	2024/02/06 16:30	30,6	38,7	---	---
5342	2024/02/06 16:30	30,7	38,7	---	---
5343	2024/02/06 16:30	30,7	38,7	---	---
5344	2024/02/06 16:30	30,7	38,7	---	---
5345	2024/02/06 16:30	30,7	38,7	---	---
5346	2024/02/06 16:30	30,7	38,7	---	---
5347	2024/02/06 16:30	30,7	38,7	---	---
5348	2024/02/06 16:30	30,6	38,7	---	---
5349	2024/02/06 16:30	30,6	38,7	---	---
5350	2024/02/06 16:30	30,6	38,7	---	---
5351	2024/02/06 16:31	30,4	38,7	---	---
5352	2024/02/06 16:31	30,4	38,7	---	---
5353	2024/02/06 16:31	30,4	38,7	---	---
5354	2024/02/06 16:31	30,4	38,7	---	---
5355	2024/02/06 16:31	30,4	38,7	---	---
5356	2024/02/06 16:31	30,4	38,7	---	---
5357	2024/02/06 16:31	30,5	38,7	---	---
5358	2024/02/06 16:31	30,5	38,7	---	---
5359	2024/02/06 16:31	30,5	38,7	---	---
5360	2024/02/06 16:31	30,5	38,7	---	---
5361	2024/02/06 16:31	30,5	38,7	---	---
5362	2024/02/06 16:31	30,5	38,7	---	---

Table C.2.15:Stack length of 55 mm positioned at 40 mm: Voltage and current.

473	39.0 V	1.0 A	06/02/24 16:21:14		
474	39.0 V	1.0 A	06/02/24 16:21:24		
475	39.0 V	1.0 A	06/02/24 16:21:34		
476	39.0 V	1.1 A	06/02/24 16:21:44		
477	39.0 V	1.0 A	06/02/24 16:21:54		
478	38.8 V	1.1 A	06/02/24 16:22:04		
479	39.0 V	1.0 A	06/02/24 16:22:14		
480	39.0 V	1.1 A	06/02/24 16:22:24		
481	39.0 V	1.1 A	06/02/24 16:22:34		
482	39.0 V	1.0 A	06/02/24 16:22:44		
483	39.0 V	1.0 A	06/02/24 16:22:54		
484	39.0 V	1.1 A	06/02/24 16:23:04		
485	39.0 V	1.0 A	06/02/24 16:23:14		
486	39.0 V	1.1 A	06/02/24 16:23:24		
487	39.0 V	1.0 A	06/02/24 16:23:34		
488	39.0 V	1.0 A	06/02/24 16:23:44		
489	39.0 V	1.0 A	06/02/24 16:23:54		
490	39.0 V	1.0 A	06/02/24 16:24:04		
491	39.0 V	1.0 A	06/02/24 16:24:14		
492	39.0 V	1.0 A	06/02/24 16:24:24		
493	39.0 V	1.1 A	06/02/24 16:24:34		
494	38.8 V	1.0 A	06/02/24 16:24:44		
495	39.0 V	1.0 A	06/02/24 16:24:54		
496	39.0 V	1.0 A	06/02/24 16:25:04		
497	39.0 V	1.0 A	06/02/24 16:25:14		
498	39.0 V	1.0 A	06/02/24 16:25:24		
499	39.0 V	1.0 A	06/02/24 16:25:34		
500	39.0 V	1.0 A	06/02/24 16:25:44		
501	39.0 V	1.0 A	06/02/24 16:25:54		
502	39.0 V	1.0 A	06/02/24 16:26:04		
503	39.0 V	1.0 A	06/02/24 16:26:14		
504	39.0 V	1.1 A	06/02/24 16:26:24		
505	39.0 V	1.0 A	06/02/24 16:26:34		
506	39.0 V	1.0 A	06/02/24 16:26:44		
507	39.0 V	1.0 A	06/02/24 16:26:54		
508	39.0 V	1.0 A	06/02/24 16:27:04		
509	39.0 V	1.0 A	06/02/24 16:27:14		
510	39.0 V	1.0 A	06/02/24 16:27:24		
511	39.0 V	1.0 A	06/02/24 16:27:34		
512	39.0 V	1.0 A	06/02/24 16:27:44		
513	39.0 V	1.0 A	06/02/24 16:27:54		
514	39.0 V	1.0 A	06/02/24 16:28:04		
515	39.0 V	1.1 A	06/02/24 16:28:14		
516	39.0 V	1.0 A	06/02/24 16:28:24		
517	39.0 V	1.0 A	06/02/24 16:28:34		
518	39.0 V	1.0 A	06/02/24 16:28:44		
519	39.0 V	1.0 A	06/02/24 16:28:54		
520	39.0 V	1.0 A	06/02/24 16:29:04		
521	39.0 V	1.0 A	06/02/24 16:29:14		
522	39.0 V	1.0 A	06/02/24 16:29:24		
523	39.0 V	1.0 A	06/02/24 16:29:34		
524	39.0 V	1.0 A	06/02/24 16:29:44		
525	39.0 V	1.0 A	06/02/24 16:29:54		
526	39.0 V	1.0 A	06/02/24 16:30:04		
527	38.8 V	1.0 A	06/02/24 16:30:14		
528	38.8 V	1.0 A	06/02/24 16:30:24		
529	39.0 V	1.0 A	06/02/24 16:30:34		

Table C.2.16: Stack length of 55 mm positioned at 40 mm: Mean and amplitude pressure.

10360	2024/02/06	16:28:31	000079.8	kpa
10361	2024/02/06	16:28:33	000079.8	kpa
10362	2024/02/06	16:28:35	000079.8	kpa
10363	2024/02/06	16:28:37	000079.8	kpa
10364	2024/02/06	16:28:39	000079.8	kpa
10365	2024/02/06	16:28:41	000079.8	kpa
10366	2024/02/06	16:28:43	000079.8	kpa
10367	2024/02/06	16:28:45	000079.8	kpa
10368	2024/02/06	16:28:47	000079.7	kpa
10369	2024/02/06	16:28:49	000079.7	kpa
10370	2024/02/06	16:28:51	000079.7	kpa
10371	2024/02/06	16:28:53	000079.7	kpa
10372	2024/02/06	16:28:55	000079.7	kpa
10373	2024/02/06	16:28:57	000079.7	kpa
10374	2024/02/06	16:28:59	000079.7	kpa
10375	2024/02/06	16:29:01	000079.6	kpa
10376	2024/02/06	16:29:03	000079.6	kpa
10377	2024/02/06	16:29:05	000079.6	kpa
10378	2024/02/06	16:29:07	000079.6	kpa
10379	2024/02/06	16:29:09	000079.6	kpa
10380	2024/02/06	16:29:11	000079.6	kpa
10381	2024/02/06	16:29:13	000079.6	kpa
10382	2024/02/06	16:29:15	000079.6	kpa
10383	2024/02/06	16:29:17	000079.6	kpa
10384	2024/02/06	16:29:19	000079.6	kpa
10385	2024/02/06	16:29:21	000079.6	kpa
10386	2024/02/06	16:29:23	000079.5	kpa
10387	2024/02/06	16:29:25	000079.5	kpa
10388	2024/02/06	16:29:27	000079.5	kpa
10389	2024/02/06	16:29:29	000079.5	kpa
10390	2024/02/06	16:29:31	000079.5	kpa
10391	2024/02/06	16:29:33	000079.5	kpa
10392	2024/02/06	16:29:35	000079.5	kpa
10393	2024/02/06	16:29:37	000079.5	kpa
10394	2024/02/06	16:29:39	000079.5	kpa
10395	2024/02/06	16:29:41	000079.5	kpa
10396	2024/02/06	16:29:43	000079.4	kpa
10397	2024/02/06	16:29:45	000079.4	kpa
10398	2024/02/06	16:29:47	000079.4	kpa
10399	2024/02/06	16:29:49	000079.4	kpa
10400	2024/02/06	16:29:51	000079.4	kpa
10401	2024/02/06	16:29:53	000079.4	kpa
10402	2024/02/06	16:29:55	000079.4	kpa
10403	2024/02/06	16:29:57	000079.4	kpa
10404	2024/02/06	16:29:59	000079.4	kpa
10405	2024/02/06	16:30:01	000079.3	kpa

Table C.2.17: Stack length of 65 mm positioned at 40 mm: T1-T4

5278	2024/02/19 16:38	25.2	30.1	23.6	25.0
5279	2024/02/19 16:38	25.2	30.0	23.6	25.0
5280	2024/02/19 16:38	25.2	30.0	23.6	25.0
5281	2024/02/19 16:38	25.2	30.0	23.6	25.0
5282	2024/02/19 16:38	25.2	30.0	23.6	25.0
5283	2024/02/19 16:38	25.2	30.0	23.6	25.0
5284	2024/02/19 16:38	25.2	30.1	23.6	25.0
5285	2024/02/19 16:38	25.2	30.1	23.6	25.0
5286	2024/02/19 16:38	25.2	30.1	23.6	25.0
5287	2024/02/19 16:38	25.2	30.1	23.6	25.0
5288	2024/02/19 16:38	25.4	30.1	23.6	25.0
5289	2024/02/19 16:38	25.4	30.2	23.6	25.0
5290	2024/02/19 16:38	25.4	30.2	23.6	25.0
5291	2024/02/19 16:38	25.4	30.2	23.6	25.0
5292	2024/02/19 16:38	25.4	30.2	23.6	25.0
5293	2024/02/19 16:38	25.4	30.2	23.6	25.0
5294	2024/02/19 16:38	25.4	30.2	23.6	25.0
5295	2024/02/19 16:38	25.4	30.2	23.6	25.0
5296	2024/02/19 16:38	25.4	30.2	23.8	25.0
5297	2024/02/19 16:38	25.4	30.2	23.8	25.0
5298	2024/02/19 16:38	25.4	30.2	23.8	25.0
5299	2024/02/19 16:38	25.4	30.1	23.8	25.0
5300	2024/02/19 16:38	25.4	30.1	23.8	25.0
5301	2024/02/19 16:38	25.4	30.1	23.8	25.0
5302	2024/02/19 16:38	25.4	30.1	23.8	25.0
5303	2024/02/19 16:38	25.4	30.1	23.8	25.0
5304	2024/02/19 16:38	25.4	30.1	23.8	25.0
5305	2024/02/19 16:38	25.4	30.0	23.8	25.0
5306	2024/02/19 16:38	25.4	30.0	24.0	25.0
5307	2024/02/19 16:38	25.4	30.0	24.0	25.0
5308	2024/02/19 16:38	25.4	30.0	24.0	25.0
5309	2024/02/19 16:38	25.4	30.0	24.0	25.0
5310	2024/02/19 16:38	25.4	30.0	24.0	25.0
5311	2024/02/19 16:38	25.4	30.0	23.8	25.0
5312	2024/02/19 16:38	25.4	30.0	23.8	25.0
5313	2024/02/19 16:38	25.4	30.0	23.8	25.0
5314	2024/02/19 16:38	25.4	30.0	23.8	25.0
5315	2024/02/19 16:38	25.4	30.0	23.8	25.0
5316	2024/02/19 16:38	25.4	30.0	23.8	25.0
5317	2024/02/19 16:38	25.4	30.0	23.8	25.0
5318	2024/02/19 16:38	25.4	30.0	23.8	25.0
5319	2024/02/19 16:38	25.4	30.0	23.8	25.0
5320	2024/02/19 16:38	25.4	30.0	23.8	25.0
5321	2024/02/19 16:38	25.4	30.0	23.8	25.0
5322	2024/02/19 16:38	25.4	30.0	23.6	25.0

Table C.2.18: Stack length of 65 mm positioned at 40 mm: T5-T6

5298	2024/02/19 16:38	25.4	33.2	---	---
5299	2024/02/19 16:38	25.4	33.1	---	---
5300	2024/02/19 16:38	25.4	33.1	---	---
5301	2024/02/19 16:38	25.4	33.1	---	---
5302	2024/02/19 16:38	25.4	33.2	---	---
5303	2024/02/19 16:38	25.4	33.2	---	---
5304	2024/02/19 16:38	25.4	33.2	---	---
5305	2024/02/19 16:38	25.4	33.2	---	---
5306	2024/02/19 16:38	25.4	33.2	---	---
5307	2024/02/19 16:38	25.4	33.2	---	---
5308	2024/02/19 16:38	25.4	33.2	---	---
5309	2024/02/19 16:38	25.4	33.2	---	---
5310	2024/02/19 16:38	25.4	33.2	---	---
5311	2024/02/19 16:38	25.4	33.2	---	---
5312	2024/02/19 16:38	25.4	33.2	---	---
5313	2024/02/19 16:38	25.4	33.2	---	---
5314	2024/02/19 16:38	25.4	33.2	---	---
5315	2024/02/19 16:38	25.4	33.2	---	---
5316	2024/02/19 16:38	25.4	33.2	---	---
5317	2024/02/19 16:38	25.4	33.4	---	---
5318	2024/02/19 16:38	25.4	33.4	---	---
5319	2024/02/19 16:38	25.4	33.4	---	---
5320	2024/02/19 16:38	25.4	33.4	---	---
5321	2024/02/19 16:38	25.4	33.4	---	---
5322	2024/02/19 16:38	25.4	33.4	---	---
5323	2024/02/19 16:38	25.4	33.4	---	---
5324	2024/02/19 16:38	25.4	33.4	---	---
5325	2024/02/19 16:38	25.4	33.4	---	---
5326	2024/02/19 16:38	25.4	33.2	---	---
5327	2024/02/19 16:38	25.4	33.2	---	---
5328	2024/02/19 16:38	25.4	33.2	---	---
5329	2024/02/19 16:38	25.4	33.2	---	---
5330	2024/02/19 16:38	25.4	33.2	---	---
5331	2024/02/19 16:38	25.4	33.2	---	---
5332	2024/02/19 16:38	25.4	33.2	---	---
5333	2024/02/19 16:38	25.4	33.2	---	---
5334	2024/02/19 16:38	25.4	33.2	---	---
5335	2024/02/19 16:38	25.4	33.2	---	---
5336	2024/02/19 16:38	25.4	33.2	---	---
5337	2024/02/19 16:38	25.4	33.2	---	---
5338	2024/02/19 16:38	25.4	33.2	---	---
5339	2024/02/19 16:38	25.4	33.2	---	---
5340	2024/02/19 16:38	25.4	33.2	---	---
5341	2024/02/19 16:38	25.4	33.2	---	---

Table C.2.19: Stack length of 65 mm positioned at 40 mm: Voltage and current.

482	39.1 V	1.1 A	19/02/24 16:30:03		
483	39.1 V	1.1 A	19/02/24 16:30:13		
484	39.1 V	1.1 A	19/02/24 16:30:23		
485	39.1 V	1.1 A	19/02/24 16:30:33		
486	39.1 V	1.1 A	19/02/24 16:30:43		
487	39.1 V	1.1 A	19/02/24 16:30:53		
488	39.1 V	1.1 A	19/02/24 16:31:03		
489	39.1 V	1.1 A	19/02/24 16:31:13		
490	39.1 V	1.1 A	19/02/24 16:31:23		
491	39.1 V	1.1 A	19/02/24 16:31:33		
492	39.1 V	1.1 A	19/02/24 16:31:43		
493	39.1 V	1.1 A	19/02/24 16:31:53		
494	39.1 V	1.1 A	19/02/24 16:32:03		
495	39.1 V	1.1 A	19/02/24 16:32:13		
496	39.1 V	1.1 A	19/02/24 16:32:23		
497	39.1 V	1.1 A	19/02/24 16:32:33		
498	39.1 V	1.1 A	19/02/24 16:32:43		
499	39.1 V	1.1 A	19/02/24 16:32:53		
500	39.1 V	1.1 A	19/02/24 16:33:03		
501	39.1 V	1.1 A	19/02/24 16:33:13		
502	39.1 V	1.1 A	19/02/24 16:33:23		
503	39.1 V	1.1 A	19/02/24 16:33:33		
504	39.1 V	1.1 A	19/02/24 16:33:43		
505	39.1 V	1.1 A	19/02/24 16:33:53		
506	39.1 V	1.1 A	19/02/24 16:34:03		
507	39.1 V	1.1 A	19/02/24 16:34:13		
508	39.1 V	1.1 A	19/02/24 16:34:23		
509	39.1 V	1.1 A	19/02/24 16:34:33		
510	39.1 V	1.1 A	19/02/24 16:34:43		
511	39.1 V	1.1 A	19/02/24 16:34:53		
512	39.1 V	1.1 A	19/02/24 16:35:03		
513	39.1 V	1.1 A	19/02/24 16:35:13		
514	39.1 V	1.1 A	19/02/24 16:35:23		
515	39.1 V	1.1 A	19/02/24 16:35:33		
516	39.1 V	1.1 A	19/02/24 16:35:43		
517	39.1 V	1.1 A	19/02/24 16:35:53		
518	39.1 V	1.1 A	19/02/24 16:36:03		
519	39.1 V	1.1 A	19/02/24 16:36:13		
520	39.1 V	1.1 A	19/02/24 16:36:23		
521	39.1 V	1.1 A	19/02/24 16:36:33		
522	39.1 V	1.1 A	19/02/24 16:36:43		
523	39.1 V	1.1 A	19/02/24 16:36:53		
524	39.1 V	1.1 A	19/02/24 16:37:03		
525	39.1 V	1.1 A	19/02/24 16:37:13		
526	39.1 V	1.1 A	19/02/24 16:37:23		
527	39.1 V	1.1 A	19/02/24 16:37:33		
528	39.1 V	1.1 A	19/02/24 16:37:43		
529	39.1 V	1.1 A	19/02/24 16:37:53		
530	39.1 V	1.1 A	19/02/24 16:38:03		
531	39.1 V	1.1 A	19/02/24 16:38:13		
532	39.1 V	1.1 A	19/02/24 16:38:23		
533	39.1 V	1.1 A	19/02/24 16:38:33		
534	39.1 V	1.1 A	19/02/24 16:38:43		
535	39.1 V	1.1 A	19/02/24 16:38:53		
536	39.1 V	1.1 A	19/02/24 16:39:03		
537	39.1 V	1.1 A	19/02/24 16:39:13		
538	39.1 V	1.1 A	19/02/24 16:39:23		
539	39.1 V	1.1 A	19/02/24 16:39:33		

Table C.2.20: Stack length of 65 mm positioned at 40 mm: Mean and amplitude pressure.

20564	2024/02/19	16:45:57	000064.9	kpa
20565	2024/02/19	16:45:59	000064.9	kpa
20566	2024/02/19	16:46:01	000064.9	kpa
20567	2024/02/19	16:46:03	000064.9	kpa
20568	2024/02/19	16:46:05	000064.9	kpa
20569	2024/02/19	16:46:07	000064.9	kpa
20570	2024/02/19	16:46:09	000064.9	kpa
20571	2024/02/19	16:46:11	000064.9	kpa
20572	2024/02/19	16:46:13	000064.9	kpa
20573	2024/02/19	16:46:15	000064.9	kpa
20574	2024/02/19	16:46:17	000064.9	kpa
20575	2024/02/19	16:46:19	000064.8	kpa
20576	2024/02/19	16:46:21	000064.8	kpa
20577	2024/02/19	16:46:23	000064.8	kpa
20578	2024/02/19	16:46:25	000064.8	kpa
20579	2024/02/19	16:46:27	000064.8	kpa
20580	2024/02/19	16:46:29	000064.7	kpa
20581	2024/02/19	16:46:31	000064.7	kpa
20582	2024/02/19	16:46:33	000064.7	kpa
20583	2024/02/19	16:46:35	000064.7	kpa
20584	2024/02/19	16:46:37	000064.7	kpa
20585	2024/02/19	16:46:39	000064.7	kpa
20586	2024/02/19	16:46:41	000064.7	kpa
20587	2024/02/19	16:46:43	000064.6	kpa
20588	2024/02/19	16:46:45	000064.6	kpa
20589	2024/02/19	16:46:47	000064.6	kpa
20590	2024/02/19	16:46:49	000064.6	kpa
20591	2024/02/19	16:46:51	000064.6	kpa
20592	2024/02/19	16:46:53	000064.6	kpa
20593	2024/02/19	16:46:55	000064.6	kpa
20594	2024/02/19	16:46:57	000064.6	kpa
20595	2024/02/19	16:46:59	000064.6	kpa
20596	2024/02/19	16:47:01	000064.6	kpa
20597	2024/02/19	16:47:03	000064.5	kpa
20598	2024/02/19	16:47:05	000064.5	kpa
20599	2024/02/19	16:47:07	000064.5	kpa
20600	2024/02/19	16:47:09	000064.5	kpa
20601	2024/02/19	16:47:11	000064.5	kpa
20602	2024/02/19	16:47:13	000064.5	kpa
20603	2024/02/19	16:47:15	000064.5	kpa
20604	2024/02/19	16:47:17	000064.4	kpa
20605	2024/02/19	16:47:19	000064.4	kpa
20606	2024/02/19	16:47:21	000064.4	kpa
20607	2024/02/19	16:47:23	000064.4	kpa
20608	2024/02/19	16:47:25	000064.4	kpa

C.3 Stacks positioned at 50 mm.

Table C.3.1: Stack length of 25 mm positioned at 50 mm: T1-T4

3651	2024/02/14 14:13	25,1	31	23,6	26,8
3652	2024/02/14 14:13	25,1	31	23,6	26,8
3653	2024/02/14 14:13	25,1	30,8	23,6	26,8
3654	2024/02/14 14:13	25,1	30,8	23,6	26,8
3655	2024/02/14 14:13	25,1	30,8	23,6	26,7
3656	2024/02/14 14:13	25,1	30,8	23,6	26,7
3657	2024/02/14 14:13	25,1	30,8	23,6	26,7
3658	2024/02/14 14:13	25,1	30,8	23,6	26,7
3659	2024/02/14 14:13	25,1	30,8	23,6	26,7
3660	2024/02/14 14:13	25,1	30,8	23,6	26,8
3661	2024/02/14 14:13	25,1	30,8	23,6	26,8
3662	2024/02/14 14:13	25,1	30,8	23,6	26,8
3663	2024/02/14 14:13	25,1	30,8	23,6	26,8
3664	2024/02/14 14:13	25,1	31	23,6	26,8
3665	2024/02/14 14:13	25,1	31	23,6	26,8
3666	2024/02/14 14:13	25,1	31	23,6	26,8
3667	2024/02/14 14:13	25,1	31	23,6	26,8
3668	2024/02/14 14:13	25,1	31	23,6	26,8
3669	2024/02/14 14:13	25,1	31,1	23,6	26,8
3670	2024/02/14 14:13	25,1	31,1	23,6	26,8
3671	2024/02/14 14:13	25,1	31,1	23,6	26,8
3672	2024/02/14 14:13	25,1	31,1	23,6	26,8
3673	2024/02/14 14:13	25,1	31,1	23,6	26,8
3674	2024/02/14 14:13	25,1	31,1	23,6	26,8
3675	2024/02/14 14:13	25,1	31,1	23,6	26,8
3676	2024/02/14 14:13	25,1	31,1	23,6	26,8
3677	2024/02/14 14:14	25,1	31,1	23,7	26,8
3678	2024/02/14 14:14	25,1	31,1	23,7	26,8
3679	2024/02/14 14:14	25,1	31,1	23,7	26,8
3680	2024/02/14 14:14	25,1	31,1	23,7	26,8
3681	2024/02/14 14:14	25,1	31,1	23,7	26,8
3682	2024/02/14 14:14	25,1	31,1	23,7	26,8
3683	2024/02/14 14:14	25,1	31,1	23,7	26,8
3684	2024/02/14 14:14	25,1	31,1	23,7	26,8
3685	2024/02/14 14:14	25,1	31,1	23,7	26,8
3686	2024/02/14 14:14	25,1	31,1	23,7	26,8
3687	2024/02/14 14:14	25,1	31,1	23,6	26,8
3688	2024/02/14 14:14	25,1	31,1	23,6	26,8
3689	2024/02/14 14:14	25,1	31,1	23,6	26,8
3690	2024/02/14 14:14	25,1	31,1	23,6	26,8
3691	2024/02/14 14:14	25,1	31,1	23,6	26,8
3692	2024/02/14 14:14	25,1	31,1	23,6	26,8
3693	2024/02/14 14:14	25,1	31,1	23,6	26,8

Table C.3.2: Stack length of 25 mm positioned at 50 mm: T5-T6

3791	2024/02/14 14:13	26	34	- - -	- - -
3792	2024/02/14 14:13	26	34	- - -	- - -
3793	2024/02/14 14:13	26	34	- - -	- - -
3794	2024/02/14 14:13	26	34	- - -	- - -
3795	2024/02/14 14:13	26	34	- - -	- - -
3796	2024/02/14 14:13	26,1	34	- - -	- - -
3797	2024/02/14 14:13	26,1	34	- - -	- - -
3798	2024/02/14 14:13	26,1	34	- - -	- - -
3799	2024/02/14 14:13	26,2	34	- - -	- - -
3800	2024/02/14 14:13	26,2	34	- - -	- - -
3801	2024/02/14 14:13	26,2	34	- - -	- - -
3802	2024/02/14 14:13	26,1	34	- - -	- - -
3803	2024/02/14 14:13	26,1	34	- - -	- - -
3804	2024/02/14 14:13	26,1	34	- - -	- - -
3805	2024/02/14 14:13	26,1	34	- - -	- - -
3806	2024/02/14 14:13	26,1	34	- - -	- - -
3807	2024/02/14 14:13	26,1	34	- - -	- - -
3808	2024/02/14 14:13	26,2	34	- - -	- - -
3809	2024/02/14 14:13	26,2	34	- - -	- - -
3810	2024/02/14 14:13	26,2	34	- - -	- - -
3811	2024/02/14 14:14	26,2	34	- - -	- - -
3812	2024/02/14 14:14	26,2	34,1	- - -	- - -
3813	2024/02/14 14:14	26,2	34,1	- - -	- - -
3814	2024/02/14 14:14	26,2	34,1	- - -	- - -
3815	2024/02/14 14:14	26,2	34,2	- - -	- - -
3816	2024/02/14 14:14	26,2	34,2	- - -	- - -
3817	2024/02/14 14:14	26,1	34,2	- - -	- - -
3818	2024/02/14 14:14	26,1	34,1	- - -	- - -
3819	2024/02/14 14:14	26,1	34,1	- - -	- - -
3820	2024/02/14 14:14	26,1	34,1	- - -	- - -
3821	2024/02/14 14:14	26,1	34,1	- - -	- - -
3822	2024/02/14 14:14	26,1	34,1	- - -	- - -
3823	2024/02/14 14:14	26,1	34,1	- - -	- - -
3824	2024/02/14 14:14	26,1	34,1	- - -	- - -
3825	2024/02/14 14:14	26,1	34,1	- - -	- - -
3826	2024/02/14 14:14	26,1	34,1	- - -	- - -
3827	2024/02/14 14:14	26,1	34,2	- - -	- - -
3828	2024/02/14 14:14	26,1	34,2	- - -	- - -
3829	2024/02/14 14:14	26,1	34,2	- - -	- - -
3830	2024/02/14 14:14	26,1	34,2	- - -	- - -
3831	2024/02/14 14:14	26,1	34,2	- - -	- - -
3832	2024/02/14 14:14	26,2	34,2	- - -	- - -
3833	2024/02/14 14:14	26,2	34,2	- - -	- - -
3834	2024/02/14 14:14	26,2	34,2	- - -	- - -
3835	2024/02/14 14:14	26,2	34,2	- - -	- - -

Table C3.3: Stack length of 25 mm positioned at 50 mm: Voltage and current.

400	39.1 V	1.1 A	14/02/24 16:30:11		
401	39.1 V	1.1 A	14/02/24 16:30:21		
402	39.1 V	1.1 A	14/02/24 16:30:31		
403	39.1 V	1.1 A	14/02/24 16:30:41		
404	39.1 V	1.1 A	14/02/24 16:30:51		
405	39.1 V	1.1 A	14/02/24 16:31:01		
406	39.1 V	1.1 A	14/02/24 16:31:11		
407	39.1 V	1.1 A	14/02/24 16:31:21		
408	39.1 V	1.1 A	14/02/24 16:31:31		
409	39.1 V	1.1 A	14/02/24 16:31:41		
410	39.1 V	1.1 A	14/02/24 16:31:51		
411	39.1 V	1.1 A	14/02/24 16:32:01		
412	39.1 V	1.1 A	14/02/24 16:32:11		
413	39.1 V	1.1 A	14/02/24 16:32:21		
414	39.1 V	1.1 A	14/02/24 16:32:31		
415	39.1 V	1.1 A	14/02/24 16:32:41		
416	39.1 V	1.1 A	14/02/24 16:32:51		
417	39.1 V	1.1 A	14/02/24 16:33:01		
418	39.1 V	1.1 A	14/02/24 16:33:11		
419	39.1 V	1.1 A	14/02/24 16:33:21		
420	39.1 V	1.1 A	14/02/24 16:33:31		
421	39.1 V	1.1 A	14/02/24 16:33:41		
422	39.1 V	1.1 A	14/02/24 16:33:51		
423	39.1 V	1.1 A	14/02/24 16:34:01		
424	39.1 V	1.1 A	14/02/24 16:34:11		
425	39.1 V	1.1 A	14/02/24 16:34:21		
426	39.1 V	1.1 A	14/02/24 16:34:31		
427	39.1 V	1.1 A	14/02/24 16:34:41		
428	39.1 V	1.1 A	14/02/24 16:34:51		
429	39.1 V	1.1 A	14/02/24 16:35:01		
430	39.1 V	1.1 A	14/02/24 16:35:11		
431	39.1 V	1.1 A	14/02/24 16:35:21		
432	39.1 V	1.1 A	14/02/24 16:35:31		
433	39.1 V	1.1 A	14/02/24 16:35:41		
434	39.1 V	1.1 A	14/02/24 16:35:51		
435	39.1 V	1.1 A	14/02/24 16:36:01		
436	39.1 V	1.1 A	14/02/24 16:36:11		
437	39.1 V	1.1 A	14/02/24 16:36:21		
438	39.1 V	1.1 A	14/02/24 16:36:31		
439	39.1 V	1.1 A	14/02/24 16:36:41		
440	39.1 V	1.1 A	14/02/24 16:36:51		
441	39.1 V	1.1 A	14/02/24 16:37:01		
442	39.1 V	1.1 A	14/02/24 16:37:11		
443	39.1 V	1.1 A	14/02/24 16:37:21		
444	39.1 V	1.1 A	14/02/24 16:37:31		
445	39.1 V	1.1 A	14/02/24 16:37:41		
446	39.1 V	1.1 A	14/02/24 16:37:51		
447	39.1 V	1.1 A	14/02/24 16:38:01		
448	39.1 V	1.1 A	14/02/24 16:38:11		
449	39.1 V	1.1 A	14/02/24 16:38:21		
450	39.1 V	1.1 A	14/02/24 16:38:31		
451	39.1 V	1.1 A	14/02/24 16:38:41		
452	39.1 V	1.1 A	14/02/24 16:38:51		
453	39.1 V	1.1 A	14/02/24 16:39:01		
454	39.1 V	1.1 A	14/02/24 16:39:11		
455	39.1 V	1.1 A	14/02/24 16:39:21		
456	39.1 V	1.1 A	14/02/24 16:39:31		

Table C3.4: Stack length of 25 mm positioned at 50 mm: Mean and amplitude pressure.

2024/02/14	14:18:12	000045.3	kpa
2024/02/14	14:18:14	000045.3	kpa
2024/02/14	14:18:16	000045.3	kpa
2024/02/14	14:18:18	000045.3	kpa
2024/02/14	14:18:20	000045.3	kpa
2024/02/14	14:18:22	000045.3	kpa
2024/02/14	14:18:24	000045.2	kpa
2024/02/14	14:18:26	000045.2	kpa
2024/02/14	14:18:28	000045.2	kpa
2024/02/14	14:18:30	000045.2	kpa
2024/02/14	14:18:32	000045.2	kpa
2024/02/14	14:18:34	000045.2	kpa
2024/02/14	14:18:36	000045.2	kpa
2024/02/14	14:18:38	000045.2	kpa
2024/02/14	14:18:40	000045.2	kpa
2024/02/14	14:18:42	000045.1	kpa
2024/02/14	14:18:44	000045.1	kpa
2024/02/14	14:18:46	000045.1	kpa
2024/02/14	14:18:48	000045.1	kpa
2024/02/14	14:18:50	000045.1	kpa
2024/02/14	14:18:52	000045.1	kpa
2024/02/14	14:18:54	000045.0	kpa
2024/02/14	14:18:56	000045.0	kpa
2024/02/14	14:18:58	000045.0	kpa
2024/02/14	14:19:00	000045.0	kpa
2024/02/14	14:19:02	000045.0	kpa
2024/02/14	14:19:04	000045.0	kpa
2024/02/14	14:19:06	000045.0	kpa
2024/02/14	14:19:08	000045.0	kpa
2024/02/14	14:19:10	000044.9	kpa
2024/02/14	14:19:12	000044.9	kpa
2024/02/14	14:19:14	000044.9	kpa
2024/02/14	14:19:16	000044.9	kpa
2024/02/14	14:19:18	000044.9	kpa
2024/02/14	14:19:20	000044.9	kpa
2024/02/14	14:19:22	000044.8	kpa
2024/02/14	14:19:24	000044.8	kpa
2024/02/14	14:19:26	000044.8	kpa
2024/02/14	14:19:28	000044.8	kpa
2024/02/14	14:19:30	000044.8	kpa
2024/02/14	14:19:32	000044.8	kpa
2024/02/14	14:19:34	000044.8	kpa
2024/02/14	14:19:36	000044.7	kpa
2024/02/14	14:19:38	000044.7	kpa
2024/02/14	14:19:40	000044.7	kpa

Table C3.5: Stack length of 35 mm positioned at 50 mm: T1-T4

4086	2024/02/29 16:00	24.0	28.6	22.9	24.7
4087	2024/02/29 16:00	23.9	28.6	22.9	24.7
4088	2024/02/29 16:00	23.9	28.6	22.9	24.7
4089	2024/02/29 16:00	23.9	28.6	22.9	24.7
4090	2024/02/29 16:00	23.9	28.6	22.9	24.7
4091	2024/02/29 16:00	23.9	28.6	22.9	24.7
4092	2024/02/29 16:00	24.0	28.6	22.9	24.7
4093	2024/02/29 16:00	24.0	28.6	22.9	24.7
4094	2024/02/29 16:00	24.0	28.6	22.9	24.7
4095	2024/02/29 16:00	24.0	28.6	22.9	24.7
4096	2024/02/29 16:00	24.0	28.6	22.9	24.7
4097	2024/02/29 16:00	24.0	28.6	22.9	24.7
4098	2024/02/29 16:00	24.0	28.7	22.9	24.7
4099	2024/02/29 16:00	24.0	28.7	22.9	24.7
4100	2024/02/29 16:00	24.0	28.7	22.9	24.7
4101	2024/02/29 16:00	24.0	28.7	22.9	24.7
4102	2024/02/29 16:00	24.0	28.7	22.9	24.7
4103	2024/02/29 16:00	24.0	28.7	22.9	24.7
4104	2024/02/29 16:00	24.0	28.8	22.9	24.7
4105	2024/02/29 16:00	24.0	28.8	22.9	24.7
4106	2024/02/29 16:00	24.0	28.8	22.9	24.7
4107	2024/02/29 16:00	24.0	28.8	22.9	24.7
4108	2024/02/29 16:00	24.0	28.8	22.9	24.7
4109	2024/02/29 16:00	24.0	28.8	22.9	24.7
4110	2024/02/29 16:00	24.0	28.8	22.9	24.7
4111	2024/02/29 16:00	24.0	28.8	22.9	24.7
4112	2024/02/29 16:00	24.0	28.8	22.9	24.7
4113	2024/02/29 16:00	24.0	28.8	22.9	24.7
4114	2024/02/29 16:00	24.0	28.7	22.9	24.7
4115	2024/02/29 16:00	24.0	28.7	22.9	24.7
4116	2024/02/29 16:00	24.0	28.7	22.9	24.7
4117	2024/02/29 16:00	24.0	28.7	22.9	24.7
4118	2024/02/29 16:00	24.0	28.7	22.9	24.7
4119	2024/02/29 16:00	24.0	28.6	22.9	24.7
4120	2024/02/29 16:00	24.0	28.6	22.9	24.7
4121	2024/02/29 16:00	24.0	28.6	22.9	24.7
4122	2024/02/29 16:00	24.0	28.6	22.9	24.7
4123	2024/02/29 16:00	24.0	28.6	22.9	24.7
4124	2024/02/29 16:00	24.0	28.6	22.9	24.7
4125	2024/02/29 16:00	24.0	28.6	22.9	24.7
4126	2024/02/29 16:00	24.0	28.6	22.9	24.7
4127	2024/02/29 16:00	24.0	28.6	22.9	24.7
4128	2024/02/29 16:00	24.0	28.6	22.9	24.7
4129	2024/02/29 16:00	24.0	28.6	22.9	24.7
4130	2024/02/29 16:00	24.0	28.7	22.9	24.7

Table C3.6: Stack length of 35 mm positioned at 50 mm: T5-T6

4062	2024/02/29 16:00	25.0	32.1	---	---
4063	2024/02/29 16:00	25.0	32.1	---	---
4064	2024/02/29 16:00	25.0	32.1	---	---
4065	2024/02/29 16:00	25.0	32.1	---	---
4066	2024/02/29 16:00	25.0	32.1	---	---
4067	2024/02/29 16:00	25.0	32.1	---	---
4068	2024/02/29 16:00	25.0	32.1	---	---
4069	2024/02/29 16:00	25.0	32.1	---	---
4070	2024/02/29 16:00	25.0	32.1	---	---
4071	2024/02/29 16:00	25.0	32.1	---	---
4072	2024/02/29 16:00	25.0	32.1	---	---
4073	2024/02/29 16:00	25.0	32.1	---	---
4074	2024/02/29 16:00	25.0	32.1	---	---
4075	2024/02/29 16:00	25.0	32.1	---	---
4076	2024/02/29 16:00	25.0	32.1	---	---
4077	2024/02/29 16:00	25.0	32.1	---	---
4078	2024/02/29 16:00	25.0	32.1	---	---
4079	2024/02/29 16:00	25.0	32.1	---	---
4080	2024/02/29 16:00	25.1	32.1	---	---
4081	2024/02/29 16:00	25.1	32.1	---	---
4082	2024/02/29 16:00	25.1	32.1	---	---
4083	2024/02/29 16:00	25.1	32.1	---	---
4084	2024/02/29 16:00	25.1	32.1	---	---
4085	2024/02/29 16:00	25.1	32.1	---	---
4086	2024/02/29 16:00	25.0	32.1	---	---
4087	2024/02/29 16:00	25.0	32.1	---	---
4088	2024/02/29 16:00	25.0	32.1	---	---
4089	2024/02/29 16:00	25.0	32.1	---	---
4090	2024/02/29 16:00	25.0	32.1	---	---
4091	2024/02/29 16:00	25.0	32.2	---	---
4092	2024/02/29 16:00	25.0	32.2	---	---
4093	2024/02/29 16:00	25.0	32.2	---	---
4094	2024/02/29 16:00	25.0	32.2	---	---
4095	2024/02/29 16:00	25.0	32.2	---	---
4096	2024/02/29 16:00	25.0	32.2	---	---
4097	2024/02/29 16:00	25.0	32.2	---	---
4098	2024/02/29 16:00	25.0	32.2	---	---
4099	2024/02/29 16:00	25.0	32.2	---	---
4100	2024/02/29 16:00	25.0	32.2	---	---
4101	2024/02/29 16:00	25.0	32.2	---	---
4102	2024/02/29 16:00	24.8	32.2	---	---
4103	2024/02/29 16:00	24.8	32.1	---	---
4104	2024/02/29 16:00	24.8	32.1	---	---
4105	2024/02/29 16:00	24.8	32.1	---	---
4106	2024/02/29 16:00	24.8	32.1	---	---

Table C3.7: Stack length of 35 mm positioned at 50 mm: Voltage and current.

317	37.3 V	1.1 A	29/02/24 15:23:49		
318	37.3 V	1.1 A	29/02/24 15:23:59		
319	37.3 V	1.1 A	29/02/24 15:24:09		
320	37.3 V	1.1 A	29/02/24 15:24:19		
321	37.3 V	1.1 A	29/02/24 15:24:29		
322	37.3 V	1.1 A	29/02/24 15:24:39		
323	37.3 V	1.1 A	29/02/24 15:24:49		
324	37.3 V	1.1 A	29/02/24 15:24:59		
325	37.3 V	1.1 A	29/02/24 15:25:09		
326	37.3 V	1.1 A	29/02/24 15:25:19		
327	37.3 V	1.1 A	29/02/24 15:25:29		
328	37.3 V	1.1 A	29/02/24 15:25:39		
329	37.3 V	1.1 A	29/02/24 15:25:49		
330	37.3 V	1.1 A	29/02/24 15:25:59		
331	37.3 V	1.1 A	29/02/24 15:26:09		
332	37.3 V	1.1 A	29/02/24 15:26:19		
333	37.3 V	1.1 A	29/02/24 15:26:29		
334	37.3 V	1.1 A	29/02/24 15:26:39		
335	37.3 V	1.1 A	29/02/24 15:26:49		
336	37.3 V	1.1 A	29/02/24 15:26:59		
337	37.3 V	1.1 A	29/02/24 15:27:09		
338	37.3 V	1.1 A	29/02/24 15:27:19		
339	37.3 V	1.1 A	29/02/24 15:27:29		
340	37.3 V	1.1 A	29/02/24 15:27:39		
341	37.3 V	1.1 A	29/02/24 15:27:49		
342	37.3 V	1.1 A	29/02/24 15:27:59		
343	37.3 V	1.1 A	29/02/24 15:28:09		
344	37.3 V	1.1 A	29/02/24 15:28:19		
345	37.3 V	1.1 A	29/02/24 15:28:29		
346	37.3 V	1.1 A	29/02/24 15:28:39		
347	37.3 V	1.1 A	29/02/24 15:28:49		
348	37.3 V	1.1 A	29/02/24 15:28:59		
349	37.3 V	1.1 A	29/02/24 15:29:09		
350	37.3 V	1.1 A	29/02/24 15:29:19		
351	37.3 V	1.1 A	29/02/24 15:29:29		
352	37.3 V	1.1 A	29/02/24 15:29:39		
353	37.3 V	1.1 A	29/02/24 15:29:49		
354	37.3 V	1.1 A	29/02/24 15:29:59		
355	37.3 V	1.1 A	29/02/24 15:30:09		
356	37.3 V	1.1 A	29/02/24 15:30:19		
357	37.3 V	1.1 A	29/02/24 15:30:29		
358	37.3 V	1.0 A	29/02/24 15:30:39		
359	37.3 V	1.1 A	29/02/24 15:30:49		
360	37.3 V	1.1 A	29/02/24 15:30:59		
361	37.3 V	1.1 A	29/02/24 15:31:09		

Table C3.8: Stack length of 35 mm positioned at 50 mm: Mean and amplitude pressure.

11557	2024/02/29	15:58:34	000021.8	kpa
11558	2024/02/29	15:58:36	000021.8	kpa
11559	2024/02/29	15:58:38	000021.8	kpa
11560	2024/02/29	15:58:40	000021.8	kpa
11561	2024/02/29	15:58:42	000021.8	kpa
11562	2024/02/29	15:58:44	000021.8	kpa
11563	2024/02/29	15:58:46	000021.8	kpa
11564	2024/02/29	15:58:48	000021.8	kpa
11565	2024/02/29	15:58:50	000021.8	kpa
11566	2024/02/29	15:58:52	000021.7	kpa
11567	2024/02/29	15:58:54	000021.7	kpa
11568	2024/02/29	15:58:56	000021.7	kpa
11569	2024/02/29	15:58:58	000021.7	kpa
11570	2024/02/29	15:59:00	000021.7	kpa
11571	2024/02/29	15:59:02	000021.7	kpa
11572	2024/02/29	15:59:04	000021.7	kpa
11573	2024/02/29	15:59:06	000021.7	kpa
11574	2024/02/29	15:59:08	000021.7	kpa
11575	2024/02/29	15:59:10	000021.7	kpa
11576	2024/02/29	15:59:12	000021.7	kpa
11577	2024/02/29	15:59:14	000021.7	kpa
11578	2024/02/29	15:59:16	000021.7	kpa
11579	2024/02/29	15:59:18	000021.6	kpa
11580	2024/02/29	15:59:20	000021.6	kpa
11581	2024/02/29	15:59:22	000021.6	kpa
11582	2024/02/29	15:59:24	000021.6	kpa
11583	2024/02/29	15:59:26	000021.6	kpa
11584	2024/02/29	15:59:28	000021.6	kpa
11585	2024/02/29	15:59:30	000021.6	kpa
11586	2024/02/29	15:59:32	000021.6	kpa
11587	2024/02/29	15:59:34	000021.6	kpa
11588	2024/02/29	15:59:36	000021.6	kpa
11589	2024/02/29	15:59:38	000021.5	kpa
11590	2024/02/29	15:59:40	000021.5	kpa
11591	2024/02/29	15:59:42	000021.5	kpa
11592	2024/02/29	15:59:44	000021.5	kpa
11593	2024/02/29	15:59:46	000021.5	kpa
11594	2024/02/29	15:59:48	000021.5	kpa
11595	2024/02/29	15:59:50	000021.5	kpa
11596	2024/02/29	15:59:52	000021.5	kpa
11597	2024/02/29	15:59:54	000021.5	kpa
11598	2024/02/29	15:59:56	000021.5	kpa
11599	2024/02/29	15:59:58	000021.4	kpa
11600	2024/02/29	16:00:00	000021.4	kpa
11601	2024/02/29	16:00:02	000021.4	kpa

Table C3.9: Stack length of 45 mm positioned at 50 mm: T1-T4

5491	2024/03/05 16:36	22.2	30.1	21.1	24.0
5492	2024/03/05 16:36	22.2	30.1	21.1	24.0
5493	2024/03/05 16:36	22.2	30.1	21.1	24.1
5494	2024/03/05 16:36	22.2	30.1	21.1	24.1
5495	2024/03/05 16:36	22.2	30.1	21.1	24.1
5496	2024/03/05 16:36	22.2	30.1	21.1	24.1
5497	2024/03/05 16:36	22.2	30.1	21.1	24.1
5498	2024/03/05 16:36	22.2	30.1	21.1	24.1
5499	2024/03/05 16:36	22.2	30.1	21.1	24.1
5500	2024/03/05 16:36	22.2	30.1	21.1	24.1
5501	2024/03/05 16:36	22.2	30.1	21.1	24.1
5502	2024/03/05 16:36	22.2	30.1	21.1	24.1
5503	2024/03/05 16:36	22.2	30.1	21.1	23.6
5504	2024/03/05 16:36	22.2	30.1	21.1	23.6
5505	2024/03/05 16:36	22.2	30.1	21.1	23.6
5506	2024/03/05 16:36	22.2	30.2	21.1	23.6
5507	2024/03/05 16:36	22.2	30.2	21.1	23.6
5508	2024/03/05 16:36	22.2	30.2	21.1	24.2
5509	2024/03/05 16:36	22.2	30.2	21.1	24.2
5510	2024/03/05 16:36	22.2	30.2	21.1	24.2
5511	2024/03/05 16:36	22.2	30.2	21.1	24.2
5512	2024/03/05 16:36	22.2	30.2	21.1	24.2
5513	2024/03/05 16:36	22.2	30.2	21.1	24.1
5514	2024/03/05 16:36	22.2	30.2	21.1	24.1
5515	2024/03/05 16:36	22.2	30.2	21.1	24.1
5516	2024/03/05 16:36	22.2	30.2	21.1	24.1
5517	2024/03/05 16:36	22.2	30.2	21.1	24.1
5518	2024/03/05 16:36	22.2	30.2	21.1	24.1
5519	2024/03/05 16:36	22.2	30.2	21.1	24.3
5520	2024/03/05 16:36	22.2	30.2	21.1	24.3
5521	2024/03/05 16:36	22.2	30.1	21.1	24.3
5522	2024/03/05 16:36	22.2	30.1	21.1	24.3
5523	2024/03/05 16:36	22.2	30.1	21.1	24.3
5524	2024/03/05 16:36	22.2	30.1	21.1	23.5
5525	2024/03/05 16:36	22.2	30.1	21.1	23.5
5526	2024/03/05 16:36	22.2	30.0	21.1	23.5
5527	2024/03/05 16:36	22.2	30.0	21.1	23.5
5528	2024/03/05 16:36	22.2	30.0	21.1	23.5
5529	2024/03/05 16:36	22.2	30.0	21.1	24.1
5530	2024/03/05 16:36	22.2	30.0	21.1	24.1
5531	2024/03/05 16:36	22.2	30.0	21.1	24.1
5532	2024/03/05 16:36	22.2	30.1	21.1	24.1
5533	2024/03/05 16:36	22.2	30.1	21.1	24.1
5534	2024/03/05 16:36	22.2	30.1	21.1	23.9
5535	2024/03/05 16:36	22.2	30.1	21.1	23.9

Table C3.10: Stack length of 45 mm positioned at 50 mm: T5-T6.

5376	2024/03/05 16:35	23.1	30.6	---	---
5377	2024/03/05 16:35	23.1	30.6	---	---
5378	2024/03/05 16:35	23.1	30.6	---	---
5379	2024/03/05 16:35	23.1	30.6	---	---
5380	2024/03/05 16:35	23.1	30.6	---	---
5381	2024/03/05 16:35	23.1	30.6	---	---
5382	2024/03/05 16:36	23.1	30.6	---	---
5383	2024/03/05 16:36	23.1	30.6	---	---
5384	2024/03/05 16:36	23.1	30.6	---	---
5385	2024/03/05 16:36	23.1	30.6	---	---
5386	2024/03/05 16:36	23.1	30.6	---	---
5387	2024/03/05 16:36	23.1	30.6	---	---
5388	2024/03/05 16:36	23.1	30.7	---	---
5389	2024/03/05 16:36	23.1	30.7	---	---
5390	2024/03/05 16:36	23.1	30.7	---	---
5391	2024/03/05 16:36	23.1	30.7	---	---
5392	2024/03/05 16:36	23.1	30.7	---	---
5393	2024/03/05 16:36	23.1	30.7	---	---
5394	2024/03/05 16:36	23.1	30.7	---	---
5395	2024/03/05 16:36	23.1	30.7	---	---
5396	2024/03/05 16:36	23.1	30.7	---	---
5397	2024/03/05 16:36	23.1	30.6	---	---
5398	2024/03/05 16:36	23.1	30.6	---	---
5399	2024/03/05 16:36	23.1	30.6	---	---
5400	2024/03/05 16:36	23.1	30.6	---	---
5401	2024/03/05 16:36	23.1	30.6	---	---
5402	2024/03/05 16:36	23.1	30.6	---	---
5403	2024/03/05 16:36	23.1	30.7	---	---
5404	2024/03/05 16:36	23.1	30.7	---	---
5405	2024/03/05 16:36	23.1	30.7	---	---
5406	2024/03/05 16:36	23.1	30.7	---	---
5407	2024/03/05 16:36	23.1	30.7	---	---
5408	2024/03/05 16:36	23.1	30.7	---	---
5409	2024/03/05 16:36	23.1	30.7	---	---
5410	2024/03/05 16:36	23.1	30.7	---	---
5411	2024/03/05 16:36	23.1	30.7	---	---
5412	2024/03/05 16:36	23.1	30.7	---	---
5413	2024/03/05 16:36	23.1	30.7	---	---
5414	2024/03/05 16:36	23.1	30.7	---	---
5415	2024/03/05 16:36	23.1	30.7	---	---
5416	2024/03/05 16:36	23.1	30.7	---	---
5417	2024/03/05 16:36	23.1	30.7	---	---
5418	2024/03/05 16:36	23.1	30.7	---	---
5419	2024/03/05 16:36	23.1	30.7	---	---
5420	2024/03/05 16:36	23.1	30.7	---	---

Table C3.11: Stack length of 45 mm positioned at 50 mm: Voltage and current.

506	39.1 V	1.1 A	05/03/24 16:32:04		
507	39.1 V	1.1 A	05/03/24 16:32:14		
508	39.1 V	1.1 A	05/03/24 16:32:24		
509	39.1 V	1.1 A	05/03/24 16:32:34		
510	39.1 V	1.0 A	05/03/24 16:32:44		
511	39.1 V	1.1 A	05/03/24 16:32:54		
512	39.1 V	1.1 A	05/03/24 16:33:04		
513	39.1 V	1.1 A	05/03/24 16:33:14		
514	39.1 V	1.1 A	05/03/24 16:33:24		
515	39.1 V	1.1 A	05/03/24 16:33:34		
516	39.1 V	1.1 A	05/03/24 16:33:44		
517	39.1 V	1.0 A	05/03/24 16:33:54		
518	39.1 V	1.1 A	05/03/24 16:34:04		
519	39.1 V	1.0 A	05/03/24 16:34:14		
520	39.1 V	1.0 A	05/03/24 16:34:24		
521	39.1 V	1.1 A	05/03/24 16:34:34		
522	39.1 V	1.1 A	05/03/24 16:34:44		
523	39.1 V	1.0 A	05/03/24 16:34:54		
524	39.1 V	1.1 A	05/03/24 16:35:04		
525	39.1 V	1.0 A	05/03/24 16:35:14		
526	39.1 V	1.1 A	05/03/24 16:35:24		
527	39.1 V	1.1 A	05/03/24 16:35:34		
528	39.1 V	1.0 A	05/03/24 16:35:44		
529	39.1 V	1.0 A	05/03/24 16:35:54		
530	39.1 V	1.1 A	05/03/24 16:36:04		
531	39.1 V	1.1 A	05/03/24 16:36:14		
532	39.1 V	1.1 A	05/03/24 16:36:24		
533	39.1 V	1.1 A	05/03/24 16:36:34		
534	39.1 V	1.0 A	05/03/24 16:36:44		
535	39.1 V	1.0 A	05/03/24 16:36:54		
536	39.1 V	1.1 A	05/03/24 16:37:04		
537	39.1 V	1.1 A	05/03/24 16:37:14		
538	39.1 V	1.0 A	05/03/24 16:37:24		
539	39.1 V	1.0 A	05/03/24 16:37:34		
540	39.1 V	1.1 A	05/03/24 16:37:44		
541	39.1 V	1.1 A	05/03/24 16:37:54		
542	39.1 V	1.1 A	05/03/24 16:38:04		
543	39.1 V	1.1 A	05/03/24 16:38:14		
544	39.1 V	1.1 A	05/03/24 16:38:24		
545	39.1 V	1.0 A	05/03/24 16:38:34		
546	39.1 V	1.0 A	05/03/24 16:38:44		
547	39.1 V	1.0 A	05/03/24 16:38:54		
548	39.1 V	1.1 A	05/03/24 16:39:04		
549	39.1 V	1.1 A	05/03/24 16:39:14		
550	39.1 V	1.0 A	05/03/24 16:39:24		

Table C3.12: Stack length of 45 mm positioned at 50 mm: Mean and amplitude pressure.

22936	3/5/2024	16:36:16	61.9	kpa
22937	3/5/2024	16:36:18	61.9	kpa
22938	3/5/2024	16:36:20	61.9	kpa
22939	3/5/2024	16:36:22	61.9	kpa
22940	3/5/2024	16:36:24	61.9	kpa
22941	3/5/2024	16:36:26	61.9	kpa
22942	3/5/2024	16:36:28	61.9	kpa
22943	3/5/2024	16:36:30	61.8	kpa
22944	3/5/2024	16:36:32	61.8	kpa
22945	3/5/2024	16:36:34	61.8	kpa
22946	3/5/2024	16:36:36	61.8	kpa
22947	3/5/2024	16:36:38	61.8	kpa
22948	3/5/2024	16:36:40	61.8	kpa
22949	3/5/2024	16:36:42	61.8	kpa
22950	3/5/2024	16:36:44	61.8	kpa
22951	3/5/2024	16:36:46	61.7	kpa
22952	3/5/2024	16:36:48	61.7	kpa
22953	3/5/2024	16:36:50	61.7	kpa
22954	3/5/2024	16:36:52	61.7	kpa
22955	3/5/2024	16:36:54	61.7	kpa
22956	3/5/2024	16:36:56	61.7	kpa
22957	3/5/2024	16:36:58	61.7	kpa
22958	3/5/2024	16:37:00	61.6	kpa
22959	3/5/2024	16:37:02	61.6	kpa
22960	3/5/2024	16:37:04	61.6	kpa
22961	3/5/2024	16:37:06	61.6	kpa
22962	3/5/2024	16:37:08	61.6	kpa
22963	3/5/2024	16:37:10	61.6	kpa
22964	3/5/2024	16:37:12	61.6	kpa
22965	3/5/2024	16:37:14	61.6	kpa
22966	3/5/2024	16:37:16	61.6	kpa
22967	3/5/2024	16:37:18	61.5	kpa
22968	3/5/2024	16:37:20	61.5	kpa
22969	3/5/2024	16:37:22	61.5	kpa
22970	3/5/2024	16:37:24	61.5	kpa
22971	3/5/2024	16:37:26	61.5	kpa
22972	3/5/2024	16:37:28	61.5	kpa
22973	3/5/2024	16:37:30	61.5	kpa
22974	3/5/2024	16:37:32	61.5	kpa
22975	3/5/2024	16:37:34	61.4	kpa
22976	3/5/2024	16:37:36	61.4	kpa
22977	3/5/2024	16:37:38	61.4	kpa
22978	3/5/2024	16:37:40	61.4	kpa
22979	3/5/2024	16:37:42	61.4	kpa
22980	3/5/2024	16:37:44	61.4	kpa

Table C3.13: Stack length of 55 mm positioned at 50 mm: T1-T4.

4880	2024/02/15 14:30	23.5	31.0	22.2	26.4
4881	2024/02/15 14:30	23.5	31.0	22.2	26.4
4882	2024/02/15 14:30	23.5	31.0	22.2	26.4
4883	2024/02/15 14:30	23.5	31.0	22.2	26.4
4884	2024/02/15 14:30	23.5	31.0	22.2	26.4
4885	2024/02/15 14:30	23.5	31.0	22.2	26.4
4886	2024/02/15 14:30	23.5	31.0	22.2	26.4
4887	2024/02/15 14:30	23.5	31.0	22.2	26.4
4888	2024/02/15 14:30	23.5	31.0	22.2	26.4
4889	2024/02/15 14:30	23.5	31.0	22.2	26.4
4890	2024/02/15 14:30	23.5	31.0	22.2	26.3
4891	2024/02/15 14:30	23.5	31.0	22.2	26.3
4892	2024/02/15 14:30	23.5	31.0	22.2	26.3
4893	2024/02/15 14:30	23.5	31.0	22.2	26.3
4894	2024/02/15 14:30	23.5	31.0	22.2	26.3
4895	2024/02/15 14:30	23.5	31.0	22.2	26.4
4896	2024/02/15 14:30	23.5	31.0	22.2	26.4
4897	2024/02/15 14:30	23.5	31.0	22.2	26.4
4898	2024/02/15 14:30	23.5	31.0	22.2	26.4
4899	2024/02/15 14:30	23.5	31.0	22.2	26.4
4900	2024/02/15 14:30	23.5	31.0	22.2	26.5
4901	2024/02/15 14:30	23.5	31.0	22.2	26.5
4902	2024/02/15 14:30	23.5	31.0	22.2	26.5
4903	2024/02/15 14:30	23.5	31.0	22.2	26.5
4904	2024/02/15 14:31	23.5	31.0	22.2	26.5
4905	2024/02/15 14:31	23.5	31.0	22.2	26.6
4906	2024/02/15 14:31	23.5	31.0	22.2	26.6
4907	2024/02/15 14:31	23.5	31.0	22.2	26.6
4908	2024/02/15 14:31	23.5	31.0	22.2	26.6
4909	2024/02/15 14:31	23.5	31.0	22.2	26.6
4910	2024/02/15 14:31	23.5	31.0	22.2	26.6
4911	2024/02/15 14:31	23.5	31.0	22.2	26.6
4912	2024/02/15 14:31	23.5	31.0	22.2	26.6
4913	2024/02/15 14:31	23.5	31.0	22.2	26.6
4914	2024/02/15 14:31	23.5	31.0	22.2	26.6
4915	2024/02/15 14:31	23.5	31.0	22.2	26.6
4916	2024/02/15 14:31	23.5	31.0	22.2	26.6
4917	2024/02/15 14:31	23.5	31.0	22.2	26.6
4918	2024/02/15 14:31	23.5	31.0	22.2	26.6
4919	2024/02/15 14:31	23.5	31.0	22.2	26.6
4920	2024/02/15 14:31	23.5	31.0	22.2	26.6
4921	2024/02/15 14:31	23.5	31.0	22.2	26.6
4922	2024/02/15 14:31	23.5	31.0	22.2	26.6
4923	2024/02/15 14:31	23.5	31.0	22.2	26.6
4924	2024/02/15 14:31	23.5	31.0	22.2	26.6
4925	2024/02/15 14:31	23.5	31.0	22.2	26.6

Table C3.14: Stack length of 55 mm positioned at 50 mm: T5-T6.

5517	2024/02/15 14:30	23.7	33.8	---	---
5518	2024/02/15 14:30	23.7	33.8	---	---
5519	2024/02/15 14:30	23.7	33.8	---	---
5520	2024/02/15 14:30	23.7	33.8	---	---
5521	2024/02/15 14:30	23.7	33.8	---	---
5522	2024/02/15 14:30	23.7	33.8	---	---
5523	2024/02/15 14:30	23.7	33.8	---	---
5524	2024/02/15 14:30	23.7	33.8	---	---
5525	2024/02/15 14:30	23.7	33.8	---	---
5526	2024/02/15 14:30	23.7	33.8	---	---
5527	2024/02/15 14:30	23.7	33.8	---	---
5528	2024/02/15 14:30	23.7	33.8	---	---
5529	2024/02/15 14:30	23.7	33.8	---	---
5530	2024/02/15 14:30	23.7	33.8	---	---
5531	2024/02/15 14:30	23.7	33.8	---	---
5532	2024/02/15 14:30	23.7	33.8	---	---
5533	2024/02/15 14:30	23.7	33.8	---	---
5534	2024/02/15 14:30	23.7	33.8	---	---
5535	2024/02/15 14:30	23.7	33.8	---	---
5536	2024/02/15 14:30	23.7	33.8	---	---
5537	2024/02/15 14:30	23.7	33.8	---	---
5538	2024/02/15 14:30	23.7	33.8	---	---
5539	2024/02/15 14:30	23.7	33.8	---	---
5540	2024/02/15 14:30	23.7	33.8	---	---
5541	2024/02/15 14:30	23.7	33.8	---	---
5542	2024/02/15 14:30	23.7	33.8	---	---
5543	2024/02/15 14:30	23.7	33.8	---	---
5544	2024/02/15 14:30	23.7	33.8	---	---
5545	2024/02/15 14:30	23.7	33.8	---	---
5546	2024/02/15 14:30	23.7	33.8	---	---
5547	2024/02/15 14:30	23.7	33.8	---	---
5548	2024/02/15 14:30	23.7	33.8	---	---
5549	2024/02/15 14:30	23.7	33.8	---	---
5550	2024/02/15 14:30	23.7	33.8	---	---
5551	2024/02/15 14:30	23.7	33.8	---	---
5552	2024/02/15 14:31	23.7	33.8	---	---
5553	2024/02/15 14:31	23.7	33.8	---	---
5554	2024/02/15 14:31	23.7	33.8	---	---
5555	2024/02/15 14:31	23.7	33.8	---	---
5556	2024/02/15 14:31	23.7	33.8	---	---
5557	2024/02/15 14:31	23.7	33.8	---	---
5558	2024/02/15 14:31	23.7	33.8	---	---
5559	2024/02/15 14:31	23.7	33.8	---	---
5560	2024/02/15 14:31	23.7	33.8	---	---
5561	2024/02/15 14:31	23.7	33.8	---	---
5562	2024/02/15 14:31	23.7	33.8	---	---

Table C3.15: Stack length of 55 mm positioned at 50 mm: Voltage and current.

519	39.1 V	1.1 A	15/02/24 14:24:09		
520	39.1 V	1.1 A	15/02/24 14:24:19		
521	39.1 V	1.1 A	15/02/24 14:24:29		
522	39.1 V	1.1 A	15/02/24 14:24:39		
523	39.1 V	1.1 A	15/02/24 14:24:49		
524	39.1 V	1.1 A	15/02/24 14:24:59		
525	39.1 V	1.1 A	15/02/24 14:25:09		
526	39.1 V	1.1 A	15/02/24 14:25:19		
527	39.1 V	1.1 A	15/02/24 14:25:29		
528	39.1 V	1.1 A	15/02/24 14:25:39		
529	39.1 V	1.1 A	15/02/24 14:25:49		
530	39.1 V	1.1 A	15/02/24 14:25:59		
531	39.1 V	1.1 A	15/02/24 14:26:09		
532	39.1 V	1.1 A	15/02/24 14:26:19		
533	39.1 V	1.1 A	15/02/24 14:26:29		
534	39.1 V	1.1 A	15/02/24 14:26:39		
535	39.1 V	1.1 A	15/02/24 14:26:49		
536	39.1 V	1.1 A	15/02/24 14:26:59		
537	39.1 V	1.1 A	15/02/24 14:27:09		
538	39.1 V	1.1 A	15/02/24 14:27:19		
539	39.1 V	1.1 A	15/02/24 14:27:29		
540	39.1 V	1.1 A	15/02/24 14:27:39		
541	39.1 V	1.1 A	15/02/24 14:27:49		
542	39.1 V	1.1 A	15/02/24 14:27:59		
543	39.1 V	1.1 A	15/02/24 14:28:09		
544	39.1 V	1.1 A	15/02/24 14:28:19		
545	39.1 V	1.1 A	15/02/24 14:28:29		
546	39.1 V	1.1 A	15/02/24 14:28:39		
547	39.1 V	1.1 A	15/02/24 14:28:49		
548	39.1 V	1.1 A	15/02/24 14:28:59		
549	39.1 V	1.1 A	15/02/24 14:29:09		
550	39.1 V	1.1 A	15/02/24 14:29:19		
551	39.1 V	1.1 A	15/02/24 14:29:29		
552	39.1 V	1.1 A	15/02/24 14:29:39		
553	39.1 V	1.1 A	15/02/24 14:29:49		
554	39.1 V	1.1 A	15/02/24 14:29:59		
555	39.1 V	1.1 A	15/02/24 14:30:09		
556	39.1 V	1.1 A	15/02/24 14:30:19		
557	39.1 V	1.1 A	15/02/24 14:30:29		
558	39.1 V	1.1 A	15/02/24 14:30:39		
559	39.1 V	1.1 A	15/02/24 14:30:49		
560	39.1 V	1.1 A	15/02/24 14:30:59		
561	39.1 V	1.1 A	15/02/24 14:31:09		
562	39.1 V	1.1 A	15/02/24 14:31:19		
563	39.1 V	1.1 A	15/02/24 14:31:29		

Table C3.16: Stack length of 55 mm positioned at 50 mm: Mean and amplitude pressure.

6991	2024/02/15	14:35:39	000019.9	kpa
6992	2024/02/15	14:35:41	000019.9	kpa
6993	2024/02/15	14:35:43	000019.9	kpa
6994	2024/02/15	14:35:45	000019.9	kpa
6995	2024/02/15	14:35:47	000019.9	kpa
6996	2024/02/15	14:35:49	000019.9	kpa
6997	2024/02/15	14:35:51	000019.9	kpa
6998	2024/02/15	14:35:53	000019.9	kpa
6999	2024/02/15	14:35:55	000019.9	kpa
7000	2024/02/15	14:35:57	000019.8	kpa
7001	2024/02/15	14:35:59	000019.8	kpa
7002	2024/02/15	14:36:01	000019.8	kpa
7003	2024/02/15	14:36:03	000019.8	kpa
7004	2024/02/15	14:36:05	000019.8	kpa
7005	2024/02/15	14:36:07	000019.8	kpa
7006	2024/02/15	14:36:09	000019.8	kpa
7007	2024/02/15	14:36:11	000019.8	kpa
7008	2024/02/15	14:36:13	000019.8	kpa
7009	2024/02/15	14:36:15	000019.8	kpa
7010	2024/02/15	14:36:17	000019.8	kpa
7011	2024/02/15	14:36:19	000019.8	kpa
7012	2024/02/15	14:36:21	000019.8	kpa
7013	2024/02/15	14:36:23	000019.7	kpa
7014	2024/02/15	14:36:25	000019.7	kpa
7015	2024/02/15	14:36:27	000019.7	kpa
7016	2024/02/15	14:36:29	000019.7	kpa
7017	2024/02/15	14:36:31	000019.7	kpa
7018	2024/02/15	14:36:33	000019.7	kpa
7019	2024/02/15	14:36:35	000019.7	kpa
7020	2024/02/15	14:36:37	000019.7	kpa
7021	2024/02/15	14:36:39	000019.7	kpa
7022	2024/02/15	14:36:41	000019.7	kpa
7023	2024/02/15	14:36:43	000019.7	kpa
7024	2024/02/15	14:36:45	000019.7	kpa
7025	2024/02/15	14:36:47	000019.7	kpa
7026	2024/02/15	14:36:49	000019.7	kpa
7027	2024/02/15	14:36:51	000019.7	kpa
7028	2024/02/15	14:36:53	000019.6	kpa
7029	2024/02/15	14:36:55	000019.6	kpa
7030	2024/02/15	14:36:57	000019.6	kpa
7031	2024/02/15	14:36:59	000019.6	kpa
7032	2024/02/15	14:37:01	000019.6	kpa
7033	2024/02/15	14:37:03	000019.6	kpa
7034	2024/02/15	14:37:05	000019.6	kpa
7035	2024/02/15	14:37:07	000019.6	kpa

Table C3.17: Stack length of 65 mm positioned at 50 mm: T1-T4.

5867	2024/03/05 13:12	23.6	31.4	22.9	25.0
5868	2024/03/05 13:12	23.6	31.4	22.9	25.0
5869	2024/03/05 13:12	23.6	31.4	22.9	25.0
5870	2024/03/05 13:13	23.6	31.4	22.9	25.0
5871	2024/03/05 13:13	23.6	31.4	22.9	25.0
5872	2024/03/05 13:13	23.6	31.4	22.9	25.0
5873	2024/03/05 13:13	23.6	31.4	22.9	25.0
5874	2024/03/05 13:13	23.6	31.4	22.9	25.0
5875	2024/03/05 13:13	23.6	31.4	22.9	24.9
5876	2024/03/05 13:13	23.6	31.4	22.9	24.9
5877	2024/03/05 13:13	23.6	31.4	22.9	24.9
5878	2024/03/05 13:13	23.6	31.4	22.9	24.9
5879	2024/03/05 13:13	23.6	31.4	22.9	24.9
5880	2024/03/05 13:13	23.6	31.4	22.9	25.0
5881	2024/03/05 13:13	23.6	31.4	22.9	25.0
5882	2024/03/05 13:13	23.6	31.4	22.9	25.0
5883	2024/03/05 13:13	23.6	31.4	22.9	25.0
5884	2024/03/05 13:13	23.6	31.4	22.9	25.0
5885	2024/03/05 13:13	23.6	31.4	22.9	25.0
5886	2024/03/05 13:13	23.6	31.4	22.9	25.2
5887	2024/03/05 13:13	23.6	31.4	22.9	25.2
5888	2024/03/05 13:13	23.6	31.4	22.9	25.2
5889	2024/03/05 13:13	23.6	31.4	22.9	25.2
5890	2024/03/05 13:13	23.6	31.4	22.9	25.2
5891	2024/03/05 13:13	23.6	31.4	22.9	25.5
5892	2024/03/05 13:13	23.6	31.4	22.9	25.5
5893	2024/03/05 13:13	23.6	31.4	22.9	25.5
5894	2024/03/05 13:13	23.6	31.4	22.9	25.5
5895	2024/03/05 13:13	23.6	31.4	22.9	25.5
5896	2024/03/05 13:13	23.6	31.4	22.9	25.4
5897	2024/03/05 13:13	23.6	31.4	22.9	25.4
5898	2024/03/05 13:13	23.6	31.4	22.9	25.4
5899	2024/03/05 13:13	23.6	31.4	22.9	25.4
5900	2024/03/05 13:13	23.6	31.4	22.9	25.4
5901	2024/03/05 13:13	23.6	31.4	22.9	25.3
5902	2024/03/05 13:13	23.6	31.4	22.9	25.3
5903	2024/03/05 13:13	23.6	31.4	22.9	25.3
5904	2024/03/05 13:13	23.6	31.4	22.9	25.3
5905	2024/03/05 13:13	23.6	31.4	22.9	25.3
5906	2024/03/05 13:13	23.6	31.4	22.9	25.3
5907	2024/03/05 13:13	23.6	31.4	22.9	25.2
5908	2024/03/05 13:13	23.6	31.4	22.9	25.2
5909	2024/03/05 13:13	23.6	31.4	22.9	25.2

Table C3.18: Stack length of 65 mm positioned at 50 mm: T5-T6.

5803	2024/03/05 13:12	24.5	34.3	---	---
5804	2024/03/05 13:12	24.5	34.3	---	---
5805	2024/03/05 13:12	24.5	34.3	---	---
5806	2024/03/05 13:12	24.5	34.3	---	---
5807	2024/03/05 13:12	24.5	34.3	---	---
5808	2024/03/05 13:12	24.5	34.3	---	---
5809	2024/03/05 13:12	24.5	34.3	---	---
5810	2024/03/05 13:12	24.5	34.3	---	---
5811	2024/03/05 13:12	24.5	34.3	---	---
5812	2024/03/05 13:12	24.3	34.3	---	---
5813	2024/03/05 13:12	24.3	34.3	---	---
5814	2024/03/05 13:12	24.3	34.3	---	---
5815	2024/03/05 13:12	24.3	34.3	---	---
5816	2024/03/05 13:12	24.3	34.3	---	---
5817	2024/03/05 13:12	24.3	34.3	---	---
5818	2024/03/05 13:12	24.3	34.3	---	---
5819	2024/03/05 13:12	24.3	34.3	---	---
5820	2024/03/05 13:12	24.3	34.3	---	---
5821	2024/03/05 13:13	24.6	34.3	---	---
5822	2024/03/05 13:13	24.6	34.3	---	---
5823	2024/03/05 13:13	24.6	34.3	---	---
5824	2024/03/05 13:13	24.6	34.3	---	---
5825	2024/03/05 13:13	24.6	34.3	---	---
5826	2024/03/05 13:13	24.6	34.3	---	---
5827	2024/03/05 13:13	24.3	34.3	---	---
5828	2024/03/05 13:13	24.3	34.3	---	---
5829	2024/03/05 13:13	24.3	34.3	---	---
5830	2024/03/05 13:13	24.3	34.3	---	---
5831	2024/03/05 13:13	24.3	34.3	---	---
5832	2024/03/05 13:13	24.3	34.3	---	---
5833	2024/03/05 13:13	24.2	34.3	---	---
5834	2024/03/05 13:13	24.2	34.3	---	---
5835	2024/03/05 13:13	24.2	34.3	---	---
5836	2024/03/05 13:13	24.3	34.3	---	---
5837	2024/03/05 13:13	24.3	34.3	---	---
5838	2024/03/05 13:13	24.3	34.3	---	---
5839	2024/03/05 13:13	24.2	34.3	---	---
5840	2024/03/05 13:13	24.2	34.3	---	---
5841	2024/03/05 13:13	24.2	34.3	---	---
5842	2024/03/05 13:13	24.2	34.3	---	---
5843	2024/03/05 13:13	23.5	34.3	---	---
5844	2024/03/05 13:13	23.5	34.3	---	---
5845	2024/03/05 13:13	23.5	34.3	---	---
5846	2024/03/05 13:13	23.7	34.3	---	---

Table 3.19: Stack length of 65 mm positioned at 50 mm: Voltage and current.

544	39.1 V	1.1 A	05/03/24 13:08:05		
545	39.1 V	1.1 A	05/03/24 13:08:15		
546	39.1 V	1.1 A	05/03/24 13:08:25		
547	39.1 V	1.0 A	05/03/24 13:08:35		
548	39.1 V	1.1 A	05/03/24 13:08:45		
549	39.1 V	1.1 A	05/03/24 13:08:55		
550	39.1 V	1.1 A	05/03/24 13:09:05		
551	39.1 V	1.1 A	05/03/24 13:09:15		
552	39.1 V	1.1 A	05/03/24 13:09:25		
553	39.1 V	1.1 A	05/03/24 13:09:35		
554	39.1 V	1.0 A	05/03/24 13:09:45		
555	39.1 V	1.1 A	05/03/24 13:09:55		
556	39.1 V	1.0 A	05/03/24 13:10:05		
557	39.1 V	1.0 A	05/03/24 13:10:15		
558	39.1 V	1.1 A	05/03/24 13:10:25		
559	39.1 V	1.1 A	05/03/24 13:10:35		
560	39.1 V	1.1 A	05/03/24 13:10:45		
561	39.1 V	1.1 A	05/03/24 13:10:55		
562	39.1 V	1.1 A	05/03/24 13:11:05		
563	39.1 V	1.1 A	05/03/24 13:11:15		
564	39.1 V	1.0 A	05/03/24 13:11:25		
565	39.1 V	1.1 A	05/03/24 13:11:35		
566	39.1 V	1.0 A	05/03/24 13:11:45		
567	39.1 V	1.1 A	05/03/24 13:11:55		
568	39.1 V	1.1 A	05/03/24 13:12:05		
569	39.1 V	1.1 A	05/03/24 13:12:15		
570	39.1 V	1.1 A	05/03/24 13:12:25		
571	39.1 V	1.1 A	05/03/24 13:12:35		
572	39.1 V	1.0 A	05/03/24 13:12:45		
573	39.1 V	1.1 A	05/03/24 13:12:55		
574	39.1 V	1.1 A	05/03/24 13:13:05		
575	39.1 V	1.1 A	05/03/24 13:13:15		
576	39.1 V	1.1 A	05/03/24 13:13:25		
577	39.1 V	1.0 A	05/03/24 13:13:35		
578	39.1 V	1.1 A	05/03/24 13:13:45		
579	39.1 V	1.1 A	05/03/24 13:13:55		
580	39.1 V	1.1 A	05/03/24 13:14:05		
581	39.1 V	1.1 A	05/03/24 13:14:15		
582	39.1 V	1.1 A	05/03/24 13:14:25		
583	39.1 V	1.0 A	05/03/24 13:14:35		
584	39.1 V	1.1 A	05/03/24 13:14:45		
585	39.1 V	1.1 A	05/03/24 13:14:55		
586	39.1 V	1.1 A	05/03/24 13:15:05		
587	39.1 V	1.1 A	05/03/24 13:15:15		
588	39.1 V	1.1 A	05/03/24 13:15:25		

Table C3.20: Stack length of 65 mm positioned at 50 mm: Mean and amplitude pressure.

20055	2024/03/05	13:12:26	000060.6	kpa
20056	2024/03/05	13:12:28	000060.6	kpa
20057	2024/03/05	13:12:30	000060.6	kpa
20058	2024/03/05	13:12:32	000060.6	kpa
20059	2024/03/05	13:12:34	000060.5	kpa
20060	2024/03/05	13:12:36	000060.5	kpa
20061	2024/03/05	13:12:38	000060.5	kpa
20062	2024/03/05	13:12:40	000060.5	kpa
20063	2024/03/05	13:12:42	000060.5	kpa
20064	2024/03/05	13:12:44	000060.5	kpa
20065	2024/03/05	13:12:46	000060.5	kpa
20066	2024/03/05	13:12:48	000060.5	kpa
20067	2024/03/05	13:12:50	000060.4	kpa
20068	2024/03/05	13:12:52	000060.4	kpa
20069	2024/03/05	13:12:54	000060.4	kpa
20070	2024/03/05	13:12:56	000060.4	kpa
20071	2024/03/05	13:12:58	000060.4	kpa
20072	2024/03/05	13:13:00	000060.4	kpa
20073	2024/03/05	13:13:02	000060.4	kpa
20074	2024/03/05	13:13:04	000060.4	kpa
20075	2024/03/05	13:13:06	000060.3	kpa
20076	2024/03/05	13:13:08	000060.3	kpa
20077	2024/03/05	13:13:10	000060.3	kpa
20078	2024/03/05	13:13:12	000060.3	kpa
20079	2024/03/05	13:13:14	000060.3	kpa
20080	2024/03/05	13:13:16	000060.3	kpa
20081	2024/03/05	13:13:18	000060.3	kpa
20082	2024/03/05	13:13:20	000060.3	kpa
20083	2024/03/05	13:13:22	000060.2	kpa
20084	2024/03/05	13:13:24	000060.2	kpa
20085	2024/03/05	13:13:26	000060.2	kpa
20086	2024/03/05	13:13:28	000060.2	kpa
20087	2024/03/05	13:13:30	000060.2	kpa
20088	2024/03/05	13:13:32	000060.2	kpa
20089	2024/03/05	13:13:34	000060.2	kpa
20090	2024/03/05	13:13:36	000060.2	kpa
20091	2024/03/05	13:13:38	000060.1	kpa
20092	2024/03/05	13:13:40	000060.1	kpa
20093	2024/03/05	13:13:42	000060.1	kpa
20094	2024/03/05	13:13:44	000060.1	kpa
20095	2024/03/05	13:13:46	000060.1	kpa
20096	2024/03/05	13:13:48	000060.1	kpa
20097	2024/03/05	13:13:50	000060.1	kpa
20098	2024/03/05	13:13:52	000060.1	kpa

APPENDIX D: Excel data for simulation results.

D.1 Five stacks positioned at 30 mm.

Table D.1.1: Stack length of 25 mm positioned at 30 mm.

0,842056	374,7404293	370,5672306	7,759467025	108,6485706
0,854349	374,726357	370,5237616	7,463503271	107,4795002
0,866641	374,7119695	370,4815127	7,167665391	106,3430839
0,878933	374,6972901	370,4403794	6,872208389	105,2358951
0,891225	374,6823123	370,400302	6,577372382	104,1603883
0,903518	374,6670456	370,3611721	6,283400709	103,1156163
0,91581	374,651499	370,3229057	5,99051879	102,1002003
0,928102	374,635681	370,2854344	5,698926924	101,1125944
0,940394	374,6196	370,2487014	5,408805842	100,1510684
0,952687	374,6032638	370,2126589	5,12031859	99,21392398
0,964979	374,58668	370,1772647	4,833607846	98,29946867
0,977271	374,5698559	370,1424841	4,54880263	97,40640187
1,001856	374,5352698	370,0750611	3,987849478	95,70452526
1,023982	374,503481	370,016027	3,489917092	94,2277964
1,046108	374,4709887	369,9582883	2,999875701	92,82222983
1,068234	374,4378898	369,9017949	2,517335363	91,4723699
1,09036	374,4041414	369,8461819	2,043161195	90,1935001
1,112486	374,3698295	369,7914422	1,576923946	88,97113888
1,134612	374,334908	369,7372039	1,120550222	87,81938544
1,156738	374,2994522	369,6835095	0,676896998	86,72393192
1,178864	374,2633938	369,6299929	0,273463038	85,69693271
1,20099	374,2267655	369,5767595	0,274007219	84,72320932
1,223116	374,1899241	369,5234708	0,705260285	83,8121891
1,245242	374,1524011	369,4702961	1,120455191	82,94822655
1,289494	374,0753967	369,3634451	1,939244724	81,39983253
1,328584	374,0059781	369,2689005	2,651829196	80,13474116
1,367673	373,9351834	369,1744593	3,349312759	78,93940024
1,406763	373,8630434	369,0804805	4,031389198	77,782542
1,445852	373,7899939	368,9868381	4,703670457	76,64150019
1,484942	373,7158215	368,8942141	5,363668305	75,4999756
1,524031	373,6404422	368,8029952	6,01106075	74,34239104
1,563121	373,5638506	368,7133964	6,646476011	73,15641736
1,6413	373,4072112	368,5407645	7,886193995	70,64435666
1,719479	373,2462064	368,3774291	9,088127421	67,95412583
1,797658	373,0811719	368,2231287	10,25709445	65,12778316
1,875837	372,9124803	368,0765325	11,39713216	62,23118558
1,954016	372,7405253	367,9355847	12,51133277	59,33310592
2,032195	372,5657118	367,7980011	13,60206034	56,48836689
2,110374	372,3884487	367,6616623	14,67121333	53,73198978
2,188553	372,2091387	367,5248101	15,7204478	51,08173225
2,344911	371,8462594	367,2435083	17,76769129	46,11750898
2,501269	371,4794392	366,9481641	19,75476128	41,591374
2,657627	371,1109511	366,6343876	21,69322907	37,49184509
2,813985	370,7421783	366,2991282	23,59271988	33,82971279
2,970343	370,3745594	365,9396491	25,46331814	30,62057502
3,126701	370,0087477	365,5540615	27,31233207	27,88813097
3,283059	369,6453896	365,1411202	29,14703853	25,64662016
3,439418	369,284621	364,7006142	30,97204906	23,89649632
3,595776	368,9266243	364,2333829	32,79154398	22,62012846
3,752134	368,5712856	363,7410522	34,60740006	21,78752089
3,908492	368,2185057	363,226098	36,4206633	21,35531332
4,06485	367,8682205	362,6915756	38,23108352	21,27368774
4,221208	367,5203331	362,1407949	40,037316	21,49080655
4,377566	367,1747583	361,577107	41,83727424	21,95630079
4,533924	366,831444	361,0037436	43,62836278	22,62347876
4,690282	366,4903678	360,423702	45,40770517	23,45054058
5,002998	365,8151789	359,257303	48,91564328	25,40433273
5,315714	365,1489802	358,0908688	52,34410308	27,64604183
5,62843	364,4926719	356,9375986	55,67640172	30,0158302
5,941146	363,8460983	355,8050271	58,90124251	32,41586717
6,253863	363,2104265	354,7002345	62,01008902	34,77021919

Table D.1.2: Stack length of 35 mm positioned at 30 mm.

0,782830379	375,276945	374,458357	5,046156219	34,46034212
0,794825442	375,271838	374,433779	4,963206043	34,13188805
0,806820504	375,266551	374,409099	4,878234967	33,81312816
0,818815566	375,26108	374,384311	4,791288481	33,50345281
0,830810628	375,255424	374,359413	4,702412794	33,20227863
0,84280569	375,249578	374,3344	4,611646658	32,90914761
0,866795815	375,2373	374,28402	4,424730376	32,34380987
0,890785939	375,224229	374,233164	4,230851544	31,80436569
0,912377051	375,211772	374,186982	4,050691231	31,33843864
0,933968163	375,198644	374,140412	3,865453047	30,88860401
0,955559275	375,184833	374,093456	3,67540426	30,45281814
0,977150387	375,170328	374,046123	3,480802385	30,02928474
0,998741499	375,15512	373,99842	3,2819102	29,61631984
1,020332611	375,139198	373,950357	3,078963228	29,21255847
1,041923723	375,122194	373,901774	2,870383746	28,82025257
1,063514835	375,104442	373,852847	2,65837103	28,4340212
1,085105947	375,085989	373,803664	2,443337693	28,05217063
1,106697059	375,066754	373,754107	2,22521938	27,6753517
1,128288171	375,046807	373,704296	2,004462235	27,30158964
1,149879283	375,026067	373,654126	1,781090406	26,93154142
1,171470395	375,004611	373,60371	1,555556226	26,56358556
1,193061507	374,982354	373,552947	1,328072859	26,19834828
1,214652619	374,959378	373,501941	1,099267672	25,83447403
1,236243731	374,935597	373,450592	0,870029922	25,47257859
1,257834843	374,911094	373,398998	0,642515855	25,11153097
1,279425955	374,885779	373,347058	0,423596711	24,75194516
1,301017067	374,859732	373,294867	0,241048492	24,39286831
1,344199291	374,8047	373,189136	0,425773637	23,67825201
1,383063292	374,752694	373,092898	0,854239387	23,03720863
1,421927294	374,698314	372,995523	1,305862015	22,39838997
1,460791295	374,641614	372,896931	1,76747369	21,76215378
1,538519298	374,523009	372,696659	2,708508483	20,4976592
1,616247301	374,396216	372,491075	3,673438125	19,24928911
1,693975304	374,261263	372,279122	4,661982182	18,0257848
1,771703308	374,11858	372,059888	5,673288385	16,83699222
1,849431311	373,968736	371,83254	6,706156756	15,69334654
1,927159314	373,812339	371,596294	7,759260828	14,60531123
2,004887317	373,650009	371,350473	8,831196117	13,58261869
2,08261532	373,482365	371,094542	9,920486873	12,63376752
2,160343323	373,31001	370,828143	11,02560021	11,76563294
2,238071326	373,133525	370,551096	12,14496227	10,98324879
2,393527332	372,770865	369,965613	14,41838386	9,686381992
2,548983338	372,397796	369,34015	16,72925242	8,74371741
2,704439345	372,017671	368,678517	19,06464218	8,139330514
2,859895351	371,632792	367,985078	21,41355723	7,846960558
3,015351357	371,245607	367,265509	23,76368215	7,83044501
3,170807363	370,857595	366,524862	26,10567275	8,055034562
3,326263369	370,470121	365,768564	28,43035204	8,48331728
3,481719375	370,084251	365,001633	30,73006176	9,080576569
3,637175381	369,700742	364,22852	32,99860567	9,815479528
3,792631388	369,319976	363,452401	35,23184404	10,66487628
4,1035434	368,569357	361,91049	39,5713135	12,56644944
4,383364211	367,906257	360,540561	43,32730579	14,45827347
4,663185022	367,255912	359,198224	46,93402954	16,43456556
4,943005833	366,61813	357,889165	50,38965486	18,44048494
5,222826644	365,993496	356,618288	53,69563242	20,43050994
5,502647455	365,381412	355,387218	56,85600577	22,37727153
5,782468266	364,781035	354,196413	59,87533245	24,26185747
6,342109889	363,617635	351,935569	65,53367607	27,79271655

Table D.1.3: Stack length of 45 mm positioned at 30 mm.

0,6359372	375,7945353	373,5279446	4,479952963	48,25028675
0,6449997	375,7914323	373,554651	4,452163595	47,51729392
0,6540623	375,7882391	373,5797851	4,423552898	46,8266577
0,6631248	375,7849539	373,6033827	4,394097105	46,17587403
0,6721874	375,7815747	373,6254804	4,363773598	45,56258939
0,68125	375,7780998	373,6461144	4,332561573	44,98460187
0,6903125	375,7745273	373,665322	4,300441891	44,43975007
0,6993751	375,7708555	373,6831387	4,267397885	43,92613109
0,7084377	375,7670827	373,6995997	4,23341423	43,44194788
0,7175002	375,763159	373,7142018	4,198026112	42,99660619
0,7265628	375,7591273	373,7275293	4,161639232	42,57655891
0,7356253	375,754988	373,7396348	4,124268401	42,17963023
0,7446879	375,7507395	373,7505531	4,085906484	41,80439821
0,7537505	375,7463802	373,7603172	4,046546799	41,44959722
0,762813	375,7419085	373,7689593	4,006184376	41,11400703
0,7718756	375,7373229	373,776511	3,964815658	40,79647285
0,7809381	375,7326218	373,7830028	3,922438292	40,4958907
0,7990633	375,7227398	373,791871	3,833606664	39,95574838
0,8141118	375,7142122	373,7967472	3,757153777	39,54253829
0,8291603	375,7053289	373,798937	3,677816905	39,16485089
0,8442088	375,6961173	373,7989171	3,595866531	38,81460307
0,8592574	375,6865374	373,7964626	3,511073703	38,49268988
0,8743059	375,676619	373,792012	3,423718013	38,19236159
0,8893544	375,666321	373,7853578	3,333586909	37,91429379
0,9044029	375,6556752	373,7768996	3,240950986	37,6528713
0,9194514	375,6446585	373,7666027	3,145722599	37,40735945
0,9345	375,6332668	373,7545414	3,047943543	37,17566274
0,9495485	375,6214753	373,7406534	2,947541696	36,95676164
0,964597	375,6093222	373,7253037	2,844787659	36,74674032
0,9796455	375,5967833	373,7084604	2,739605297	36,54508444
0,9946941	375,5838552	373,6901842	2,632038733	36,35030393
1,0247911	375,5563938	373,6482613	2,407565736	35,97851406
1,0517515	375,5304867	373,606823	2,19925085	35,65290619
1,0787119	375,5032941	373,5619676	1,984157968	35,32913387
1,1056723	375,4748117	373,5140015	1,762624755	35,00296302
1,1595931	375,4148859	373,4117631	1,306598056	34,33520484
1,2063852	375,3589596	373,3152699	0,896962574	33,72885569
1,2531773	375,2992292	373,2121947	0,491053215	33,08719297
1,2999695	375,2357736	373,1033361	0,250129133	32,40304571
1,3467616	375,1685766	372,9893983	0,586468946	31,67330458
1,3935537	375,097639	372,870945	1,064293349	30,89806547
1,4403458	375,0231108	372,7483905	1,576373409	30,07996877
1,487138	374,9451456	372,6220148	2,11072346	29,22350156
1,5807222	374,7796749	372,3583786	3,231049181	27,42751862
1,6743065	374,6023332	372,0802558	4,413951517	25,55787601
1,7678907	374,4144234	371,7873137	5,653917264	23,66868843
1,861475	374,2171146	371,4788791	6,945668883	21,80466089
1,9550592	374,0117081	371,1542324	8,28348527	20,00940435
2,0486435	373,7994514	370,8128043	9,661549967	18,31709941
2,1422278	373,5815011	370,454281	11,07401154	16,75227113
2,235812	373,3589129	370,0786787	12,51511324	15,3305624
2,3293963	373,1326351	369,6863538	13,97929545	14,06006019
2,4229805	372,903506	369,2779685	15,46127276	12,94279314
2,5165648	372,6722564	368,8544367	16,95609575	11,9761911
2,610149	372,4395156	368,4168628	18,45919548	11,15439726
2,7037333	372,2058194	367,9664819	19,96640685	10,46939566
2,8909018	371,7378312	367,0346182	22,97452681	9,457828216
3,0780703	371,2702859	366,0675368	25,96120781	8,876595881
3,2652388	370,805241	365,0754639	28,90677114	8,649110286
3,4524073	370,3437264	364,0666187	31,79805956	8,713481106
3,6395758	369,8868635	363,0497427	34,6234088	9,005674905
3,8267443	369,4349869	362,0309688	37,37668006	9,480524091
4,0139129	368,988414	361,0161117	40,05338705	10,09552905
4,2010814	368,5474005	360,0098253	42,65141653	10,81659959
4,3882499	368,1120298	359,0156895	45,17042867	11,61637855
4,7625869	367,2583263	357,0762433	49,97894026	13,34759468
5,1369239	366,426872	355,2083407	54,49316495	15,18549664
5,5112609	365,6169039	353,417867	58,73004806	17,05370689
5,885598	364,8278054	351,7074473	62,70933271	18,89570102
6,259935	364,0589072	350,0766922	66,45143101	20,67540223

Table D.1.4: Stack length of 55 mm positioned at 30 mm.

0,71747	352,2839473	347,298039	2,918451031	106,3258305
0,73091	352,27925	347,196158	2,89271897	109,4494776
0,74435	352,2743387	347,086744	2,864949407	112,5836465
0,75778	352,2692079	346,971491	2,835122705	115,6039427
0,77122	352,2638521	346,852336	2,803222426	118,4004239
0,78466	352,258266	346,731268	2,769235267	120,8885277
0,7981	352,2524443	346,610236	2,733150674	123,0121625
0,81153	352,2463823	346,490744	2,694962643	124,7519665
0,82497	352,2400752	346,374131	2,654666905	126,1084147
0,83841	352,2335182	346,261387	2,612261711	127,101255
0,86529	352,2196306	346,050177	2,521137685	128,1889923
0,88947	352,2057967	345,884371	2,428600873	127,9810704
0,91124	352,1926057	345,747564	2,339832189	127,4066976
0,93301	352,1787217	345,621299	2,246089258	126,5666476
0,95478	352,1640478	345,505745	2,146880882	125,4847205
0,97655	352,1486552	345,399101	2,042838827	124,235724
0,99832	352,1324937	345,301198	1,933800085	122,8373733
1,02009	352,1155539	345,211394	1,819867323	121,3122978
1,06362	352,0797789	345,049403	1,580687396	118,0109769
1,10716	352,0410257	344,913265	1,32433177	114,3847343
1,1507	351,9991312	344,801411	1,051354818	110,5056106
1,19424	351,9540492	344,711031	0,764241249	106,4585986
1,23778	351,9057729	344,639121	0,470263825	102,3268469
1,28131	351,8543627	344,58264	0,219917251	98,18739427
1,32485	351,79992	344,538453	0,332562518	94,11004592
1,36839	351,742345	344,503799	0,656995377	90,14393148
1,41193	351,6817395	344,476203	1,024149494	86,32450728
1,45547	351,6181938	344,453681	1,413826011	82,67369581
1,54254	351,4829372	344,412775	2,241321624	75,94774935
1,62962	351,3374146	344,371575	3,123077598	69,95313829
1,71669	351,1825666	344,32365	4,052607835	64,61468234
1,80377	351,0194023	344,265027	5,024526817	59,83528707
1,89084	350,8489372	344,193857	6,033584989	55,51739401
1,97792	350,6721634	344,109621	7,074663128	51,57498272
2,065	350,4900278	344,0125	8,142743397	47,93838067
2,15207	350,3034166	343,902954	9,232927132	44,5547052
2,23915	350,1131453	343,781467	10,34050822	41,38601807
2,32622	349,919954	343,648426	11,46104538	38,40659678
2,4133	349,7245058	343,504076	12,59041275	35,60018311
2,50037	349,5273892	343,348521	13,72483327	32,95741795
2,58745	349,3291208	343,181769	14,86089852	30,47359266
2,67453	349,1301511	343,003773	15,99557381	28,14676371
2,7616	348,9308697	342,814484	17,1261927	25,97624391
2,84868	348,7316111	342,613896	18,25044222	23,9614719
2,93575	348,5326611	342,402076	19,36634266	22,10124242
3,1099	348,1369093	341,946009	21,56508905	18,82986156
3,26664	347,7836989	341,500072	23,50253497	16,37725696
3,42338	347,4342097	341,023604	25,39524641	14,34950383
3,58011	347,0889044	340,519861	27,24019877	12,70645848
3,73685	346,7482811	339,993079	29,03541459	11,39744871
3,89359	346,4125162	339,447021	30,78026468	10,37989837
4,05032	346,0817648	338,88581	32,4748949	9,608379104
4,20706	345,756138	338,313329	34,12017239	9,041969032
4,3638	345,4356647	337,733088	35,71734279	8,645109672
4,52053	345,120326	337,148195	37,2679261	8,387486405
4,83401	344,5048353	335,97797	40,2388941	8,164569719
5,14748	343,9088525	334,815266	43,04344742	8,256689892
5,46095	343,3319845	333,672139	45,69497025	8,554343732
5,77442	342,7734462	332,556526	48,20477688	8,983663378
6,0879	342,2324859	331,473808	50,58384467	9,492054884

Table D.1.5: Stack length of 65 mm positioned at 65 mm.

0,83374	367,6305339	366,104418	2,655670473	47,38983358
0,852457	367,6233873	366,041183	2,575801947	47,67361877
0,871174	367,6158472	365,977237	2,492115884	47,94174921
0,889891	367,6079049	365,912681	2,40461783	48,19178276
0,908608	367,5995515	365,847619	2,313321521	48,4215049
0,927325	367,5907787	365,782145	2,218250983	48,62894933
0,964759	367,5719322	365,650404	2,016976245	48,96888105
1,002193	367,5513055	365,518061	1,801130727	49,20206611
1,039627	367,5288427	365,385589	1,571159835	49,32261078
1,077061	367,5044832	365,25344	1,327689501	49,32650859
1,114495	367,4781679	365,121973	1,071612025	49,21287555
1,151929	367,4498405	364,991437	0,804483578	48,98375846
1,189363	367,419447	364,861974	0,530116211	48,64355564
1,226797	367,386925	364,733642	0,267221382	48,19853975
1,264232	367,3523108	364,60642	0,198309648	47,65639141
1,301666	367,3154842	364,480224	0,464389025	47,02574598
1,376534	367,2350366	364,230081	1,125714949	45,54692455
1,451402	367,1455483	363,981839	1,843564051	43,82797311
1,52627	367,047018	363,73383	2,604437531	41,93562515
1,601138	366,9395223	363,484265	3,403550031	39,93295083
1,676006	366,8232558	363,231412	4,238656659	37,8747746
1,750874	366,6985237	362,973704	5,107676051	35,80660557
1,825742	366,5657268	362,709806	6,008341795	33,76479485
1,900611	366,4253446	362,438651	6,938408911	31,77734096
1,975479	366,2779162	362,159442	7,895622442	29,86496634
2,050347	366,1240206	361,871636	8,877672818	28,04224784
2,125215	365,9642583	361,574921	9,882212422	26,31870294
2,200083	365,7992356	361,269185	10,90687417	24,69977676
2,349819	365,456428	360,631361	13,0046799	21,78073698
2,499556	365,099519	359,960159	15,15481181	19,2740154
2,649292	364,7324814	359,25889	17,33974874	17,14982789
2,799028	364,3582584	358,531078	19,54512071	15,37289432
2,948764	363,9797371	357,780946	21,7561658	13,90080792
3,098501	363,599255	357,012788	23,96032488	12,69135682
3,248237	363,2186245	356,230711	26,14730917	11,70557293
3,397973	362,8392411	355,438526	28,30885931	10,90898711
3,547709	362,4621633	354,639687	30,43847678	10,27186911
3,697446	362,0881773	353,837268	32,53118002	9,768973757
3,847182	361,7178546	353,033971	34,58328114	9,379106526
3,996918	361,3515999	352,232143	36,59217908	9,084574415
4,296391	360,6325981	350,643064	40,47382948	8,708503517
4,595863	359,9315466	349,079516	44,17308409	8,572452424
4,895336	359,2491331	347,550665	47,69120041	8,611455715
5,194808	358,5851261	346,062566	51,03349697	8,779402195
5,494281	357,9390868	344,619355	54,20812521	9,041014113
5,793753	357,3104109	343,223294	57,22432586	9,371174914
6,093226	356,6984014	341,875417	60,0917338	9,75075887

D.2 Five stacks positioned at 40 mm.

Table D.2.1: Stack length of 25 mm positioned at 40 mm.

0,969827	365,5560612	361,2350538	6,191497493	93,57159
0,998648	365,5108275	361,1711587	5,471802077	90,47519923
1,02747	365,4642421	361,1134078	4,765503467	87,54270449
1,056291	365,4164103	361,0604705	4,074972078	84,79400147
1,085113	365,367429	361,0110303	3,402015435	82,24197051
1,113934	365,3173835	360,9639241	2,747962473	79,88849102
1,142756	365,2663475	360,918215	2,113916571	77,72544084
1,171577	365,2143708	360,8733156	1,501023856	75,74069373
1,22922	365,1078582	360,783241	0,373117185	72,19744841
1,281099	365,0093468	360,7014559	0,72730001	69,43323932
1,332978	364,9082789	360,6183242	1,644323245	66,98241081
1,384856	364,8048379	360,533603	2,522246102	64,77474977
1,436735	364,6990912	360,447312	3,355965014	62,75749674
1,488614	364,5910043	360,3595812	4,145753522	60,89006664
1,540492	364,4805409	360,2705723	4,89526493	59,14032101
1,592371	364,367668	360,1804405	5,609238959	57,48236015
1,64425	364,2523564	360,0892812	6,291240545	55,89917117
1,748007	364,0143297	359,9045635	7,58242799	52,8540639
1,841389	363,7917492	359,7356078	8,671202918	50,22316403
1,93477	363,561485	359,5641299	9,707238269	47,64647461
2,028152	363,3238931	359,3897597	10,70223995	45,1048553
2,121534	363,0794934	359,2118938	11,66695839	42,58917082
2,214915	362,828921	359,029705	12,60985603	40,10327184
2,308297	362,5728778	358,842179	13,53762953	37,65975194
2,401679	362,3120974	358,6482149	14,45561083	35,27585718
2,49506	362,0473143	358,4467123	15,36803499	32,97075473
2,588442	361,7792375	358,2366374	16,27824418	30,76365829
2,681824	361,5085316	358,0170774	17,18884987	28,67244903
2,775205	361,2358048	357,7872817	18,10185602	26,712676
2,961969	360,6870877	357,2946309	19,9419635	23,24768206
3,148732	360,1357725	356,7576726	21,80298631	20,4059088
3,335495	359,584663	356,1775185	23,68697381	18,19291667
3,522258	359,0356657	355,5575864	25,59201172	16,57761891
3,709022	358,4900743	354,902671	27,51365405	15,50609555
3,895785	357,9489169	354,2186509	29,44561137	14,90833271
4,082548	357,4127816	353,5113836	31,38055531	14,71320876
4,269312	356,8823978	352,7877331	33,31008034	14,83974245
4,456075	356,3580008	352,0529692	35,22635572	15,22580018
4,642838	355,8398553	351,312392	37,12145619	15,81024756
4,829602	355,3282297	350,5705273	38,98845499	16,54246874
5,016365	354,8232948	349,8310722	40,82135141	17,38138902
5,389891	353,8342213	348,373687	44,36233199	19,22255161
5,763418	352,8724376	346,9519313	47,72466179	21,1970737
6,136945	351,9387221	345,576101	50,896407	23,19033706

Table D.2.2: Stack length of 35 mm positioned at 40 mm.

0,806092	316,8474458	314,9085096	1,178471987	18,87737039
0,838897	316,8292412	314,9135194	0,997115165	18,4697286
0,871702	316,8101346	314,9143236	0,814814231	18,1740663
0,904508	316,7901145	314,9106435	0,63249896	17,99303064
0,937313	316,769173	314,9022665	0,451157121	17,92340726
0,970118	316,7473041	314,889111	0,272336625	17,95438414
1,002924	316,7244983	314,8712711	0,10400752	18,0677648
1,068534	316,6761446	314,8234642	0,273524763	18,41989667
1,134145	316,624111	314,7624314	0,615068192	18,81960479
1,199756	316,5684264	314,692475	0,945465974	19,13532593
1,265366	316,509154	314,6177258	1,264329002	19,28689585
1,330977	316,446363	314,5414521	1,570961099	19,2487647
1,396588	316,3801442	314,4658394	1,865433732	19,03285773
1,462198	316,3106129	314,3921042	2,148682943	18,66883118
1,527809	316,2379075	314,3207474	2,421819792	18,19018544
1,59342	316,1621882	314,251806	2,685975517	17,62744733
1,65903	316,0836354	314,1850426	2,942270493	17,00604283
1,724641	316,0024469	314,1200697	3,191740226	16,34637188
1,790251	315,9188342	314,0564274	3,435292772	15,6645893
1,921473	315,7455588	313,9305071	3,9085975	14,29616826
2,039572	315,5835314	313,8171064	4,320767756	13,08500481
2,157671	315,4171069	313,7010952	4,722898912	11,93188525
2,27577	315,2473462	313,5807296	5,117041126	10,85788401
2,393869	315,0753311	313,4544793	5,505188879	9,87818868
2,511969	314,901999	313,3213306	5,889062143	9,000115372
2,630068	314,7281374	313,1807459	6,2701423	8,22514062
2,748167	314,5543968	313,0325944	6,649684343	7,550570821
2,866266	314,3813064	312,8770757	7,02870152	6,970848008
2,984365	314,2092898	312,7146396	7,407947578	6,478631841
3,102464	314,0386814	312,5459104	7,787916107	6,06566229
3,220564	313,8697424	312,3716197	8,16885613	5,723408567
3,338663	313,7026745	312,1925523	8,550798947	5,443523805
3,456762	313,5376322	312,0095047	8,933592644	5,218140108
3,574861	313,3747323	311,823254	9,316939848	5,04003982
3,69296	313,214062	311,6345381	9,700435412	4,902734636
3,81106	313,0556853	311,4440426	10,08360069	4,8004798
3,929159	312,8996479	311,2523937	10,46591322	4,728243505
4,047258	312,7459808	311,0601557	10,8468319	4,681656894
4,165357	312,5947036	310,8678317	11,22581724	4,656950415
4,401555	312,2993557	310,4851839	11,97524792	4,656934828
4,637754	312,0135573	310,1066326	12,71114615	4,712658003
4,873952	311,7372435	309,7344058	13,43046255	4,808381357
5,11015	311,4702574	309,3699023	14,13088127	4,93396537
5,346349	311,2124379	309,0144131	14,81053255	5,07991494
5,582547	310,9635609	308,6685884	15,4681799	5,240717598
5,818745	310,7233988	308,3329688	16,10310953	5,411308144
6,054944	310,4916935	308,0077417	16,71492489	5,588686511

Table D.2.3: Stack length of 45 mm positioned at 40 mm.

0,909798	365,2689916	359,6245712	3,874151917	139,8124041
0,931662	365,2555296	359,4937568	3,738412028	137,4813465
0,953527	365,2415649	359,3785244	3,597070709	134,9289129
0,975391	365,2270827	359,2771738	3,450289968	132,2375985
0,997256	365,2120683	359,1880122	3,298243015	129,474165
1,01912	365,1965101	359,1096907	3,141082014	126,6818416
1,062849	365,1636781	358,9770253	2,812531923	121,2232189
1,106578	365,128483	358,8703562	2,466067167	116,0136844
1,150307	365,0908142	358,7823598	2,103245706	111,1191839
1,194036	365,0505636	358,7077329	1,72569353	106,547583
1,237765	365,0076124	358,6421805	1,335521153	102,2755961
1,281493	364,9618404	358,5828227	0,935967395	98,26278398
1,325222	364,9131257	358,5277706	0,535759004	94,46833175
1,368951	364,8613736	358,4757346	0,207911558	90,86006819
1,41268	364,806554	358,4257547	0,43455539	87,41614288
1,456409	364,7484291	358,3770473	0,865549175	84,12312612
1,500138	364,6869694	358,3289351	1,318917706	80,97274002
1,543867	364,6221567	358,2809158	1,784042803	77,95995031
1,631325	364,482281	358,1822509	2,737239238	72,31453948
1,718782	364,3286907	358,0784437	3,712732591	67,14113457
1,80624	364,1614918	357,9675503	4,706879925	62,3870111
1,893698	363,9810103	357,8482255	5,716990882	57,99780896
1,981156	363,7877841	357,7196482	6,740600752	53,92400925
2,068614	363,5825345	357,5813151	7,775955391	50,12311554
2,156071	363,3661276	357,4328798	8,821806908	46,56048461
2,243529	363,1395318	357,2740417	9,877127795	43,20954763
2,330987	362,9037772	357,1044801	10,94099079	40,05130582
2,418445	362,6599195	356,9238313	12,01248374	37,07326677
2,505903	362,4090079	356,731696	13,09064393	34,26807166
2,59336	362,15206	356,5276675	14,17442788	31,63202307
2,680818	361,8900429	356,311369	15,26270961	29,16367536
2,768276	361,6238599	356,0824925	16,35429223	26,86260053
2,943192	361,0833194	355,5863275	18,54074201	22,76071708
3,100616	360,5897608	355,0964311	20,50767165	19,62794309
3,25804	360,0932182	354,5670499	22,46594744	16,99640729
3,415464	359,5960668	354,0007053	24,40940665	14,83331722
3,572888	359,1006926	353,4012769	26,33160495	13,09172453
3,730312	358,6084659	352,7727532	28,22786575	11,72719175
3,887736	358,1206126	352,1198226	30,09376278	10,68897125
4,04516	357,638037	351,4472296	31,92581823	9,928265082
4,202584	357,1613338	350,7595132	33,72133588	9,400471262
4,360008	356,6908849	350,0608709	35,47829163	9,06609522
4,517432	356,2269253	349,3550829	37,19521299	8,890943311
4,83228	355,3190149	347,9388587	40,50507994	8,874601693
5,147128	354,4372075	346,5267858	43,64822875	9,215987922
5,461976	353,5814354	345,1342854	46,62576709	9,787739783
5,776824	352,7509044	343,7717382	49,44094802	10,50263072
6,091672	351,9447299	342,446342	52,09938519	11,29820232

Table D.2.4: Stack length of 55 mm positioned at 40 mm.

0,91886	387,2835492	385,4153147	2,658573823	57,29109
0,948841	387,263766	385,2981571	2,490949038	58,9901033
0,978822	387,2427	385,1703146	2,313217276	60,86604667
1,008803	387,2203003	385,0319463	2,12572128	62,898226
1,038784	387,1965176	384,8832847	1,928852944	65,06523095
1,068765	387,1713041	384,7246598	1,723062843	67,34308063
1,098746	387,1446136	384,5565372	1,508878064	69,70295831
1,128727	387,1164009	384,3795627	1,286956397	72,10915645
1,158708	387,0866224	384,1946029	1,058257451	74,51779492
1,18869	387,0552357	384,0027726	0,824309087	76,8769092
1,218671	387,0221993	383,805438	0,588455606	79,12822143
1,248652	386,9874618	383,6041884	0,360406611	81,21064399
1,278633	386,9510477	383,4007722	0,211580308	83,06499705
1,338595	386,8729065	382,9964578	0,563210604	85,8679602
1,398557	386,7873955	382,6036617	1,116781083	87,34912589
1,458519	386,6944241	382,2313285	1,710367041	87,4835028
1,518481	386,5939267	381,8849843	2,331597142	86,39955767
1,578444	386,4858666	381,5662522	2,976133422	84,33296436
1,638406	386,370265	381,273657	3,642602191	81,5533847
1,698368	386,2472026	381,003861	4,33037109	78,30680363
1,75833	386,1168177	380,7527841	5,038943021	74,787822
1,878254	385,8352589	380,2872905	6,516997839	67,52319933
1,998179	385,5276003	379,8545832	8,074627153	60,28549945
2,118103	385,1963785	379,4365961	9,709003305	53,35765206
2,238027	384,8445008	379,0197338	11,41597111	46,88016309
2,357952	384,4750267	378,5945527	13,18991326	40,90608115
2,477876	384,0910016	378,1545352	15,02383488	35,45041263
2,5978	383,6953313	377,6951808	16,9096153	30,51281769
2,717725	383,2906932	377,213473	18,83836008	26,08489005
2,837649	382,8794825	376,7075812	20,80078913	22,15196684
2,957573	382,463789	376,1766707	22,78760545	18,69378598
3,077498	382,0453967	375,6207509	24,78981242	15,68520232
3,197422	381,6257986	375,0405342	26,7989602	13,09712394
3,317346	381,2062221	374,4372968	28,80731647	10,89762521
3,437271	380,7876589	373,812746	30,80796471	9,053075344
3,557195	380,3708966	373,1688929	32,79484663	7,529277166
3,797044	379,5457356	371,8355391	36,70223916	5,268107495
4,012908	378,8135062	370,5915863	40,13120116	4,020306781
4,228771	378,0928517	369,3196945	43,45945197	3,335132375
4,444635	377,3841693	368,0304256	46,67717009	3,082294562
4,660499	376,6880044	366,7348782	49,77764055	3,138356293
4,876363	376,004039	365,4408044	52,75859281	3,431682114
5,092227	375,3322201	364,1558766	55,62033224	3,895047794
5,30809	374,6719822	362,8850381	58,36468571	4,488411597
5,523954	374,0226644	361,6319438	60,99393911	5,179455787
5,955682	372,7561654	359,1975039	65,93623398	6,688082147
6,344237	371,650418	357,091821	70,04023043	8,142672571

Table D.2.5: Stack length of 65 mm positioned at 40 mm.

0,869974	370,1383	361,4943	3,881190677	170,9135139
0,896847	370,1214	361,4235	3,723207971	167,7693749
0,92372	370,1036	361,3623	3,558096481	164,5051034
0,950593	370,0852	361,31	3,386038046	161,1648321
0,977466	370,066	361,2656	3,207252925	157,7883262
1,004339	370,0459	361,228	3,022003075	154,4099259
1,031212	370,025	361,1964	2,830544279	151,0516548
1,058085	370,0032	361,1697	2,633176858	147,7329613
1,084958	369,9806	361,1471	2,430214721	144,4678723
1,138704	369,9323	361,1105	2,009186389	138,1383967
1,19245	369,88	361,0821	1,57010403	132,09236
1,246196	369,8234	361,0582	1,116712761	126,3382192
1,299942	369,7623	361,036	0,657415686	120,8710304
1,353689	369,6964	361,013	0,245700726	115,6772291
1,407435	369,6256	360,9878	0,435321706	110,7390338
1,461181	369,5495	360,9591	0,922145879	106,0373381
1,514927	369,468	360,9262	1,441901748	101,5534035
1,568673	369,3811	360,8885	1,978564242	97,26969223
1,622419	369,2886	360,8457	2,527076354	93,17020119
1,676165	369,1906	360,7975	3,085844258	89,24057756
1,783657	368,9781	360,6844	4,232857703	81,83248806
1,891149	368,7443	360,5493	5,418356807	74,96905881
1,998641	368,4903	360,3922	6,642035999	68,58062527
2,106133	368,2176	360,2133	7,903695015	62,62742908
2,213625	367,928	360,0127	9,20261731	57,0720675
2,321117	367,6235	359,7904	10,53739939	51,89054875
2,428609	367,3061	359,5463	11,90587945	47,06929303
2,536102	366,978	359,2801	13,30515124	42,60042089
2,643594	366,641	358,9917	14,73165525	38,47822017
2,751086	366,2971	358,681	16,18132173	34,6967485
2,858578	365,9478	358,3482	17,64974081	31,2482538
2,96607	365,5947	357,9936	19,13233086	28,12228173
3,073562	365,2391	357,6179	20,62449212	25,30539862
3,181054	364,882	357,222	22,12174074	22,78142871
3,396038	364,1683	356,3767	25,10970441	18,51130783
3,589524	363,5286	355,5601	27,77884305	15,47995333
3,78301	362,8947	354,7001	30,40934676	13,08814564
3,976496	362,2685	353,8048	32,98780523	11,23423081
4,169981	361,6516	352,8836	35,50220257	9,8091697
4,363467	361,0447	351,9436	37,94527571	8,735785473
4,556953	360,4482	350,9919	40,31148023	7,940350522
4,750439	359,8625	350,0347	42,59784286	7,363784651
4,943925	359,2875	349,0772	44,80318165	6,959715532
5,13741	358,7232	348,1234	46,92771077	6,691842537
5,524382	357,6254	346,2437	50,94357934	6,431995409
5,911353	356,5674	344,411	54,66165058	6,455088849
6,298325	355,5468	342,6363	58,10075172	6,668337331

D.3 Five stacks positioned at 50 mm.

Table D.3.1: Stack length of 25 mm positioned at 50 mm.

0,99019898	347,246959	344,353747	2,601651213	53,86531865
1,02163102	347,201906	344,286005	2,138792985	52,96640742
1,05306305	347,155445	344,220205	1,689124747	52,07616713
1,08449508	347,107615	344,156368	1,253727043	51,18808217
1,11592711	347,058439	344,094485	0,834629451	50,29832947
1,14735915	347,007933	344,034517	0,441467703	49,40526391
1,17879118	346,956079	343,976393	0,174333371	48,5088576
1,21022321	346,903047	343,920013	0,429995447	47,6101447
1,24165524	346,848786	343,865254	0,795014184	46,71074749
1,27308728	346,79317	343,811975	1,151840038	45,81249675
1,30451931	346,736275	343,760025	1,498994087	44,91716799
1,33595134	346,67813	343,709251	1,836837965	44,02631701
1,36738337	346,618725	343,659498	2,164481906	43,141195
1,39881541	346,558061	343,610639	2,481632834	42,26257944
1,46167947	346,432981	343,514772	3,085511187	40,52804779
1,52454353	346,302937	343,42074	3,650630494	38,8243153
1,5874076	346,168005	343,327677	4,179830135	37,1515372
1,65027166	346,02829	343,234769	4,676260383	35,50928202
1,71313573	345,883931	343,141294	5,143245692	33,89713213
1,77599979	345,735097	343,046605	5,58418813	32,31522931
1,83886386	345,581989	342,950119	6,002460546	30,76453905
1,90172792	345,424828	342,851302	6,401334377	29,24688043
2,02745605	345,099645	342,644291	7,15647453	26,32570601
2,15318418	344,761429	342,422716	7,868953481	23,5742687
2,27891231	344,412351	342,183994	8,557453481	21,01769133
2,40464044	344,054256	341,926451	9,235298697	18,67550834
2,53036857	343,689261	341,64878	9,91550627	16,56475709
2,6560967	343,318977	341,350581	10,60595323	14,69334673
2,78182483	342,945024	341,031986	11,31306962	13,06319993
2,90755296	342,568803	340,693742	12,04076757	11,66922381
3,03328109	342,191487	340,337078	12,79083492	10,50067376
3,15900922	341,81405	339,963577	13,563416	9,542634291
3,28473735	341,437298	339,575051	14,35740302	8,777474072
3,41046548	341,061896	339,173443	15,17076599	8,186172766
3,53619361	340,688386	338,760727	16,00084577	7,74941157
3,78764987	339,949238	337,912316	17,69406311	7,2419215
4,0139605	339,293842	337,12843	19,2437902	7,146230145
4,24027113	338,649308	336,335016	20,79927643	7,301766237
4,46658177	338,016383	335,538767	22,34583147	7,64705314
4,6928924	337,395886	334,746379	23,86938938	8,122487628
4,91920303	336,788087	333,962026	25,35990258	8,690761544
5,14551367	336,193351	333,189679	26,80880501	9,317129041
5,3718243	335,611689	332,431593	28,21053997	9,980449942
5,59813493	335,043	331,689309	29,56117469	10,66512112
6,0507562	333,944864	330,259237	32,10091045	12,02664023

Table D.3.2: Stack length of 35 mm positioned at 50 mm.

0,670905	320,3046	318,1522	3,028858	30,94923
0,700188	320,2876	318,1288	2,908467	30,33991
0,729471	320,2698	318,1057	2,780668	29,73957
0,758754	320,2509	318,083	2,646607	29,14764
0,788037	320,2311	318,0605	2,507349	28,56372
0,81732	320,2102	318,0384	2,363837	27,98755
0,875886	320,1651	317,9947	2,068048	26,85819
0,934452	320,1155	317,9517	1,764097	25,75923
0,993018	320,0614	317,9092	1,456371	24,69062
1,051584	320,0029	317,8668	1,148872	23,65252
1,11015	319,94	317,8243	0,84537	22,64525
1,168717	319,8729	317,7813	0,550395	21,66925
1,227283	319,8017	317,7374	0,275239	20,72505
1,285849	319,7266	317,6925	0,131219	19,81325
1,344415	319,6479	317,6462	0,357162	18,93445
1,402981	319,5658	317,5982	0,619674	18,08926
1,461547	319,4803	317,5481	0,872435	17,27824
1,520113	319,3918	317,4959	1,119915	16,50183
1,637246	319,2069	317,3835	1,591547	15,05382
1,754378	319,0124	317,2599	2,032581	13,74442
1,87151	318,81	317,1244	2,449749	12,56984
1,988642	318,6012	316,9766	2,84901	11,52423
2,105774	318,3874	316,8166	3,236563	10,59928
2,222907	318,1698	316,645	3,617815	9,785287
2,340039	317,9497	316,4627	3,997058	9,071872
2,457171	317,7281	316,2705	4,377403	8,448617
2,574303	317,5057	316,0696	4,760874	7,905503
2,691436	317,2834	315,8611	5,148574	7,433209
2,808568	317,0617	315,6462	5,540852	7,023265
2,9257	316,8411	315,4259	5,937495	6,668099
3,159965	316,4054	314,9747	6,739838	6,088261
3,370803	316,0203	314,5592	7,468473	5,698254
3,581641	315,6432	314,1397	8,197017	5,405371
3,792479	315,2748	313,7193	8,92017	5,191804
4,003317	314,9158	313,3012	9,632509	5,040104
4,214155	314,5663	312,8875	10,33016	4,939422
4,424993	314,2265	312,4799	11,00966	4,879154
4,635831	313,8965	312,0797	11,66886	4,852551
4,846669	313,576	311,6878	12,30617	4,85294
5,057507	313,265	311,305	12,92077	4,875942
5,268345	312,9634	310,9315	13,51236	4,917199
5,479183	312,6708	310,5677	14,08092	4,973769
5,690021	312,3871	310,2137	14,62662	5,043281
6,111697	311,8451	309,5351	15,65397	5,208128

Table D.3.3: Stack length of 45 mm positioned at 50 mm.

0,815883	366,6214	363,9571	3,805145333	73,71424884
0,827172	366,6158	363,9311	3,759689269	73,04541241
0,849751	366,6041	363,8783	3,664297476	71,81516526
0,87233	366,5915	363,8238	3,55998693	70,80037855
0,894908	366,5782	363,7673	3,44971476	69,93207483
0,917487	366,5644	363,7086	3,333711807	69,20498172
0,940066	366,5499	363,6474	3,212110156	68,61559081
0,985224	366,5193	363,5184	2,956482163	67,73698603
1,030381	366,4861	363,3783	2,681044958	67,32458034
1,075539	366,45	363,2256	2,38601952	67,35122225
1,120696	366,411	363,0599	2,072677523	67,74756163
1,165854	366,369	362,8818	1,742775999	68,42027196
1,211011	366,3237	362,6927	1,398532368	69,26314488
1,256169	366,2752	362,4946	1,043077231	70,16681844
1,301326	366,2232	362,2898	0,682648441	71,02839476
1,346484	366,1678	362,0809	0,342374435	71,7589224
1,391641	366,109	361,8707	0,254292935	72,28797591
1,436799	366,0464	361,6614	0,592547975	72,56568247
1,481957	365,98	361,4554	0,992385231	72,56255974
1,572272	365,8358	361,0601	1,831184379	71,70390117
1,662587	365,6759	360,6915	2,697189919	69,8084251
1,752902	365,5003	360,3521	3,578385341	67,07262236
1,843217	365,3088	360,0405	4,470530733	63,73693304
1,933532	365,1018	359,7529	5,371634063	60,033555
2,023847	364,8795	359,4841	6,280370352	56,15474913
2,114162	364,6426	359,2286	7,196158959	52,24359162
2,204477	364,3918	358,9812	8,118920981	48,39893854
2,294792	364,1281	358,7374	9,048757005	44,68554299
2,385108	363,8525	358,4935	9,98576628	41,14401249
2,565738	363,2717	357,9898	11,88110276	34,68472221
2,728305	362,7191	357,5122	13,60920384	29,59115857
2,890872	362,1453	357,0029	15,35395296	25,18189959
3,053439	361,5552	356,458	17,1101154	21,43159803
3,216006	360,9546	355,876	18,87088986	18,29002993
3,378574	360,3474	355,258	20,63016161	15,70362969
3,541141	359,7375	354,6069	22,38101692	13,60303542
3,703708	359,1276	353,9261	24,11786418	11,92879348
3,866275	358,5201	353,2201	25,83504131	10,61677878
4,028842	357,9169	352,4935	27,52771883	9,608628261
4,19141	357,3193	351,751	29,19180609	8,853143717
4,353977	356,7284	350,9966	30,82392865	8,306286519
4,516544	356,1449	350,2345	32,42137435	7,930730652
4,841678	355,0024	348,7042	35,50265909	7,540406572
5,166813	353,893	347,1771	38,42727621	7,539413533
5,491947	352,8176	345,6697	41,19144235	7,794646195
5,817081	351,7762	344,1933	43,79485792	8,216199398
6,142216	350,7679	342,7561	46,24066186	8,740005058

Table D.3.4: Stack length of 55 mm positioned at 50 mm.

0,735914	318,0058	313,8955	0,147893527	0,149109739
0,757095	317,9938	313,9307	0,072026968	0,212092832
0,778275	317,9814	313,9618	0,066877913	0,634020616
0,820636	317,9559	314,0128	0,248525433	1,600323056
0,862996	317,9292	314,0498	0,449724868	2,635190106
0,905357	317,9011	314,0746	0,655829104	3,681021156
0,947718	317,8717	314,0891	0,868154269	4,693444005
0,990078	317,8408	314,0948	1,084772515	5,638191235
1,032439	317,8085	314,0935	1,303718831	6,496153219
1,0748	317,7746	314,0863	1,523809536	7,25899587
1,117161	317,7393	314,0743	1,743954484	7,924675598
1,159521	317,7023	314,0586	1,963102665	8,495341075
1,201882	317,6638	314,0398	2,18034462	8,97585393
1,286603	317,5819	313,9956	2,605487681	9,699521821
1,371325	317,4935	313,9445	3,015270716	10,14520221
1,456046	317,3986	313,8884	3,406377498	10,36737687
1,540768	317,2973	313,8283	3,777169677	10,40949212
1,625489	317,1898	313,7648	4,126768578	10,31471629
1,71021	317,0763	313,6983	4,455351787	10,11878884
1,794932	316,9573	313,6285	4,763934704	9,850690319
1,879653	316,8332	313,5555	5,054111909	9,533870674
1,964374	316,7043	313,4788	5,327819871	9,187243782
2,049096	316,5712	313,3984	5,587144258	8,82590221
2,133817	316,4343	313,3139	5,834175892	8,461649796
2,218539	316,2943	313,2251	6,070907496	8,103457736
2,387981	316,0072	313,0348	6,522808897	7,435186212
2,54048	315,7422	312,8491	6,909507948	6,896250952
2,692978	315,4736	312,6504	7,284419299	6,425890486
2,845477	315,2031	312,4398	7,651713625	6,023527469
2,997975	314,9325	312,2189	8,015063749	5,683887031
3,150474	314,6631	311,989	8,376198535	5,399619982
3,302972	314,3959	311,752	8,736438717	5,161456921
3,455471	314,1318	311,5092	9,096122091	4,962001496
3,607969	313,8714	311,2621	9,455343793	4,793346122
3,760468	313,6153	311,0121	9,813803756	4,650115316
3,912966	313,3637	310,7602	10,17107363	4,52720344
4,065465	313,1169	310,5075	10,52665125	4,42063125
4,217963	312,8751	310,2549	10,87997921	4,327370241
4,370462	312,6383	310,003	11,23050347	4,245119208
4,52296	312,4068	309,7525	11,57770209	4,172127006
4,827957	311,9589	309,2583	12,25967352	4,04757147
5,132954	311,5312	308,7746	12,92321799	3,948369171
5,437951	311,1232	308,3034	13,56611914	3,869711393
5,742948	310,7342	307,8463	14,18664655	3,80851308
6,047945	310,3634	307,4039	14,78369025	3,762589031

Table D.3.5: Stack length of 65 mm positioned at 50 mm.

0,75711	365,1997	360,402	4,313674028	66,15103848
0,781351	365,1859	360,468	4,211106538	64,87675512
0,803167	365,1731	360,5172	4,113160982	63,9569041
0,824983	365,1597	360,5564	4,009778699	63,27749562
0,8468	365,1459	360,5851	3,900891675	62,87819271
0,868616	365,1316	360,6022	3,786468665	62,81563413
0,890432	365,1168	360,6064	3,666522161	63,15309299
0,912249	365,1015	360,5961	3,541094965	63,95585125
0,934065	365,0857	360,5694	3,410260909	65,2840346
0,955882	365,0694	360,5246	3,274123911	67,17586463
0,977698	365,0526	360,4607	3,132794795	69,63520079
1,021331	365,0173	360,273	2,835527535	75,97049875
1,064963	364,98	360,012	2,519871641	83,62270778
1,108596	364,9405	359,6914	2,187553182	91,7091942
1,152229	364,8987	359,3307	1,840621753	99,36014465
1,195862	364,8545	358,9504	1,481512113	105,9135421
1,239495	364,8078	358,5692	1,11345533	110,996974
1,283127	364,7585	358,2012	0,742271781	114,5014363
1,32676	364,7065	357,8559	0,388693669	116,4987847
1,414026	364,5937	357,252	0,547691342	116,9106539
1,501291	364,4683	356,7638	1,347435652	113,6290337
1,588557	364,3296	356,3797	2,171821826	108,0280521
1,675822	364,1767	356,0796	3,002539048	101,2489335
1,763088	364,0092	355,8406	3,831593016	94,07928939
1,850353	363,8267	355,6423	4,655359815	86,9862856
1,937619	363,6291	355,4687	5,473215812	80,20850061
2,024884	363,4165	355,3079	6,285674154	73,8462931
2,11215	363,1895	355,1517	7,094138584	67,92595077
2,286681	362,6961	354,8265	8,712237734	57,33807657
2,443759	362,2107	354,5108	10,17809073	49,12524252
2,600837	361,6927	354,1606	11,66485801	41,99245014
2,757915	361,1481	353,77	13,17969131	35,82874355
2,914993	360,5828	353,3362	14,7254345	30,54360482
3,072071	360,0024	352,8587	16,30154863	26,0459587
3,229149	359,4118	352,3387	17,90440435	22,25065136
3,386226	358,8154	351,779	19,52812774	19,07586626
3,543304	358,2164	351,1829	21,16582623	16,44711831
3,700382	357,6181	350,5553	22,80893255	14,27934879
3,85746	357,0227	349,9003	24,45006125	12,50819144
4,014538	356,4319	349,2227	26,08140679	11,06787349
4,171616	355,8471	348,5269	27,6960542	9,90133525
4,328694	355,2693	347,8173	29,28807528	8,960290847
4,485772	354,6991	347,0975	30,85254588	8,204363349
4,799928	353,584	345,6445	33,88054974	7,084789882
5,114084	352,5024	344,1843	36,76430238	6,392360626
5,42824	351,4552	342,7334	39,49309445	5,98775108
5,742396	350,4418	341,3034	42,06309377	5,779039241
6,056552	349,4612	339,9029	44,4756826	5,702314205